Co-occurrence of aerobic ammonia oxidation, anaerobic ammonia oxidation and nitrite oxidation in oxic riverbeds and their relationships with net nitrification efficiency

Liao Ouyang

Submitted in partial fulfilment of the requirements of the Degree of Doctor of Philosophy

I, Liao Ouyang, confirm that the research included within this thesis is my own work or that where it has been carried out in collaboration with, or supported by others, that this is duly acknowledged below and my contribution indicated. Previously published material is also acknowledged below.

I attest that I have exercised reasonable care to ensure that the work is original, and does not to the best of my knowledge break any UK law, infringe any third party's copyright or other Intellectual Property Right, or contain any confidential material.

I accept that the College has the right to use plagiarism detection software to check the electronic version of the thesis.

I confirm that this thesis has not been previously submitted for the award of a degree by this or any other university.

Signature: liao ouyang

Date: 07/01/2019

This research project was supervised by Professor Mark Trimmer and was supported by the Queen Mary University of London (QMUL)-China Scholarship Council (CSC) Joint Scholarship.

The molecular work was carried out in collaboration with Dr Boyd A. McKew in University of Essex.

Abstract

In short term, re-mineralized nitrogen as ammonia can either be conserved in an ecosystem through its complete oxidation to nitrate e.g. 'efficient nitrification' or lost via oxidation to N_2 gas e.g., 'inefficient nitrification'. Here, ^{15}N tracers and molecular analyses were used to characterize the 'nitrification efficiency' in relation to aerobic ammonia oxidation, anaerobic ammonia oxidation (anammox) and nitrite oxidation across a range of oxic riverbeds. Here $^{15}NO_2^-$ from $^{15}NH_4^+$ was rapidly consumed by anammox/denitrification and/or nitrite oxidation and although the total rate of ammonia oxidation (i.e. $^{15}NO_3^- + {}^{15}N_2$) was conserved, nitrification efficiency varied from 22.2% to 99.7%. Nitrification efficiency was highest where the contribution from anammox to N_2 production (*ra*) was lowest, and maximal where anammox was absent, suggesting competition between nitrite oxidation and anammox for nitrite. Nitrification efficiency was also highest where the abundance of *nxr*B gene (*Nitrospira* + *Nitrobacter*) was greatest, along with the highest abundance of comammox *Nitrospira amo*A gene. These results reveal a gradient in riverbed nitrification efficiency that was related primarily to *Nitrospira* dominating the nitrite oxidizing bacteria (NOB). A preincubation of soluble reactive phosphorus (SRP) selectively increased the degree of nitrification efficiency in some riverbed sediments by stimulating nitrite oxidation. Furthermore, anammox was more important where the abundance of *hzs*B and *amo*A genes were greatest, indicating an interaction between aerobic and anaerobic ammonia oxidation. In these oxic riverbeds, aerobic ammonia oxidizing microorganisms (AOM) and anammox bacteria may aggregate together, AOM consumed oxygen at a rate of 22.28 nmol g^{-1} h^{-1} and competed with heterotrophic respiration for 8% of the total oxygen consumption, making oxygen limited in the aggregates and thus enabling anammox. Furthermore, the aerobic ammonia oxidation can provide nitrite to sustain the anammox bacteria.

Table of Contents

List of Figures

List of Tables

Chapter 1 : Introduction

1.1. Nitrogen and its ecological significance

Nitrogen is a key element for the living organisms and is critical in the amino acids and proteins synthesis process. As many of the original plant species living in terrestrial, freshwater and marine ecosystems are with low levels of available nitrogen, it controls the primary production of these ecosystems (Vitousek et al. 1997). Although 78% of the atmosphere is made of nitrogen gas, most of the environmental systems are nitrogen limited as the nitrogen gas cannot be used directly by most microorganisms. In the preindustrial world, lightning and biological nitrogen fixation (BNF) are two natural processes that can convert unreactive N_2 gas to reactive nitrogen and then the reactive nitrogen can be used by the biological system (Galloway et al. 1995). Compared with lighting, the contribution of BNF is always significantly greater. In the preindustrial world, the rates of formation and loss of reactive nitrogen are approximately in balance.

Human activities have remarkably increased the bioavailable nitrogen loading into the biosphere (Gruber and Galloway 2008) through the combustion of fossil fuels, fertilization and cultivation (Galloway et al. 1995, Vitousek et al. 1997). Globally, human activities converted N_2 to reactive forms at about the same rate as BNF, thus doubled the turnover rates of the nitrogen cycle of the entire earth. The increase of the nitrogen availability has substantially accelerated the productivity and biomass accumulation, however, it also brings some negative consequences.

The formation process and the further distribution of reactive nitrogen can affect the atmosphere. For example, the emission of oxides of nitrogen (NO and NO_2) can enhance the O_3 concentration in troposphere, form photochemical smog and acidic rains,

also, they are involved in the formation of fine particles (PM), which are associated with air pollution and adverse health effects. The release of N_2O, although not stable, can enhance the greenhouse effect (Vitousek et al. 1997). Furthermore, changes in nitrogen can alter the global cycle of carbon, affecting both CO_2 and CH_4 concentrations in the atmosphere (Galloway et al. 2008). Furthermore, the imbalance of the formation and the removal of the reactive nitrogen would cause the accumulation of NO_3^- in soils. In rivers receiving substantial amounts of anthropogenic nitrogen input, the accumulation of nitrate may cause eutrophication and harmful algal bloom, decreasing the water quality (Vitousek et al. 1997, Boyer et al. 2006), further reduce the biological diversity of the ecosystem.

1.2. Nitrogen cycle

Nitrogen exists in a wide variety of chemical forms in the environment, the oxidation states range from -3 (NH_4^+) to +5 (NO_3^-) .The nitrogen cycle is a combination of processes between various nitrogen chemical forms (Gruber and Galloway 2008). Nitrogen cycle mainly consists of nitrogen fixation, ammonification, nitrification, denitrification, dissimilatory nitrate reduction to ammonium (DNRA) and anaerobic ammonium oxidation (anammox). The relationships among them are illustrated in the Figure 1.1 (Trimmer et al. 2003).

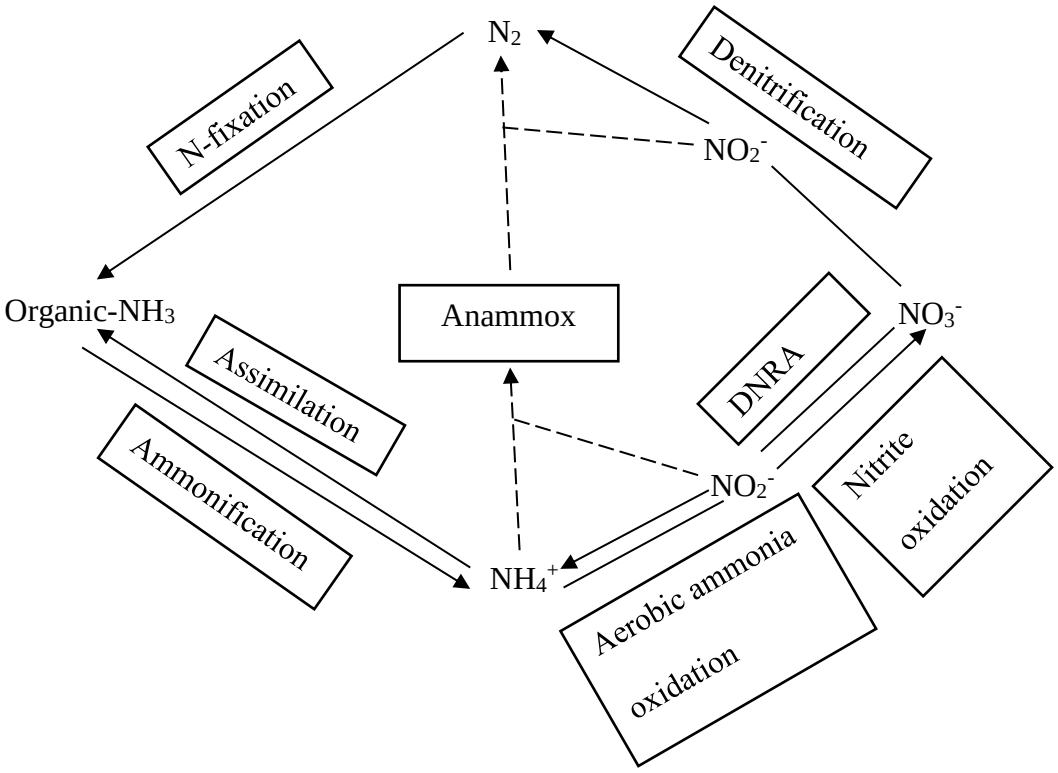

Figure 1.1. Main processes in nitrogen cycle, based on (Trimmer et al. 2003).

Nitrogen fixation is a process that nitrogen gas is converted into ammonia or other molecules available to living organisms. It is an important source for biologically available nitrogen and it is critical for maintaining the productivity of the ecosystems (Capone 2001, Jetten 2008). Biological nitrogen fixation is mediated enzymatically by the nitrogenase complex. Nitrogen fixation can occur in a wide variety of autotrophic and heterotrophic bacteria and archaea (Raymond et al. 2004). *Nif*H is a gene marker that widely used for detecting the nitrogen fixation microorganisms in the environment (Zehr et al. 2003).

Ammonification or nitrogen mineralization is a process that organic N is hydrolysed and catabolised by heterotrophic organisms and release NH_4^+ (Herbert 1999). The released NH_4^+ can then either be oxidized or assimilated and incorporated into

organic molecules by a variety of aerobic and anaerobic organisms. Ammonification occurs in both oxic and anoxic sediments and is always coupled to heterotrophic carbon mineralization (Herbert 1999).

Nitrification is a fundamental process in all ecosystems as it connects the most reduced and oxidised sides of the nitrogen (Herbert 1999). The conventional nitrification is the oxidation of NH_4^+ to NO_3^- through NO_2^-, it comprises two separate reactions and is driven by two different functional groups of microorganisms producing a set of nitrogen intermediates (Ward 2008). The oxidation of NH_4^+ to NO_2^- is governed by the ammonia oxidizing microorganisms (AOM), consists of ammonia oxidizing bacteria (AOB) and ammonia oxidizing archaea (AOA). The subsequent oxidation of NO_2^- to NO_3^- is catalysed by the nitrite oxidizing bacteria (NOB) (Ward 2008). Both processes are aerobic catabolic processes with oxygen serves as electron acceptor. Nitrification process releases N_2O into the atmosphere as a by-product (Anderson and Levine 1986). Recently, complete ammonia oxidizing bacteria (comammox) possess both ammonia and nitrite oxidizing genes and are therefore capable of the complete oxidation of ammonia to nitrate (comammox) has been identified (Daims et al. 2015, van Kessel et al. 2015, Kits et al. 2017).

Denitrification process is the reduction of nitrate to N_2 through a series of nitrogen intermediates, this process basically involves four metalloenzymes: nitrate reductase (nar), nitrite reductase (nir), nitric oxide reductase (nor) and nitrous oxide reductase (nos). It usually occurs under low-oxygen conditions and use organic matter as elector donor (Francis et al. 2007). Denitrifiers distributes widely among all the three domain life (Stein and Klotz 2016). Denitrification is an important sink for nitrogen, as it is a significant pathway for N_2 formation and, in turn, the removal of nitrogen in aquatic sediments.

Denitrification also forms N_2O, which is a highly potent greenhouse gas (Canfield et al. 2010).

Anaerobic ammonium oxidation (anammox) is a process where NH_4^+ is oxidized to N_2 gas with nitrite serving as the electron acceptor under anoxic conditions (Mulder et al. 1995, Van de Graaf et al. 1995). As an alternative way that can remove fixed nitrogen by the production of N_2 gas, the discovery of anammox changed our understanding of the N cycle on Earth. Anammox dominates N_2 production in some marine environments. Although anammox and denitrification have the same impact, it has advantage over denitrification as there was no N_2O release and no need for organic matter in anammox process (Babbin and Ward 2013).

Dissimilatory nitrate reduction to ammonium (DNRA) is the reduction of NO_3^- to NH_4^+ and it mainly occurs under anoxic conditions. Fermentative nitrate reduction and sulfur-driven nitrate reduction are two recognized pathways for DNRA (Burgin and Hamilton 2007). DNRA is thought to be favoured at anoxic, electron donor-rich zones and NO_3^- limited conditions, competes with denitrification and anammox for nitrate and nitrite (Van Den Berg et al. 2015).

1.3. Aerobic ammonia oxidation

The ammonia in the environment was mainly obtained from the decay of the organic matter. As the rate limiting step of nitrification, aerobic ammonia oxidation is a fundamental biogeochemical process in the nitrogen cycle. Aerobic ammonia oxidation to nitrite can be driven by both bacteria and archaea (Ward 2008). Bacterial aerobic ammonia oxidation was discovered over 100 years ago, it is a two-step enzymatic process, the oxidation of ammonia to NH_2OH is catalysed by ammonium monooxygenase (AMO)

(Equation 1.1) and the oxidation of NH_2OH to NO_2^- is catalysed by hydroxylamine oxidoreductase (HAO) (Equation 1.2). A recent study has found NO as an intermediate involved in this process, it is proposed that HAO oxidizes NH_2OH to NO, and then NO is oxidized to NO_2^- aerobically by an unknown enzyme (Caranto and Lancaster 2017).

$$NH_4^+ + O_2 + 2H^+ + 2e^- = NH_2OH \quad + H_2O \qquad (1.1)$$

$$NH_2OH \quad + H_2O \quad = NO_2^- + 5H^+ + 4e^- \qquad (1.2)$$

The *amo*A gene encodes the active site of α-subunit of the enzyme AMO, so it is normally used as an phylogenetic marker for the AOB (Purkhold et al. 2003). The bacterial oxidation of ammonia to nitrite is mainly caused by the *Nitrosococcu*s belong to the class 'Gammaproteobacteria' and *Nitrosomonas* and *Nitrosospira* belong to class 'Betaproteobacteria'. While AOB in Gammaproteobacteria were only observed in the marine environment, Betaproteobacteria AOB were widely distributed in diverse habitats, such as estuaries (Li et al. 2018), streams (Cooper 1983), aquaculture ponds (Lu et al. 2016, Zhou et al. 2017), lakes (Wu et al. 2010), freshwater wetlands (Lee et al. 2014) and paddy soils (Wang et al. 2014).

AOA was also confirmed to contain the archaeal *amo*A gene, dominates aerobic ammonia oxidation in some freshwater and marine habitats (Francis et al. 2005). The genetic capacity of aerobic ammonia oxidation by archaea was firstly found by the observation of the *amo*A genes from uncultured crenarchaeota in seawater (Venter et al. 2004) and soil samples (Treusch et al. 2005). The AOA was then classified to the phylum Thaumarchaeota (Pester et al. 2012). *Nitrosopumilus maritimus* strain SCM1 is the first isolated AOA and it was isolated from a marine aquarium tank (Könneke et al. 2005).

The first isolation of AOA from soil is *Candidatus.* Nitrosophaera viennensis strain EN76 (Tourna et al. 2011). The widespread of AOA was then confirmed in marine waters and the sediments (Francis et al. 2005, Lam et al. 2009), freshwater lake sediments (Herrmann et al. 2009, Wu et al. 2010, Hampel et al. 2018) and estuaries (Jin et al. 2011). More than ten strains were isolated so far and AOA was divided into four clusters: the *Nitrosopumilus* cluster (1.1a), the *Nitrosotalea* cluster (1.1a-associated), the *Nitrososphaera* cluster (1.1b) and the *Nitrosocaldus* cluster (ThAOA) (Pester et al. 2012, Liu et al. 2017). The oxidation of ammonia to NH_2OH by archaea was firstly catalysed by ammonium monooxygenase (AMO) enzyme, the NH_2OH was then catalysed to NO_2^- with NO as the intermediate by a copper-containing enzyme (Kozlowski et al. 2016). Unlike AOB, AOA do not encode HAO.

AOA and AOB coexist in most environment and the distribution of the AOA and AOB could be largely dependent on the habitat. Environmental factors such as ammonium concentration, pH, organic matters, dissolved oxygen concentration and temperature have been demonstrated to influence the niche separation of AOA and AOB (He et al. 2012, Liu et al. 2017). The study of (Erguder et al. 2009) showed that AOA might be more important in low nutrient, low pH and sulphide containing environment. AOA can grow at a ammonium concentration of 0.5-1.5 mM, while AOB can grow at a concentration of 1.5 to 25 mM and have a maximum ammonium tolerance of 50-100 mM (Nicol et al. 2011). It is reported that archaea mainly drives the marine nitrification with low ammonium concentrations (Martens-Habbena et al. 2015). Studies also showed that AOA are more abundant than AOB in acidic soils (He et al. 2012) and eutrophic lake sediments (Zhao et al. 2013). The study of (Lam et al. 2007) showed that AOA are responsible for most of the ammonia oxidation in oxic marine water and AOB are mainly responsible in the suboxic zone.

Recently, complete ammonia oxidizing bacteria (comammox) that possess both ammonia and nitrite oxidizing genes and are therefore capable of the complete oxidation of ammonia to nitrate (comammox) has been identified (Daims et al. 2015, van Kessel et al. 2015, Kits et al. 2017). *Candidatus* Nitrospira nitrosa, *Candidatus* Nitrospira nitrificans *Candidatus* Nitrospira inopinata and *Nitrospira* sp. strain Ga0074138) has been identified as the comammox *Nitrospira* to date (Camejo et al. 2017). Comammox *Nitrospira* contain novel *amo*A genes encoding ammonia monooxygenase (AMO), which is distinct from the *amo*A in AOB and AOA. They also contain genes encoding HAO and nitrite oxidoreductase (NXR), the key enzymes of bacteria ammonia oxidation and nitrite oxidation (Camejo et al. 2017, Pjevac et al. 2017).

So far comammox have been found in diverse man-made systems such as groundwater-fed rapid sand filters (Fowler et al. 2018), wastewater treatment plants (WWTPs) (Gonzalez-Martinez et al. 2016, Fan et al. 2017) and drinking water systems (Pinto et al. 2016, Wang et al. 2017), the activated sludge and biofilm samples (Chao et al. 2016), freshwater recirculating aquaculture system (Bartelme et al. 2017) and other natural habitats such as rice paddy and forest soils, brackish lake sediment and freshwater biofilm (Hu and He 2017, Pjevac et al. 2017). It is proposed that comammox *Nitrospira* might outcompete other nitrifiers under highly oligotrophic environment as they have high affinity for ammonia (Hu and He 2017).

1.4. Nitrite oxidation

Nitrite oxidation, the second step of the nitrification, is the major known biological source for nitrate. The oxidation of nitrite to nitrate is catalysed by membrane-bound enzyme nitrite oxidoreductase (NXR) (Kuypers et al. 2018). The oxidation of

nitrite to nitrate is carried out by chemolithoautotrophic nitrite oxidizing bacteria (NOB) and it can be described as follows (Equation 1.3):

$$NO_2^- + \frac{1}{2}O_2 = NO_3^- \qquad (1.3)$$

NO_2^- oxidation to NO_3^- is primarily accomplished by bacteria that belong to the unrelated genera *Nitrobacter*, *Nitrococcus*, *Nitrospina* and *Nitrospira*. The *nxr*B gene encoding the β subunit of NXR, was introduced as the functional and phylogenetic marker for *Nitrospira* and *Nitrobacter* (Pester et al. 2014).

Nitrospira is the most diverse and widespread group of NOB and it belongs to the phylum *Nitrospirae*. It is regarded as more important than *Nitrobacter* in WWTPs and aquaria (Daims et al. 2001, Pester et al. 2014). It consists of at least six phylogenetic lineages (Pester et al. 2014). Selected species in *Nitrospira* consists of *Nitrospira defluvii* (lineage I), *Nitrospira moscoviensis* (lineage II), *Nitrospira marina* (lineage IV), *Candidatus* Nitrospira bockiana (lineage V), *Nitrospira calida* (lineage VI) (Pester et al. 2014, Daims and Wagner 2018). The first isolated *Nitrospira* species, *Nitrospira marina*, was obtained from the marine water (Watson et al. 1986). The study in WWTPs showed that the distribution of *Nitrospira* populations is related to their affinities of substrates and their relationships with AOB (Maixner et al. 2006, Ushiki et al. 2017), while sub-lineage I had an advantage over sub-lineage II under higher nitrite concentrations (5 mg NO_2^- L^{-1} vs. 0.1 mg NO_2^- L^{-1}) (Maixner et al. 2006).

Nitrobacter also plays an important role in both fertilized and unfertilized soils (Vanparys et al. 2007, Fukushima et al. 2013), *Nitrobacter winogradskyi*, *Nitrobacter hamburgensis*, *Nitrobacter vulgaris* and *Nitrobacter alkalicus* are four species that belong to *Nitrobacter* (Vanparys et al. 2007). The coexistence of *Nitrospira* and *Nitrobacter* have

been found in WWTPs (Whang et al. 2009) and estuaries (Cebron and Garnier 2005). Nitrite concentration was the main factor that controlling the distribution of *Nitrospira* and *Nitrobacter*. Compared with *Nitrospira*, *Nitrobacter* have a relatively lower affinity for nitrite and a higher maximum nitrite uptake rate (Schramm et al. 1999). Inorganic carbon was also demonstrated to be a factor that driven the distribution of *Nitrospira* and *Nitrobacter*, *Nitrospira* dominated in the bioreactor with higher inorganic carbon, while *Nitrobacter* dominated in the bioreactor with lower inorganic carbon(Fukushima et al. 2013).

Compared with AOA and AOB, NOB have received less attention though the abundance of *Nitrospira* was sometimes higher than those of AOA and AOB, for example, in a marine aquaculture biofilm (Foesel et al. 2007) and river sediments (Nakamura et al. 2006).

1.5. Anaerobic ammonia oxidation

Anaerobic ammonia oxidation (anammox), an alternative microbiological process that can oxidize ammonium under anoxic conditions with nitrite serving as the electron acceptor (Mulder et al. 1995, Van de Graaf et al. 1995), has been identified as an important way to remove the fixed nitrogen into atmosphere as N_2 (Kuypers et al. 2005). The discovery of anammox changed our understanding of the N cycle, since denitrification was thought to be the only process that can remove fixed nitrogen to the atmosphere for over 100 years. The first direct evidence of the anaerobic ammonium oxidation was found by (Mulder et al. 1995) in a denitrifying fluidized bed reactor in 1995 in Delft, the Netherlands. A few years later, the direct evidence of anaerobic ammonia oxidation in a natural environment, marine sediments, was published (Thamdrup and

Dalsgaard 2002). Subsequently, based on experiments using a ^{15}N isotope labelling technique (Thamdrup and Dalsgaard 2002), more and more evidences appeared confirming that the anammox process is important in the overall nitrogen cycle.

The anammox process have been confirmed to play important roles in marine environments (Rich et al. 2008, Stevens and Ulloa 2008), estuaries (Trimmer et al. 2003, Nicholls and Trimmer 2009), subtropical mangrove-aquaculture ecosystems (Amano et al. 2011), marsh sediments (Hou et al. 2013) and paddy soils (Zhu et al. 2011). The contribution of anammox to total N_2 production ranged from negligible to approximately 70% (Trimmer et al. 2013).

In freshwater ecosystems, the first direct evidence of anammox bacteria was found in a lacustrine system, Lake Tanganyika, here, the anammox process contributed to 9–13% of the N_2 production (Schubert et al. 2006). Since then, anammox process has been confirmed to exist in some muddy lakes and rivers sediments, it contributed to 0.8–13% of the N_2 production (Penton et al. 2006, Schubert et al. 2006, Zhang et al. 2007, Zhao et al. 2013) and up to 40% in a eutrophic freshwater lake (Yoshinaga et al. 2011). To date, research for anammox in rivers were mainly focused on the muddy sediments, in these rivers, the oxygen penetrations are restricted, which can provide an ideal environment for anammox.

Environmental factors such as organic matter, nitrate and nitrite concentrations, salinity and pH can influence the distribution of anammox bacteria. Anammox bacteria was found less competitive for NO_2^- than the denitrifiers in organic-rich shallow sediments (Thamdrup and Dalsgaard 2002, Trimmer et al. 2003, Trimmer et al. 2013). Studies also showed that higher NO_3^- concentration leads to a higher nitrate reduction rate and a greater release of NO_2^- for anammox (Risgaard-Petersen et al. 2004, Rich et al. 2008, Hou et al. 2013). The study of (Terada et al. 2011) showed that higher contributions

of the anammox process to nitrogen loss were found at higher salinity environments (Li et al. 2011, Terada et al. 2011, Hou et al. 2013). Anammox bacteria was active at a wide range of temperature, with an optimal temperature of 35 °C in laboratory bioreactors (Schubert et al. 2006, Hou et al. 2013).

The first discovered anammox bacterium belongs to the phylum Planctomycetales and, while not in pure culture, was named *Candidatus* Brocadia anammoxidans (Dalsgaard et al. 2005). At least five genera (*Candidatus* Brocadia, *Candidatus* Kuenenia, *Candidatus* Scalindua, *Candidatus* Anammoxoglobus and *Candidatus* Jettenia) and 22 species have been identified using culture-independent molecular techniques (Hu et al. 2011, Sonthiphand et al. 2014, Zhou et al. 2018). Anammox bacteria have a widespread distribution in various natural habitats. Among the anammox bacteria that have been described to date, *Candidatus* Scalindua were mainly discovered in marine systems (Penton et al. 2006, Rich et al. 2008, Li et al. 2010), *Candidatus* Brocadia and *Candidatus* Kuenenia appeared to be more common in freshwater, terrestrial ecosystems and the reservoirs (Hu et al. 2011, Shen et al. 2017). The coexistence of different groups of anammox was normally found in various habitats with certain groups dominated in specific habitats (Humbert et al. 2012, Shen et al. 2015).

Base on the ^{15}N tracing studies, the metabolic pathway of anammox was firstly proposed by (Van De Graaf et al. 1997), the hydroxylamine (NH_2OH), which is most likely derived from incomplete reduction of NO_2^-, was proposed as an intermediate for the anammox reaction. Ammonium is then biologically oxidized using NH_2OH as the electron acceptor and produce hydrazine (N_2H_4), the N_2H_4 is then oxidized to N_2 gas. Based on the genomic analysis of uncultured anammox bacterium *Candidatus* Kuenenia stuttgartiensis, NO was proposed as an intermediate for the anammox reaction (Strous et al. 2006). The overall stoichiometry was then proposed as follows (Equations 1.4-1.6)

(Kartal et al. 2011). The nitrite reductase (NirS) has the potential ability to reduce nitrite to NO (Equation 1.4), then NO reacts with ammonium to produce N_2H_4.

$$NO_2^- + 2H^+ + e^- = NO + H_2O \quad (1.4)$$

$$NO + NH_4^+ + 2H^+ + 3e^- = N_2H_4 + H_2O \quad (1.5)$$

$$N_2H_4 = N_2 + 4H^+ + 4e^- \quad (1.6)$$

The enzymatic mechanism of the hydrazine (N_2H_4) synthesis was proposed as a two-step process, the reduction of the NO to NH_2OH (Equation 1.7) at the active site of the ϒ-subunit and its subsequent condensation with NH_3, which will yield N_2H_4 in the active centre of the α-subunit (Equation 1.8) (Dietl et al. 2015). Hydrazine synthesis (HZS) enzyme is the only known enzyme that can activate ammonium anaerobically (Kuypers et al. 2018). *hzs*A and *hzs*B genes encode the HZS and have been used as the gene makers for anammox.

$$NO + 3H^+ + 3e^- = NH_2OH \quad (1.7)$$

$$NH_2OH + NH_3 = N_2H_4 + H_2O \quad (1.8)$$

1.6. Rivers as important sinks for N

As a hydrological connection between terrestrial system and costal system, rivers play an important role in the N cycle. It is reported that 25% of the human added N inputs are exported to the rivers, and then are further transported to the inland-receiving waters

and coastal waters (Boyer et al. 2006). Rivers are important sinks for the bioavailable nitrogen (Mulholland et al. 2008). In short term, organic nitrogen is mineralized to ammonia, and then aerobically oxidized and conserved as nitrate through nitrification or returned to the atmosphere as N_2 through denitrification and anammox.

Denitrification was thought to be the only process that can remove the fixed nitrogen in the rivers, approximate 50% of the nitrogen entering river systems appears to be lost to denitrification (Galloway et al. 2004, Pina-Ochoa and Alvarez-Cobelas 2006, Burgin and Hamilton 2007). In rivers, both overlying water nitrification and sediment nitrification can provide nitrate for sediment denitrification (Seitzinger et al. 2006). Denitrification and nitrification are tightly coupled in spatially and temporally. It is proposed that the overlying water nitrate concentration was the main factor that influence the nitrate source of the sediment denitrification. In rivers where nitrate concentration was less than 10 μM, coupled nitrification/denitrification in the sediments appears to be the major substrate for denitrification (Seitzinger 1988), while in others the water column with nitrate concentration higher than 60 μM, the bottom water accounts for major nitrate source for denitrification (Seitzinger et al. 2006, Smith et al. 2006).

In permeable, oxic sediments, the advective flows of the porewater can enhance the supply of the oxidants and organic matter, as well as the removal of remineralization by-products, thus resulting in high metabolic activity (Rao et al. 2008). Nitrification and nitrate reduction can occur simultaneously in permeable coastal sediments and about 30% of the nitrate was reduced as N_2 gas (Koike and Hattori 1978). By adding ^{15}N tracers into sediment slurries in oxic conditions, the coupling of nitrification and dentification has been studied in permeable, oxic costal sediments (Rao et al. 2008, Gao et al. 2009, Marchant et al. 2014, Marchant et al. 2016) and suspended sediments in oxic rivers (Xia et al. 2017). These findings therefore suggest the interactions between nitrification and

denitrification are very tight in permeable coastal sediments. The availability of ammonium, nitrate, organic matter and oxygen was thought be the controlling factors for the degree of the coupled nitrification and denitrification when anammox was absent (Gao et al. 2009).

Given the widespread occurrence of anammox in various aquatic environments (Kuypers et al. 2005), affiliation between anammox and nitrification might have an important but so far neglected role in the removal of N_2 in permeable, oxic riverbeds. To date, the study of anammox in permeable, oxic riverbed is limited. Lansdown et.al found negligible anammox activity in a permeable, oxic river Leith (Lansdown et al. 2012, Lansdown et al. 2014). While in the Hampshire Avon, both anammox and denitrification contributed to the production of ^{15}N-N_2 in oxic, permeable riverbeds with the addition of $^{15}NH_4^+$, indicated the potential coupling between aerobic ammonia oxidation, denitrification and anammox (Lansdown et al. 2016). In a costal upwelling oxycline, the interactions between anammox and denitrification and nitrification were also found to co-contribute the N_2 production (Galán et al. 2017). However, these studies have so far mainly focused on the presence and the contribution of the anammox on the N_2 production, little is known about distributions and the interactions between anammox and nitrification in oxic riverbeds.

AOM and anammox bacteria are thought to be natural partners in ecosystems that the oxygen supply was limited (Schmidt et al. 2002). The coexistence of AOM and anammox have been found in the some marine oxygen minimum zones (OMZs), it is estimated that aerobic ammonia oxidation provided about 33% of the nitrite supply for the anammox (Lam et al. 2007, Lam et al. 2009). Coexistences of aerobic ammonia and nitrite oxidation, as well as anammox and denitrification was found in the Bay of Bengal OMZs, here nitrite oxidation competes with anaerobic organisms for nitrite (Bristow et

al. 2016). Coupling of nitrification with denitrification and anammox was also found in intertidal sediments in Arcachon Bay (Fernandes et al. 2016). This interaction between anammox bacteria and nitrifiers has been widely used in WWTPs called Completely Autotrophic Nitrogen-removal Over Nitrite (CANON), where partial nitrification is coupled to anammox, under reduced oxygen (Third et al. 2001, Third et al. 2001, Hao et al. 2002). Here, the partial oxidation by aerobic ammonia oxidizing microorganisms (AOM) consumes enough oxygen to keep the core of the aggregates anoxic, provide ideal environment for anammox (Nielsen et al. 2005).

Aerobic ammonia oxidation and denitrification could both potentially provide nitrite source for anammox, yet very few measurements of interactions between these organisms have been taken in riverbeds. The study of (Zhou et al. 2014) showed that denitrification can provide nitrite for anammox in muddy freshwater sediments. Other studies also proposed that both nitrification and denitrification can provide nitrite as an intermediate for anammox in the oxic-anoxic interfaces (Kuenen 2008, Zhu et al. 2013). (Lee et al. 2014) reported the distributions of AOB and anammox bacteria in freshwater marsh sediments. Anammox bacteria were also observed in the water-saturated zone in an unconfined aquifer soils, where AOB was thought to be the major source of nitrite for anammox bacteria (Wang et al. 2017). So far, however, coupled nitrification–denitrification/anammox has rarely been measured directly in permeable, oxic riverbeds.

As anammox utilize common substrates for aerobic ammonia oxidation (NH_4^+) and nitrite oxidation (NO_2^-), interactions between AOM, anammox, and NOB might be very tight in oxic riverbeds. However, in the oxic permeable riverbeds, when AOM, anammox, and NOB coexist, the fate of the ammonia remains unclear, the factors and key players that influence the overall degree of nitrification efficiency remains unsolved. Furthermore, how comammox sits in the oxic riverbeds in relation to other processes i.e.

anammox remains largely unknown, yet no measurements of interactions between comammox and anammox have been taken in oxic riverbeds.

The UK Rivers Habitat Survey (Naura et al. 2016) shows that 48% of the rivers are dominated by gravels and pebbles and 26% of sites are dominated by sands and fine sediments. Twelve rivers with permeable, oxic riverbeds from southern England were visited for this thesis. pH, oxygen and nutrient concentrations are presented in Chapter 2.

1.7. Nitrification efficiency and its regulatory environmental factors

The degree of the net nitrification efficiency, i.e., the proportion of ammonia that totally oxidized to nitrate, regulates the primary production and the degree of eutrophication in rivers (Seitzinger 1988, Vitousek et al. 1997, Boyer et al. 2006). The degree of the nitrification efficiency can be influenced by the processes of aerobic ammonia oxidation, anammox, denitrification and nitrite oxidation. The substrates concentrations (ammonium, nitrite and nitrate) are the fundamental factors that influence the nitrification efficiency. pH and oxygen concentration may also be important factors that influence the distribution of microorganisms.

Nitrogen and phosphorus are two nutrients that limit primary productivity in ecosystem. The effects of phosphorus on the nitrogen cycle process have also been widely investigated in the soils. It is proposed that phosphorus deficiency was the main reason that restrict the nitrification rates in phosphorus-poor savanna soils (Rosswall 1981). The study of (Hue and Adams 1984) showed that the effect of phosphorus on AOB was greater than NOB. Similar to this study, the positive effect of phosphorus on aerobic ammonia oxidation process has been found in various environment. For example, the study of (Minami and Fukushi 1983) showed that phosphate can slightly enhance the growth of AOB. Phosphorus was found to be an important factor affecting soil ammonia-oxidizing

activity and AOB community structure in a purple soil (Zhou et al. 2014), the aquaculture ponds (Zhou et al. 2017) and nitrifying groundwater filters (De Vet et al. 2012). However, others found a negative effect of phosphorus on aerobic ammonia oxidation in a steppe ecosystem (Zhang et al. 2013) and the intertidal sediments of the Yangtze Estuary (Zheng et al. 2014).

In contrast, others showed that phosphorus has a more important influence on the process of nitrite oxidation rather than aerobic ammonia oxidation. The study (Purchase 1974) found that the accumulation of nitrite was quite high when the P concentration is low in a grassland, implied that P deficiency affects nitrite oxidizers to a greater extent than ammonia oxidizers. In a wastewater treatment system, (Nowak et al. 1996) found a reduction of the nitrite oxidation at phosphorus concentration below 6.5 μM PO_4^--P, it is proposed that the phosphate half-saturation coefficient for *Nitrobacter* is about one order of magnitude higher than that for *Nitrosomonas*.

The effect phosphorus on denitrification have also been investigated in various environment. It is proposed that denitrifiers are more sensitive to P limitations than nitrifiers in wetland soils (White and Reddy 2003). Other studies indeed found potential denitrification rates were positively related to soluble reactive phosphorus in headwater streams (Inwood et al. 2005), and pristine and impacted prairie streams (Graham et al. 2010). However, others found the opposite results that low concentrations of total phosphorus enhance denitrification rates at the yearly scale across aquatic ecosystems (Pina-Ochoa and Alvarez-Cobelas 2006). Denitrification was also found negatively correlated with P in C-poor shallow lakes (Veraart 2012). It is proposed that P addition slowed down nitrate uptake by denitrifiers because of the imbalance of N and P supply to denitrifiers (Kim et al. 2015).

Phosphate was shown to be a strong inhibitor of the anammox activity in various systems, however, the degree of the effect varied. It is proposed that phosphate lower than 1 mM has no significant effect on anammox activity, while phosphate up to 5 mM can completely inhibited the anammox activity in a fluidized bed reactor (Van de Graaf et al. 1996). In an anammox pilot plant, phosphorus higher than 2 mM inhibited anammox activity (Jetten et al. 1998). In a lab-scale rotating biological contactor, phosphorus inhibited 37% and 80% of the anammox activity at a concentration of 1.8 mM and 3.6 mM, respectively (Pynaert et al. 2003). A higher inhibition concentration (25mM) was found in anammox biomass enriched with *Candidatus* Kuenenia stuttgartiensis (Dapena-Mora et al. 2007).

As phosphorus concentration can influence the processes of nitrification, denitrification and anammox, it could potentially influence the degree of nitrification efficiency. However, effects of phosphorus on the interaction between nitrification, denitrification and anammox remains unclear in oxic riverbeds. Here, if the availability of phosphorus regulates the degree of nitrification efficiency in these rivers was also investigated.

1.8. Structure of the thesis

This thesis consists of three main data chapters, outlined below:

Chapter 2: Simultaneous aerobic ammonia oxidation and anaerobic ammonia oxidation (anammox) in oxic riverbeds

Coupled nitrification/denitrification is a well-recognized pathway of N loss in ecosystems. However, research so far on anaerobic ammonia oxidation (anammox) has mainly focused on both the presence and contribution of anammox to N_2 production, yet

how the interaction between aerobic ammonia oxidation and anammox in permeable, oxic riverbeds is largely unknown. Here, using ^{15}N tracers, potential interactions between nitrification and anammox and/or denitrification in permeable, oxic riverbeds were investigated. Firstly, by adding $^{15}NH_4^+$ in oxic, sediment slurries, the production of $^{15}N_2$ was quantified, and the contribution of anammox to the $^{15}N_2$ was calculated. Then, to further understand how anammox works in these oxic riverbeds, the electron acceptor for anammox (NO_2^-), as well as two intermediates for the anammox reaction (NH_2OH and NO) were used to check if the anammox reaction can happen in oxic slurries without the presence of aerobic ammonia oxidation. A micro-respiration system was then used to quantify the consumption of oxygen during aerobic ammonia oxidation. Furthermore, a standard, anoxic ^{15}N isotope pairing technique was also used in homogenized, anoxic sediment slurries to confirm the anammox potential in these riverbeds. Anammox activities were also investigated at different depths of two selected riverbeds.

Chapter 3: Nitrification efficiency and the effect of soluble reactive phosphorus (SRP)

In short term, re-mineralized nitrogen as ammonia can either be conserved in an ecosystem through its complete oxidation to nitrate e.g. 'efficient nitrification' or lost via oxidation to N_2 gas e.g., 'inefficient nitrification'. The degree of net nitrification efficiency, i.e., the proportion of ammonia that is totally oxidized to nitrate, can regulate primary production and the degree of eutrophication in rivers (Seitzinger 1988, Vitousek et al. 1997, Boyer et al. 2006). In this chapter, the degree of 'nitrification efficiency' was calculated based on the oxic $^{15}NH_4^+$ oxidation experiment in chapter 2. Furthermore, the abundance of genes that could affect the degree of nitrification efficiency were quantified by qPCR amplification of total bacterial 16S rRNA genes, anammox-specific 16S rRNA,

hzo (hydrazine oxidoreductase) and *hzs*B (hydrazine synthase beta subunit) genes, AOB-specific 16S rRNA and *amo*A (ammonia monooxygenase subunit A) genes, AOA *amo*A genes, *Nitrobacter*-specific *nxr*B (nitrite oxidoreductase subunit B) genes, *Nitrospira*-specific 16S rRNA and *nxr*B genes and the comammox *Nitrospira amo*A gene. The relationships between the degree of nitrification efficiency and environmental factors as well as functional genes were also investigated. As an important environmental factor that can potentially influence the degree of nitrification efficiency, the effects of soluble reactive phosphorus (SRP) on the degree of nitrification efficiency was further investigated.

Chapter 4: Community structures of AOM, anammox bacteria and NOB across the oxic riverbeds

In chapter 3 the abundance of the main microorganisms that related to the degree of nitrification efficiency were analysed. To further identify the microorganisms that might help explain the variation in nitrification efficiency across the 12 riverbeds, the community structures of the microorganisms should be investigated. Here, Illumina MiSeq sequencings for total bacterial 16S rRNA genes, anammox 16S rRNA gene, *hzo* gene, *hzs*B gene, AOA *amo*A gene, AOB *amo*A gene, *Nitrospira nxr*B gene and comammox *Nitrospira amo*A gene were conducted to characterize the community structures of the AOA, AOB, anammox bacteria, NOB and comammox *Nitrospira* in order to identify the organisms that related to the degree of nitrification efficiency in these oxic riverbeds.

Chapter 2 : Simultaneous aerobic ammonia oxidation and anaerobic ammonia oxidation (anammox) in oxic riverbeds

In this chapter, ^{15}N tracers were used to characterize the interaction between aerobic ammonia oxidation and anaerobic ammonia oxidation (anammox) across twelve oxic riverbeds, the potential mechanism of how anammox works in oxic, permeable riverbeds was also investigated. Here $^{15}N\text{-}N_2$ was produced in $^{15}NH_4^+$ amended oxic slurries and the production ceased completely with the inhibitor of aerobic ammonia oxidation - allylthiourea (ATU). The accumulation of $^{15}N\text{-}N_2$ indicated a close affiliation between aerobic ammonia oxidation and anammox and/or denitrification. The anammox reaction could not be stimulated by adding NO_2^- or intermediates in the anammox reaction (NH_2OH and NO) with $^{15}NH_4^+$ in oxic slurries without the presence of aerobic ammonia oxidation, further confirming a direct coupling between aerobic ammonia oxidation and anammox. In these oxic riverbeds, AOM consumed oxygen at a rate of 22.28 nmol g^{-1} h^{-1} on average, competing for 8% of the total oxygen consumption through heterotrophic respiration, furthermore, there is more ammonia released through organic respiration than can be oxidised through aerobic ammonia oxidation, making oxygen limited in the aggregates and thus enabling anammox. The aerobic ammonia oxidation can provide nitrite to sustain the anammox bacteria. Anammox made a higher contribution to N_2 production (*ra*) in gravel-dominated riverbeds compared with the sand-dominated riverbeds. Anammox activity in the surface riverbed layer (0-2 cm) was higher than at depth and a significant correlation between anammox activity and porewater oxygen concentration was observed in the riverbeds (r_s = 0.90, p < 0.01), suggesting that porewater oxygen concentration may be a significant factor controlling anammox activity in these riverbeds, this could be related to aerobic ammonia oxidation as aerobic ammonia

oxidation was limited by oxygen . Under anoxic conditions, denitrification can provide an alternative source of substrates for anammox.

2.1. Introduction

Rivers are important sinks for bioavailable nitrogen (Mulholland et al. 2008). In short term, organic nitrogen is mineralized to ammonia, and then aerobically oxidized and conserved as nitrate through nitrification or 'lost' and returned to the atmosphere as N_2 gas through denitrification and anaerobic ammonia oxidation (anammox) (Trimmer and Nicholls 2009).The degree of net nitrification efficiency, i.e., the proportion of ammonia that is totally oxidized to nitrate, can regulate primary production and the degree of eutrophication in rivers (Seitzinger 1988, Vitousek et al. 1997, Boyer et al. 2006).

The coupling of nitrification to denitrification has been studied widely with ^{15}N tracers in permeable, oxic coastal sediments (Rao et al. 2008, Gao et al. 2009, Marchant et al. 2014, Marchant et al. 2016) and has also been confirmed in suspended sediments in rivers (Xia et al. 2017). Ammonium, nitrate, organic matter and oxygen are thought to control the degree of coupling between nitrification and denitrification (Gao et al. 2009) where anammox is absent. As anammox also contributes to N_2 production in various ecosystems such as marine environments (Rich et al. 2008, Stevens and Ulloa 2008), estuaries (Trimmer et al. 2003, Nicholls and Trimmer 2009), subtropical mangrove-aquaculture ecosystems (Amano et al. 2011), paddy field soils (Zhu et al. 2011), lakes, wetlands and rivers (Penton et al. 2006, Schubert et al. 2006, Zhang et al. 2007, Hu et al. 2012, Zhao et al. 2013) and can co-occur with nitrification and denitrification, it can further affect the degree of nitrification efficiency, yet the role of anammox as well as the interactions between nitrification, denitrification and anammox in permeable, oxic riverbeds remains largely unknown.

It is commonly accepted that anammox bacteria are sensitive to oxygen, as little as 1.1 μM oxygen was sufficient to completely inhibit anammox activity in bioreactors (Strous et al. 1999). Marine anammox bacteria were thought to have a higher tolerance

towards oxygen (Dalsgaard et al. 2005) and the upper limit of oxygen concentration for anammox bacteria in oxygen minimum zones (OMZs) was estimated to be 20 μmol L^{-1} (Kalvelage et al. 2011). Anammox activities were confirmed in some permeable marine sands (Neubacher et al. 2011, Evrard et al. 2013), while in others, there was no anammox activity (Gao et al. 2009, Gihring et al. 2010). In a permeable sandstone riverbed (River Leith), anammox activity was negligible (Lansdown et al. 2012, Lansdown et al. 2014). While recently, (Lansdown et al. 2016) demonstrated that both anammox and denitrification contributed to N_2 production in oxic, permeable riverbeds being coupled tightly to the oxidation of NH_4^+. Also, in a coastal oxycline anammox, denitrification and nitrification interacted to remove fixed N as N_2 gas (Galán et al. 2017). However, research so far has focused on both the presence and contribution of anammox to N_2 production, yet how anammox process linked to aerobic ammonia oxidation process in permeable, oxic riverbeds is unknown.

It was proposed that AOM and anammox might be natural partners in ecosystems with limited oxygen supply (Schmidt et al. 2002). The coexistence of AOM and anammox have been found in some OMZs and it is estimated that aerobic ammonia oxidation provided about 33% of the nitrite supply for the anammox (Lam et al. 2007, Lam et al. 2009). Coexistence of ammonia oxidation and anammox have also been found in the OMZs of the Bay of Bengal (Bristow et al. 2016), the intertidal sediments in the Arcachon Bay (Fernandes et al. 2016), freshwater marsh (Lee et al. 2014), wetland sediments (Wang et al. 2013), mangrove sediment (Wang and Gu 2014) and wetland ecosystems (Zhu et al. 2010).

In addition, both aerobic ammonia oxidation and nitrate reduction could provide a source of nitrite for anammox, yet few measurements have been carried out in rivers. (Zhou et al. 2014) showed that nitrate reduction by denitrification can provide nitrite for

anammox in muddy freshwater sediments and others have proposed that both aerobic ammonia oxidation and nitrate reduction can provide nitrite for anammox at oxic-anoxic interfaces (Kuenen 2008, Zhu et al. 2013). Wastewater treatment has taken advantage of the coupling between aerobic ammonia oxidation and anammox under a higher ambient oxygen concentration (Third et al. 2001, Hao et al. 2002). Here, the partial oxidation by AOM consumes enough oxygen to keep the core of the aggregates anoxic, provide ideal environment for anammox (Nielsen et al. 2005). However, the ecological relevance of the co-occurrence of aerobic ammonia oxidation and anammox in oxic sediments remains unclear.

To get a further understanding of the link between aerobic ammonia oxidation and anammox in oxic, permeable riverbeds, ^{15}N tracers were used to detect the interactions between aerobic ammonia oxidation and anammox in twelve oxic, permeable riverbeds, the potential mechanism of how anammox works in these riverbeds was also investigated.

2.2. Materials and Methods

2.2.1. Study sites and sampling

Samples were collected from twelve rivers from southern England between October 2015 and May 2016 (Table 2.1 and Figure 2.1). Among them, the Rivers Lambourn, Darent, Wylye, Rib, Pant, Stour (1) and Stour (2) have chalk-based, permeable gravel-dominated riverbeds, while the Rivers Marden, Hammer, Medway, Broadstone and Nadder have less permeable sand-dominated riverbeds. At each river, surface sediments (<5 cm) were collected from five different locations using Perspex cores (diameter = 9 cm). Sediment samples were then transferred to plastic zip-lock bags (VWR International) and stored in a cool bag (Thermo) for transporting back to the laboratory. Sediments samples from each river were then homogenized in the laboratory

and sub-sampled (n = 3 for each river) and stored at -20 °C for later DNA extraction and molecular analysis.

Porewater samples were also collected for each river using bespoke stainless steel mini-probes (Lansdown et al. 2014) inserted to different depths (2-16 cm) in the riverbeds (n = 5). The porewater was transferred slowly via a three-way stopcock into another open syringe barrel and a fast response microelectrode (50 µm, Unisense) and a pH meter (pH 100, VWR International) inserted to measure dissolved oxygen concentration, pH and temperature (Lansdown et al. 2014). Porewaters for dissolved inorganic nutrients (ammonia, nitrite, nitrate and soluble reactive phosphate (SRP)) analysis were filtered through pre-rinsed, 0.45µm polypropylene filters (VWR International) and preserved in 5ml polypropylene vials (VWR International). Surface water was collected and preserved as for the porewater. Water samples were stored in a cool bag (Thermo) for transfer back to the laboratory.

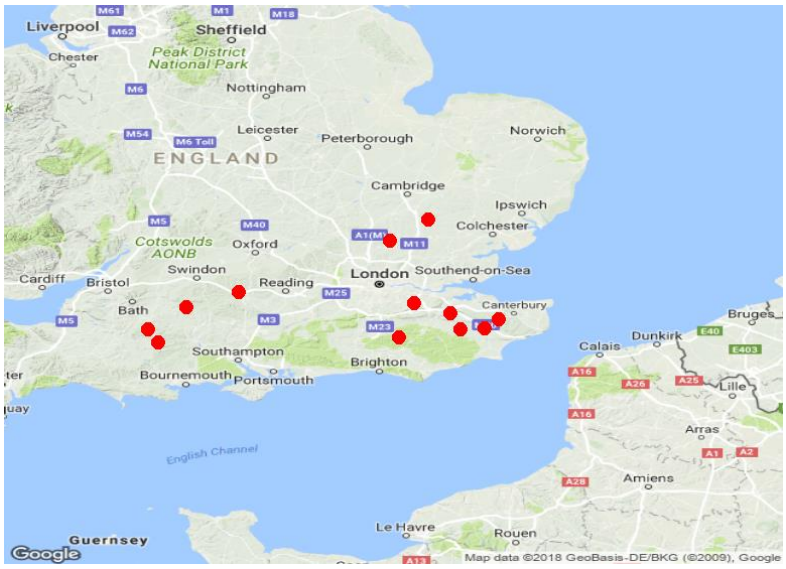

Figure 2.1. Sampling sites (copyright Google Map).

Table 2.1. Location of sampling sites and slurries experiments design.

River	Riverbed type	Latitude	Longitude	Experiments
Lambourn	Gravel-dominated	51.44089	-1.38661	Oxic and anoxic incubations for surface sediments
Darent	Gravel-dominated	51.35043	0.188336	Oxic and anoxic incubations for surface sediments
Wylye	Gravel-dominated	51.14248	-2.20331	Oxic and anoxic incubations for sediments (both surface and different depths)
Rib	Gravel-dominated	51.83917	-0.02936	Oxic and anoxic incubations for surface sediments
Pant	Gravel-dominated	52.0044	0.316916	Oxic and anoxic incubations for surface sediments
Stour (2)	Gravel-dominated	51.22574	0.957806	Oxic and anoxic incubations for surface sediments
Stour (1)	Gravel-dominated	51.15604	0.828219	Oxic and anoxic incubations for surface sediments
Marden	Sand-dominated	51.31829	-1.86	Oxic and anoxic incubations for surface sediments
Hammer	Sand-dominated	51.14607	0.610196	Oxic and anoxic incubations for surface sediments
Medway	Sand-dominated	51.26798	0.518439	Oxic and anoxic incubations for surface sediments
Broadstone	Sand-dominated	51.08326	0.05549	Oxic and anoxic incubations for surface sediments
Nadder	Sand-dominated	51.04385	-2.11182	Oxic and anoxic incubations for sediments (both surface and different depths)

2.2.2. Aerobic ammonia oxidation in oxic slurries

In the standard anoxic application of ^{15}N isotope pairing techniques, ambient porewater nitrite and nitrate are removed by a preincubation of the sediment slurries before adding any ^{15}N-tracers (Thamdrup and Dalsgaard 2002, Trimmer et al. 2003, Risgaard-Petersen et al. 2004). Here, as the primary interest is the oxic interactions between the processes, so the nitrate-free, synthetic river water (0.12g/l $NaHCO_3$, 0.04g/l $KHCO_3$, 0.07g/l $MgSO_4 \cdot 7H_2O$, 0.09g/l $CaCl_2$ $2H_2O$, pH = 7) was used instead to make the sediment slurries (Lansdown et al. 2016).

$^{15}NH_4^+$ tracing methods were used to quantify the aerobic ammonia oxidation in oxic slurries. Oxic slurries were prepared by adding approximately 3 g sediment and 2.7 ml air-saturated synthetic river water into 12 ml gas-tight vials (Exetainer, Labco). The vials were then sealed and injected with 100 µl of either 14 mM $^{15}NH_4^+$ (98 atom% ^{15}N, Sigma-Aldrich) or 14 mM $^{15}NH_4^+$ plus 2.8 mM allylthiourea (ATU) to generate a final porewater concentration of ~500 µM $^{15}NH_4^+$ and ~500 µM $^{15}NH_4^+$ plus ~100 µM ATU and then incubated on a shaker (120 rpm, Stuart SSL1) for up to 12 h. $^{15}NH_4^+$ amended samples were killed at 0h, 0.5 h, 1 h, 3 h, 4.5 h, 6 h, 9 h and 12 h, while $^{15}NH_4^+$ plus ATU treated samples were killed at 0 h, 3 h, 6 h and 12 h with 100 µl of formaldehyde (38%, w/v). Samples were stored upside down prior to ^{15}N-N_2 analysis.

To avoid any potential interference from formaldehyde on the analysis of inorganic nutrients in the slurries, a parallel set of $^{15}NH_4^+$ amended slurries was prepared solely for nutrient analyses. At each time point, samples were injected with 20µL of 1.6M NaOH to preserve the nitrite before being frozen at -20°C (Wolff et al. 1998). Samples were defrosted and centrifuged at 1200 rpm for 10 minutes and the collected supernatant frozen at -20°C prior to analysis of $^{15}NO_2^-$, $^{15}NO_3^-$, NO_2^-, NO_3^-, and NH_4^+ (see below). To measure oxygen over time in the oxic sediment slurries, a set of parallel and scaled-up

slurries (120 mL and same ratio of sediment to water) were prepared. Then, at each time point, one bottle was open and dissolved oxygen measured using a microelectrode (50µm, Unisense).

2.2.3. Screening for anammox activity in the absence of aerobic ammonia oxidation in oxic slurries

To further understand how anammox works under oxic conditions in the absence of a coupling to aerobic ammonia oxidation, oxic slurries from four riverbeds (the rivers Lambourn, Wylye, Marden and Hammer) were injected with 100 µl of either 14 mM $^{15}NH_4^+$ (98 atom% ^{15}N, Sigma-Aldrich) plus 840 µM NO_2^- with or without 2.8 mM allylthiourea (ATU) to generate a final porewater concentration of ~500 µM $^{15}NH_4^+$ and ~30 µM NO_2^- with or without ~100 µM ATU and then incubated on a shaker for up to 12h. $^{15}NH_4^+$ plus NO_2^- amended samples were killed at 0h, 0.5 h, 1 h, 3 h, 4.5 h, 6 h, 9 h and 12 h, while ATU treated samples were killed at 0 h, 3 h, 6 h and 12 h with 100 µl of formaldehyde (38%, w/v). Samples were stored upside down prior to ^{15}N-N_2 analysis. A parallel set of $^{15}NH_4^+$ plus NO_2^- amended slurries was prepared solely for nutrient analyses.

$^{15}NO_2^-$ plus $^{14}NH_4^+$ was also used to test if the anammox reaction can be stimulated in oxic slurries in the absence of a coupling to aerobic ammonia oxidation. The oxic slurries from the above four riverbeds were injected with 100 µl of either 14 mM $^{14}NH_4^+$ plus 840 µM $^{15}NO_2^-$ (98 atom% ^{15}N, Sigma-Aldrich) with or without 2.8 mM allylthiourea (ATU) to generate a final porewater concentration of ~500 µM $^{14}NH_4^+$ and ~30 µM $^{15}NO_2^-$ with or without ~100 µM ATU and then incubated on a shaker for up to 12h. Samples were killed at 0h, 0.5 h, 1 h, 3 h, 4.5 h, 6 h, 9 h and 12 h with 100 µl of formaldehyde (38%, w/v). Samples were stored upside down prior to ^{15}N-N_2 analysis. A

parallel set of $^{14}NH_4^+$ plus $^{15}NO_2^-$ with and without ATU amended slurries was prepared solely for nutrient analyses.

Two intermediates for the anammox reaction (NH_2OH and NO) (Van De Graaf et al. 1997, Strous et al. 2006, Kartal et al. 2011) were also used to test if the anammox reaction can be stimulated in oxic slurries in the absence of a coupling to aerobic ammonia oxidation. For NH_2OH stimulation experiment, oxic slurries from the river Lambourn were injected with different concentrations of NH_2OH with either $^{15}NH_4^+$ or $^{15}NH_4^+$ plus allylthiourea (ATU) stocks to generate a final porewater concentration of 1, 10 or 100 µM of NH_2OH with either ~500 µM $^{15}NH_4^+$ or ~500 µM $^{15}NH_4^+$ plus ~100 µM ATU and then incubated on a shaker for 12h. Detailed treatments and abbreviations are listed in Table 2.2. All samples were killed at 0 h and 12 h with 100 µl of formaldehyde (38%, w/v). Samples were stored upside down prior to ^{15}N-N_2 analysis.

Table 2.2. List of treatments for NH_2OH stimulation experiment.

Abbreviation	Treatment
N+A	$^{15}NH_4^+$ + ATU
N	$^{15}NH_4^+$
N+ N1+A	$^{15}NH_4^+$ + NH_2OH (1 µM) + ATU
N+N1	$^{15}NH_4^+$ + NH_2OH (1 µM)
N+ N10+A	$^{15}NH_4^+$ + NH_2OH (10 µM) + ATU
N+N10	$^{15}NH_4^+$ + NH_2OH (10 µM)
N+ N100+A	$^{15}NH_4^+$ + NH_2OH (100 µM) + ATU
N+N100	$^{15}NH_4^+$ + NH_2OH (100 µM)

PAPA NONOate (Cambridge bioscience) was used to generate NO (Kozlowski et al. 2016) to see if it can stimulate the anammox reaction in oxic conditions in the absence of a coupling to aerobic ammonia oxidation. Half of the oxic slurries were injected with 100 µl of either 60 µM, 600 µM or 6 mM PAPA NONOate to give a final nominal porewater NO concentration of either ~1, 10 and 100 µM and the slurries were then incubated at 37°C for 30 minutes to release NO. Then the oxic slurries were injected with either $^{15}NH_4^+$ or $^{15}NH_4^+$ plus allylthiourea (ATU) stocks to generate a final porewater concentration of 1, 10 or 100 µM NO with either ~500 µM $^{15}NH_4^+$ or ~500 µM $^{15}NH_4^+$ plus ~100 µM ATU and then incubated on a shaker for 12h. Detailed treatments are listed in Table 2.3. All samples were killed at 0 h and 12 h with 100 µl of formaldehyde (38%, w/v). Samples were stored upside down prior to ^{15}N-N_2 analysis.

Table 2.3. List of treatments for NO stimulation experiment.

Abbreviation	Treatment
N+A	$^{15}NH_4^+$ + ATU
N	$^{15}NH_4^+$
N+ NO100+A	$^{15}NH_4^+$ + NO (100 µM) + ATU
N+NO100	$^{15}NH_4^+$ + NO (100 µM)
N+ NO1+A	$^{15}NH_4^+$ + NO (1 µM) + ATU
N+NO1	$^{15}NH_4^+$ + NO (1 µM)
N+ NO10+A	$^{15}NH_4^+$ + NO (10 µM) + ATU
N+NO10	$^{15}NH_4^+$ + NO (10 µM)

2.2.4. Consumption of oxygen during aerobic ammonia oxidation

A micro-respiration system (Unisense) was used to quantify how much oxygen was consumed during aerobic ammonia oxidation (Cavan et al. 2017), further tracing the potential mechanism of the affiliation between aerobic ammonia oxidation and anammox. Surface sediments (~0.4 g and ~0.2 g) from the river Lambourn were added to four, 4 ml and four, 2 ml glass micro-respiration chambers, respectively. A glass-coated magnetic stirrer was then put into each chamber and half of the chambers were then filled with ~500 µM $^{15}NH_4^+$ amended synthetic river water, while the rest was filled with ~500 µM $^{15}NH_4^+$ plus ~100 µM ATU amended synthetic river water. The chambers were sealed and then placed in an eight-chamber rack, the rack was then secured in a water bath at 22 °C, with stirring at 120 rpm. The chambers were equilibrated for 30 min in the dark and then the oxygen concentrations were measured by a rapid-response, micro-oxygen electrode (OX 20, Unisense) inserted into the chamber through capillaries in the lids. At each time point, data were logged for 30 s in each chamber. A total of 20 replicated experiments was made to quantify the overall rate of change in oxygen concentration over time both with and without ATU.

2.2.5. Screening for anammox activity in anoxic slurries

A standard ^{15}N isotope pairing technique was also used in homogenized, anoxic sediment slurries to confirm their anammox potentials (Thamdrup and Dalsgaard 2002). Approximately 1 g of sediment was placed into gas-tight vials (Exetainer, Labco), which were then transferred into an anoxic glove box (CV24, Belle Technologies), where 0.9 ml of N_2-degassed synthetic river water were added and the vials sealed and preincubated overnight on a shaker (120 rpm, Stuart SSL1) to remove all residual O_2, NO_3^-, and NO_2^- (Trimmer et al. 2003). After preincubation, the vials were enriched with 100 µl of 3 mM

$^{15}NO_3^-$ (98 atom% ^{15}N, Sigma-Aldrich), 5 mM $^{15}NH_4^+$ (98 atom% ^{15}N, Sigma-Aldrich) and 5 mM $^{15}NH_4^+$ plus 3 mM $^{14}NO_3^-$ separately to give a final concentration of ~300 μM $^{15}NO_3^-$, ~500 μM $^{15}NH_4^+$ and ~500 μM $^{15}NH_4^+$ plus ~300 μM $^{14}NO_3^-$ (n = 5). $^{15}NO_3^-$ treated samples were killed with 100 μl $ZnCl_2$ (50%, w/v) at 0 h, 1 h, 2 h, 3 h and 6 h, whereas, vials with either $^{15}NH_4^+$ treated or $^{15}NH_4^+$ plus $^{14}NO_3^-$ were killed at just 0 h and 6 h. Samples were stored upside down prior to ^{15}N-N_2 analysis.

2.2.6. Depth profiles of aerobic ammonia oxidation and anammox activity

To further understand the depth profiles of aerobic ammonia oxidation and anammox potential. Sediment samples from different depths of the River Wylye (gravel-dominated riverbed) and the River Nadder (sand-dominated riverbed) were collected. At each river, 5 sediment cores were taken by a metal corer (internal dimensions: 18.5 cm). The sediment cores were then extruded and sectioned at 0-2 cm, 2-4 cm, 4-8 cm and 8-16 cm, then transferred to plastic zip-lock bags (VWR International) and stored in a cool bag (Thermo) for transporting back to the laboratory.

$^{15}NH_4^+$ tracing methods were used to quantify the production of ^{15}N-N_2 production with aerobic ammonia oxidation in oxic slurries as above (2.2.2), while a standard ^{15}N isotope pairing technique was also used in anoxic sediment slurries to confirm their anammox potentials at different depths as above (2.2.5).

2.2.7. Analytical methods

The headspaces of both the anoxic and oxic slurry samples were analysed for ^{15}N-N_2 using a continuous-flow isotope ratio mass spectrometer (Sercon 20-22, UK). To determine the concentrations of $^{15}NO_2^-$ in the $^{15}NH_4^+$ treatment slurries, the preserved supernatants were diluted and 3 ml of sample transferred into a new gas-tight vial (3 ml,

Exetainer, Exetainer, Labco), the vial capped and a 0.5 ml helium headspace (BOC) added. Samples were injected with 100 µl of sulfamic acid (4 mM in 4 M HCl) and placed on a shaker (120 rpm, Stuart SSL1) overnight to reduce $^{15}NO_2^-$ to ^{15}N-N_2. The headspace analysesd for ^{15}N-N_2 as above (Chen et al. 1990, Lansdown et al. 2016). For $^{15}NO_x^-$ ($^{15}NO_2^-$ plus $^{15}NO_3^-$) analysis, 0.3 g sponge cadmium (McIlvin and Altabet 2005) and 200 µl of 1 M imidazole, along with 3.5 ml of sample were added to each gas-tight vial (12 ml, Exetainer, Labco) and the vials were put on a shaker (120 rpm, Stuart SSL1) for 2.5 h to reduce $^{15}NO_3^-$ to $^{15}NO_2^-$ and the samples then treated as above to convert $^{15}NO_2^-$ to N_2 (McIlvin and Altabet 2005, Lansdown et al. 2016).

Dissolved inorganic nutrients (ammonium, nitrite, nitrate and soluble reactive phosphorus (SRP)) in both the riverbed porewater samples and oxic slurry incubations were analysesd by a segmented flow auto analysesr (San++, Skalar, Breda, The Netherlands) using standard colorimetric techniques (Murphy and Riley 1962).

Particle size determination was performed with a series of sieves (Endecotts Ltd, England) with different sizes, from 16 mm, 13.2, 8, 4, 1.4, 0.5, 0.25, 0.125, to 0.0625 mm and each size fraction weighted separately (Pretty et al. 2006). Grain size distribution was then calculated and classified on the Wentworth scale (Wentworth 1922): gravel (material coarser than 2 mm), sand (material between 0.0625 and 2mm), mud (silt plus clay material finer than 0.0625 mm) (Folk 1954).

Sediments for organic C and N content were acidified by HCl (2 M) to remove inorganic carbon and after dried in an oven to a constant weight, ~50 mg of sediments were transferred to tin-cups, weighted and combusted at 1,000°C in an elemental analysesr coupled to a mass-spectrometer (Sercon Integra 2, UK).

2.2.8. Calculations of anammox activity in anoxic and oxic slurries

For the anoxic slurry experiments, potential anammox activity was calculated according to (Thamdrup and Dalsgaard 2002).

$$D_{total} = P_{30} \times F_N^{-2} \quad (2.2.1)$$

$$A_{total} = F_N^{-1} \times [P_{29} + 2 \times (1 - F_N^{-1}) \times P_{30} \quad (2.2.2)$$

$$Contribution\ of\ anammox\ to\ N_2\ gas\ production\ (ra) = \frac{A_{total}}{A_{total} + D_{total}} \quad (2.2.3)$$

where D_{total} represents the production of N_2 through denitrification; A_{total} represents the production of N_2 through anammox, P_{29} and P_{30} represent the measured production rate of $^{29}N_2$ and $^{30}N_2$; F_N is the fraction of ^{15}N in NO_3^- (Thamdrup and Dalsgaard 2002), here the ^{15}N atom% of the $^{15}NO_3^-$ (98%) was used.

In the oxic $^{15}NH_4^+$ oxidation experiments, as anammox could also produce $^{30}N_2$, a mixing model was used to calculate the contribution of anammox to ^{15}N-N_2 production (Lansdown et al. 2016). This model assumes that the ^{15}N-N_2 produced solely from denitrification is equal to the ^{15}N-labelling of the NO_2^- pool.

$$^{15}N\ labelling\ of\ produced\ N_2\left(F_{p_{N_2}}\right) = \frac{1}{1 + \left(\frac{P_{29}}{2 \times P_{30}}\right)} \quad (2.2.4)$$

$$Denitrification\ (F_{N_2\ denitrification}) = F_{No_2^-} \quad (2.2.5)$$

^{15}N-N_2 produced solely through anammox assumes random pairing of one NH_4^+-N and one NO_2^--N where the production of $^{28}N_2$, $^{29}N_2$ or $^{30}N_2$ from anammox can be predicted as follows:

$$^{28}N_2(Anammox_{28}) = (1 - F_{NH_4^+}) \times (1 - F_{No_2^-}) \quad (2.2.6)$$

$$^{29}N_2(Anammox_{29}) = (F_{NH_4^+} \times (1 - F_{No_2^-})) + (F_{No_2^-} \times (1 - F_{NH_4^+})) \quad (2.2.7)$$

$$^{30}N_2(Anammox_{30}) = F_{NH_4^+} \times F_{No_2^-} \quad (2.2.8)$$

$$Anammox(F_{N_2\ anammox}) = \frac{1}{1 + (\frac{Anammox_{29}}{2 \times Anammomx_{30}})} \quad (2.2.9)$$

$$Contribution\ of\ anammox\ (\%) = 1 - \frac{F_{\mathrm{p}N_2} - F_{N_2 anammox}}{F_{N_{2denitrification}} - F_{N_2 anammox}} \quad (2.2.10)$$

Where $F_{No_2^-}$ is the proportion of ^{15}N in the NO_2^- pool (median from each time interval), $F_{NH_4^+}$ is the proportion of ^{15}N in the NH_4^+ pool (initial proportion). To calculate the contribution of anammox to ^{15}N-N_2 production using the equations above, the $F_{\mathrm{p}N_2}$ must fall between $F_{N_{2denitrification}}$ and $F_{N_2 anammox}$.

2.2.9. Statistical analyses

Statistical analyses were performed in R (version 3.4.1) under RStudio (version 1.0.143). Differences between gravel and sand-dominated riverbeds in production rates of $^{15}N\text{-}N_2$ and $^{15}N\text{-}NO_3^-$ and anammox activity were tested with linear mixed effect models using the lme4 package (Bates et al. 2015), where riverbed type as a fixed effect and river as a random effect. Significance of the fixed effect ($p < 0.05$) was determined by likelihood ratio testing between the full model and a reduced model with just a random effect.

Spearman correlation analyses were used to assess the potential correlations between environmental factors and anammox activity, which were also performed in R under the 'Hmisc' package.

Linear mixed effects models were also used to characterize the overall rates of oxygen consumption in the micro-respiration experiment, fitting 'time' and 'treatment' as fixed effects, with random effects on each chamber (1-8) nested within each replicate experiment (1-20). Significance of the fixed effect ($p < 0.05$) was determined by likelihood ratio testing between the full model and a reduced model.

2.3. Results

2.3.1. Riverbed characteristics

Grainsize of the surface sediments from the riverbeds are listed in Table 2.2. For the rivers Stour (2) and Stour (1), although surface sediments I collected for the slurry experiments were mainly consisted of sand (0.0625 and 2mm), the rivers themselves have chalk-based gravel-dominated riverbeds, so I defined them as gravel-dominated riverbeds. For the river Broadstone, the surface sediment has a greater proportion of gravels, but the riverbed itself has a sand-based riverbed (Winterbourn et al. 1992), so I classified it as

sand-dominated riverbed. Sediment organic C concentration in gravel-dominated riverbeds varied from 66±2 to 293±23 and in sand-dominated riverbeds ranged from 96±10 to 801±59 µmol g^{-1}, respectively. Sediment from the river Darent has the maximum Organic C and N concentration, while the river Hammer has the minimum Organic C and N concentrations (Table 2.4).

Porewater characteristics from the gravel and sand-dominated riverbeds are given in Figure 2.2. Both kinds of the riverbeds covered a wide range of oxygen, nitrate and ammonium concentrations. Porewater pH ranged from 6.14±0.04 to 8.08±0.03 and was significantly higher in gravel-dominated riverbeds on a chalk geology (Likelihood ratio test, p = 0.03) and at pH 6.14, the river Broadstone was clearly acidic (Figure 2.2). Oxygen concentrations varied from 94.95±25.22 µM in the river Hammer to 238.15±26.28 µM in the river Lambourn (Figure 2.2) and was slightly higher in gravels than in the sands (Likelihood ratio test, p=0.07). Nitrate varied from 70.74±6.18 µM to 484.25±20.69 µM in the gravel-dominated riverbeds and was significantly higher than in the sand, where nitrate ranged from 5.73±0.28 µM to 112.25±22.41 µM (Likelihood ratio test, p=0.03) (Figure 2.2). Average nitrite concentrations were 1.06±0.38 - 6.83±0.89 µM across all the riverbeds, with no significant difference between gravel and sand-dominated riverbeds. Ammonium concentration varied a lot across the riverbeds from 0.89±0.10 µM in the river Lambourn to 1217.2±176.97 µM in the river Medway (Figure 2.2). Soluble reactive phosphorus (SRP) ranged from 1.42±0.11 to 14.3±0.57 µM in the gravel riverbeds, and 1.43±0.11 - 6.64±1.24 µM in the sand-dominated riverbeds but with no overall difference between the gravel and sand (Figure 2.2). Compared with the sand-dominated riverbeds, the gravel-dominated riverbeds were more oxidized, with higher concentrations of nitrate and oxygen.

Table 2.4. Summary of the riverbed sediments characteristics.

River	Grainsize (%)[a] gravel	sand	mud	Organic C (μmol g^{-1}) [b]	N (μmol g^{-1}) [b]	C: N (molar ratio) [b]
Lambourn	66.1	32.9	1	222±23	21±0.4	11±1
Darent	53.1	44	2.8	801±59	61±6.3	13±0.4
Wylye	74.5	23.6	1.9	555±26	49±10.7	12±1.9
Rib	67.7	31.6	0.7	282±23	35±3.1	8±0.1
Pant	84.4	15	0.6	155±6	22±0.8	7±0
Stour (2)[c]	16.4	82.5	1.1	96±10	7±0.7	13±0.6
Stour (1)[c]	26	73	1	151±16	13±1.3	11±0.1
Marden	39.2	59.7	1	293±23	32±3	9±0.2
Hammer	0	98.9	1.1	66±2	6±0.4	12±1.1
Medway	0	97.4	2.6	244±79	14±2.4	17±2.6
Broadstone [d]	82.2	15.9	1.9	255±46	17±1.8	15±1.1
Nadder	9.9	87.4	2.7	287±114	15±6.5	22±4.3

[a] Data are mean values(n=3).

[b] Organic C, N and C: N data are mean values±1 standard error (n = 3).

[c] Overall, the rivers Stour (2) and Stour (1) were chalk based gravel-dominated riverbeds but the sediments I collected were sand dominated.

[d] River Broadstone is an acidic river and has a sand-based riverbed.

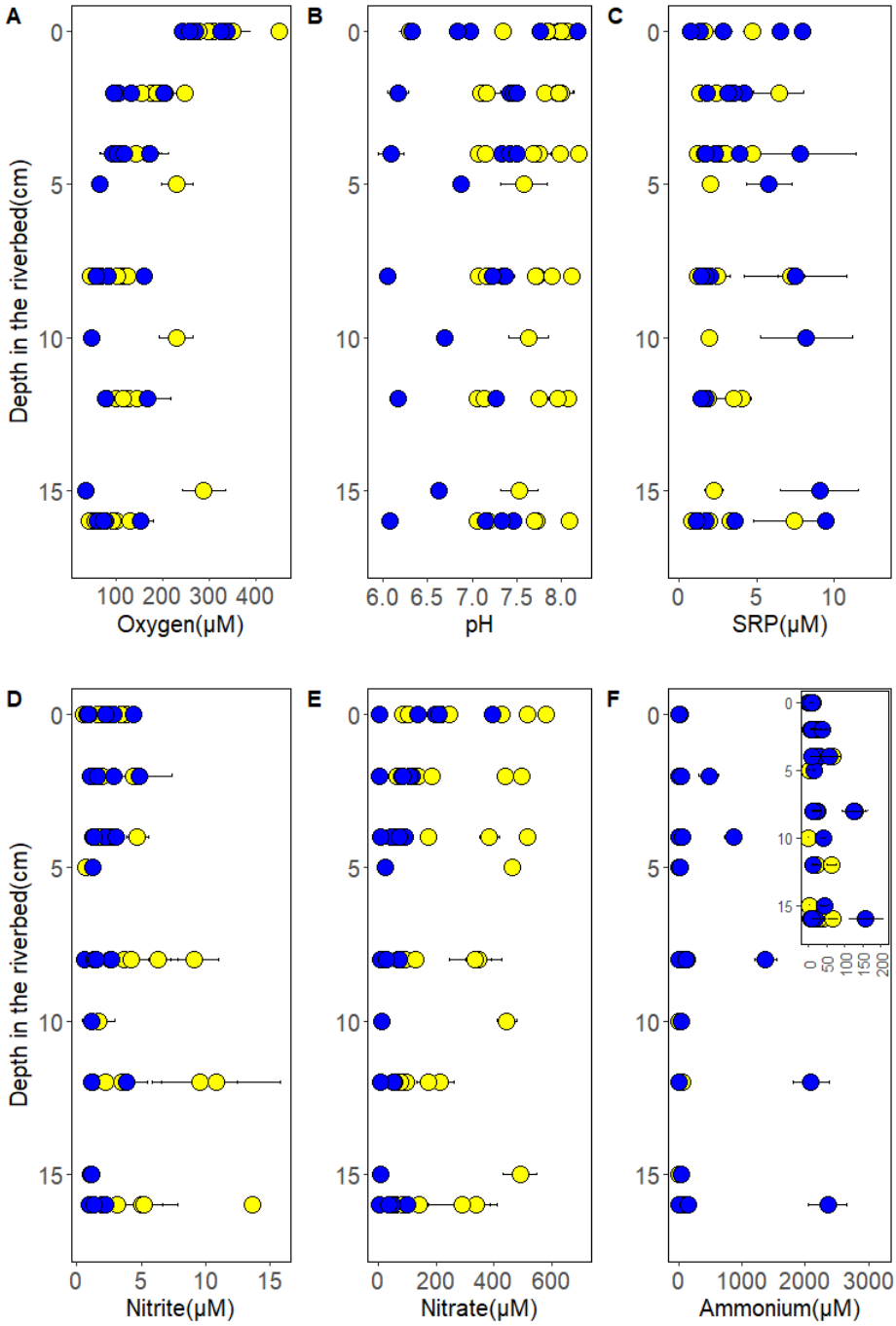

Figure 2.2. Vertical profiles of porewater dissolved oxygen concentration (A), pH (B), soluble reactive phosphorus (SRP) concentration (C), nitrite concentration (D), nitrate concentration (E) and ammonium concentration (F) in different riverbeds.

0 cm represents surface water. Data are mean values ± standard error (n = 5). Yellow and blue represent gravel and sand-dominated riverbeds respectively.

2.3.2. Aerobic ammonia oxidation and N_2 production in oxic riverbeds

$^{15}N\text{-}N_2$ was produced in $^{15}NH_4^+$ amended oxic slurries and production ceased completely with the inhibitor of aerobic ammonia oxidation bacteria - allylthiourea (ATU) (Figure 2.3). The accumulation of $^{15}N\text{-}N_2$ indicated a close affiliation between aerobic ammonia oxidation and anammox and/or denitrification, while the production of $^{15}N\text{-}NO_3^-$ suggested a closer coupling between aerobic ammonia oxidation and nitrite oxidation to nitrate, where the degree of each coupling varied across the riverbeds.

The production rate of $^{15}N\text{-}N_2$ ranged from 0.04 to 9.41 nmol g^{-1} h^{-1} but the median rates across the gravel and sand-dominated riverbeds were comparable, 6.71 and 3.83 nmol g^{-1} h^{-1}, respectively (Figure 2.4) and there was no overall significant difference in $^{15}N\text{-}N_2$ between the gravel and sand-dominated riverbeds (Table 2.5). The production rate of $^{15}N\text{-}NO_3^-$ ranged from 1.36 to 17.39 nmol g^{-1} h^{-1}, however, the median rate across the sand-dominated riverbeds was 11.15 nmol g^{-1} h^{-1}, which is significantly higher than in the gravel-dominated riverbeds on the chalk (2.08 nmol g^{-1} h^{-1}). (Figure 2.4 and Table 2.5).

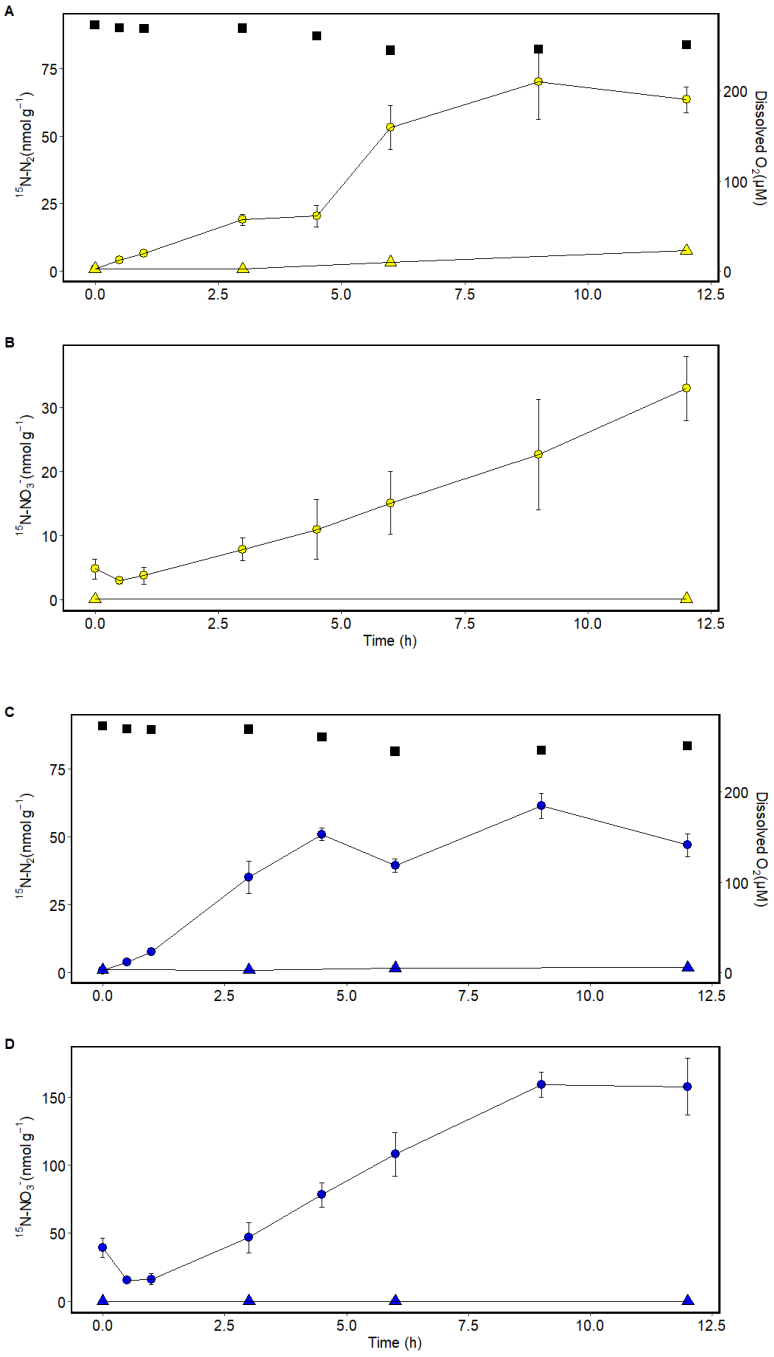

Figure 2.3. Production of ^{15}N-N_2 and ^{15}N-NO_3^- following the addition of $^{15}NH_4^+$ with and without ATU (allylthiourea) in oxic slurries from a gravel-dominated riverbed Darent (A and B) and a sand-dominated riverbed Marden (C and D).

Yellow and blue represent gravel and sand-dominated riverbeds respectively. Black squares are dissolved O_2. Circles represent $^{15}NH_4^+$ amended samples, triangles represent $^{15}NH_4^+$ plus ATU amended samples. Data are mean values ± standard error (n = 5).

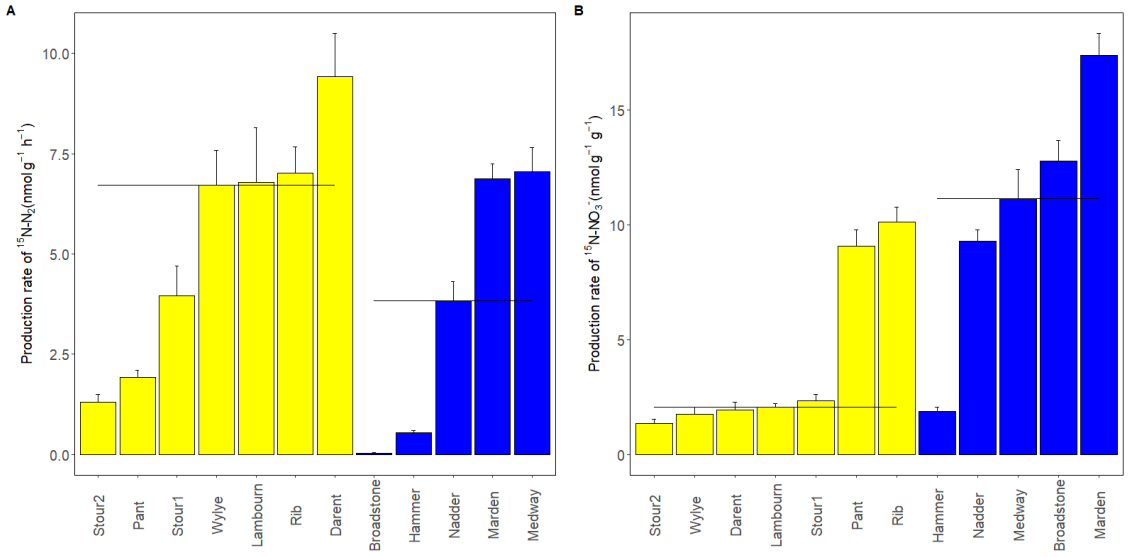

Figure 2.4. Production rates of (A) ^{15}N-N$_2$ and (B) ^{15}N-NO$_3^-$ across twelve riverbeds with the oxidation of ^{15}NH$_4^+$ in oxic slurries.

Yellow and blue represent gravel and sand-dominated riverbeds respectively. Black lines indicate the overall median values for the gravel and sand-dominated riverbeds. Data are mean values ± standard error (n = 5).

Table 2.5. Likelihood ratio test of the effect of riverbed type on rates of anammox, contribution of anammox to N$_2$ production (*ra*) from anoxic incubations, and production rates of ^{15}N-N$_2$ and ^{15}N-NO$_3^-$from oxic incubations.

Experiment	Dependent variable	Independent variable	df	$\chi 2$	*p*-value
Oxic experiment	Production rate of ^{15}N-N$_2$	type	1	0.92	0.34
	Production rate of ^{15}N-NO$_3^-$	type	1	5.30	0.02
Anoxic experiment	Denitrification rate	type	1	1.79	0.18
	Anammox rate	type	1	2.88	0.09
	Anammox contribution (*ra*)	type	1	4.15	0.04

2.3.3. Contribution of anammox to N_2 production in oxic slurries

The contribution of anammox in oxic production of $^{15}N\text{-}N_2$ was calculated based on the mixing model (Lansdown et al. 2016). Based on this model, the contribution of anammox to the $^{15}N\text{-}N_2$ can be calculated in 9 of 55 incubations. For these samples, anammox contributed 68.21 ± 8.34% (mean ± standard error) of the $^{15}N\text{-}N_2$ production (Table 2.6). However, for the majority of the samples (46 of 55 incubations), the produced $^{15}N\text{-}N_2$ were higher than predicted production of $^{15}N\text{-}N_2$ from both denitrification and anammox, suggesting the uneven distribution of the ^{15}N-labelling of the substrate pools. It is noted that in some experiments, the $Fn\text{-}N_2$ was even higher than $Fn\text{-}NH_4^+$, this might be caused by the bias from the calculations. The listed $Fn\text{-}N_2$ in the table was generated from the median of $Fn\text{-}N_2$ at each time point, as the production rates of $^{29}N\text{-}N_2$ and $^{30}N\text{-}N_2$ varied a lot at each time point, the $Fn\text{-}N_2$ might be overestimated. When plotting all of these data together using mixed effect model, a similar average $Fn\text{-}NH_4^+$ and $Fn\text{-}N_2$ (0.55 and 0.56) can be found (Table 2.9).

Table 2.6. The ^{15}N-labelling of NH_4^+, NO_2^- and N_2 pools measured during oxic incubations with $^{15}NH_4^+$ and the predicted ^{15}N-N_2 resulting from denitrification or anammox.

River	Measured			Modelled			
	F_N-NH_4^+ [a]	F_N-NO_2^- [b]	F_N-N_2 [b]	Denitrification-N_2	Anammox-N_2	*ra* (%)	ΔN_2 *
*Time series experiments with $^{15}NO_2^-$ that met model criteria***							
Lambourn	0.85	0.19	0.29	0.19	0.31	79.28	
Lambourn	0.85	0.35	0.42	0.35	0.49	47.51	
Lambourn	0.89	0.32	0.47	0.32	0.47	96.87	
Lambourn	0.84	0.38	0.49	0.38	0.53	74.12	
Darent	0.48	0.29	0.33	0.29	0.36	50.65	
Darent	0.43	0.14	0.21	0.14	0.22	90.58	
Darent	0.54	0.15	0.20	0.15	0.23	60.10	
Darent	0.51	0.19	0.27	0.19	0.27	92.62	
Darent	0.55	0.36	0.37	0.36	0.43	22.12	
Time series experiments with $^{15}NO_2^-$ that did not meet model criteria							
Lambourn	0.80	0.11	0.46	0.11	0.19		0.27
Wylye	0.67	0.01	0.36	0.01	0.01		0.35
Wylye	0.64	0.01	0.25	0.01	0.01		0.24
Wylye	0.73	0.01	0.30	0.01	0.03		0.27
Wylye	0.69	0.01	0.39	0.01	0.01		0.38
Wylye	0.65	0.01	0.24	0.01	0.01		0.24
Rib	0.60	0.05	0.67	0.05	0.10		0.57
Rib	0.64	0.05	0.70	0.05	0.09		0.61

River	F_N-NH_4^{+} [a]	F_N-NO_2^{-} [b]	F_N-N_2 [b]	Denitrification-N_2	Anammox-N_2	*ra* (%)	ΔN_2 *
Rib	0.65	0.05	0.65	0.05	0.09		0.56
Rib	0.62	0.06	0.69	0.06	0.11		0.59
Rib	0.66	0.05	0.66	0.05	0.10		0.56
Pant	0.84	0.2	0.68	0.2	0.32		0.36
Pant	0.84	0.17	0.60	0.17	0.28		0.32
Pant	0.76	0.15	0.54	0.15	0.25		0.28
Pant	0.77	0.13	0.65	0.13	0.22		0.43
Pant	0.76	0.13	0.53	0.13	0.22		0.30
Stour2	0.56	0.07	0.65	0.07	0.12		0.53
Stour2	0.57	0.05	0.72	0.05	0.09		0.62
Stour2	0.63	0.05	0.71	0.05	0.09		0.62
Stour2	0.57	0.04	0.69	0.04	0.08		0.6
Stour2	0.60	0.03	0.72	0.03	0.06		0.66
Stour1	0.52	0.05	0.71	0.05	0.08		0.62
Stour1	0.56	0.04	0.75	0.04	0.08		0.67
Stour1	0.51	0.04	0.65	0.04	0.07		0.58
Stour1	0.65	0.04	0.71	0.04	0.07		0.64
Stour1	0.55	0.04	0.72	0.04	0.08		0.64
Marden	0.64	0.13	0.63	0.13	0.22		0.42
Marden	0.55	0.15	0.67	0.15	0.23		0.44
Marden	0.59	0.09	0.67	0.09	0.16		0.50
Marden	0.57	0.14	0.65	0.14	0.22		0.43
Marden	0.63	0.10	0.69	0.10	0.17		0.52

River	F_N-NH_4^+ [a]	F_N-NO_2^- [b]	F_N-N_2 [b]	Denitrification-N_2	Anammox-N_2	*ra* (%)	ΔN_2 *
Hammer	0.71	0.04	0.67	0.04	0.07		0.59
Hammer	0.69	0.02	0.66	0.02	0.04		0.63
Hammer	0.74	0.03	0.39	0.03	0.07		0.32
Hammer	0.62	0.03	0.56	0.03	0.06		0.5
Hammer	0.61	0.03	0.67	0.03	0.06		0.61
Medway	0.50	0.11	0.55	0.11	0.19		0.36
Medway	0.49	0.22	0.54	0.22	0.31		0.24
Medway	0.46	0.15	0.54	0.15	0.23		0.32
Medway	0.38	0.18	0.51	0.18	0.24		0.27
Medway	0.44	0.25	0.56	0.25	0.32		0.24
Nadder	0.92	0.25	0.70	0.25	0.40		0.30
Nadder	0.90	0.16	0.72	0.16	0.28		0.44
Nadder	0.90	0.17	0.69	0.17	0.28		0.41
Nadder	0.89	0.16	0.72	0.16	0.27		0.45
Nadder	0.91	0.22	0.71	0.22	0.36		0.35

[a] Data represent the proportion of ^{15}N at the beginning of the experiment.

[b] Data represent the median proportion of ^{15}N from different time intervals.

* ΔN_2 is the difference between the measured ^{15}N-N_2 and the predicted ^{15}N-N_2 from the maximum model prediction.

** For a successful model, the produced ^{15}N-N_2 must fall between the predicted anammox and denitrification. Each time series experiment consisted of 5 replicates.

2.3.4. How does anammox work in oxic conditions?

To further understand how anammox works in oxic slurries, $^{15}NH_4^+$ plus $^{14}NO_2^-$ with and without allythiourea (ATU) (Treatment 3 and 4) were added into oxic slurries to test anammox activity in the absence of a coupling to aerobic ammonia oxidation. There was no significant production of both ^{29}N-N_2 and ^{30}N-N_2 in the $^{15}NH_4^+$ plus $^{14}NO_2^-$ with allythiourea (ATU) (Treatment 3) amended slurries (Figure 2.5), indicating that although both $^{15}NH_4^+$ and $^{14}NO_2^-$ were present in the porewater, the anammox process cannot happen directly without aerobic ammonia oxidation. This might be explained by the fact that when aerobic ammonia oxidation was blocked by ATU, the slurries were too oxic for anammox to proceed even when its substrates are present. Another explanation might be that the added $^{14}NO_2^-$ was oxidized to $^{14}NO_3^-$ by nitrite oxidizing bacteria (NOB) before it could be accessed by anammox. However, this is not very likely because the initial concentration of $^{14}NO_2^-$ in this experiment was about 30 nmol g^{-1} and the nitrite oxidation rate was 7.1±0.6 nmol g^{-1} h^{-1} in these riverbed slurries, which means that 21.3±1.8 nmol g^{-1} of nitrite would be turned over in the first 3 h of incubation, so nitrite would not be limited for anammox.

^{15}N-N_2 was produced in $^{15}NH_4^+$ plus $^{14}NO_2^-$ (Treatment 4) amended oxic slurries and there were no significant differences in the productions of ^{29}N-N_2 and ^{30}N-N_2 between $^{15}NH_4^+$ treatment (Treatment 2) and $^{15}NH_4^+$ plus $^{14}NO_2^-$ treatment (Treatment 4) (Figure 2.5 and Table 2.7). In comparison with $^{15}NH_4^+$ (Treatment 2) amended slurries, Fn-NO_2^- in $^{15}NH_4^+$ plus $^{14}NO_2^-$ (Treatment 4) amended slurries decreased from 0.29 to 0.179 by the dilution of the added $^{14}NO_2^-$ (Table 2.9). However, Fn-N_2 remained constant in these two treatments (Table 2.9). This indicates that when adding $^{15}NH_4^+$ into the oxic slurries, Fn-N_2 is not influenced by the external porewater Fn-NO_2^-. The coupling between aerobic ammonia oxidation and N_2 production might be an 'internal' process that happened in the

aggregates, did not influenced by the 'external' NO_2^- or NO_x^- pool. Together, this suggests that the added $^{14}NO_2^-$ to the porewater cannot be used by anammox bacteria directly in oxic conditions, further hinting at a direct affiliation between aerobic ammonia oxidation and anammox.

$^{14}NH_4^+$ plus $^{15}NO_2^-$ with and without allythiourea (ATU) (Treatment 5 and 6) were also added into oxic slurries to test anammox activity in the absence of a coupling to aerobic ammonia oxidation. Production of both $^{29}N\text{-}N_2$ and $^{30}N\text{-}N_2$ was observed in the $^{14}NH_4^+$ plus $^{15}NO_2^-$ with ATU (Treatment 5) amended slurries (Figure 2.5), indicating that $^{15}NO_2^-$ was oxidized to $^{15}N\text{-}N_2$ when aerobic ammonia oxidation was blocked. The production of $^{15}N\text{-}N_2$ in this treatment was contributed solely by denitrification, as $Fn\text{-}N_2$ equals to $Fn\text{-}NO_2^-$ (Table 2.9). This result is consistent with the findings in the $^{15}NH_4^+$ plus ATU (Treatment 1) and $^{15}NH_4^+$ plus $^{14}NO_2^-$ plus ATU (Treatment 3) amended slurries, where no anammox activity was observed. This further confirms that anammox cannot proceed when aerobic ammonia oxidation was blocked by ATU.

In the $^{14}NH_4^+$ plus $^{15}NO_2^-$ (Treatment 6) amended slurries, there was no significant production of $^{30}N\text{-}N_2$, indicating that the denitrification activity is negligible in this treatment. This might be caused by the competition between anammox and denitrifiers for $^{15}NO_2^-$. The production of $^{29}N\text{-}N_2$ in the $^{14}NH_4^+$ plus $^{15}NO_2^-$ (Treatment 6) amended slurries suggests the occurrence of anammox with the presence of aerobic ammonium oxidation. In the presence of aerobic ammonium oxidation, anammox can take some external $^{15}NO_2^-$ and outcompete denitrification.

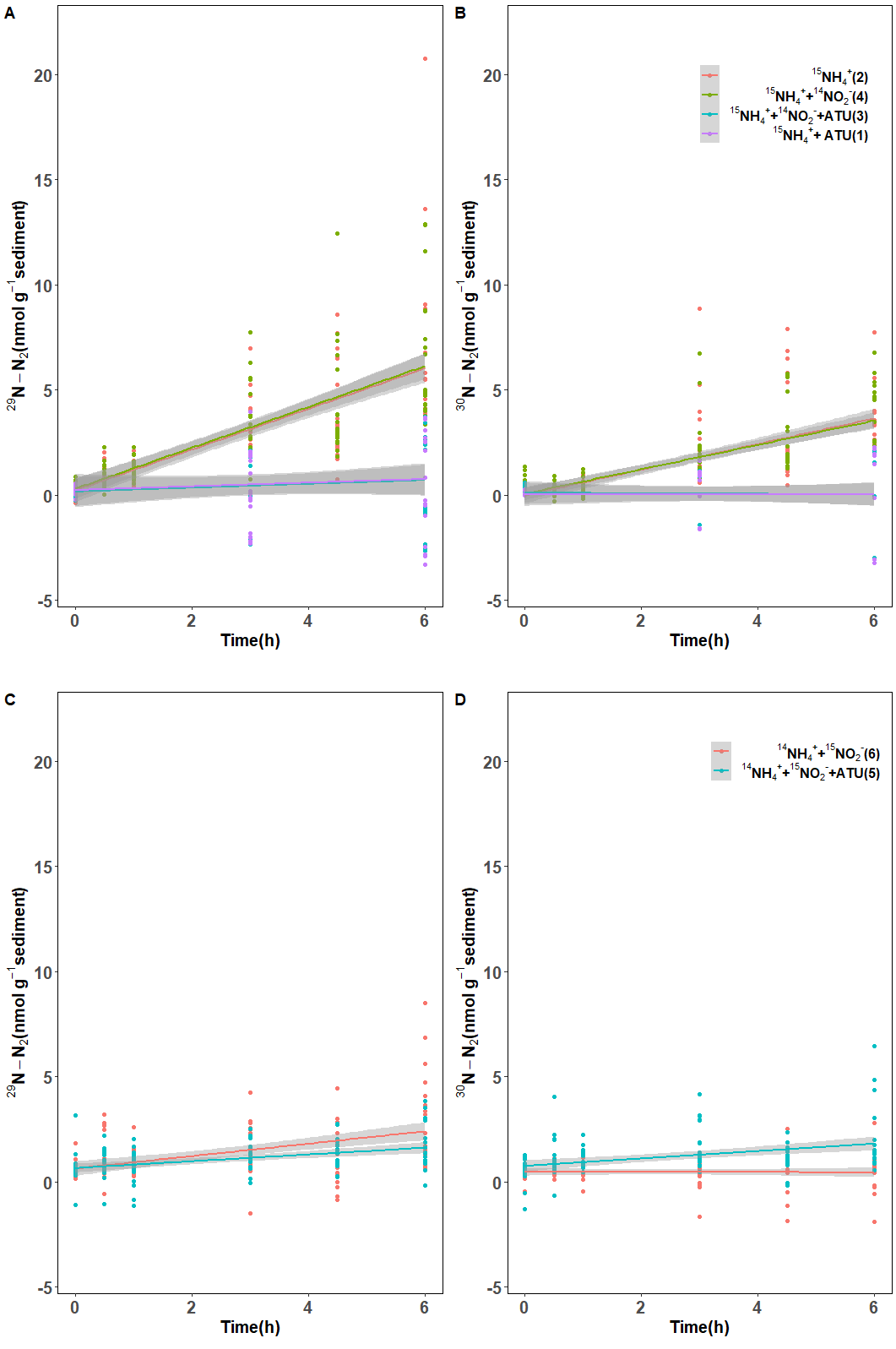

Figure 2.5. Fixed production of ^{29}N-N_2 and ^{30}N-N_2 over time for different $^{15}NH_4^+$ treatments (A and B) and $^{15}NO_2^-$ treatments (C and D) based on the mixed effect model (data from 4 rivers).

Table 2.7. Output of a linear mixed effects model testing the difference in ^{29}N-N_2 or ^{30}N-N_2 production rates between $^{15}NH_4^+$ (2), $^{15}NH_4^+$ plus ATU (1), $^{15}NH_4^+$ plus $^{14}NO_2^-$ (4) and $^{15}NH_4^+$ plus $^{14}NO_2^-$ plus ATU (3) amended sediments.

	Fixed effect	Value	s.e.	*t*-value	*P*
Production of ^{29}N-N_2	Intercept, nmol g^{-1}, $^{15}NH_4^+$ (2)	0.2396	0.3005	0.979	0.4366
	Slope, nmol g^{-1} h^{-1}, $^{15}NH_4^+$ (2)	0.9679	0.2859	3.386	0.0364*
	ΔIntercept, $^{15}NH_4^+$ plus $^{14}NO_2^-$ (4)	0.0773	0.3718	0.208	0.8355
	ΔIntercept, $^{15}NH_4^+$ plus $^{14}NO_2^-$ plus ATU (3)	-0.0698	0.4689	-0.149	0.8818
	ΔIntercept, $^{15}NH_4^+$ plus ATU (1)	0.0032	0.4689	0.007	0.9946
	ΔSlope, $^{15}NH_4^+$ plus $^{14}NO_2^-$ (4)	0.0034	0.1117	0.030	0.7958
	ΔSlope, $^{15}NH_4^+$ plus $^{14}NO_2^-$ plus ATU (3)	-0.8769	0.1276	-6.872	<0.001*
	ΔSlope, $^{15}NH_4^+$ plus ATU (1)	-0.8804	0.1276	-6.900	<0.001*
Production of ^{30}N-N_2	Intercept, nmol g^{-1}, $^{15}NH_4^+$ (2)	0.0002	0.1771	0.013	0.9900
	Slope, nmol g^{-1} h^{-1}, $^{15}NH_4^+$ (2)	0.6102	0.2011	3.035	0.0572*
	ΔIntercept, $^{15}NH_4^+$ plus $^{14}NO_2^-$ (4)	0.0783	0.2505	0.313	0.7548
	ΔIntercept, $^{15}NH_4^+$ plus $^{14}NO_2^-$ plus ATU (3)	0.1124	0.3159	0.356	0.7222

	Fixed effect	Value	s.e.	*t*-value	*P*
Production of ^{30}N-N_2	ΔIntercept, $^{15}NH_4^+$ plus ATU (1)	0.0402	0.3159	0.127	0.8988
	ΔSlope, $^{15}NH_4^+$ plus $^{14}NO_2^-$ (4)	-0.0304	0.0752	-0.404	0.6868
	ΔSlope, $^{15}NH_4^+$ plus $^{14}NO_2^-$ plus ATU (3)	-0.6235	0.0860	-7.252	<0.001*
	ΔSlope, $^{15}NH_4^+$ plus ATU (1)	-0.6076	0.0860	-7.068	<0.001*

Table 2.8. Output of a linear mixed effects model testing the difference in ^{29}N-N_2 or ^{30}N-N_2 production rates between $^{14}NH_4^+$ plus $^{15}NO_2^-$ (6) and $^{14}NH_4^+$ plus $^{15}NO_2^-$ plus ATU (5) amended sediments.

	Fixed effect	Value	s.e.	*t*-value	*P*
Production of ^{29}N-N_2	Intercept, nmol g^{-1}, $^{14}NH_4^+$ plus $^{15}NO_2^-$ (6)	0.6366	0.4011	1.587	0.1985
	Slope, nmol g^{-1} h^{-1}, $^{14}NH_4^+$ plus $^{15}NO_2^-$ (6)	0.2953	0.0851	3.472	0.0245*
	ΔIntercept, $^{14}NH_4^+$ plus $^{15}NO_2^-$ plus ATU (5)	0.0227	0.2092	0.109	0.9135
	ΔSlope, $^{14}NH_4^+$ plus $^{15}NO_2^-$ plus ATU (5)	-0.1349	0.0628	-2.146	0.0329*
Production of ^{30}N-N_2	Intercept, nmol g^{-1}, $^{14}NH_4^+$ plus $^{15}NO_2^-$ (6)	0.4802	0.4486	1.070	0.3581
	Slope, nmol g^{-1} h^{-1}, $^{14}NH_4^+$ plus $^{15}NO_2^-$ (6)	-0.0042	0.0546	-0.078	0.9411
	ΔIntercept, $^{14}NH_4^+$ plus $^{15}NO_2^-$ plus ATU (5)	0.2857	0.1649	1.732	0.0845
	ΔSlope, $^{14}NH_4^+$ plus $^{15}NO_2^-$ plus ATU (5)	0.1807	0.0495	3.647	0.0003*

Table 2.9. Summary of the $^{29}N\text{-}N_2$ and $^{30}N\text{-}N_2$ production rates (based on mixed effect model) and $Fn\text{-}N_2$, $Fn\text{-}NO_2^-$ and $Fn\text{-}NH_4^+$ in different treatments.

Treatment	$^{29}N\text{-}N_2$ production (nmol g^{-1} h^{-1})	$^{30}N\text{-}N_2$ production (nmol g^{-1} h^{-1})	$Fn\text{-}N_2$ [a]	$Fn\text{-}NO_2^-$ [b] (mean 3 or 6 h)	$Fn\text{-}NH_4^+$ [b] (mean 3 or 6h)
$^{15}NH_4^+$ plus ATU (1)	0.0875	0.0026			
$^{15}NH_4^+$ (2)	0.9679	0.6102	0.5450	0.2919/0.3233	0.6053/0.6321
$^{15}NH_4^+$ plus $^{14}NO_2^-$ plus ATU (3)	0.091	-0.0133			
$^{15}NH_4^+$ plus $^{14}NO_2^-$ (4)	0.9713	0.5798	0.5441	0.1796/0.2151	0.5787/0.6099
$^{14}NH_4^+$ plus $^{15}NO_2^-$ plus ATU (5)	0.1604	0.1765	0.6876	0.6700/0.5407	
$^{14}NH_4^+$ plus $^{15}NO_2^-$ (6)	0.2953	0		0.5855/0.4691	
$^{15}NH_4^+$ plus ATU (12 rivers) (1)[c]	0.0782	0.0065			
$^{15}NH_4^+$ (12 rivers) (2) [c]	0.7598	0.4864	0.5615	0.0918/0.1128	0.5529/0.5262

[a] $Fn\text{-}N_2$ is calculated based on the production rates of $^{29}N\text{-}N_2$ and $^{30}N\text{-}N_2$ generated from mixed effect models.

[b] $Fn\text{-}NO_2^-$ is the mean of $Fn\text{-}NO_2^-$ in 3/6 hours and $Fn\text{-}NH_4^+$ is the mean of $Fn\text{-}NH_4^+$ in 3/6 hours

[c] Results of the 12 rivers data (treatments $^{15}NH_4^+$ and $^{15}NH_4^+$ plus ATU) analysed based on mixed effect model are also listed here.

As the added $^{14}NO_2^-$ cannot be used by anammox directly in oxic conditions, two intermediates for anammox process, NH_2OH and NO (Van De Graaf et al. 1997, Strous et al. 2006, Kartal et al. 2011), were also used test if the anammox reaction can be stimulated by these intermediates in oxic slurries from the river Lambourn. Similar results were obtained as in the $^{14}NO_2^-$ addition experiment. With the addition of NH_2OH, there was no $^{15}N\text{-}N_2$ production in ATU amended samples (Figure 2.6). Also, there was no significant difference in the production of $^{15}N\text{-}N_2$ between $^{15}NH_4^+$ treatment and $^{15}NH_4^+$ plus NH_2OH treatment (Likelihood ratio test, p = 0.76, Figure 2.6), further rejected the assumption that anammox may use NH_2OH in oxic condition, further corroborating a more direct affiliation between aerobic ammonia oxidation and anammox.

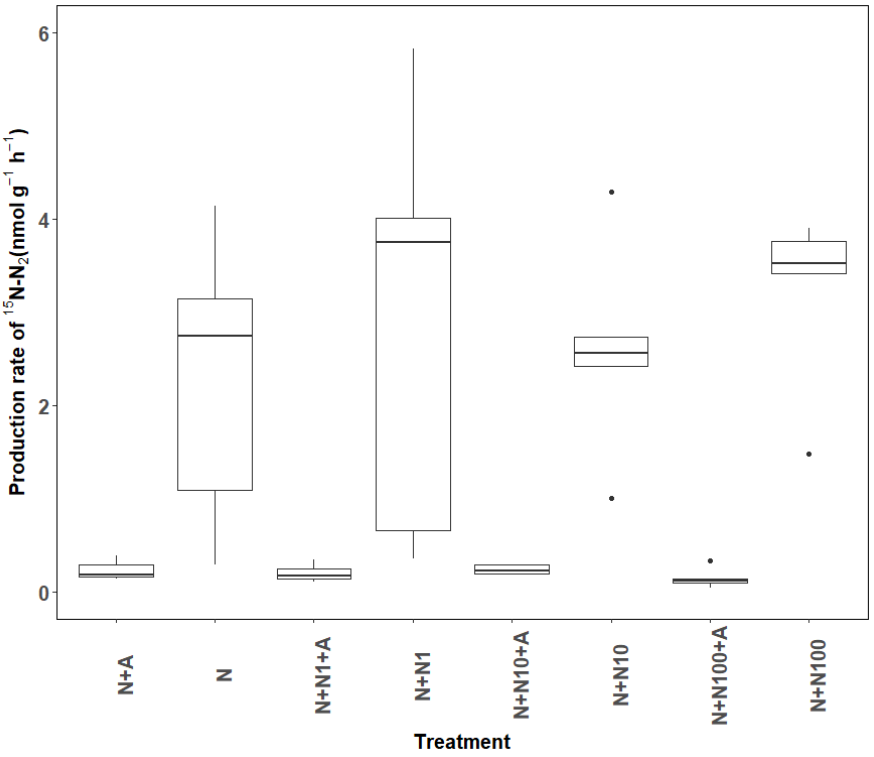

Figure 2.6. Production rates of $^{15}N\text{-}N_2$ following the addition of NH_2OH to $^{15}NH_4^+$ with and without ATU in oxic slurries from a gravel-dominated riverbed Lambourn (n = 5).

Similar results were obtained for the NO addition experiments. With the addition of NO, there was no ^{15}N-N_2 production in ATU amended samples (Figure 2.7), further rejected the assumption that anammox may use NO in oxic condition, further corroborating a more direct affiliation between aerobic ammonia oxidation and anammox. there was no significant difference for the production rate of ^{15}N-N_2 between $^{15}NH_4^+$ treatment and $^{15}NH_4^+$ plus NO treatments (Likelihood ratio test, $p = 0.14$, Figure 2.7).

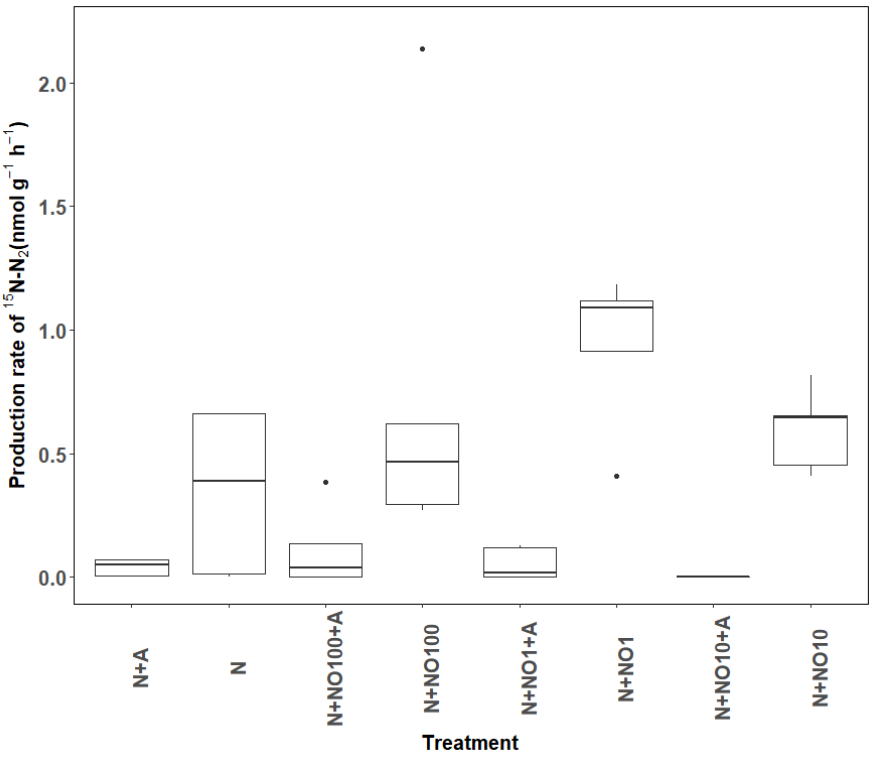

Figure 2.7. Production rates of ^{15}N-N_2 following the addition of NO to $^{15}NH_4^+$ with and without ATU in oxic slurries from a gravel-dominated riverbed Lambourn ($n = 5$).

2.3.5. Competition for oxygen during aerobic ammonia oxidation

Based on the above ^{15}N tracing experiments, a direct affiliation between aerobic ammonia oxidation and anammox was found, it was assumed that in oxic riverbeds, aerobic ammonia-oxidizing microorganisms (AOM) and anammox bacteria aggregate together. AOM consume oxygen and create a redox micro-environment for anammox.

Oxygen micro-electrodes were used to measure oxygen consumption in the presence of either $^{15}NH_4^+$ or $^{15}NH_4^+$ plus ATU amended slurries. The difference oxygen consumption rates between $^{15}NH_4^+$ and $^{15}NH_4^+$ plus ATU amended should be caused by AOM. Twenty replicate measurements of oxygen consumption were conducted in eight chambers, significant rates of oxygen consumption were observed in all the chambers (Figure 2.8).

The overall rate of change in oxygen concentration over time for $^{15}NH_4^+$ and $^{15}NH_4^+$ plus ATU amended samples is shown in Figure 2.9. Here the change in oxygen was modelled as a fixed effect of both time and treatment with random intercepts and slopes fitted as nested random effects on each chamber within each replicate. The average oxygen consumption rate in $^{15}NH_4^+$ amended samples was 277.07 nmol g^{-1} h^{-1}, while the difference in oxygen consumption rates between $^{15}NH_4^+$ and $^{15}NH_4^+$ plus ATU amended sample was 22.28 nmol g^{-1} h^{-1} (Table 2.10). Although the difference between these two treatments was not significant (Table 2.10), this difference suggests that oxygen was being consumed by AOM with a rate of 22.28 nmol g^{-1} h^{-1}. Power analysis indicated that only if 710 replicates were conducted for each treatment, a 90% chance of detecting a difference can be achieved at a significance level of 0.05, which would have been too time consuming to conduct. Further, there was a good agreement between AOM oxygen consumption rate and average ammonia oxidation rate in the river Lambourn, which is 8.85 nmol g^{-1} h^{-1} and 17.7 nmol g^{-1} h^{-1} oxygen would be consumed during aerobic ammonia oxidation. AOM would have to compete for 8% of the total oxygen being consumed with heterotrophic respiration, thus making AOM oxygen limited. In the river Lambourn, the C:N ratio of the organic matter was 11±1, which means that organic respiration could release 25.19 nmol N g^{-1} h^{-1}, as only 8.85 nmol g^{-1} h^{-1} of the released N would be oxidised through aerobic ammonia oxidation, the remaining 16.34 nmol g^{-1} h^{-1} N thus making the system not N limited but oxygen limited.

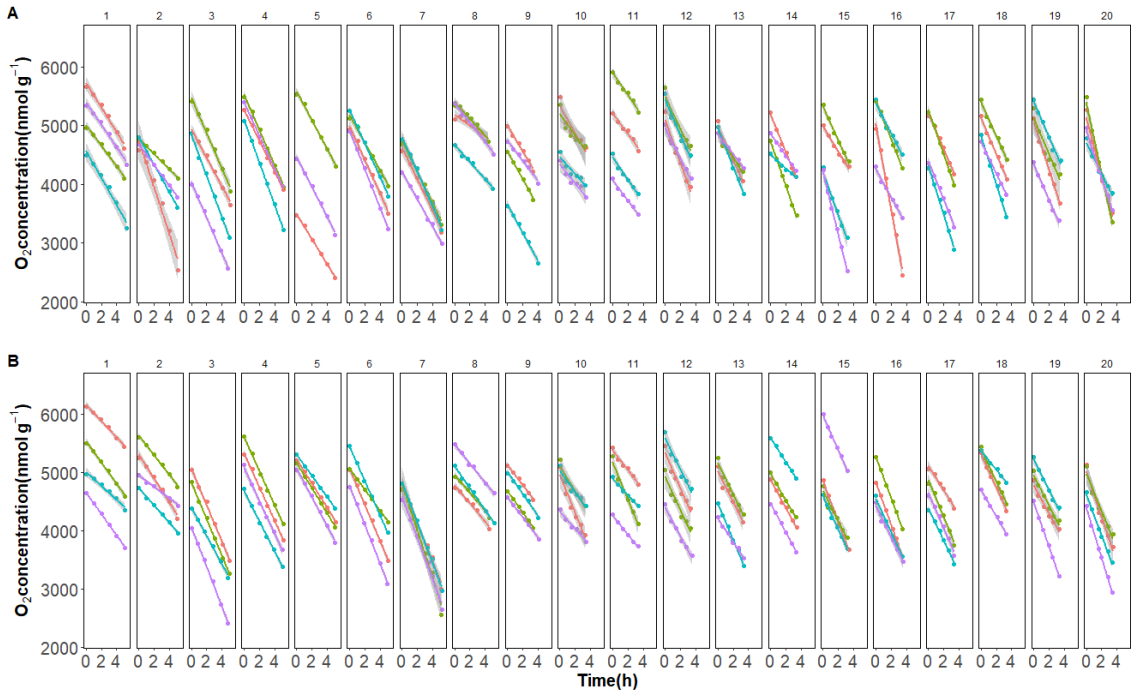

Figure 2.8. Plot of all 20 replicate measurements of oxygen consumption in eight chambers.

(For each replicate experiment (1-20), four rate measurements were made (different coloured symbols) with $^{15}NH_4^+$ amended chambers (A) and $^{15}NH_4^+$ plus ATU amended chambers (B)).

Table 2.10. Output of a linear mixed effects model testing the difference in oxygen consumption rates between $^{15}NH_4^+$and $^{15}NH_4^+$ plus ATU amended sediments.

Fixed effect	Value	s.e.	*t*-value	*P*
Intercept, nmol g^{-1}, $^{15}NH_4^+$	4920.69	48.44	101.59	<0.01
Slope, nmol g^{-1} h^{-1}, $^{15}NH_4^+$	-277.07	10.18	-27.22	<0.01
ΔIntercept,$^{15}NH_4^+$ plus ATU	42.94	68.28	0.63	0.53
ΔSlope, $^{15}NH_4^+$ plus ATU	22.28	14.35	1.55	0.12

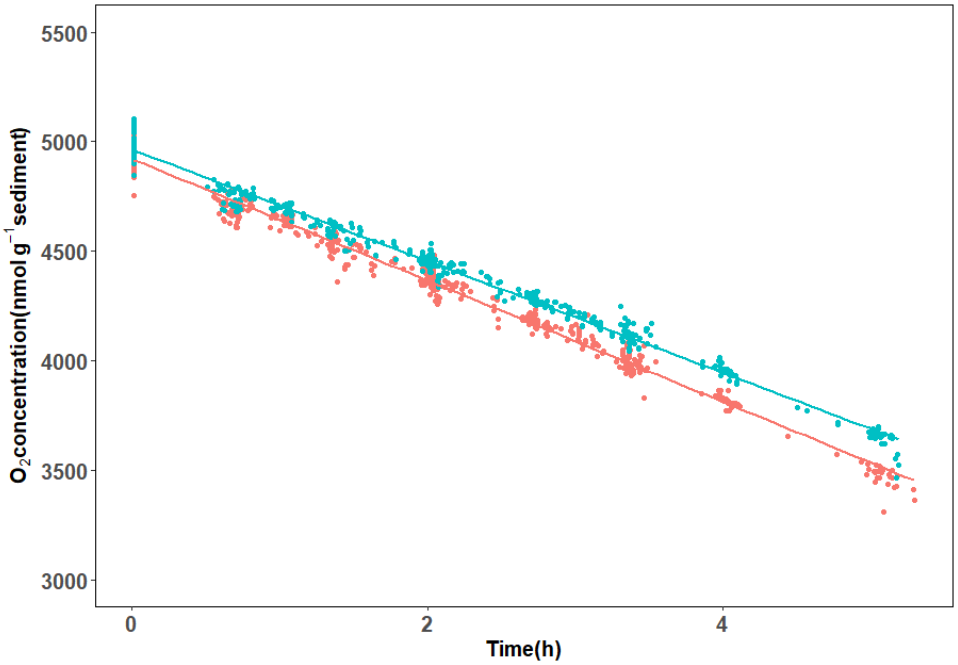

Figure 2.9. Fitted oxygen concentration changes over time for different treatments based on the mixed effect model.

(Red dots represent $^{15}NH_4^+$ amended samples while green dots represent $^{15}NH_4^+$ plus ATU amended samples).

2.3.6. Confirmation of anammox potential in anoxic slurries

Anammox activities were checked in anoxic slurries from these twelve riverbeds. Except for the acidic sandy river, Broadstone, potential anammox activity was confirmed in all other riverbeds by the production of $^{29}N_2$ in $^{15}NH_4^+$ and $^{14}NO_3^-$ amended anoxic slurries (Figure 2.10). There was no significant production of $^{29}N_2$ in $^{15}NH_4^+$ only amended samples (Figure 2.10), which suggested that there was no anaerobic ammonia oxidation coupled to the reduction of metal oxides (Luther et al. 1997). The production of $^{29}N_2$ and $^{30}N_2$ in the $^{15}NO_3^-$ amended slurries (Figure 2.10) confirmed the potential occurrence of both denitrification and anammox under anoxia.

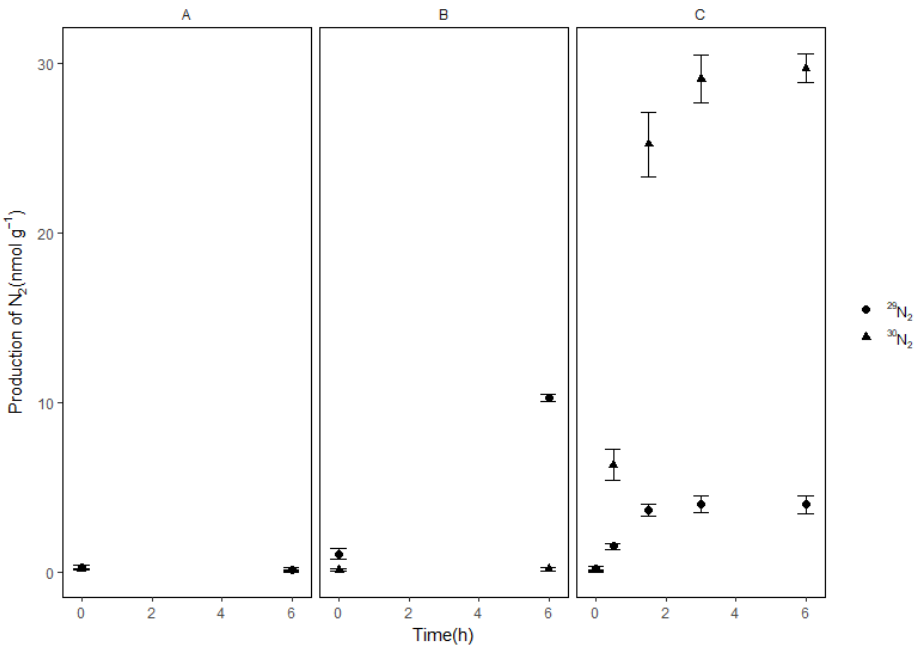

Figure 2.10. Examples of $^{29}N_2$ and $^{30}N_2$ production in anoxic slurries amended with $^{15}NH_4^+$ (A), $^{15}NH_4^+$+ $^{14}NO_3^-$ (B) and $^{15}NO_3^-$ (C).

(Data are mean values ± 1 standard error (*n* = 5)).

Both the rate of anammox and its contribution to N_2 production (*ra*%) were calculated from the production of $^{29}N_2$ and $^{30}N_2$ in $^{15}NO_3^-$ amended slurries. As shown in Figure 2.11, anammox activity varied from 0.2 to 10.5 nmol N g^{-1} h^{-1} across the riverbeds, and anammox contributed to 4.1~16.7% of N_2 production under anoxia. Anammox made a higher contribution to N_2 production in gravel-dominated riverbeds compared with the sand-dominated riverbeds (Figure 2.11 and Table 2.5). Though there was no significant difference between gravel and sand-dominated riverbeds in denitrification activity, the anammox activity in gravel was slightly higher than in the sand-dominated riverbeds (Table 2.5).

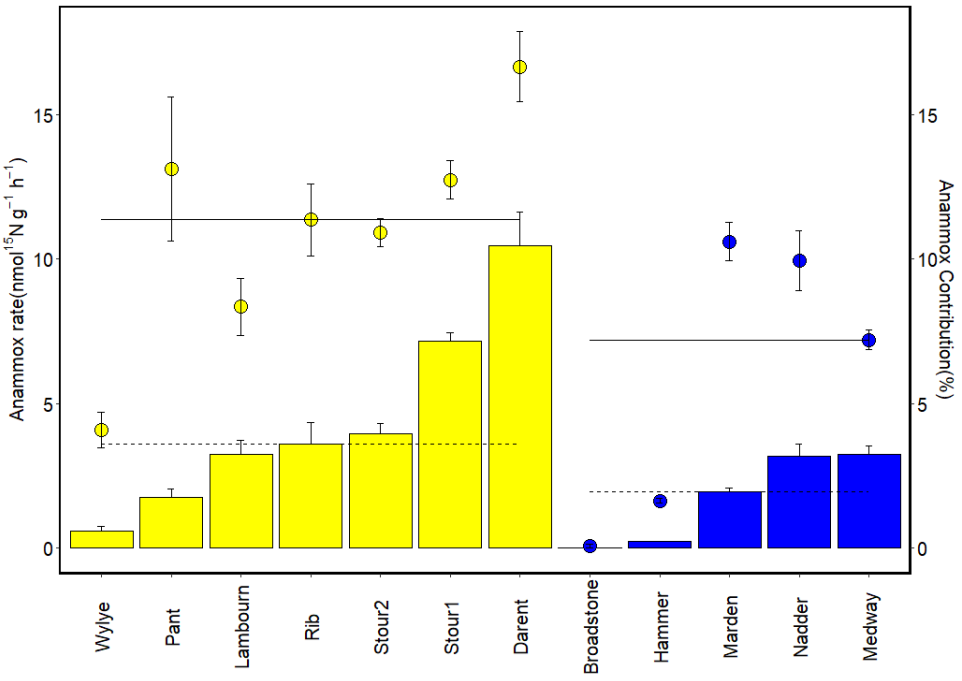

Figure 2.11. Potential anammox activity across riverbeds, both anammox activity and anammox contribution to total N_2 production (*ra*), as measured in anoxic slurries. Yellow and blue represent gravel and sand-dominated riverbeds respectively. Black lines indicate the overall median values for the gravel and sand-dominated riverbeds. Data are mean values ± standard error (n = 5).

Anammox activity positively correlated with denitrification activity (Spearman's rank correlation, r_s (60) =0.88, $p < 0.001$) in anoxic slurries (Figure 2.12). Although the contribution of anammox and denitrification to the N_2 production in oxic slurries cannot be calculated due to the heterogeneity in the ^{15}N-labelling of the substrate pools in the majority of the samples (46 of 55 incubations). The production rate of ^{15}N-N_2 in oxic $^{15}NH_4^+$ oxidation slurries positively correlated with both anammox activity and denitrification activity as measured in anoxic slurries (Spearman's rank correlation, r_s =0.48, $p < 0.001$ and r_s =0.47, $p < 0.001$), as well as the contribution of anammox to the total N_2 production (*ra*) as measured in anoxic slurries (r_s =0.39 , $p < 0.001$, Figure 2.12).

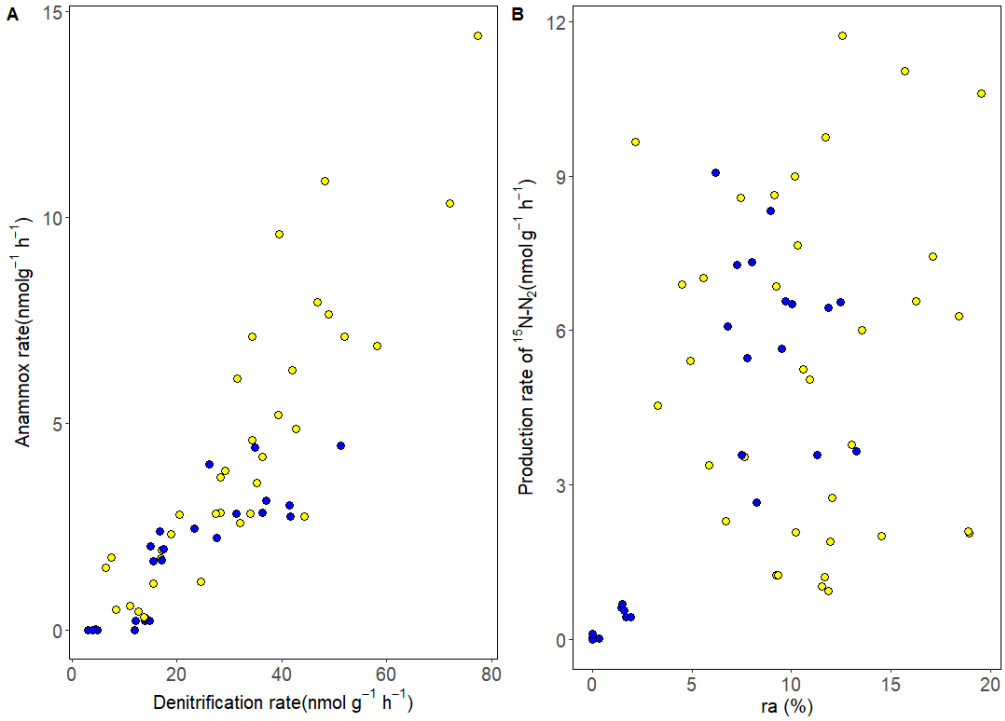

Figure 2.12. Correlations between (A) anammox activity and denitrification activity as measured in anoxic slurries and (B) contribution of anammox to N_2 production (*ra*) as measured in anoxic slurries and production rate of ^{15}N-N_2 measured in oxic slurries. Yellow and blue represent gravel and sand-dominated riverbeds respectively.

2.3.7. Anammox activity at different depth

To understand the pattern of anammox activity along with the riverbed depth, sediments from different depths of the river Wylye (gravel-dominated) and the river Nadder (sand-dominated) were incubated with ^{15}N tracers under both oxic and anoxic conditions to detect the potential anammox activity and its contribution to total N_2 production. In the river Wylye, the production rates of ^{15}N-N_2 in oxic slurries ranged from 0.59 to 1.64 nmol N g^{-1} h^{-1} (Figure 2.13) with slightly higher rates at the surface (0-2cm), compared with deeper layer (8-16cm) (likelihood ratio test, p = 0.08). The production rates of ^{15}N-N_2 ranged from 1.65 to 1.93 nmol N g^{-1} h^{-1} in the river Nadder (Figure 2.13), with no significant difference between depths (likelihood ratio test, p = 0.96).

Anammox activities as measured in anoxic slurries varied from 0.64 to 3.15 nmol N g^{-1} h^{-1} in the river Wylye (Figure 2.13) and decayed with depth (likelihood ratio test, $p < 0.01$), while contribution of anammox to N_2 production (*ra*) varied from 8.67 to 10.81% (Figure 2.13), with no significant difference between depths (likelihood ratio test, $p = 0.81$). Anammox activity in anoxic slurries, varied from 1.37 to 2.23 nmol N g^{-1} h^{-1} in the river Nadder (Figure 2.13) and anammox activity was significantly higher in upper 0-2cm layer, compared to the deeper 8-16cm layer (likelihood ratio test, $p = 0.04$). The contribution of anammox to N_2 production (*ra*) varied from 3.50 to 6.53% (Figure 2.13), with no significant difference between depths (likelihood ratio test, $p = 0.49$). Overall, the anammox activity was significantly higher in the top layer (0-2cm) than at depth of the sediments (likelihood ratio test, $p < 0.01$). A positive correlation between anammox activity and porewater oxygen concentration was observed in the riverbeds ($r_s = 0.90$, $p < 0.01$), suggesting that porewater oxygen concentration maybe an important factor that influence the anammox activity.

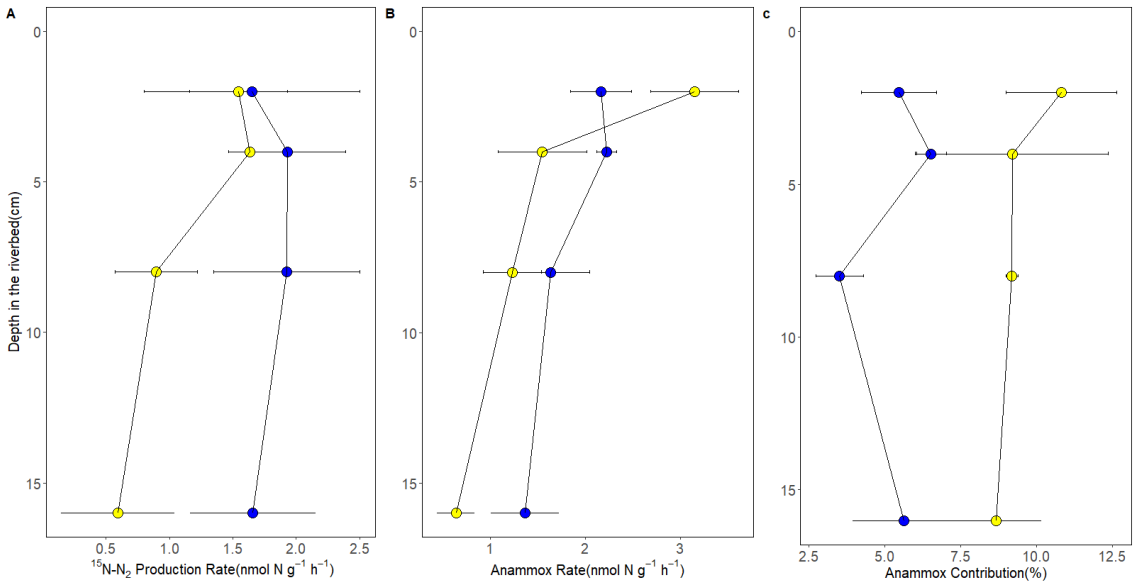

Figure 2.13. Anammox activity and anammox contribution to total N_2 production at different depth.

(Data are mean values ± 1 standard error (n = 5). Yellow and blue represent a gravel and a sand-dominated riverbed (Wylye and Nadder) respectively.)

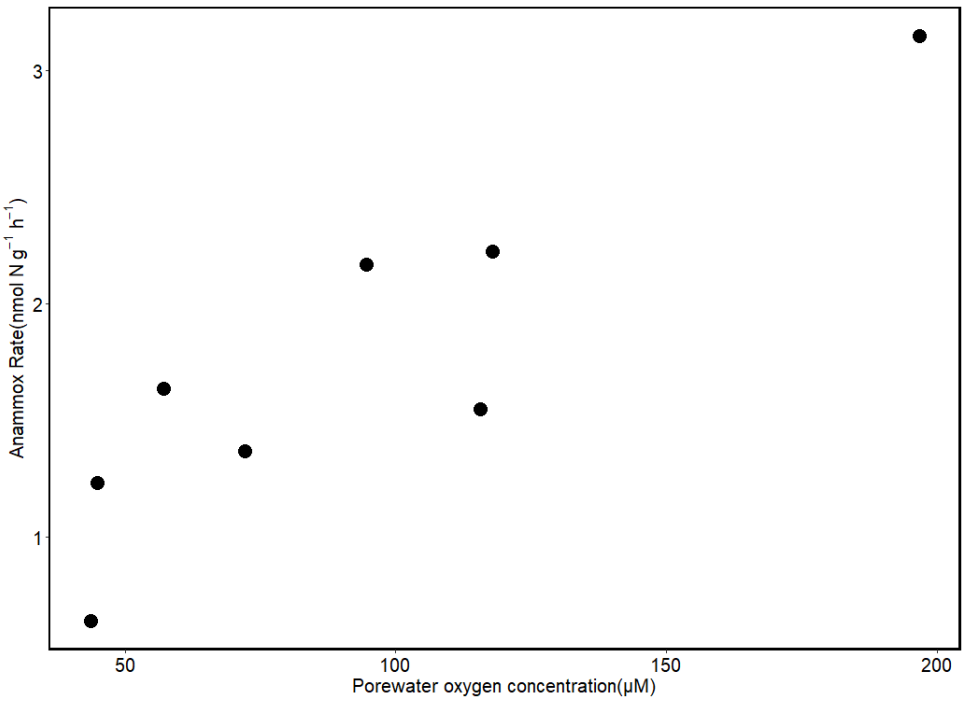

Figure 2.14. Correlations between porewater oxygen concentration and potential anammox activity as measured in anoxic slurries.

2.4. Discussion

The production of ^{15}N-N_2 in $^{15}NH_4^+$ amended oxic slurries confirmed the affiliation of nitrification, anammox and/or denitrification in permeable, oxic riverbeds. The production of ^{15}N-N_2 ceased completely with the addition of ATU, suggesting the dependence of anammox and/or denitrification on aerobic ammonia oxidation. Both anammox and denitrification contributed to the production of ^{15}N-N_2 in these oxic slurries, however, the contribution of anammox to the ^{15}N-N_2 production cannot be calculated for the majority of the samples as the produced ^{15}N-N_2 was higher than the predicted values from the mixing model. This suggests an uneven distribution of the ^{15}N in the substrate pools (De Brabandere et al. 2014, Lansdown et al. 2016). In these samples, both the accumulated concentration of $^{15}NO_2^-$ and the proportion of $^{15}NO_2^-$ to total NO_2^- were quite low (Fn-NO_2^- = 0.09), suggesting rapid consumption of $^{15}NO_2^-$ by anammox/denitrification and/or nitrite oxidizing bacteria and that the $^{15}NO_2^-$ was consumed before mixing uniformly with the surrounding porewater NO_2^- pool. Also, direct oxidation of $^{15}NH_4^+$ to $^{15}NO_3^-$ by comammox *Nitrospira* may contribute to the heterogeneity in the ^{15}N-labelling of the NO_2^- pool (Jensen et al. 2009, De Brabandere et al. 2014).

$^{15}NH_4^+$ plus $^{14}NO_2^-$ plus ATU (Treatment 3) was added into oxic slurries to test the anammox reaction without the presence of aerobic ammonia oxidation (Ginestet et al. 1998, Subbarao et al. 2006). Results showed that anammox process cannot happen in oxic slurries when aerobic ammonia oxidation was inhibited. This was further confirmed by the results from $^{14}NH_4^+$ plus $^{15}NO_2^-$ plus ATU (Treatment 5) amended slurries, where the produced ^{15}N-N_2 was contributed solely by denitrification. With the presence of ATU, the anammox process cannot happen directly even if both substrates for anammox exist in the porewater. This might be explained by the fact that the slurries were too oxic for

anammox to proceed. Another explanation might be that the added NO_2^- was oxidized to NO_3^- by nitrite oxidizing bacteria (NOB) before it could be accessed by anammox. However, this is not very likely because the initial concentration of NO_2^- in this experiment was about 30 nmol g^{-1} and the nitrite oxidation rate was 7.1±0.6 nmol g^{-1} h^{-1} in these riverbed slurries, which means that 21.3±1.8 nmol g^{-1} of nitrite would be turned over in the first 3 h of incubation, so nitrite would not be limited for anammox.

Without the presence of ATU, the production of ^{15}N-N_2 in $^{15}NH_4^+$ plus $^{14}NO_2^-$ (Treatment 4) amended oxic slurries again suggests a coupling between aerobic ammonia oxidation and N_2 production, this indicates that the N_2 production cannot proceed before the first step of aerobic ammonium oxidation. However, even with different NO_2^- pools, there was no significant difference between the productions of ^{15}N-N_2 in $^{15}NH_4^+$ plus $^{14}NO_2^-$ (Treatment 4) and $^{15}NH_4^+$ (Treatment 2), this suggests that the 'external' NO_2^- is not limiting for the production of ^{15}N-N_2.

These results further hinting that the substrate pools 'outside' and 'inside' the aggregates may be different (De Brabandere et al. 2014, Lansdown et al. 2016), this also help explain the heterogeneity of the substrate pools. The production of ^{29}N-N_2 in $^{14}NH_4^+$ plus $^{15}NO_2^-$ (Treatment 6) further confirmed the occurrence of anammox with the presence of aerobic ammonium oxidation. In the presence of aerobic ammonium oxidation, anammox reaction can be stimulated and outcompete denitrification.

The affiliation between aerobic ammonia oxidation and anammox was further confirmed as neither the addition of NH_2OH nor NO (two intermediates in the anammox reaction) (Van De Graaf et al. 1997, Strous et al. 2006, Kartal et al. 2011) plus $^{15}NH_4^+$ with ATU could stimulate the anammox reaction in the oxic slurries.

In the oxic slurries, nitrifier-denitrification may also contribute to the production of N_2, they are only considered to make N_2O, which could in turn be reduced to N_2 even

by another process or by a novel nitrifier-denitrifier metabolism (Wrage et al. 2001, Schmidt et al. 2004, Shaw et al. 2006). In this study, the AOA *amo*A gene was more abundant than its AOB variant in all riverbeds. The proportions of AOA *amo*A and AOB *amo*A to bacterial 16S rRNA gene were 0.28%-1.32% and 0.09%-1.1%, respectively (see Chapter 3). The AOB sequences in this study was closely related to genus *Nitrosospira* (see Chapter 4). Some *Nitrosospira* were demonstrated to carry out nitrifier-denitrification, however, the N_2O production only represented 0.03-0.7% of the total NO_2^- produced through nitrification (Shaw et al. 2006). Furthermore, their abilities of making N_2O was much lower than *Nitrosomonas* (Shaw et al. 2006). So nitrifier-denitrification may exist in these sediments, but it could not be the main process that drives the production of N_2. In this study, the ^{15}N labelling of the N_2 pool (Fn-N_2) was not influenced by the external NO_2^- pool (Treatment 2 and 4). However, in the nitrifier-denitrification process, up to 13.5%. of the ^{15}N labelling of the N_2O pool (Shaw et al. 2006) and the N_2 pool (Schmidt et al. 2004) was influenced by the exogenous NO_2^- pool. This difference further confirms that the production of N_2 in this study could not be solely contributed by nitrifier-denitrification.

The oxygen consumption experiment showed that oxygen was being consumed by AOM and heterotrophic respiration. AOM would have to compete for 8% of the total oxygen consumption with heterotrophic respiration, thus making AOM oxygen limited. It has been reported that AOM are poor competitors for oxygen when compared with heterotrophic bacteria, because AOM have a lower affinity for oxygen (Gieseke et al. 2001). Furthermore, more ammonia released through organic respiration than can be oxidised through aerobic ammonia oxidation, suggesting that the aggregates would not be ammonia limited but oxygen limited. Although the porewater oxygen concentrations

were high in the riverbeds, oxygen will be limited in the aggregates thus supporting anammox.

Although the contribution of anammox and denitrification to the N_2 production in oxic slurries cannot be calculated due to the heterogeneity in the ^{15}N-labelling of the substrate pools. The positive correlation between the production rate of ^{15}N-N_2 measured in oxic slurries and contribution of anammox to N_2 production (*ra*) as measured in anoxic slurries (Figure 2.12), further hinting the consistency of the contribution of anammox to N_2 production in both oxic and anoxic slurries.

In the surface layers, higher concentrations of porewater oxygen were observed and a significant correlation between anammox activity and porewater oxygen concentration was observed in the examined riverbeds ($r_s = 0.90$, $p < 0.01$), suggesting that porewater oxygen concentration maybe a significant factor controlling anammox activity in the examined riverbeds, this could be related to aerobic ammonia oxidation. As AOM compete for 8% of the oxygen with heterotrophic respiration, with higher oxygen concentrations, aerobic ammonia oxidation could thus provide more substrates for anammox. The availability of nitrite was reported to be the limiting factor for anammox process in aquatic systems (Meyer et al. 2005, Trimmer et al. 2005). In these oxic riverbeds, as aerobic ammonia oxidation provides nitrite for anammox and aerobic ammonia oxidation is oxygen limited, making porewater oxygen concentration become the controlling factor for anammox activity.

Stable isotope experiments in anoxic slurries further confirmed the anammox potential in every other river except for the river Broadstone and anammox activity varied from 0.2 to 10.5 nmol N g^{-1} h^{-1} across the riverbeds and anammox contributed to 4.1~16.7% of N_2 production, these values are within the reported rates in other rivers (Schubert et al. 2006, Zhao et al. 2013, Lansdown et al. 2016). The distribution of anammox bacteria and

their contribution to the loss of fixed nitrogen is influenced by local environmental conditions, such as organic content (Thamdrup and Dalsgaard 2002, Trimmer et al. 2003, Trimmer et al. 2013) and NO_x^- concentration (Risgaard-Petersen et al. 2004, Rich et al. 2008, Hou et al. 2013). Anammox made a higher contribution to N_2 production in gravel-dominated riverbeds compared with the sand-dominated riverbeds, which may be caused by the higher porewater oxygen and nitrate concentration in gravel-dominated riverbeds. As anammox was directly coupled with aerobic ammonia oxidation and aerobic ammonia oxidation was limited by the oxygen, higher oxygen concentration in gravel-dominated riverbeds could contribute a higher degree of aerobic ammonia oxidation, thus provide more nitrite for anammox.

Spearman's rank correlation analysis showed a significant correlation between the anammox rates and denitrification rates in anoxic slurries (Figure 2.12), indicating a further potential coupling between anammox and denitrification through nitrite in these riverbeds, denitrification may provide nitrite for the anammox bacteria in anoxic conditions. Previous studies have also indicated the coupling between anammox and denitrification in various sediments (Wang et al. 2012, Hou et al. 2013, Shan et al. 2016), it is proposed that most denitrifying bacteria are heterotrophic and capable of utilizing organic matter to generate nitrite and ammonium for the anammox bacteria (Hou et al. 2013, Shan et al. 2016).

Therefore, the mechanisms affecting anammox in oxic riverbeds may be summarised as follows. In these oxic riverbeds, AOM and anammox may aggregate together, as in suspended sediments particles (Zhang et al. 2017), big granules in wastewater treatment plants (Ma et al. 2015) and marine snow aggregates (Kalvelage et al. 2011), aerobic ammonia oxidation competes for 8% of the total oxygen consumption with heterotrophic respiration, furthermore, there is more ammonia released through

organic respiration than can be oxidised through aerobic ammonia oxidation, making oxygen limited in the aggregates and thus enabling anammox. Furthermore, the aerobic ammonia oxidation can provide nitrite to sustain the anammox bacteria. Under anoxic conditions, denitrification can provide an alternative source of substrates for anammox.

Chapter 3 : Nitrification efficiency and the effect of soluble reactive phosphorus (SRP)

In Chapter 2, the affiliation between aerobic ammonia oxidation and anammox was confirmed and the relationships between the microorganisms involved in these processes are of interest. In this chapter, 'nitrification efficiency' (the proportion of the ammonia that oxidized to nitrate) and its relationship with aerobic ammonia oxidation, anaerobic ammonia oxidation (anammox) and nitrite oxidation across a range of oxic riverbeds was characterized. The degree of nitrification efficiency varied from 22.2% to 99.7%. the degree of nitrification efficiency was highest where the contribution from anammox to N_2 production (*ra*) was lowest, and maximal where anammox was absent, suggesting competition between nitrite oxidation and anammox for nitrite. The degree of nitrification efficiency was also highest where the abundance of *nxr*B gene (*Nitrospira* + *Nitrobacter*) was greatest, along with the highest abundance of comammox *Nitrospira* *amo*A gene. The results reveal a gradient in riverbed nitrification efficiency that was related primarily to *Nitrospira* dominating the nitrite oxidising bacteria (NOB) and being separated from anammox. A positive correlation between the degree of nitrification efficiency and riverbed porewater soluble reactive phosphorus (SRP) concentration was found, suggesting that the availability of the phosphorus may be related to the degree of the nitrification efficiency. Adding SRP directly to the riverbed sediment slurries selectively increased the degree of nitrification efficiency in some riverbeds by stimulating nitrite oxidation. Furthermore, anammox was more important where the abundance of *hzs*B and *amo*A genes were greater, indicating an interaction between aerobic and anaerobic ammonia oxidation--supported by oxygen.

3.1. Introduction

In short term, re-mineralized nitrogen as ammonia can either be conserved in an ecosystem through its complete oxidation to nitrate e.g. 'efficient nitrification' or lost via oxidation to N_2 gas e.g., 'inefficient nitrification'. The degree of net nitrification efficiency can regulate primary production and the degree of eutrophication in rivers. Apart from aerobic ammonia oxidation, anammox and denitrification, aerobic nitrite oxidation, the process that is responsible for the oxidation of nitrite to nitrate, also plays an important role in controlling the degree of nitrification efficiency.

As anammox utilizes the substrates for both aerobic ammonia oxidation (NH_4^+) and nitrite oxidation (NO_2^-), competition between AOM, anammox, and NOB might be strong where these processes interact. Wastewater treatment has taken advantage of the prevalence of coupled nitrification and anammox (Sliekers et al. 2002), where competition between anammox and NOB for nitrite is thought to control the ammonia removal efficiency. However, the ecological relevance of the coexistence of AOM, anammox, and NOB in oxic sediments remains unclear.

Aerobic ammonia oxidation can be driven by the *amo*A gene in both ammonia oxidizing bacteria and archaea (AOB and AOA). The *amo*A gene encodes the active site of the α-subunit of the enzyme ammonia monooxygenase (AmoA) and it is a phylogenetic marker for the AOB (Purkhold et al. 2003). Aerobic ammonia archaea (AOA) have also been confirmed to contain the archaeal *amo*A gene and dominate aerobic ammonia oxidation in some freshwater and marine habitats (Francis et al. 2005). The oxidation of nitrite to nitrate is carried out by chemolithoautotrophic nitrite-oxidizing bacteria (NOB), *Nitrospira* is the most diverse and widespread group of NOB and *Nitrobacter* also plays an important role in some WWTP and aquaria system (Vanparys et al. 2007, Fukushima et al. 2013). The *nxr*B gene, which encodes the β-subunit of nitrite oxidoreductase (NXR),

was introduced as the functional and phylogenetic marker for *Nitrospira* and *Nitrobacter* (Pester et al. 2014). The anammox specific 16S rRNA gene and hydrazine oxidoreductase (*hzo*) gene have been widely used to identify and quantify anammox in coastal, estuarial and riverine sediments (Li et al. 2011, Trimmer et al. 2013, Lansdown et al. 2016). The hydrazine synthase gene *hzs*, that can encode the hydrazine synthase protein, was identified as the unique biomarker for anammox bacteria (Harhangi et al. 2012).

For over a century it was understood that further oxidation of this nitrite to nitrate was always catalysed by a separate group of microorganisms (the NOB) until the recent discovery of bacteria that possess both ammonia and nitrite oxidizing genes and are therefore capable of the complete oxidation of ammonia to nitrate (comammox) (Daims et al. 2015, Kits et al. 2017). So far comammox bacteria have been found in diverse man-made systems such as groundwater-fed rapid sand filters (Fowler et al. 2018), wastewater treatment plants (WWTPs) (Chao et al. 2016, Gonzalez-Martinez et al. 2016, Fan et al. 2017), drinking water systems (Pinto et al. 2016, Wang et al. 2017) and other natural habitats such as rice paddy and forest soils, brackish lake sediment and freshwater biofilms (Hu and He 2017, Pjevac et al. 2017). However, how comammox is related to other processes in the environment remains largely unknown. If comammox coexists with anammox, comammox bacteria could potentially 'hide' nitrite from anammox bacteria and, in turn, increase the degree of nitrification efficiency. However, to date, no measurements of the interactions between comammox and anammox have been undertaken.

Although some research has shown relationships between AOA and AOB (Zhao et al. 2013, Liu et al. 2017), AOA, AOB and NOB (Fukushima et al. 2013), AOA, AOB and anammox (Lee et al. 2014, Wang et al. 2014), AOA, AOB and denitrifiers (Kim et al. 2016) and AOA, AOB, comammox and NOB (Bartelme et al. 2017, Fowler et al. 2018)

in various sediments, the focus was on individual processes and organismal abundance, rather than their interaction and co-occurrence of simultaneous processes. To our knowledge, the interactions between AOM, anammox and NOB in permeable, oxic riverbeds, as well as their contributions to the degree of nitrification efficiency have not been characterized. Here, the degree of nitrification efficiency of a range of permeable, oxic riverbeds along with the abundance of the AOM, anammox, NOB and comammox was characterized in order to identify the key factors that control the degree of nitrification efficiency in permeable, oxic riverbeds.

Phosphorus is often considered to be the limiting nutrient for primary production in rivers and plays a key role in the accelerated growth of aquatic plants in freshwaters, as well as in eutrophication. The initial results in this chapter show a correlation between concentration of porewater soluble reactive phosphorus (SRP) and the degree of nitrification efficiency, hinting at the possibility that the availability of phosphorus may influence the processes involved in regulating the degree of nitrification efficiency. It was proposed that phosphorus can stimulate the nitrification process mainly by accelerating aerobic ammonia oxidation (Rosswall 1981, Minami and Fukushi 1983, Hue and Adams 1984, De Vet et al. 2012, Zhou et al. 2014). In contrast, others showed that phosphorus has a more important influence on the process of nitrite oxidation rather than ammonia oxidation (Purchase 1974, Nowak et al. 1996). Potential denitrification rates were also found to be positively related to SRP in streams (Inwood et al. 2005, Graham et al. 2010, Lansdown et al. 2016), while other studies showed the opposite (Pina-Ochoa and Alvarez-Cobelas 2006, Veraart 2012). For the anammox process, it is reported that phosphate lower than 1 mM has no significant effect on anammox activity, while high than 2 mM can completely inhibit anammox activity (Van de Graaf et al. 1996, Jetten et al. 1998, Pynaert et al. 2003). However, effects of phosphorus on the interactions between

nitrification, denitrification and anammox remains unclear in natural settings. Here, an additional experiment was conducted to seek the influence of SRP on the degree of nitrification efficiency.

3.2. Materials and Methods

3.2.1. Nitrification efficiency

Nitrification efficiencies and the total rates of ammonia oxidation were calculated from the rate of production of both $^{15}N\text{-}N_2$ and $^{15}N\text{-}NO_3^-$ in the oxic, $^{15}NH_4^+$ oxidation experiments as described in chapter 2. The rate of total ammonium oxidation was the sum of $^{15}N\text{-}N_2$ and $^{15}N\text{-}NO_3^-$, and nitrification efficiency was defined as the proportion of $^{15}N\text{-}NO_3^-$ production to total ammonium oxidation.

$$Total\ ammomium\ oxidation\ rate = \left(^{15}N\_N_2 + {}^{15}N\_NO_3^-\right) production \text{ rate} \quad (3.1)$$

$$Nitrification\ efficiency(\%) = \frac{^{15}N\_NO_3^- production \text{ rate}}{\left(^{15}N\_N_2 + {}^{15}N\_NO_3^-\right) production\ rate} \quad (3.2)$$

3.2.2. DNA extraction and qPCR

To get more detailed information about the microorganisms that contribute the degree of nitrification efficiency, the preserved surface sediments from the twelve riverbeds (as described in Chapter 2) were further analysed for the gene abundances. DNA was extracted from sediment from each river using a PowerSoil DNA Isolation Kit (MO BIO Laboratories) according to the manufacturer's instructions and its concentration and quality determined with a NanoDrop spectrophotometer (UV-Vis, Thermos Scientific). The abundance of genes that could affect the degree of nitrification efficiency

were quantified by qPCR. Amplification of total bacterial 16S rRNA genes, anammox-specific 16S rRNA, *hzo* (hydrazine oxidoreductase) and *hzs*B (hydrazine synthase beta subunit) genes, AOB-specific 16S rRNA and *amo*A (ammonia monooxygenase subunit A) genes, AOA *amo*A genes, *Nitrobacter*-specific *nxr*B genes, *Nitrospira*-specific 16S rRNA and *nxr*B (nitrite oxidoreductase subunit B) genes and the comammox *Nitrospira amo*A gene was performed separately using SensiFAST SYBR No-ROX Kit (Bioline) on a CFX384 Real-Time PCR Detection System (BioRad). The list of primer pairs used and their annealing temperatures are described in Table 3.1. Each sample was performed in triplicate, and the amplicons of target gene (with known gene copies) was used to construct standard curves (see below). Gene abundances were then quantified by the absolute quantification method against internal DNA standards curves of the target gene amplicons with 10-fold serial dilutions. PCR reactions were run in a 15µl volume containing 200nM of primers and 1µl of DNA template. Cycle conditions were 95°C for 3min, followed by 40 cycles of denaturation at 95°C for 5s and then annealing/extension at 60°C for 30s. A melting curve analysis was performed after completion of PCR to confirm the amplification of a single product. Standard curve coefficients of variation and efficiencies were as follows: total bacterial 16S rRNA (R^2 = 0.989, efficiency = 82.8%), anammox-specific 16S rRNA (R^2 = 0.993, efficiency = 73.8%), *hzo* (R^2 = 0.987, efficiency = 84.9%) and *hzs*B (R^2 = 0.991, efficiency = 80.4%), AOB-specific 16S rRNA (R^2 = 0.996, efficiency = 85.8%) and AOB *amo*A (R^2 = 0.989, efficiency = 65.6%), AOA *amo*A (R^2 = 0.996, efficiency = 75%), *Nitrobacter*-specific *nxr*B (R^2 = 0.997, efficiency = 86.5%), *Nitrospira*-specific 16S rRNA (R^2 = 0.997, efficiency = 88.3%), *Nitrospira*-specific *nxr*B (R^2 = 0.997, efficiency = 80.0%) and comammox *Nitrospira amo*A (R^2 = 0.998, efficiency = 89.1%). To further investigate the correlations between the gene abundances and the activities of aerobic ammonia oxidation and anammox, as well as the

degrees of nitrification efficiency, the results of the qPCR were expressed as the number of gene copies g^{-1} of sediment (dry weight) as well as their relative abundances to total bacterial 16S rRNA gene.

Standard curve for qPCR of each gene was generated based on the absolute gene copies of a target gene amplicon with 10-fold serial dilutions. Amplicons of the target genes were prepared by PCR amplifications with the specific primers (Table 3.1). PCR amplification of each gene was performed separately in a total volume of 20 µl in a 96 Well Thermal Cycler (Applied Biosystems). Each PCR mixture contained 1 µl of template DNA, 10 µl of PCR Reaction Mix (ReadyMix RED Taq, Sigma-Aldrich) and 200 nM of each primer. Thermal cycling was carried out by using an initial denaturation step of 95°C for 3 min, followed by 35 cycles of denaturation at 94°C for 30 s, annealing temperature for 30 s, and extension at 72°C for 30 s. Cycling was completed by a final extension step of 72°C for 7 min. A negative control (without template DNA) was added for each PCR amplification. The PCR products were examined on 1% (w/v) ethidium bromide-stained agarose gels and purified using the PCR Clean-up Kit (GenElute, Sigma), the concentration of amplicon was determined using a Quant-iT PicoGreen dsDNA assay Kit (Life Technologies) on a NanoDrop 3300 fluorospectrometer (Thermo Scientific). Based on the concentration and size of the amplicon of the target gene, the concentration of the target amplicon can be converted to copies/µl using the following equation and then used as standards for qPCR (McKew and Smith 2015).

$$\frac{^{*}6.023 \times 10^{23}\ (copies/mol)) \times concentration\ of\ target(g/\mu l)}{660\ (g/mol)} \qquad (3.3)$$

*Avogadro's number

Table 3.1. Primers used for qPCR and sequencing.

Specificity	Primer Sequence	Tm(°C)	Reference
Bacteria 16S rRNA	Bakt_341F: CCTACGGGNGGCWGCAG	57	(Herlemann et al. 2011)
	Bakt_805R: GACTACHVGGGTATCTAATCC		
Anammox 16S rRNA	A438f: GTCRGGAGTTADGAAATG	55	(Humbert et al. 2012)
	A684r: ACCAGAAGTTCCACTCTC		
hzo	hzocl1F1: TGYAAGACYTGYCAYTGG	51	(Schmid et al. 2008)
	hzocl1R2: ACTCCAGATRTGCTGACC		
*hzs*B	HzsB_396F: ARGGHTGGGGHAGYTGGAAG	59	(Wang et al. 2012)
	HzsB_742R: GTYCCHACRTCATGVGTCTG		
AOB 16S rRNA	CTO189f A/B: GGAGRAAAGCAGGGGATCG	57	(Kowalchuk et al. 1997)
	CTO189f C: GGAGGAAAGTAGGGGATCG		
	CTO654R: CTAGCYTTGTAGTTTCAAACGC		
AOB *amo*A	AmoA-1F: GGGGTTTCTACTGGTGGT	60	(Wang and Gu 2013)
	AmoA-2R: CCCCTCKGSAAAGCCTTCTTC		

Specificity	Primer Sequence	Tm(°C)	Reference
AOA *amo*A	CrenamoA-23F: ATGGTCTGGCTWAGACG	60	(Tourna et al. 2008)
	CrenamoA-616R: GCCATCCATCTGTATGTCCA		
*Nitrobacter nxr*B	NxrB 1F: ACGTGGAGACCAAGCCGGG	55	(Geets et al. 2007)
	NxrB 1R: CCGTGCTGTTGAYCTCGTTGA		
Nitrospira 16S rRNA	EUB338f: ACTCCTACGGGAGGCAGC	58	(Regan et al. 2002)
	NTspa0685r: CGGGAATTCCGCGCTC		
*Nitrospira nxr*B	*nxr*B169f: TACATGTGGTGGAACA	56	(Pester et al. 2014)
	*nxr*B638r: CGGTTCTGGTCRATCA		
Comammox *Nitrospira*	Ntsp-*amo*A *162F:* GGATTTCTGGNTSGATTGGA	48	(Fowler et al. 2018)
*amo*A	Ntsp-*amo*A *359R:* WAGTTNGACCACCASTACCA		

3.2.3. Effects of soluble reactive phosphorus (SRP) on the degree of nitrification efficiency

Oxic slurries were prepared by adding approximately 3 g sediment and 2.7 ml air-saturated synthetic river water into 12 ml gas-tight vials (Exetainer, Labco). The vials were then sealed and half of them were injected with KH_2PO_4 to give a final, notional, SRP concentration of 500 µM and incubated on a shaker for 15h. After preincubation, the vials were then injected with 200 µl of either 7.25 mM $^{15}NH_4^+$ (98 atom% ^{15}N, Sigma-Aldrich) or 7.25 mM $^{15}NH_4^+$ plus 7.25 mM KH_2PO_4 to generate a final porewater concentration of ~500 µM $^{15}NH_4^+$ and ~500 µM $^{15}NH_4^+$ plus ~500 µM SRP and then incubated on a shaker (120 rpm, Stuart SSL1) for 6 h. Details of experimental design are listed in Table 3.2. Samples were centrifuged at 2000 rpm for 15min after analysed for ^{15}N-N_2, then the supernatants were transferred to plastic vials (polypropylene, VWR International) and preserved at -20°C before further analysis of $^{15}NO_2^-$, $^{15}NO_3^-$, NO_2^-, NO_3^-, and SRP.

Table 3.2. Experimental design for the effect of SRP on the degree of nitrification efficiency.

Abbreviation	Treatment	Preincubation(15h) with SRP	Tracers/SRP added
A	$^{15}NH_4^+$	no	$^{15}NH_4^+$
A+SRP	$^{15}NH_4^+$ +SRP	no	$^{15}NH_4^+$ +SRP
P+A	Preincubation+$^{15}NH4^+$	yes	$^{15}NH_4^+$
P+A+SRP	Preincubation+$^{15}NH_4^+$ +SRP	yes	$^{15}NH_4^+$ +SRP

Research by Purchase (Purchase 1974) indicated that a higher SRP concentration may stimulate the second step of nitrification, nitrite oxidation, in agricultural soils. To test the effects of SRP on nitrite oxidation, a similar experiment was conducted as above, experimental design is described below (Table 3.3). In this experiment, a final porewater concentration of ~300 µM $^{15}NO_2^-$ and ~300 µM $^{15}NO_2^-$ plus ~500 µM SRP was set. Samples were centrifuged at 2000 rpm for 15min, then the supernatants were transferred to plastic vials (polypropylene, VWR International) and preserved at -20℃ before further analysis of $^{15}NO_2^-$ and $^{15}NO_3^-$, NO_2^-, NO_3^-, and SRP.

Table 3.3. Experimental design for the effect of SRP on nitrite oxidation process.

Abbreviation	Treatment	Preincubation(15h) with SRP	Tracers/SRP added
N	$^{15}NO_2^-$	no	$^{15}NO_2^-$
N+SRP	$^{15}NO_2^-$ +SRP	no	$^{15}NO_2^-$ +SRP
P+N	Preincubation+$^{15}NO_2^-$	yes	$^{15}NO_2^-$
P+N+SRP	Preincubation+$^{15}NO_2^-$ +SRP	yes	$^{15}NO_2^-$ +SRP

When measuring the SRP concentrations in the above experiments, I noticed that the SRP concentrations decreased quickly and the rate of decline varied a lot between the different riverbed slurries, which means that the availability of the SRP for different riverbed slurries varied during and between the experiments. To further understand the fate of the additional SRP in the slurries, the SRP decreasing process was traced with sediment samples from two rivers. Slurries were prepared as above, the vials were then

injected with 200 µl of either 7.25 mM $^{15}NH_4^+$ (98 atom% ^{15}N, Sigma-Aldrich) or 7.25 mM $^{15}NH_4^+$ plus 7.25 mM KH_2PO_4 to generate a final porewater concentration of ~500 µM $^{15}NH_4^+$ and ~500 µM $^{15}NH_4^+$ plus ~500 µM SRP and then incubated on a shaker (120 rpm, Stuart SSL1) for up to 24 h. Samples were then analysed for SRP at 0 h, 0.25 h, 0.5 h, 1 h, 2 h, 3 h, 4.5 h, 6 h, 8 h and 24 h. Briefly, samples were centrifuged at 2000 rpm for 15min, then the supernatants were transferred to plastic vials (polypropylene, VWR International) and preserved at -20℃ before further analysis of SRP concentration. The remaining sediment samples were then dried in an oven before quantification of both inorganic and organic phosphorus concentrations.

3.2.4. Analytical methods

Analysis of $^{15}N\text{-}N_2$, $^{15}NO_2^-$, $^{15}NO_3^-$, NO_2^-, NO_3^-, and SRP were conducted as described in Chapter 2. Inorganic phosphorus concentrations were determined using HCl extraction method (Aspila et al. 1976). Briefly, 0.15 g dried sediment samples and 15 ml of 1M HCl were added into a 15ml glass vial, vials were then incubated on a shaker (80rpm, Stuart SSL1) for 16h, samples were filtered, diluted and analysed by a segmented flow auto analyser (San++, Skalar, Breda, The Netherlands) using standard colorimetric techniques (Murphy and Riley 1962). Total phosphorus concentration was quantified using a revised total phosphorus detection protocol (kindly provided by Sarah Seco Leite in QMUL) (Nelson 1987). Briefly, 0.02 g dried sediment samples were added into 15 ml glass vial, then 1.5 g potassium persulphate and 10 ml of 0.5 M sulphuric acid were added to each sample, vials were then autoclaved at 121°C for 40 min. The samples were then diluted for 100 times and then analysed on a segmented flow auto analyser for SRP as above. Organic phosphorus was determined from the difference between total phosphorus and inorganic phosphorus.

3.2.5. Statistical analyses

Statistical analyses were performed in R (version 3.4.1). Differences between gravel and sand-dominated riverbeds in the degree of nitrification efficiency, total ammonia oxidation rate, and gene abundance were tested with linear mixed effect models using the lme4 package (Bates et al. 2015). Riverbed type was fitted as a fixed effect and each river as a random effect. Significance of the fixed effect ($p < 0.05$) was determined by likelihood ratio testing between the full model and a reduced model.

Any relationships between microbial functional gene abundances and porewater chemistries and the degree of nitrification efficiency were analysed using redundancy analysis (RDA) in the Vegan package in R (Oksanen et al. 2017). Spearman correlation analysis was used to assess the potential correlations between environmental factors and the degree of nitrification efficiency and gene abundance, which were also performed in R under the in the 'Hmisc' package.

Differences between various SRP treatments in the degree of nitrification efficiency, production of $^{15}N\text{-}N_2$, production of $^{15}N\text{-}NO_3^-$ were tested with linear mixed effect models using the lme4 package (Bates et al. 2015). Treatment was fitted as a fixed effect and each replicate or river as a random effect. Significance of the fixed effect ($p < 0.05$) was determined by likelihood ratio testing between the full model and a reduced model.

3.3. Results

3.3.1. Nitrification efficiency

The rate of total ammonia oxidation ranged from 2.44 to 24.16 nmol g^{-1} h^{-1} but the median rates across the gravel and sand riverbeds were comparable, 10.06 and 13.23 nmol g^{-1} h^{-1}, respectively (Figure 3.1), with no overall significant difference (Likelihood ratio

test, p = 0.17, Table 3.4). In contrast, the degree of nitrification efficiency varied from 22.2% to 99.7% across the riverbeds and was significantly lower in the gravel-dominated riverbeds (median 38.77%), compared to the sand-dominated riverbeds (median 71.38%, Likelihood ratio test, $p < 0.01$, Table 3.4).

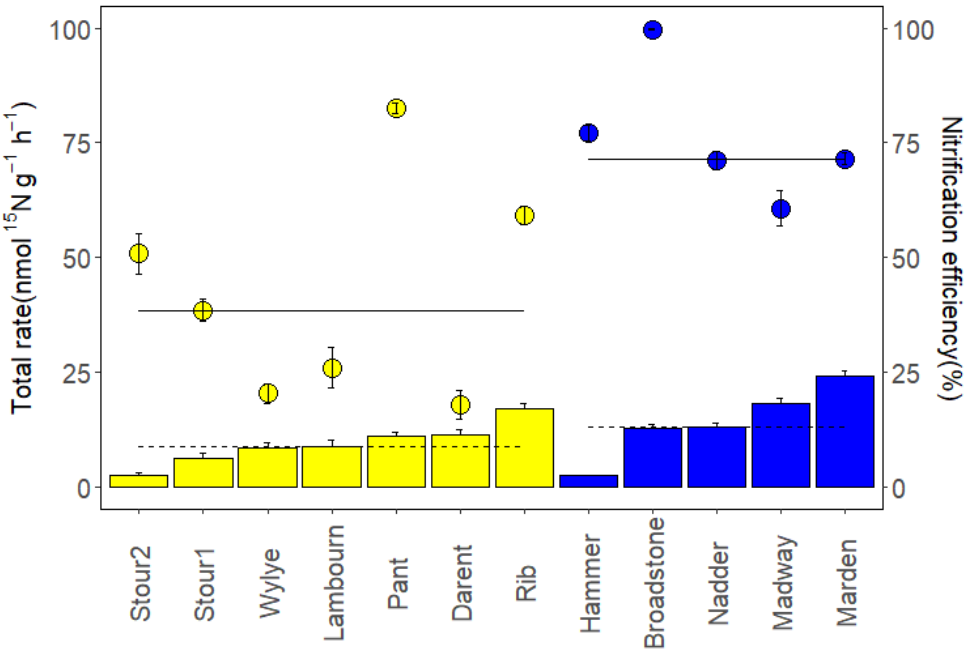

Figure 3.1. Total $^{15}N\text{-}NH_4^+$ oxidation rate (production rate of $^{15}N\text{-}N_2$ plus $^{15}N\text{-}NO_3^-$) and the degree of nitrification efficiency across the twelve riverbeds, as measured in oxic slurries.

(Yellow and blue represent gravel and sand-dominated riverbeds respectively. Black lines indicate the overall median values for the gravel and sand-dominated riverbeds (n = 7 and 5, respectively). Data are mean values ± standard error (n = 5).)

Table 3.4. Likelihood ratio test of the effect of riverbed type on rates of total ammonia oxidation and the degree of nitrification efficiency from oxic incubations.

Experiment	Dependent variable	Independent variable	df	$\chi 2$	*p*-value
Oxic incubations	Rate of total $^{15}NH_4^+$ oxidation	type	1	1.91	0.17
	Nitrification efficiency	type	1	7.05	<0.01

3.3.2. Microbial abundance of AOM, anammox bacteria and NOB

Total bacterial 16S rRNA gene abundance ranged from 8.9×10^7 (River Hammer) to 5.6×10^8 (River Wylye) copies g^{-1} dry sediment, and there was no significant difference between gravel and sand-dominated riverbeds (Likelihood ratio test, $p = 0.13$).

Genes responsible for aerobic ammonia oxidation (AOB 16S rRNA, AOB *amoA* and AOA *amoA*) were quantified. AOA *amo*A gene abundance varied from 3.3×10^5 to 4.4×10^6 copies g^{-1} dry sediment, while AOB *amo*A gene abundance varied from 1.57×10^5 to 2.3×10^6 copies g^{-1} dry sediment (Figure 3.3). There was no significant difference in the total *amo*A gene abundance (AOA+AOB) between gravel and sands (Likelihood ratio test, $p = 0.15$), the proportions of total *amo*A gene to total bacteria between gravel and sand-dominated riverbeds also showed no significant difference (Likelihood ratio test, $p = 0.18$). The minimum total *amo*A gene abundance, along with the lowest rate of total ammonia oxidation, were observed in the river Hammer (Figure 3.2). The relative abundance (proportion) of total *amo*A to total bacterial 16S rRNA correlated well with the total *amo*A gene copies (Figure 3.4, $r_s = 0.63$, $p < 0.01$). Both the abundance of AOB *amo*A genes and AOB 16S rRNA genes were positively correlated with the AOA *amo*A gene (Figure 3.3 and Table 3.5). Also, AOB *amo*A genes and AOB 16S rRNA genes were positively correlated (Table 3.5). The maximum abundance of AOA *amo*A was found in

the river Marden, where the highest total ammonium oxidation rate was also observed. Both AOB 16S rRNA and *amo*A gene abundance peaked at the river Pant. The proportions of AOA *amo*A and AOB *amo*A to bacterial 16S rRNA were 0.28%-1.32% and 0.09%-1.1%, respectively. AOB 16S rRNA gene abundance varied from 1.2×10^5 to 9.9×10^5 copies g^{-1} dry sediment and the proportion of AOB 16S rRNA gene to bacteria 16S rRNA were 0.07%-0.49%.

Anammox related genes (anammox 16S rRNA, *hzo* and *hzs*B gene) were quantified for the riverbeds. The abundance of *hzs*B was greater than *hzo* in all riverbeds (Figure 3.3), with abundance from 1.6×10^5 to 2.9×10^6 copies g^{-1} dry sediment across the riverbeds (Figure 3.2) and there was no significant difference between gravel and sand (Likelihood ratio test, $p = 0.12$). The abundance of *hzo* genes and anammox 16S rRNA genes correlated well with the *hzs*B genes (Table 3.5), with the abundance of 9.8×10^4 - 5.8×10^5 copies g^{-1} dry sediment and 4.2×10^4 -1.2×10^6 copies g^{-1} dry sediment, respectively (Figure 3.3). The contribution from anammox to N_2 gas production measured in anoxic slurries was also positively correlated with *hzs*B gene abundance ($r_s = 0.30$, $p = 0.04$). In the acidic river Broadstone, where no significant anammox activity was recorded, the lowest abundance of anammox 16S rRNA and *hzo* genes were also recorded. The highest gene abundance of *hzo* was recorded in River Wylye; while the highest gene abundances of *hzs*B and anammox 16S rRNA gene were measured in River Rib. The relative abundance (proportion) of *hzs*B to total bacterial 16S rRNA correlated well with the *hzs*B gene copies (Figure 3.4, $r_s = 0.78$, $p < 0.01$). The proportions of *hzo* gene and *hzs*B gene to bacterial 16S rRNA gene ranged from 0.03-0.13% and 0.07-0.95%. Anammox 16S rRNA gene copies were 4.2×10^4 -1.2×10^6 copies g^{-1} dry sediment across the riverbeds, the proportions of anammox 16S rRNA gene to bacterial 16S rRNA gene abundance were 0.02-0.38%.

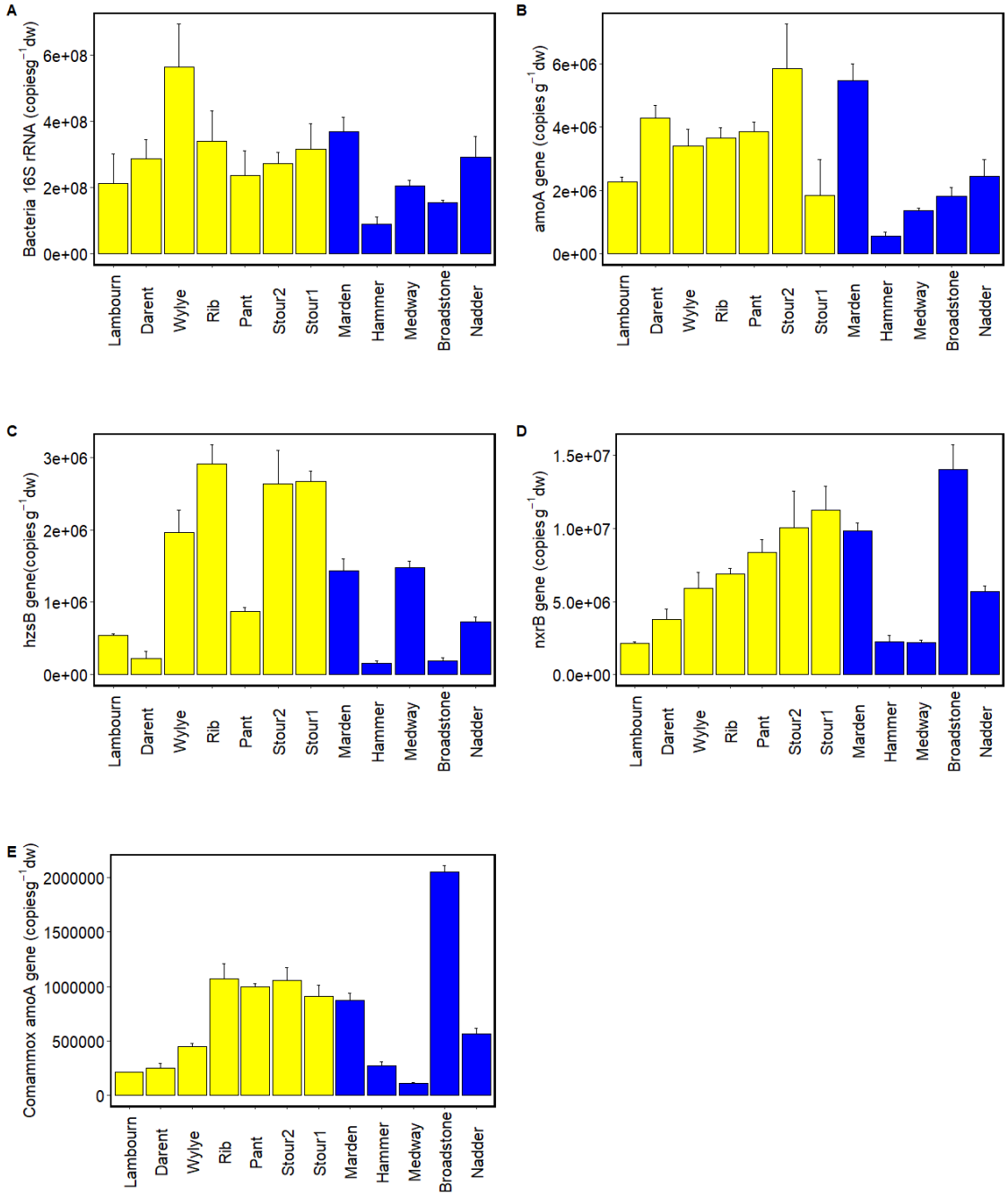

Figure 3.2. Abundance of targeted genes across the twelve riverbeds. A: Total bacteria 16S rRNA gene. B: Total *amo*A genes (AOA and AOB). C: The *hzs*B gene. D: Total *nxr*B genes (*Nitrospira* and *Nitrobacter*). E: Comammox *Nitrospira amo*A gene. Yellow and blue represent gravel and sand-dominated riverbeds respectively. Bars indicate mean values ± standard error (n = 3 for each individual river).

Abundances of nitrite oxidation related genes (*Nitrospira* 16S rRNA, *Nitrospira nxr*B and *Nitrobacter nxr*B) were detected in all sediment samples. The highest total *nxr*B gene abundance as well as its relative abundance to total bacteria was observed in the acidic river Broadstone, along with the highest degree of nitrification efficiency (Figure 3.1 and 3.2). The relative abundance (proportion) of *nxr*B to total bacterial 16S rRNA gene correlated well with the *nxr*B gene copies (Figure 3.4, $r_s = 0.67$, $p < 0.01$). *Nitrospira nxr*B gene abundance ranged from 1.6×10^6 to 1.4×10^7 copies g^{-1} dry sediment across all riverbeds and the proportion of the *Nitrospira nxr*B gene to bacterial 16S rRNA genes were 0.9%-8.8% across the riverbeds. Compared with *Nitrospira nxr*B gene, *Nitrobacter nxr*B had a relatively low abundance, *Nitrobacter nxr*B gene abundance varied from 2.0×10^5 to 7.7×10^5 copies g^{-1} dry sediment, with the proportions to bacterial 16S rRNA ranged from 0.1% to 0.3%. The ratio of the relative abundance of *Nitrospira* to *Nitrobacter* ranged from 2.9 to 50.6 (Figure 3.3). The abundance of *Nitrospira* 16S rRNA genes was 1.6×10^6 -6.2×10^6 copies g^{-1} dry sediment and correlated well with the *Nitrospira nxr*B gene (Figure 3.3 and Table 3.5), represented 0.8 %-2.3 % of the total bacterial 16S rRNA gene abundance.

Furthermore, comammox *Nitrospira amo*A gene abundance (which is a phylogenetically distinct form of the *amo*A gene not picked up by AOB *amo*A primers) ranged from 1.1×10^5 to 2.0×10^6 copies g^{-1} dry sediment (Figure 3.2) and correlated well with the *Nitrospira nxr*B gene abundance (Figure 3.3 and Table 3.5), the proportion of the comammox *Nitrospira amo*A gene to bacterial 16S rRNA genes was 0.06%-1.32% across the riverbeds. The relative abundance (proportion) of comammox *Nitrospira amo*A to total bacterial 16S rRNA correlated well with the comammox *Nitrospira amo*A gene copies (Figure 3.4, $r_s = 0.84$, $p < 0.01$).

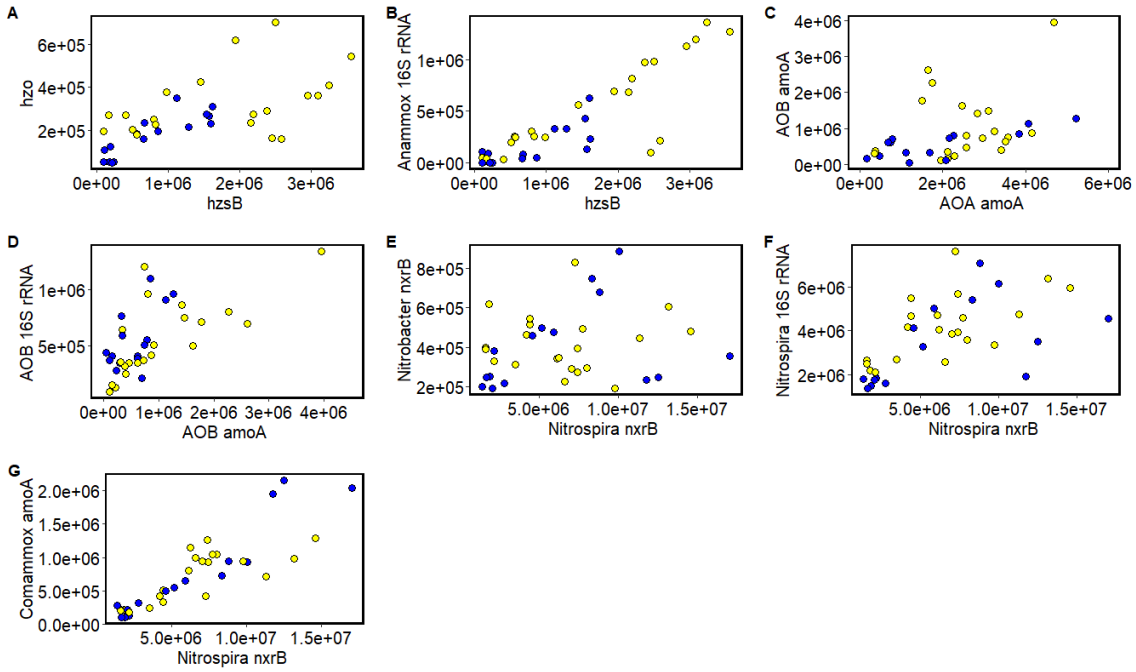

Figure 3.3. Gene abundance and their correlations. (A) *hzs*B and *hzo*; (B) *hzs*B and anammox 16S rRNA; (C) AOA *amo*A and AOB *amo*A; (D) AOB *amo*A and AOB 16S rRNA; (E) *Nitrospira nxr*B and *Nitrobacter nxr*B; (F) *Nitrospira nxr*B and *Nitrospira* 16S rRNA; (G) *Nitrospira nxr*B and Comammox *Nitrospira amo*A.

Yellow and blue represent gravel and sand-dominated riverbeds respectively.

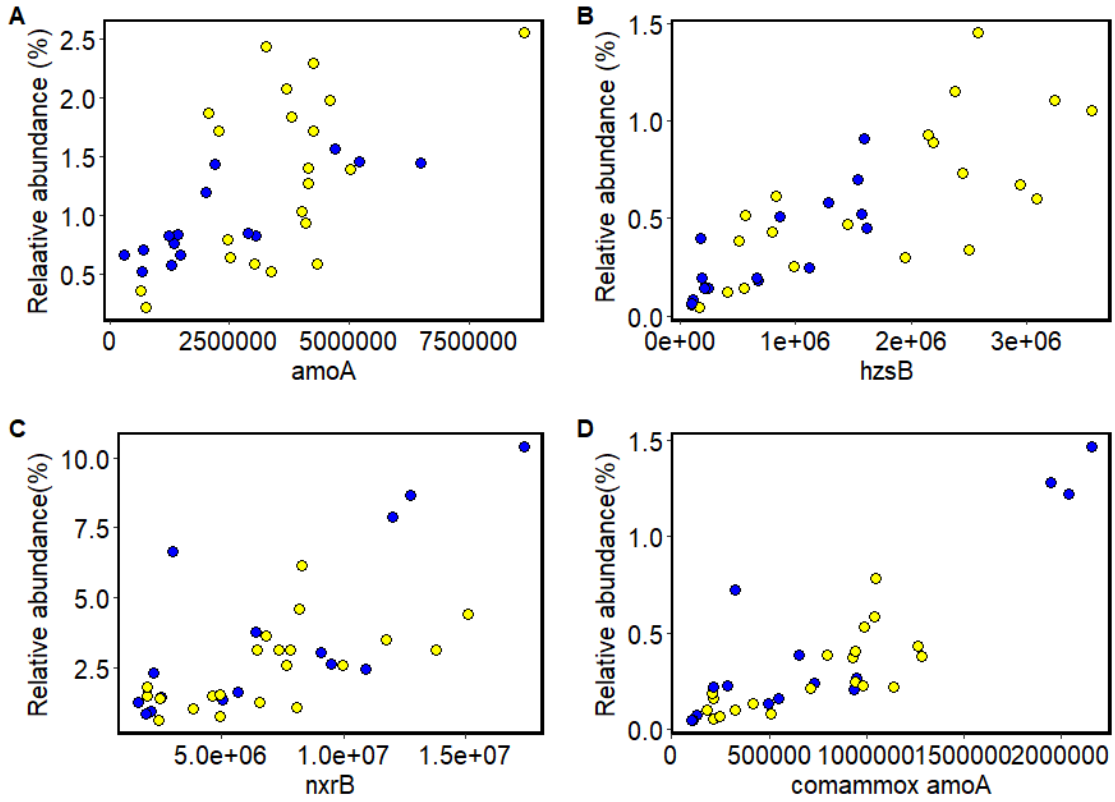

Figure 3.4. Correlations between relative abundance of targeted genes to total bacterial 16S rRNA gene and the abundance of the target genes. A: Total *amo*A genes (AOA and AOB). B: The *hzs*B gene. C: Total *nxr*B genes (*Nitrospira* and *Nitrobacter*). D: Comammox *Nitrospira amo*A gene.

Yellow and blue represent gravel and sand-dominated riverbeds respectively (n = 3 for each individual river).

Table 3.5. Spearman's correlation analyses of the abundances of different genes.

	Anammox 16S rRNA	*hzo*	*hzs*B	AOA *amo*A	AOB 16S rRNA	AOB *amo*A	*Nitrobacter nxr*B	*Nitrospira* 16S rRNA	*Nitrospira* nxrB	Comammox *amo*A
Anammox 16S rRNA	1									
hzo	0.70*	1								
*hzs*B	0.86*	0.64*	1							
AOA *amo*A	0.40*	0.57*	0.31	1						
AOB 16S rRNA	0.26	0.61*	0.34*	0.53*	1					
AOB *amo*A	0.38*	0.46*	0.37*	0.42*	0.64*	1				
*Nitrobacter nxr*B	0.15	0.47*	0.29	0.57*	0.50*	0.07	1			
Nitrospira 16S rRNA	0.44*	0.60*	0.59*	0.61*	0.64*	0.30	0.72*	1		
*Nitrospira nxr*B	0.18	0.09	0.33*	0.27	0.47*	0.39*	0.20	0.57*	1	
Comammox *amo*A	0.11	-0.12	0.17	0.15	0.25	0.18	-0.08	0.33*	0.86*	1

*$p < 0.05$

3.3.3. Cell-specific ammonia oxidation rates

Cell-specific ammonia oxidation rates were calculated from the total ammonia oxidation rates and the *amo*A gene copy numbers. The rate of ammonia oxidized per AOA or AOB cell was calculated separately by dividing the total ammonia oxidation rates. Here, assuming each genome of AOA contains 1.0 gene copy and each genome of AOB contains 2.5 *amo*A gene copies (Wang et al. 2012). Cell-specific ammonia oxidation activities for AOA ranged from 0.7-25.2 fmol $cell^{-1}$ h^{-1} (Table 3.6), all of them were higher compared with the cell-specific rates from the pure culture (0.08-0.59 fmol $cell^{-1}$ h^{-1}) (Könneke et al. 2005, Treusch et al. 2005). Cell-specific ammonia oxidation activity for AOB ranged from 2.9-230 fmol $copies^{-1}$ h^{-1} (Table 3.6), extraordinarily high specific rates were found in the rivers Lambourn and Broadstone, others were within the range of the cell-specific rates from the pure culture (0.9-83 fmol $cell^{-1}$ h^{-1}) (Belser 1979, Ward et al. 1989). These results suggest that AOA could not account for aerobic ammonia oxidation solely, AOB were also involved in the oxic ammonia oxidation. Although the gene abundances of AOA *amo*A were higher than AOB *amo*A in all the riverbeds, the contribution of AOA to the aerobic ammonia oxidation might not be as important as AOB.

Table 3.6. Estimates of cell specific ammonia oxidation rates of AOA and AOB.

River	Cell specific ammonia oxidation rate (fmol $cell^{-1}$ h^{-1})	
	AOA[a]	AOB[a]
Lambourn	5.08	230.25
Darent	3.29	34.14
Wylye	3.07	33.54
Rib	5.43	86.08
Pant	6.77	12.35
Stour (2)	0.75	2.92
Stour (1)	5.93	20.53
Marden	5.54	55.98
Hammer	7.36	27.12
Medway	25.26	58.53
Broadstone	7.78	197.74
Nadder	7.14	53.11

[a] Here, assuming each genome of AOA contains 1.0 gene copy and each genome of AOB contains 2.5 *amo*A gene copies (Wang et al. 2012).

3.3.4. Factors influencing the degree of nitrification efficiency

Redundancy analysis was performed to evaluate how functional gene abundances were related to the porewater chemistries and the degree of nitrification efficiency. The RDA results (Figure 3.5) showed that the abundance of both *hzs*B and *nxr*B genes were positively correlated with *amo*A gene (r_s = 0.36, p = 0.03 and r_s = 0.41, p = 0.01, respectively). On the other hand, *nxr*B and comammox *Nitrospira amo*A genes separated well from *hzs*B. A positive correlation between the degree of nitrification efficiency and

the abundance of *nxr*B gene (Table 3.7) was also observed. The abundance of the *amo*A gene was positively correlated with pH and nitrite (Table 3.7) and the same pattern was also found for the *hzs*B gene (Table 3.7).

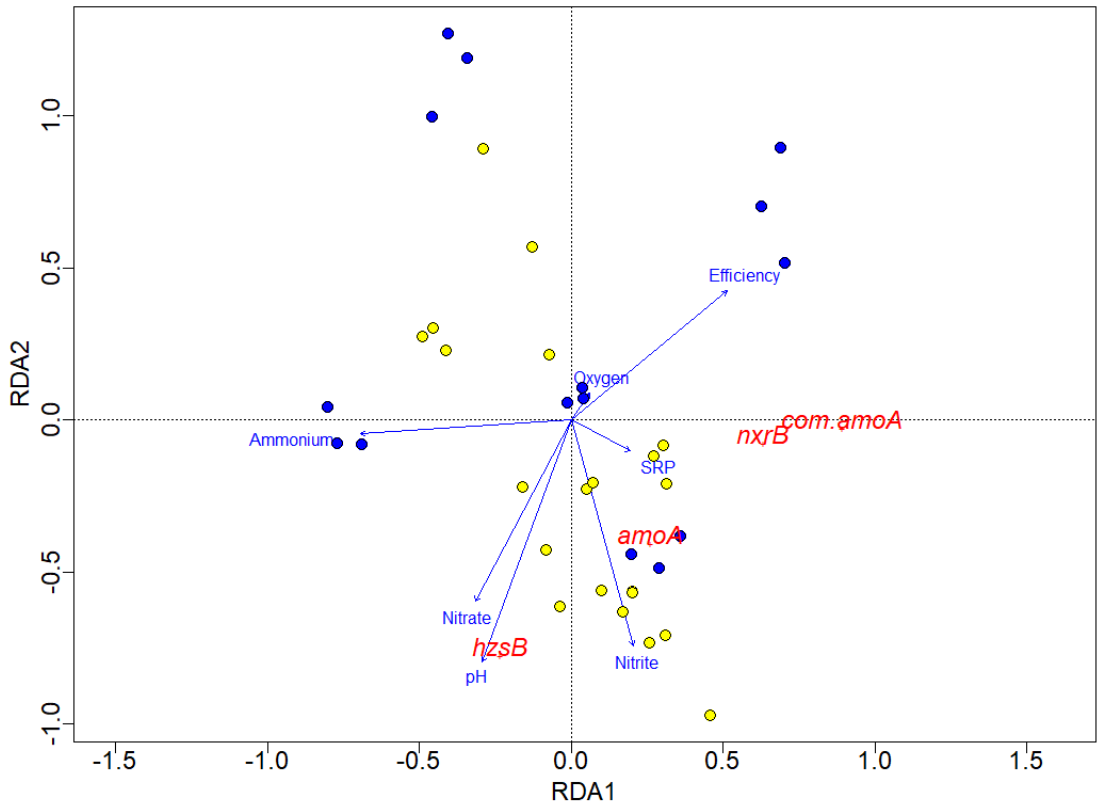

Figure 3.5. Redundancy analysis plot of the relationship between either functional gene abundances of *amo*A, *hzs*B, *nxr*B and comammox *Nitrospira amo*A (*com.amo*A), and nitrification efficiency and porewater chemistries across in gravel (yellow) and sand-dominated (blue) riverbeds.

(The first and second canonical axes represented 53% and 31% of the variation, respectively. High degree of nitrification efficiency correlates with a high functional gene abundance for NOB and comammox).

Table 3.7. Spearman's correlation analyses of gene abundances and environmental factors.

	pH	Oxygen	Nitrite	Nitrate	Ammonium	SRP	Efficiency	*ra*	Total ammonia oxidation
*amo*A	0.48*	0.13	0.34*	0.17	-0.23	0.03	-0.21	0.51*	0.32
*hzs*B	0.40*	-0.11	0.38*	0.38*	0.19	0.05	-0.25	0.34*	0.17
*nxr*B	-0.22	-0.06	0.19	-0.26	0.16	0.08	0.33*	0.11	0.12
Comammox *amo*A	-0.26	-0.04	0.20	-0.19	0.05	0.22	0.47*	-0.01	0.03
P.*amo*A [a]	0.22	0.29	0.27	-0.04	-0.28	0.23	0.06	0.39*	0.04
P.*hzs*B [a]	0.15	-0.08	0.28	0.19	0.22	0.06	-0.12	0.28	-0.04
P.*nxr*B [a]	-0.67*	0.10	-0.11	-0.44*	-0.26	0.07	0.64*	-0.38*	0.10
P.Comammox *amo*A [a]	-0.65*	0.16	-0.08	-0.37*	-0.27	0.07	0.66*	-0.45*	0.07
pH	1								

	pH	Oxygen	Nitrite	Nitrate	Ammonium	SRP	Efficiency	*ra*	Total ammonia oxidation
Oxygen	0.23	1							
Nitrite	0.65*	-0.02	1						
Nitrate	0.60*	0.56*	0.21	1					
Ammonium	-0.13	-0.53*	-0.25	-0.35*	1				
SRP	0.33	-0.06	0.71*	-0.10	0.02	1			
Efficiency	-0.52*	-0.23	0.11	-0.58*	0.05	0.49*	1		
ra	0.66*	0.08	0.46*	0.05	0.17	0.22	-0.40*	1	
Total ammonia oxidation	0.27	-0.13	0.32	-0.02	-0.06	0.04	0.24	0.16	1

[a] Relative abundance of target gene to total bacterial 16S rRNA gene; * $p < 0.05$

3.3.5. Effects of SRP on the degree of nitrification efficiency

Spearman's correlation test showed a positive correlation between the degree of nitrification efficiency and riverbed porewater SRP concentration ($r(s)$=0.51, $p < 0.01$, Table 3.7), which suggests that phosphorus might influence the degree of the nitrification efficiency by the availability of phosphorus influencing the distribution of bacteria governing the degree of nitrification efficiency. To further test this hypothesis, different $^{15}NH_4^+$ and SRP treatments were conducted in oxic slurries from eight riverbeds along this gradient in efficiency.

Among them, only the results from the river Wylye and Nadder met the hypothesis. With a preincubation of 15h with SRP (treatments P+A and P+A+SRP), the nitrification efficiencies increased significantly in the slurries from the rivers Wylye and Nadder (Figure 3.6 and Table 3.8). Figure.3.7 shows a significant decrease in the production rate of $^{15}N\text{-}N_2$ ($p = 0.03$) and a significant increase in $^{15}N\text{-}NO_3^-$ production ($p = 0.04$) in the preincubation treatments (treatments P+A and P+A+SRP) in the river Wylye. A similar trend was also observed in the river Nadder, where the production of $^{15}N\text{-}NO_3^-$ increased ($p < 0.01$) while the production of $^{15}N\text{-}N_2$ decreased ($p < 0.01$) after a preincubation with SRP. However, total ammonia oxidation rates did not change significantly among different treatments ($p = 0.08$ and $p = 0.24$ in the river Wylye and Nadder, respectively), suggesting for these two rivers, SRP may have accelerated the rate of nitrite oxidation to nitrate. However, a preincubation with SRP has no significant influence on the degree of nitrification efficiency in the riverbed slurries from the rivers Darent and Marden. For the remaining riverbeds, nitrification efficiencies decreased after a preincubation with SRP (Figure 3.6 and Table 3.8).

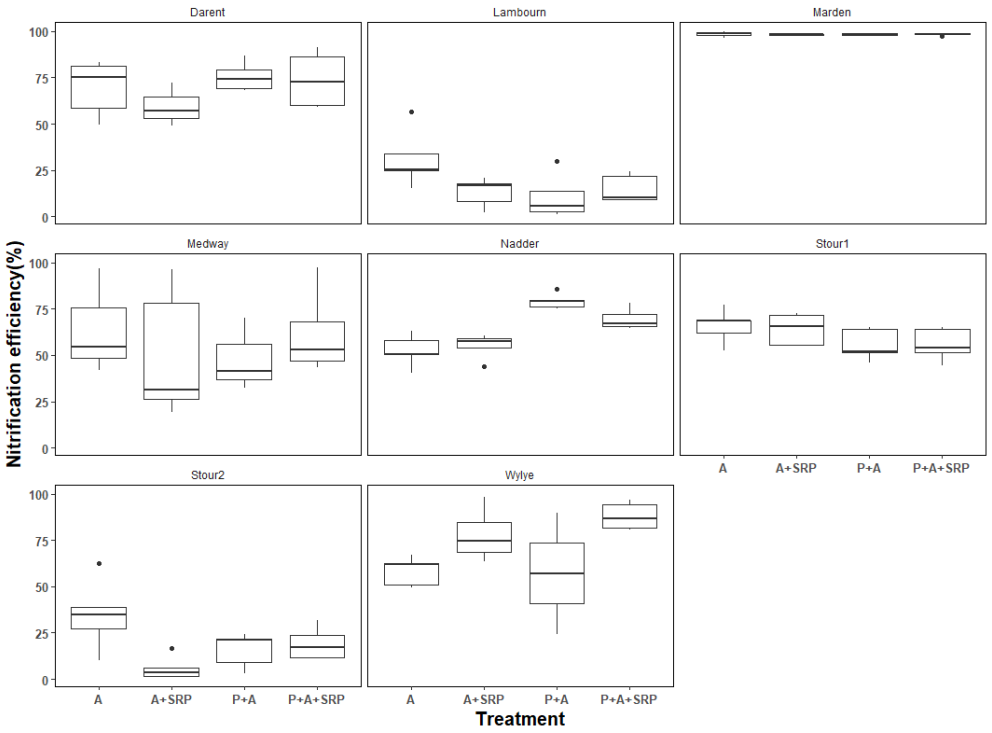

Figure 3.6. Nitrification efficiencies under different $^{15}NH_4^+$ and SRP treatments in oxic slurries for eight riverbeds.

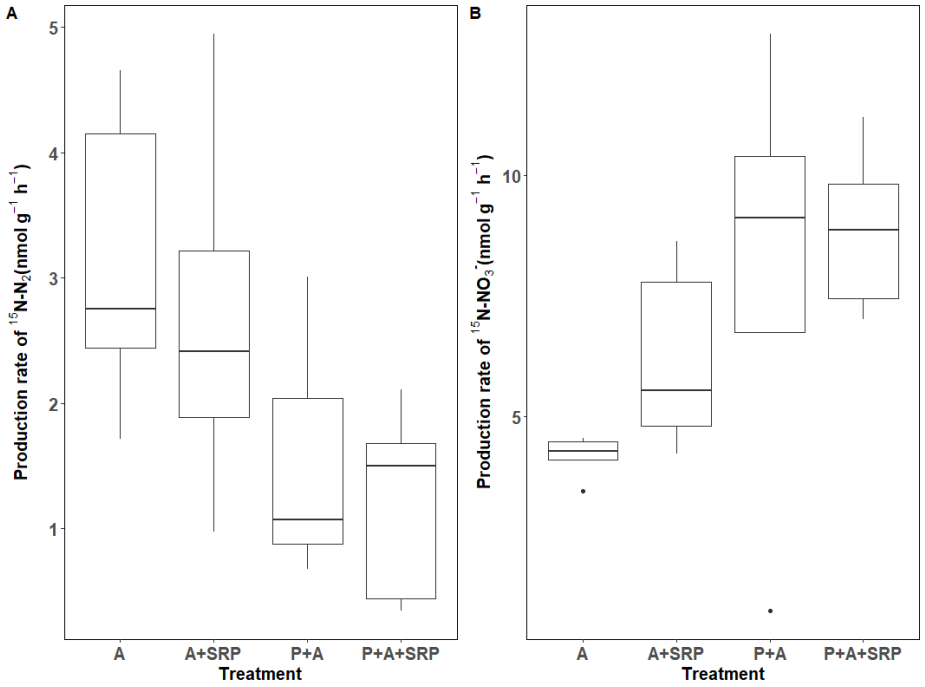

Figure 3.7. Production rates of $^{15}N\text{-}N_2$ and $^{15}N\text{-}NO_3^-$ under different $^{15}NH_4^+$ and SRP treatments for the river Wylye (chalk-based gravel dominated riverbed).

Table 3.8. Results from likelihood ratio test on linear mixed effect models testing the effect of treatment on the degree of nitrification efficiency.

River	Dependent variable	Independent variable	Df	$\chi 2$	*p*-value
Lambourn	efficiency	treatment	3	10.11	0.02
Darent	efficiency	treatment	3	4.19	0.24
Wylye	efficiency	treatment	3	10.35	0.02
Stour (2)	efficiency	treatment	3	13.5	<0.01
Stour (1)	efficiency	treatment	3	9.15	0.03
Marden	efficiency	treatment	3	0.32	0.96
Medway	efficiency	treatment	3	14.33	<0.01
Nadder	efficiency	treatment	3	31.82	<0.01

Sediment slurries from four rivers (the rivers Wylye, Nadder, Marden and Medway) were further examined for the influence of SRP on nitrite oxidation. Among them, the rivers Wylye and Nadder have shown increases in the degree of nitrification efficiency with a preincubation of SRP. While the other two rivers were chosen because a preincubation with SRP has either decreased (the river Medway) or not affected (the river Marden) the degree of nitrification efficiency. The production rate of $^{15}NO_3^-$ in preincubation treatments (treatments P+N and P+N+SRP) increased significantly when compared with $^{15}NO_2^-$ solely treatment (treatment N) ($p = 0.02$ and $p = 0.01$, respectively, Figure 3.8). While adding SRP without preincubation (treatment N+SRP) has no significant influence on the production rate of $^{15}NO_3^-$ ($p = 0.13$, Figure 3.8). These results indicated that a preincubation with SRP can selectively accelerate the nitrite oxidation, thus increasing the production of nitrate and the degree of the nitrification efficiency in some sediment slurries.

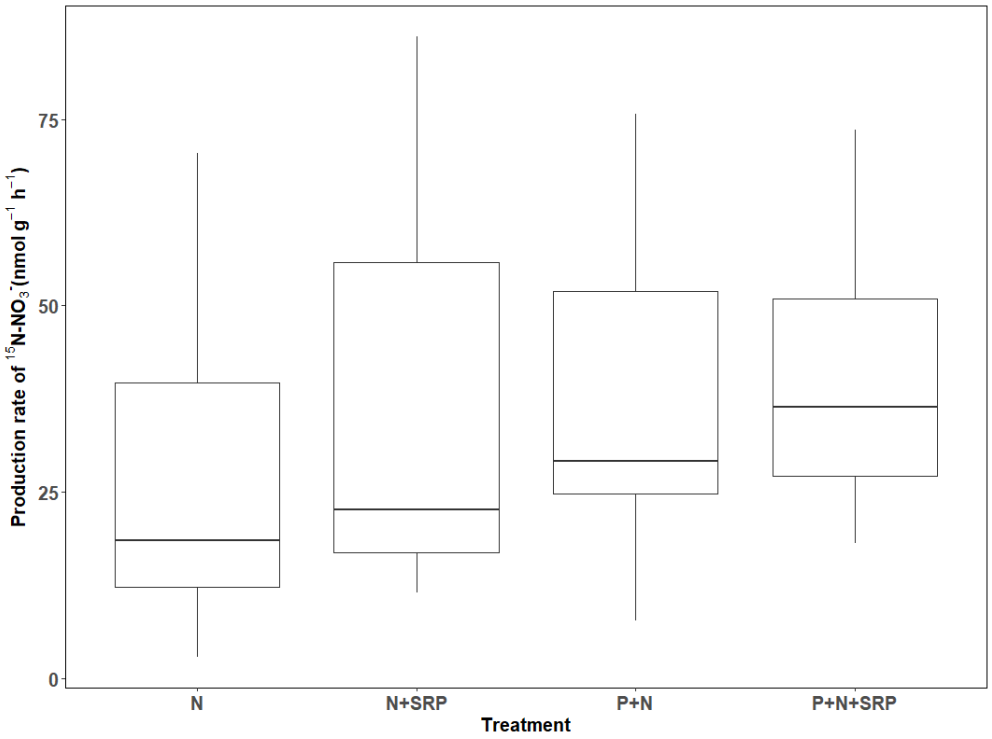

Figure 3.8. Production rate of $^{15}N\text{-}NO_3^-$ under different $^{15}NO_2^-$ and SRP treatments in oxic slurries from four rivers.

The different effects of SRP on the degree of nitrification efficiency might be caused by the different availability of the SRP in the sediment. During the experiment, the SRP concentration decreased rapidly in the slurries (Figure 3.9) most likely through adsorption (Hanrahan et al. 2003), precipitation (Williams et al. 1971) or bounded assimilation into biofilms, but the magnitude of decrease varied between the different riverbed sediments. SRP decay coefficient was calculated based on the log transformed SRP concentration (in treatment $^{15}NH_4^+$+SRP) changes over time (the first 3 h) (Figure 3.10). During the experiments, the availability of SRP differed between the riverbed sediments and the level of treatment was not consistent across the slurries, i.e., SRP was not at steady-state, thus making it difficult to quantify the effect of SRP on the degree of nitrification efficiency in batch incubations.

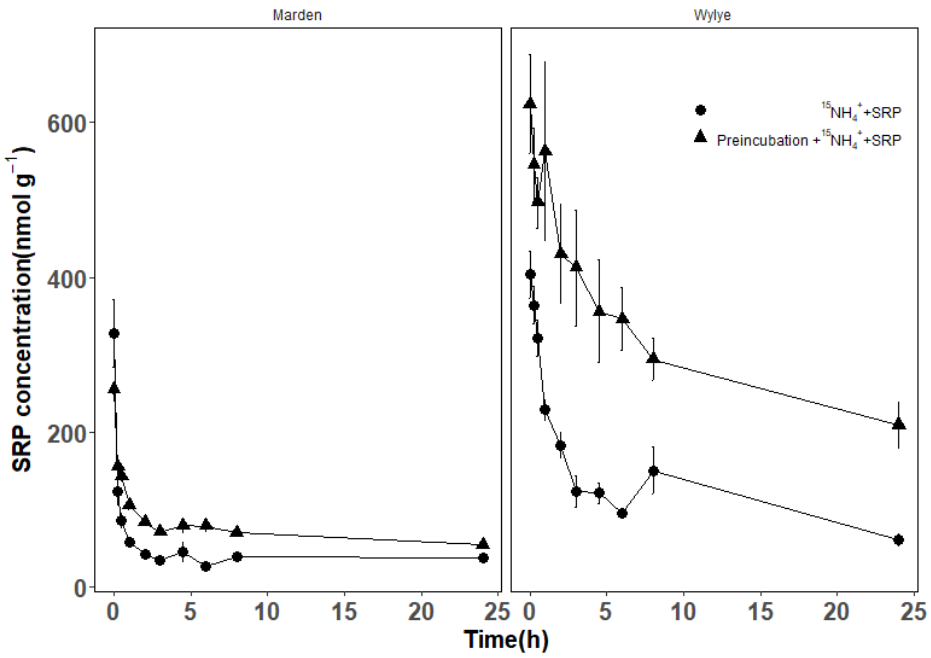

Figure 3.9. SRP concentration changes with time in $^{15}NH_4^+$ +SRP (A+SRP) and Preincubation+$^{15}NH_4^+$ +SRP (P+A+SRP) treatments in riverbed slurries of Marden and Wylye.

(Data are mean values ± 1 standard error (n = 5)).

Total inorganic phosphorus pool and organic phosphorus concentration for the sediments were then analysed to further tracing the fate of the decreased SRP in the sediment. However, the results showed that the background inorganic phosphorus pool and organic phosphorus concentration were far higher than the amount of SRP that added into each sample (500 μM/~483nmol g^{-1})) (Figure 3.11), making it impossible to trace the fate of the SRP in the riverbed sediments.

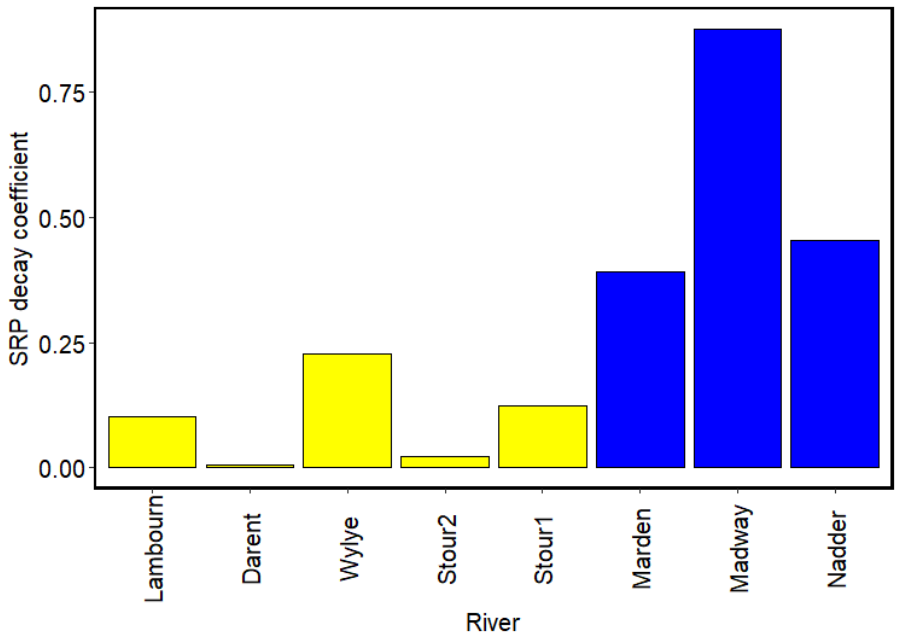

Figure 3.10. The decay coefficient of SRP in oxic slurries across eight riverbeds.

(SRP decay coefficient was calculated based on the log transferred SRP concentration changes over time (the first 3 h). Yellow represents gravel-dominate riverbed and blue represents sand-dominated riverbed).

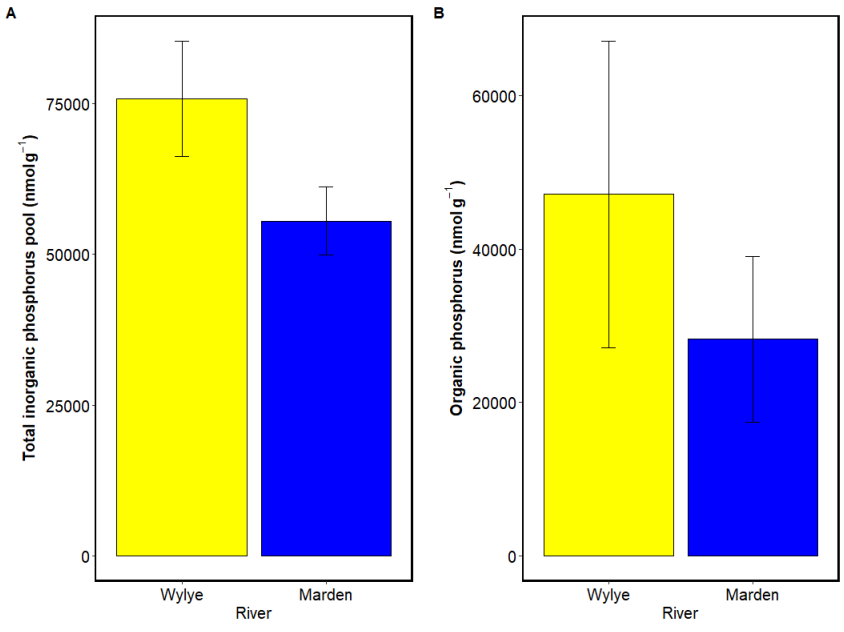

Figure 3.11. Total inorganic phosphorus pool (A) and organic phosphorus content (B) in riverbed sediments from river Marden and Wylye.

(Data are mean values ± 1 standard error (*n*=10)).

3.4. Discussion

The ^{15}N tracer experiments and molecular analyses confirmed the co-existence of aerobic ammonia oxidation, anammox and nitrite oxidation in these permeable, oxic riverbeds. Both anammox and nitrite oxidation are dependent on the nitrite that is generated by aerobic ammonia oxidation. Although the total rate of ammonia oxidation remained relatively constant across the gravel and sand riverbeds (10.06 and 13.23 nmol g^{-1} h^{-1}, respectively), the degree of nitrification efficiency varied significantly (Figure 3.1). The degree of nitrification efficiency was higher in sands, along with a lower contribution from anammox to N_2 production (*ra*), and was maximal where anammox was absent, suggesting potential competition between aerobic nitrite oxidation and anammox for nitrite (Kuenen 2008).

The degree of nitrification efficiency was positively correlated with the abundance of *nxr*B gene, suggesting that differences in the degree of nitrification efficiency across the riverbeds may be related to NOB. High temperature (Hellinga et al. 1998), high ammonia (Vadivelu et al. 2007), high nitrite/nitrous acid (Vadivelu et al. 2006, Wang et al. 2014), high salt (Ye et al. 2009), and low dissolved oxygen concentrations (Blackburne et al. 2008, Ma et al. 2009, Ma et al. 2015) have been identified to selectively inhibit or limit NOB growth in waste water treatment reactors, leading to nitritation/anammox or nitritation/denitrification, i.e., partial nitrification prior to the reduction of NO_2^- to N_2 gas. Here, however, our results showed a decrease in the degree of nitrification efficiency as porewaters became more oxidized, suggesting that competition for nitrite between NOB and anammox might be the main factor influencing the degree of nitrification efficiency across our riverbeds.

The abundance of *Nitrospira* was 1-2 orders of magnitude greater than *Nitrobacter*, which may imply a competitive advantage of *Nitrospira* over *Nitrobacter* in

these rivers. The degree of nitrification efficiency was also positively correlated with the ratio of the relative abundance of *Nitrospira* to *Nitrobacter* (r_s=0.62, p<0.01), further suggesting that the degree of nitrification efficiency across the riverbeds was mainly driven by the abundance and the distribution of *Nitrospira*. Similar to our results, the predominant role of *Nitrospira* over *Nitrobacter* in nitrite oxidation has been found in paddy soils (Wang et al. 2015). It has also been reported that *Nitrospira* is more likely to dominate nitrite oxidation under both low ammonia and nitrite concentrations (Blackburne et al. 2007). In our riverbeds, the low porewater nitrite concentrations (1.06-6.83µM) may provide an ideal environment for *Nitrospira*.

Furthermore, comammox *Nitrospira amo*A gene abundance correlated well with *Nitrospira nxr*B gene abundance and represented about 6%-21% of the *Nitrospira nxr*B gene abundance (Figure 3.3). As genomic copy numbers of *nxr*B varied from two to six copies in different *Nitrospira* (Pester et al. 2014), while only one copy of *amo*A and *nxr*B per genome is present in comammox *Nitrospira* (Daims et al. 2015, Palomo et al. 2018), comammox *Nitrospira* may represents a higher proportion of *Nitrospira* in these rivers. As far as we know, this is the first report of comammox *Nitrospira* in oxic riverbeds, where this finding suggests that it may play an important role in conserving fixed nitrogen. For example, the presence of comammox *Nitrospira* may help explain high nitrification efficiencies as ammonia would be oxidised intracellularly completely through to NO_3^-, avoiding the release of NO_2^-, and thereby its potential oxidation by anammox bacteria. Also, direct oxidation of $^{15}NH_4^+$ to $^{15}NO_3^-$ by comammox *Nitrospira* may contribute to the heterogeneity in the ^{15}N-labelling of the substrate pools in the oxic $^{15}NH_4^+$ oxidation experiments (Jensen et al. 2009, De Brabandere et al. 2014).

The contribution from anammox to N_2 production (*ra)* was higher in gravel-dominated riverbeds and, further, positively correlated with the abundance of *hzs*B gene

(r_s = 0.30, p = 0.04, Table 3.7). The separation between *hzs*B and *nxr*B (Figure 3.5) suggests competition between anammox and NOB for nitrite. The production of ^{15}N-N_2 in the oxic $^{15}NH_4^+$ oxidation experiments, suggests that aerobic ammonia oxidation and anammox and/or denitrification are co-contributing to the removal of fixed nitrogen in these oxic riverbeds. The affiliation of AOA/AOB and anammox bacteria was also reflected in their correlated abundances, as well as their clustering in the RDA analysis (Table 3.5 and Figure 3.5). Furthermore, the contribution from anammox to N_2 production (*ra*) was positively correlated with the abundance of *amo*A (r_s=0.51, p<0.01, Table 3.7), further hinting at the potential affiliation between anammox and AOA/AOB. In these oxic riverbeds, aerobic ammonia oxidation competes for 8% of the oxygen with microbial respiration, making the oxygen limited in the aggregates supporting anammox. Furthermore, the aerobic ammonia oxidation can provide nitrite to sustain the anammox bacteria.

The AOA *amo*A gene was more abundant than its AOB variant in all riverbeds, indicating the predominant role of AOA in these riverbeds. In this sense, the findings differ from the observation of a dominant role for AOB in the oxidation of ammonia in muddy lake sediments (Zhu et al. 2013). The availability of ammonia has been shown to govern niche separation in AOA and AOB in sediments and it has been proposed that AOA favour low ammonia, unfertilized soils, while AOB favour high ammonia-based fertilized soils (Martens-Habbena et al. 2009, Verhamme et al. 2011, Hink et al. 2018). Also, the AOA have been found to be better adapted to relatively high pH, for example, in alkaline soils (Wang et al. 2015). The relatively low ammonium concentration and slightly higher pH, especially in gravel-dominated riverbeds on the chalk, may provide an ideal environmental for AOA. Although the AOA *amo*A gene was more abundant than its AOB variant in all rivers, the estimates of cell-specific activity showed that the

contribution of AOB to aerobic ammonia oxidation is also important. The abundance of the *hzs*B gene was also positively correlated with porewater pH and nitrite, indicating that anammox prefers sediment with higher nitrite concentrations, as previously suggested (Meyer et al. 2005, Zhu et al. 2013, Lansdown et al. 2016).

Spearman's correlation test showed a positive correlation between the degree of nitrification efficiency and riverbed porewater SRP concentration ($r(s)$=0.51, $p < 0.01$), suggesting that phosphorus may be related to the degree of the nitrification efficiency. A preincubation with SRP selectively increased the degree of nitrification efficiency in the rivers Wylye and Nadder. $^{15}NO_2^-$ oxidation experiment with a preincubation with SRP further indicated that a preincubation with SRP can selectively accelerate the nitrite oxidation, thus increasing the production of nitrate and the degree of nitrification efficiency in some sediment slurries. This result is consistent with the finding that a higher SRP concentration can stimulate nitrite oxidation in agricultural soils and an activated sludge plant (Purchase 1974, Nowak et al. 1996). However, as SRP was not at steady-state when conducting these experiments, it was difficult to quantify and explain the different effects of SRP on the degree of nitrification efficiency in batch incubations.

In summary, results in this chapter show a clear gradient in the degree of nitrification efficiency across oxic riverbeds, that was related primarily to differences in the abundance of NOB where *Nitrospira* dominates the NOB and separates from anammox. The confirmed presence of comammox *Nitrospira* in oxic riverbeds may also significantly enhance the degree of nitrification efficiency, as complete nitrification in a single organism results in nitrite being concealed from anammox bacteria. Anammox therefore appears to be tightly affiliated with AOA and AOB and contributes to the removal of fixed nitrogen in oxic, permeable riverbeds. A preincubation of SRP is likely

to stimulate nitrite oxidation in some riverbeds thus increasing the degree of the nitrification efficiency.

Chapter 4 : Community structures of AOM, anammox bacteria and NOB across the oxic riverbeds

In chapter 3 I presented the nitrification efficiency and the abundance of the main microorganisms that drives the degree of nitrification efficiency, now I am going to focus on the identification of the microorganisms that related to the degree of nitrification efficiency in these riverbeds. Based on Illumina MiSeq amplicon sequencing, the identifications and community structures of AOA, AOB, anammox bacteria, NOB and comammox *Nitrospira* across these twelve oxic riverbeds were analysed in this chapter. Community structures of AOA and AOB were investigated by sequencing their *amo*A (ammonia monooxygenase subunit A) genes. The AOB *amo*A gene sequences obtained from these oxic riverbeds were all assigned to *Nitrosospira*, while the AOA *amo*A gene sequences were closely related to *Nitrosopumilus maritimus*, *Nitrosophaera viennensis* and some *amo*A sequences from uncultured archaea soils or WWTP. Anammox bacteria communities were assessed by amplicon sequencing 16S rRNA, *hzo* (hydrazine oxidoreductase) and *hzs*B (hydrazine synthase beta subunit) genes. Phylogenetic analyses of all these three genes showed that most of the anammox sequences were closely affiliated to *Candidatus* Brocadia. Community structure of NOB was determined by sequencing the *Nitrospira nxr*B (nitrite oxidoreductase subunit B) gene, which reveal that *Nitrospira nxr*B gene sequences mainly clustered with *Nitrospira moscoviensis and Nitrospira marina* species. Sequencing of the comammox *Nitrospira amo*A gene showed the comammox *Nitrospira* sequences clustered with *Candidatus* Nitrospira nitrificans, *Candidatus* Nitrospira inopinata and uncultured bacteria clones from groundwater-fed rapid sand filters in Denmark, Clade B comammox *Nitrospira* make up 79.5%-94.7% of the comammox abundance in these rivers and are more abundant than clade A comammox

Nitrospira. These results indicated that these permeable, oxic riverbeds are likely to have selected for distinct nitrification and anammox communities. pH and SRP concentration were the main factors that influence the community structure of AOB, while the community structure of AOA was mainly driven by ammonium concentration. Nitrite concentration was the main factor that influence the community structure of *Nitrospira* and comammox *Nitrospira.* The community structure of anammox was influenced by ammonium and nitrite concentrations.

4.1. Introduction

In chapter 3 the abundance of the main microorganisms that related to the degree of nitrification efficiency were analysed. To further understand the community structure that might help explain the variation in nitrification efficiency across the 12 riverbeds, the community structures of the microorganisms should be investigated.

Both ammonia oxidizing bacteria and archaea (AOB and AOA) can contribute to the aerobic oxidation of ammonia to nitrite. The AOB mainly consist of species from the genus *Nitrosococcu*s, belonging to the class 'Gammaproteobacteria' and *Nitrosomonas* and *Nitrosospira* genera belonging to class 'Betaproteobacteria' (Purkhold et al. 2003). Whilst AOB from Gammaproteobacteria are only typically observed in the marine environment, Betaproteobacteria AOB are widely distributed in diverse habitats, such as freshwater marsh wetland (Lee et al. 2014), estuaries (Li et al. 2018), aquaculture ponds (Lu et al. 2016, Zhou et al. 2017), lakes (Wu et al. 2010) and paddy soils (Wang et al. 2014).

The archaea responsible for aerobic ammonia oxidation to nitrite were classified into the phylum Thaumarchaeota (Pester et al. 2012). More than ten strains have been isolated so far and AOA are divided into four clusters: the *Nitrosopumilus* cluster (1.1a), the *Nitrosotalea* cluster (1.1a-associated), the *Nitrososphaera* cluster (1.1b) and the *Nitrosocaldus* cluster (ThAOA) (Pester et al. 2012, Liu et al. 2017). The widespread distribution of AOA has then been confirmed in marine water columns and sediments (Francis et al. 2005, Lam et al. 2009), freshwater lake sediments (Herrmann et al. 2009, Wu et al. 2010, Hampel et al. 2018) and estuaries (Jin et al. 2011).

The oxidation of nitrite to nitrate is primarily accomplished by bacteria that belong to the unrelated genera *Nitrobacter*, *Nitrococcus*, *Nitrospina* and *Nitrospira*. *Nitrospira* is the most diverse and widespread group of NOB and *Nitrospira* is regarded as more

important in WWTP and aquaria than *Nitrobacter* (Daims et al. 2001, Pester et al. 2014). *Nitrospira* consists of at least six phylogenetic lineages (Pester et al. 2014). Selected species within the *Nitrospira* genus include *Nitrospira marina* isolated from ocean water, *Nitrospira defluvii* and *Nitrospira japonica* isolated from activated sludge, *Nitrospira moscoviensis* isolated from heating pipes and *Candidatus* Nitrospira inopinata (comammox) in hot groundwater (56 °C) (Daims et al. 2015). The distributions of *Nitrospira* populations in WWTPs were caused by affinities of substrates and relationships with AOB (Maixner et al. 2006, Ushiki et al. 2017). Nitrite concentration has also been reported to drive the community structure of *Nitrospira* and it has been suggested that higher nitrite concentrations (5 mg NO_2^- L^{-1} vs. 0.1 mg NO_2^- L^{-1}) select for *Nitrospira delfluvii* but supressed *Nitrospira moscoviensis* (Maixner et al. 2006).

At least five genera (*Candidatus* Brocadia, *Candidatus* Kuenenia, *Candidatus* Scalindua, *Candidatus* Anammoxoglobus and *Candidatus* Jettenia which all branch deeply within the Plantomycetes phylum) and 22 species have been identified using culture-independent molecular techniques (Hu et al. 2011, Sonthiphand et al. 2014, Zhou et al. 2018). Anammox bacteria have a widespread distribution in various natural habitats. Among the anammox bacteria that have been described to date, *Candidatus* Scalindua appear to be the most widespread genus in marine ecosystems (Penton et al. 2006, Rich et al. 2008, Li et al. 2010), while *Candidatus* Brocadia and *Candidatus* Kuenenia appear to be more common in freshwater, terrestrial ecosystems and the reservoirs (Hu et al. 2011, Shen et al. 2017). The coexistence of different groups of anammox was normally found in various habitats with certain groups dominated in specific habitats (Humbert et al. 2012, Shen et al. 2015).

Recently, complete ammonia oxidizing bacteria (comammox) that possess both ammonia and nitrite oxidizing genes and are therefore capable of the complete oxidation

of ammonia to nitrate (comammox) has been identified (Daims et al. 2015, van Kessel et al. 2015, Kits et al. 2017). Comammox *Nitrospira* contain novel *amo*A genes encoding ammonia monooxygenase (AMO), which is distinct from the *amo*A in AOB and AOA. They also contain genes encoding nitrite oxidoreductase (NXR), the key enzymes of bacteria nitrite oxidation, but these genes are not distinct from classical NOB (Camejo et al. 2017, Pjevac et al. 2017, Palomo et al. 2018). All known comammox organisms belong to *Nitrospira* lineage II (Daims and Wagner 2018) and they have been divided into clade A and clade B comammox *Nitrospira* (Palomo et al. 2018). *Candidatus* Nitrospira nitrosa, *Candidatus* Nitrospira nitrificans, *Candidatus* Nitrospira inopinata and *Nitrospira* sp. strain Ga0074138 are the main comammox-like *Nitrospira* bacteria identified to date (Camejo et al. 2017).

In this chapter, community structures of AOM, anammox bacteria, NOB and comammox *Nitrospira* across these 12 oxic riverbeds were evaluated. The aims are: (i) to explore the taxonomic diversity of the microorganisms across these rivers, (ii) to find out the key factors that shaping the community structures, (iii) to find out the community structure that might help explain the variation in nitrification efficiency.

4.2. Materials and Methods

4.2.1. Collection of sediments and DNA extraction

Sediment collection and Sediment DNA extraction was described in Chapter 3.

4.2.2. Illumina sequencing

Amplicon libraries for the bacterial 16S rRNA gene, anammox 16S rRNA gene, *hzo* gene, *hzs*B gene, AOA *amo*A gene, AOB *amo*A gene, *Nitrospira nxr*B gene and comammox *Nitrospira* specific amoA gene were prepared using primers containing the

same target region as the qPCR primers (see Chapter 3) but flanked with Illumina Nextera overhang sequences. A 28-cycle (bacterial 16S rRNA gene) or 30-cycles (all other genes) PCR was conducted using their specific annealing temperatures (see Chapter 3, Table 3.1) in a 96 Well Thermal Cycler (Applied Biosystems). Amplicons were then purified using AMPureXP SPRI beads (Beckman Coulter) and then an 8-cycle index PCR was conducted to attach dual indices and Illumina sequencing adapters using the Nextera XT Index Kit (Illumina). Amplicons were again purified using AMPureXP SPRI beads and then quantified using a Quant-iT PicoGreen dsDNA assay Kit (Life Technologies) on a NanoDrop 3300 fluorospectrometer (Thermo Scientific). Amplicons were then pooled in equimolar concentrations and then purified and concentrated using the GenElute PCR Clean-up Kit (Sigma-Aldrich). The amplicon libraries were quality checked using a DNA 1000 kit on a 2100 Bioanalyser (Agilent) before sequencing was performed on the Illumina MiSeq platform using a MiSeq reagent kit V3 (2×300 bp) at The Earlham Institute (Norwich, UK).

4.2.3. Sequences analyses

The sequencing reads were demultiplexed by the Nextera XT indexes and analysed within BioLinux as described in (Dumbrell et al. 2016). The reads were quality trimmed using Sickle (Joshi and Fass 2011), error corrected using SPAdes (Bankevich et al. 2012) with the BayesHammer algorithm (Nikolenko et al. 2013) and pair-end aligned using PEAR (Zhang et al. 2013) within PANDAseq (Masella et al. 2012). The reads were dereplicated, sorted by abundance and clustered into operational taxonomic units (OTUs) using the VSEARCH centroid algorithm (Rognes et al. 2016) at the 0.97 level. All singleton OTUs were removed, along with all chimeric sequences using denovo and reference based (for 16S rRNA reads) chimera checking with UCHIME (Edgar et al.

2011). Bacterial and anammox 16S rRNA centroid sequences from each OTU were assigned taxonomic identities with the RDP classifier (Wang et al. 2007). Phylogenies were constructed for the most abundant OTUs (with sequences numbers representing greater than 0.1% of the total sequences numbers by using neighbour-joining method (Saitou and Nei 1987) with representative genes in MEGA7 (Kumar et al. 2016). For the 16S rRNA gene sequences, multiple sequences alignment was performed using MUSCLE (Multiple Sequence Comparison by Log-Expectation) (Edgar 2004). For the functional genes, sequence alignment was performed on condon-aligned deduced amino acid sequences using MUSCLE and 1000 replicates were used to generate the bootstrap values.

4.2.4. Community structure analyses

Sequences and community analyses were conducted with the 'vegan' package (Oksanen et al. 2017) in R. To compare the relative diversity of communities in each river and to estimate the completeness of sampling. Numbers of sequences and OTUs for each river were calculated based on the sum of the 3 replicates from each river and the sample-size-based Rarefaction/Extrapolation (R/E) curves were generated using 'iNEXT' and 'ggiNEXT' functions in the 'iNEXT' (Hsieh et al. 2016) and 'ggplot2' (Wickham 2016) packages in R. The species richness estimator (Chao1) and diversity index (Shannon) were generated for each river using 'diversity' and 'estimateR' function in the 'vegan' package, respectively. The coverages of sequencing libraries were calculated as described by (Dang et al. 2008), using $C = [1 - (n_1/N)] \times 100$, where n_1 is the number of unique OTUs, and N is the total number of sequences in a library.

Non-metric Multidimensional scaling analysis (NMDS) was used to ordinate the samples based on their distance matrices and the relative distance between the points represents the relative dissimilarity of the samples. NMDS was conducted using the

function ‘metaMDS’, where the distance matrices of the samples were evaluated by Bray-Curtis dissimilarity calculation. Environmental vectors were then fitted onto the NMDS ordination using ‘envfit’ function to evaluate influence of the environmental factors on community compositions. A permutational multivariate analysis of variance (PERMANOVA) was performed using the ‘adonis’ function at 999 permutations to test if the community compositions between gravel and sand-dominated riverbeds are significantly different. The raw reads were deposited into the NCBI Sequence Read Archive (SRA) database (Accession Number: PRJNA497462).

4.2.5. Statistical analyses

Any relationships between the relative proportions of aerobic AOB, anammox and NOB (OTUs that assigned to these groups) sequences to total bacterial 16S rRNA sequence abundance and porewater chemistries and nitrification efficiency were analysed using redundancy analysis (RDA) in the ‘vegan’ package in R (Oksanen et al. 2017).

Spearman correlation analysis was used to assess the potential correlations between environmental factors and community richness, diversity and relative abundance of clades, which were also performed in R under the in the ‘Hmisc’ package.

4.3. Results

4.3.1. Bacterial 16S rRNA community structures

A total of 828,543 bacterial 16S rRNA sequences were obtained from the riverbeds which were assigned to a total of 3,393 OTUs at a similarity threshold of 0.97. The Good's coverage estimator indicated that more than 79.2% of OTUs were picked up for this study from the samples (Table 4.1). Rarefaction curves of all these riverbeds tend to approach the saturation plateaus (Figure 4.1), indicating that the bacteria in these

riverbeds could be well-represented by this library. Chao1 richness estimator and Shannon diversity indices ranged from 2,146 to 2,862 and from 6.1 to 6.7, respectively in these riverbed samples (Table 4.1). The highest bacterial richness (Chao1) occurred in the river Medway, while the highest bacterial diversity (Shannon) occurred in the river Stour (2). Both the Shannon index and Chao 1 estimator were positively correlated with porewater soluble reactive phosphorus (SRP) concentration ($r_{(s)}$ = 0.58, p = 0.04 and $r_{(s)}$ = 0.64, p = 0.02, respectively), indicating that sediment samples from the rivers that with higher SRP concentration may support more diverse bacteria.

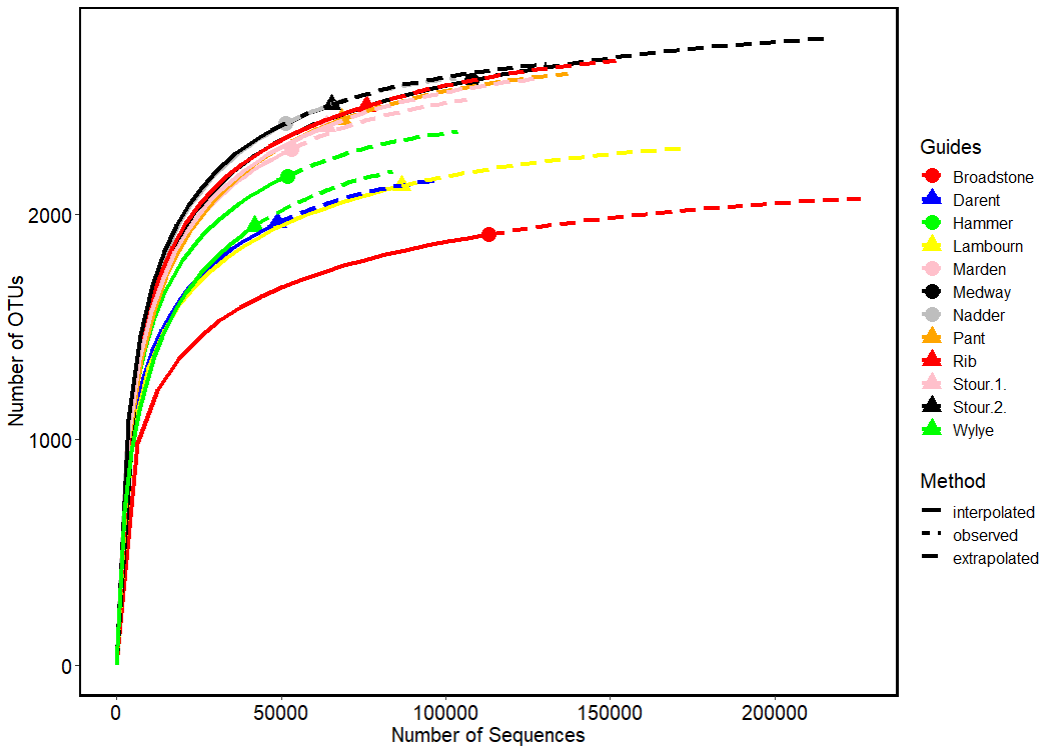

Figure 4.1. Rarefaction/Extrapolation curves of bacterial 16S rRNA sequences from different riverbeds.

(The solid lines represent the rarefaction (interpolation) curves and the dashed lines represent the extrapolation curves, the points/triangles between solid and dashed lines represent the observed sample sizes)

Table 4.1. Diversity of Bacterial 16S rRNA sequences in each riverbed.

River	No. of sequences	No. of OTUs	Shannon	Chao 1	Coverage (%)
Lambourn	86699	2124	6.28	2347.87	85.92
Darent	48822	1963	6.42	2228.47	82.88
Wylye	41911	1947	6.10	2305.82	79.20
Rib	75873	2480	6.59	2767.79	86.13
Pant	68502	2421	6.42	2689.27	84.55
Stour (2)	65331	2486	6.70	2723.05	86.73
Stour (1)	63721	2391	6.56	2685.25	84.53
Marden	53279	2291	6.62	2601.57	83.59
Hammer	51870	2171	6.55	2438.79	83.74
Medway	107945	2595	6.52	2862.07	87.90
Broadstone	113108	1912	6.12	2143.06	85.93
Nadder	51482	2403	6.58	2667.32	84.23

A total of 40 bacterial phyla were identified in these samples with RDP classifier. The relative abundances of 14 phyla that represented higher than 1% frequency in at least one riverbed are shown in Figure 4.2. Proteobacteria was the most abundant phyla in all of the samples, accounting for 35.3-55.0% of the total number of sequences. Planctomycetes and Nitrospirae accounted for 1.4-6.3% and 0.6-2.7% of the total number sequences, respectively.

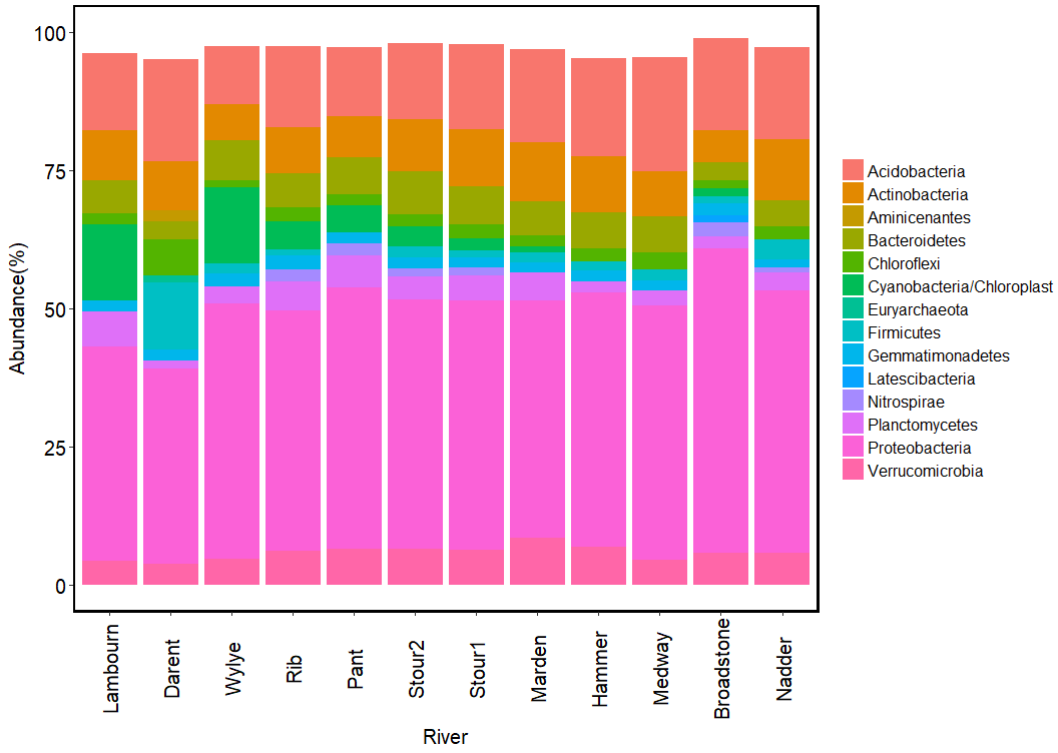

Figure 4.2. Distribution of bacteria in all riverbeds at phylum level. (Taxa represented occurred at 1% frequency in at least one sample. *Proteobacteria* was the most dominant phylum across all riverbeds).

To further understand the bacterial community structure that might help explain the variation in the degree of nitrification efficiency across the 12 riverbeds, relative proportions of AOB, anammox bacteria and NOB (OTUs that assigned to these groups) within the total bacterial 16S rRNA sequences were calculated. The RDA plot (Figure 4.3) clearly clustered the microbial communities into gravel or sand riverbeds. The distribution of NOB positively correlated with AOB ($r_s = 0.73$, $p < 0.01$), while being separated from anammox (Figure 4.3). The degree of nitrification efficiency was positively correlated with the proportion of NOB in the total bacterial community ($r_s = 0.54$, $p < 0.01$).

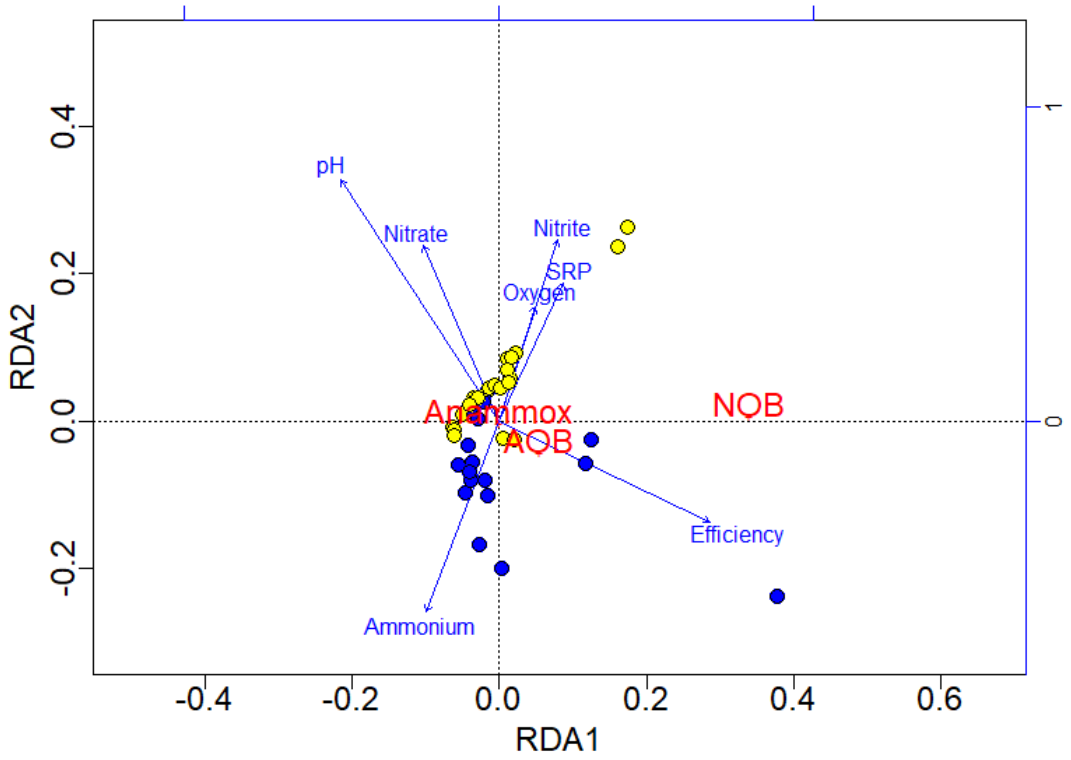

Figure 4.3. Redundancy analysis plot of the relationship between relative sequence proportions of AOB, anammox and NOB and nitrification efficiency and porewater chemistries across in gravel (yellow) and sand (blue) riverbeds.

(The first and second canonical axes represented 98.3% and 1.6% of the variation, respectively. High degree of nitrification efficiency correlates with a high proportion of NOB in total bacteria community).

4.3.2. Community structures of anammox bacteria across riverbeds

To investigate the biodiversity of anammox bacteria in these riverbeds, the 16S rRNA gene was sequenced using anammox-specific 16S rRNA primer. A total of 1,625,551 sequences were obtained, which were assigned to a total of 38 OTUs at a similarity threshold of 0.97. For the acidic river Broadstone, where no anammox activity was observed, only 14 of these OTUs were detected (Table 4.2). Rarefaction curve of the river Broadstone also shows an extremely low sequence depth (Figure 4.4), so the river

Broadstone was omitted from the further community analysis. Rarefaction curves of the other rivers tend to approach the saturation plateau (Figure 4.4), indicating that these riverbeds were sampled sufficiently. The Good's coverage estimator indicated that more than 85.7% of OTUs were picked up from the other riverbeds, further indicating that this library has captured the majority of the anammox 16S rRNA sequence types in the riverbeds with the primers used. The Chao1 richness estimator predicted the presence of 17-31 OTUs in each location, with Shannon diversity indices ranging from 0.29 to 1.76. The highest richness occurred in the river Rib, along with the highest diversity. There was a positive correlation between Chao 1 richness and contribution of anammox to N_2 production (*ra*) ($r_{(s)}$ = 0.58, p = 0.04), indicating that the rivers that with a higher *ra* support more diverse anammox bacteria.

Table 4.2. Diversity of Anammox 16S rRNA sequences in each riverbed.

River	No. of sequences	No. of OTUs	Shannon	Chao 1	Coverage (%)
Lambourn	146222	21	1.14	22.00	90.48
Darent	75900	21	1.01	21.75	85.71
Wylye	144163	20	0.57	20.50	90.00
Rib	168546	30	1.76	30.50	93.33
Pant	148125	25	1.32	25.00	96.00
Stour (2)	161821	29	1.62	30.00	93.10
Stour (1)	212234	22	1.48	22.50	90.91
Marden	162159	19	0.29	19.50	89.47
Hammer	114194	17	1.23	17.00	94.12
Medway	158513	24	1.33	24.00	95.83
Broadstone	4145	14	0.33	15.00	78.57
Nadder	129529	21	0.46	22.50	85.71

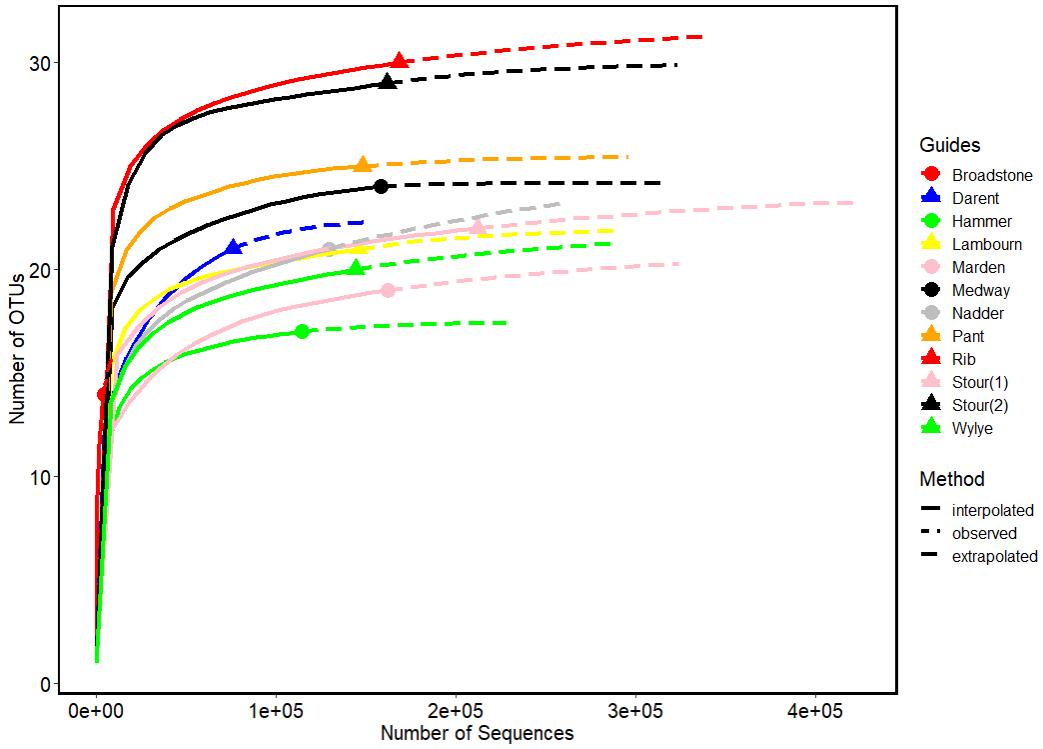

Figure 4.4. Rarefaction/Extrapolation curves of anammox 16S rRNA sequences from different riverbeds.

(The solid lines represent the rarefaction (interpolation) curves and the dashed lines represent the extrapolation curves, the points/triangles between solid and dashed lines represent the observed sample sizes)

The ordination and dissimilarity of anammox OTUs between the samples were assessed with non-metric multidimensional scaling (NMDS) analysis. NMDS ordination (without the river Broadstone) showed that the community composition in the river Hammer is different from the other rivers (Figure 4.5). The envfit analysis showed that pH and ammonium are the most important factors that influence the anammox community compositions (r^2 = 0.39, p <0.01, and r^2 = 0.37, p <0.01, respectively). PERMANOVA analysis showed that anammox community compositions between the gravel and sand-dominated riverbeds are significantly different (p < 0.01).

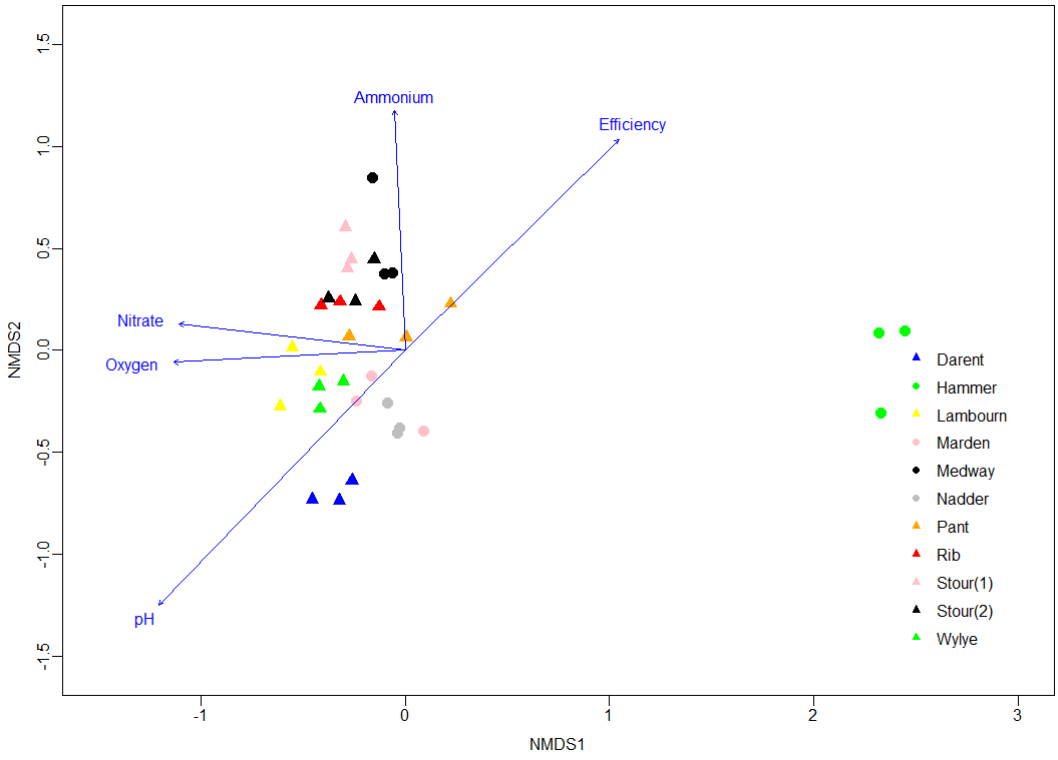

Figure 4.5. Non-metric multidimensional scaling analysis of the distributions of anammox 16S rRNA sequences based on Bray-Curtis dissimilarities.

(Dissimilarity in community composition is represented as distance in the diagram. Gravel and sand-dominated riverbed samples were mapped as triangles and circles, respectively. Rivers were mapped was different colours. Environmental factors were fitted to the ordination with arrow length proportional to the correlation between variables and ordination axes. Only vectors with $p < 0.05$ are shown. The river Broadstone was omitted as the sequences number was extremely low).

Phylogenetic analysis of anammox 16S rRNA sequences and related sequences deposited in GenBank showed that OTUs were divided into four clades (Figure 4.6). Most of the OTUs in Clade 1, Clade 2 and Clade 3 were closely affiliated to *Candidatus.* Brocadia. The dominant OTU1, represented 55.6% of the total sequences and was identical (100% sequence identity) to an uncultured clone found in sediments of the River

Seine in France. Others are identical, or very similar, to Chinese estuary sediments, wetlands, a lake in Finland and a Japanese paddy field. Interestingly, OTU17, in Clade 4, is phylogenetically distinct from other OTUs, which seems restricted to river Pant and is closely related to *Candidatus*.Scalindua. The majority OTUs are found in most riverbeds but there are some differences in their distribution. Figure 4.7 shows the relative abundances of different clades of anammox 16S rRNA in different riverbeds. Clade 1 was the most dominant clade in all of these riverbeds and varied from 61.08% in the river Darent to 99.55% in the river Hammer, while Clade 4 was only observed in the River Pant. It is noted that although the river Broadstone showed no significant anammox activity, 14 OTUs were detected. The most abundant OTU in the river Broadstone was OTU 3 and it represented 94.1% of its total sequences number. This OTU was also found in all the other rivers, and the relative abundances ranged from 0.26% (the river Hammer) to 37.99% (the river Darent). The OTU 3 belongs to Clade 2, and this clade was the second dominant clade in all other riverbeds, hinting its wide distribution in these riverbeds. However, the low gene abundance of the OUT 3 in the river Broadstone contributed a negligible anammox activity.

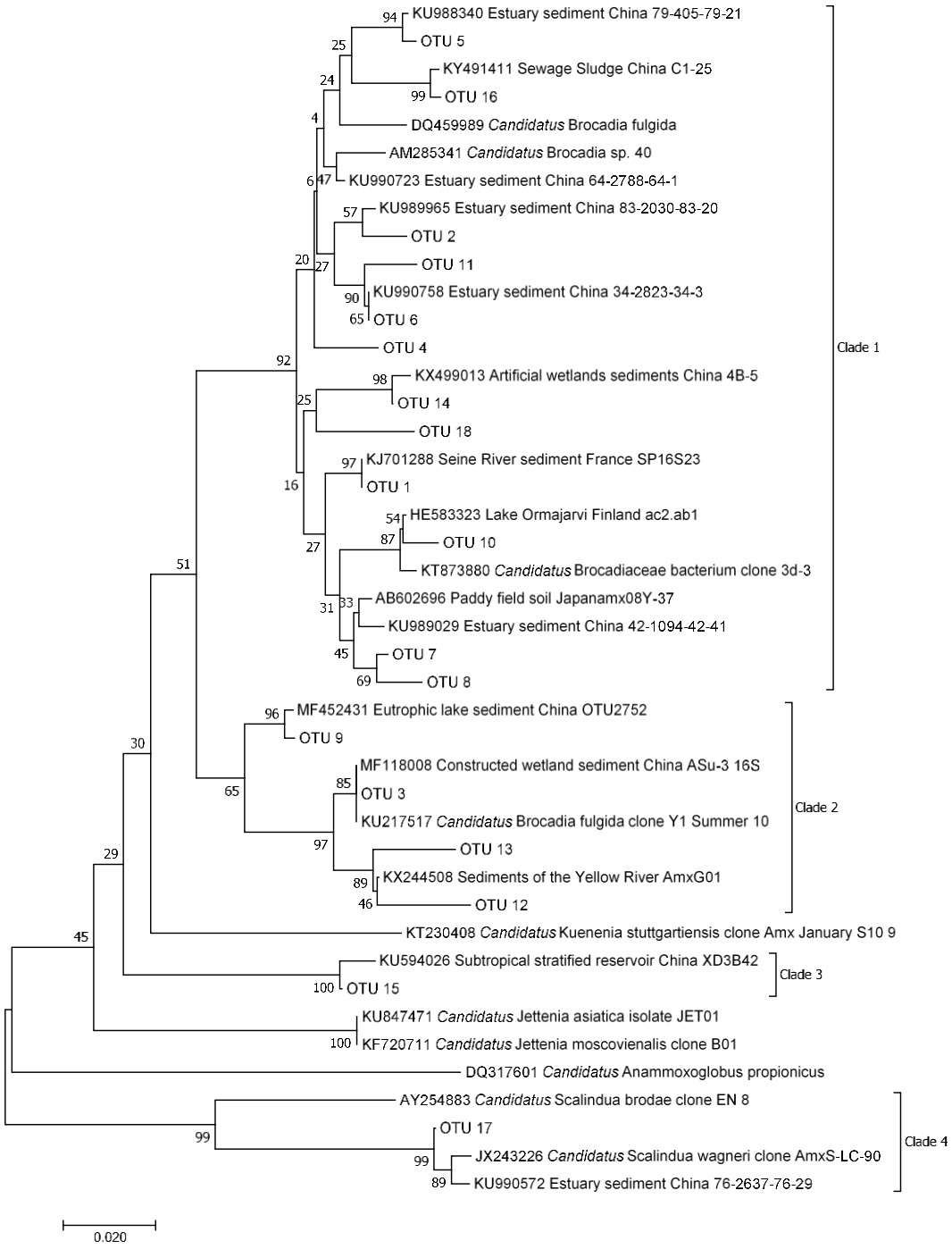

Figure 4.6. Phylogenetic analysis of the anammox 16S rRNA sequences using the neighbour-joining method.

(Tree was constructed from the 18 most abundant OTUs (OTUs that sequences numbers represent higher than 0.1% of the total sequences number). Bootstrap values are indicated at the branch nodes. The scale bar represents a 2% sequence divergence. OTUs are numbered by the order of sequence abundance, i.e., OTU 1 was the most abundant OTU).

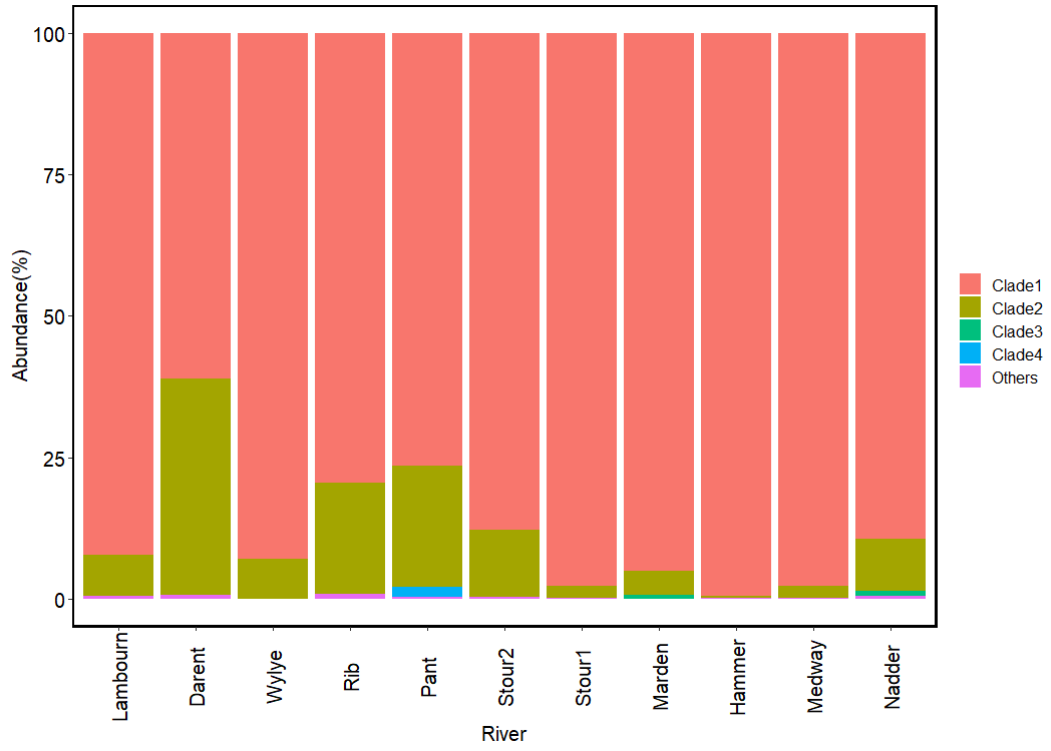

Figure 4.7. Relative abundances of anammox 16S rRNA within each clade (based on phylogenetic tree) in each riverbed.

The anammox *hzo* gene was also sequenced. A total of 871,422 sequences were obtained which were assigned to a total of 65 OTUs at a similarity threshold of 0.97. For the acidic river Broadstone, where no anammox activity was observed, only 11 OTUs were picked up (Table 4.3). Similar as the results from anammox 16S rRNA sequencing, the rarefaction curve of the river Broadstone also shows an extremely low sequence depth (Figure 4.8), so the river Broadstone was omitted from the further community analysis. Rarefaction curves of the other rivers tend to approach the saturation plateaus (Figure 4.8), indicating that these riverbeds were sampled sufficiently. The Good's coverage estimator indicated that more than 80.7% of OTUs were picked up from all the other riverbeds. The Chao1 richness estimator predicted the presence of 17-45 OTUs in each location, with Shannon diversity indices ranging from 0.45 to 1.94. Similar to the results from anammox

16S rRNA sequencing, the highest bacterial richness occurred in the river Rib, while the highest bacterial diversity occurred in the river Medway.

Table 4.3. Diversity of *hzo* gene sequences in each riverbed.

river	No. of sequences	No. of OTUs	Shannon	Chao 1	Coverage (%)
Lambourn	80966	26	1.69	36.00	80.77
Darent	63799	29	1.74	30.50	89.66
Wylye	88169	28	1.68	31.00	89.29
Rib	125185	43	1.71	45.00	90.70
Pant	67744	26	0.45	28.00	84.62
Stour (2)	88685	39	1.30	39.00	100.00
Stour (1)	85599	28	1.40	29.00	92.86
Marden	90275	24	1.21	24.00	95.83
Hammer	45059	16	1.06	16.75	81.25
Medway	73420	34	1.94	40.00	88.24
Broadstone	1331	11	0.81	12.00	81.82
Nadder	82672	29	1.43	34.00	82.76

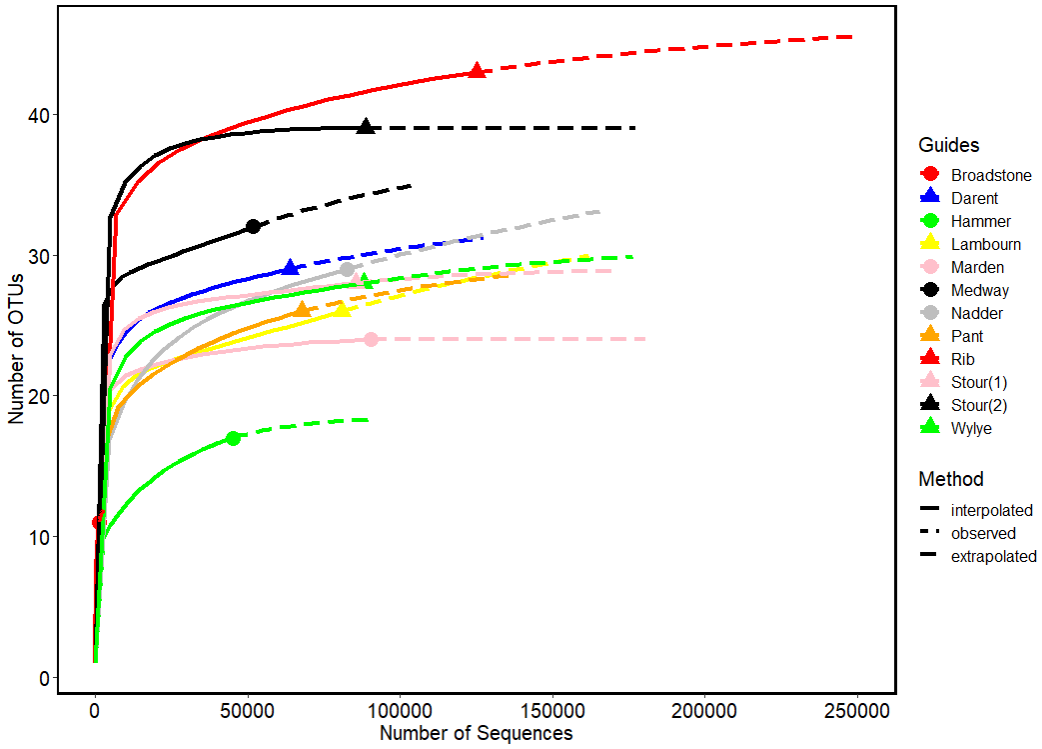

Figure 4.8. Rarefaction/Extrapolation curves of *hzo* gene sequences from different riverbeds.

(The solid lines represent the rarefaction (interpolation) curves and the dashed lines represent the extrapolation curves, the points/triangles between solid and dashed lines represent the observed sample sizes)

The plotting of NMDS (without the rivers Broadstone and Hammer) showed that the communities in the gravel-dominated riverbeds tend to cluster together (Figure 4.9). The envfit analysis showed that the ammonium and nitrite were the most important factors that influence the anammox communities ($r^2 = 0.57$, $p < 0.01$ and $r^2 = 0.46$, $p < 0.01$). PERMANOVA analysis showed no significant difference between the anammox community compositions in gravel and sand-dominated riverbeds ($p = 0.11$).

Phylogenetic analysis of *hzo* sequences showed that the OTUs could be grouped into four clusters and most of the OTUs in Clade 1, Clade 2 and Clade 3 were closely

affiliated to *Candidatus*. Brocadia (Figure 4.10). The dominant OTU1, represented 41.2% of the total sequences and has 98% sequence identity to an uncultured clone (SPhzo15) found in sediments of the River Seine in France. Others are similar to *hzo* sequences from freshwater lake sediments or estuarine sediments. OTU5 and OTU27 in Clade 4 are phylogenetically distinct from other OTUs, closely related to *Candidatus* Scalindua. Figure 4.11 shows the relative abundances of different clusters of *hzo* in different riverbeds. Sequences from Clade 1 were the most dominant in all of these riverbeds except for the river Pant and ranged from 91.99% in Medway to 99.70% in Nadder. However, Clade 4 was the most abundant clade in the River Pant and presented 91.05% of the total sequences. Different from the other riverbeds, OTU34 was the most abundant OTU in the river Broadstone. Although with a low sequences number (952), it represented 71.5% of the total sequences. It has a 97% similarity to an uncultured anammox bacterium clone (QTWAna25) in the water column of the Dongjiang River (China) (JX069733) and has a 90% similarity to OTU1 in this study. OTU34 was also observed in the rivers Hammer and Nadder, represented 0.2% and <0.01% of the total sequences number, respectively. It indicates that this OTU may prefer acidic sandy riverbeds.

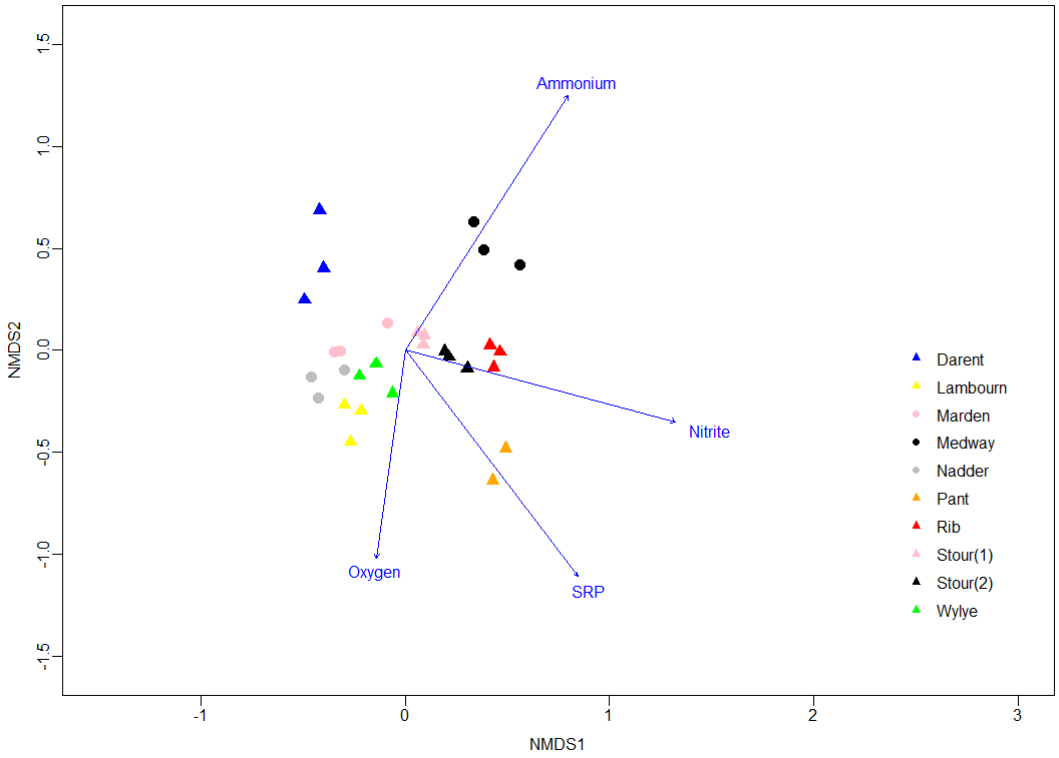

Figure 4.9. Non-metric multidimensional scaling analysis of the community structures of anammox *hzo* sequences based on Bray-Curtis dissimilarities.

(Dissimilarity in community composition is represented as distance in the diagram. Gravel and sand-dominated riverbed samples were mapped as triangles and circles, respectively. Rivers were mapped was different colours. Environmental factors were fitted to the ordination with arrow length proportional to the correlation between variables and ordination axes. Only vectors with $p < 0.05$ are shown. The rivers Broadstone and Hammer were omitted as their sequence numbers were too low.).

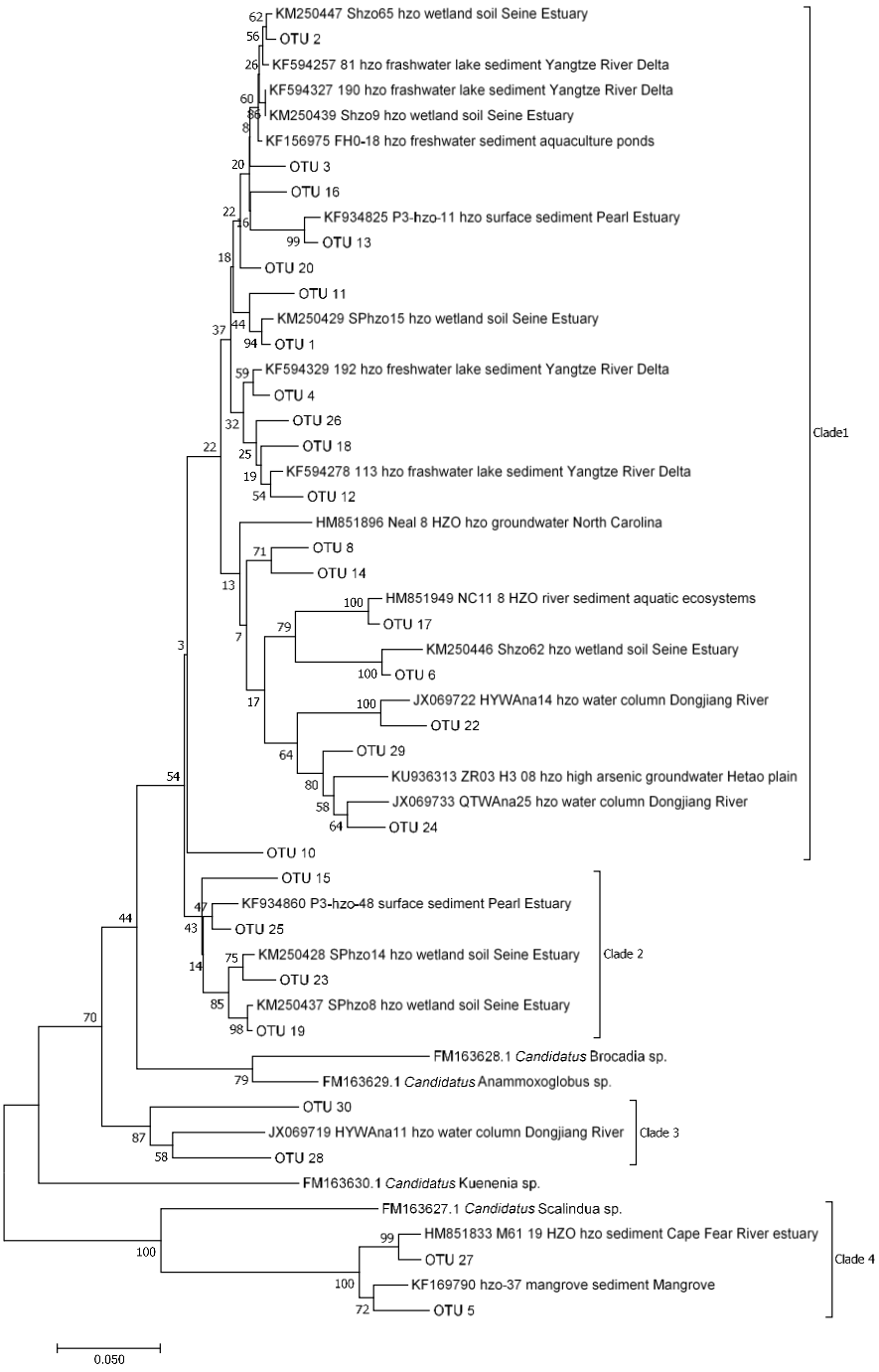

Figure 4.10. Phylogenetic analysis of the anammox *hzo* amino acid sequences using the neighbour-joining method.

(Tree was constructed from the 29 most abundant OTUs (OTUs that sequences numbers represent higher than 0.1% of the total sequences number). Bootstrap values are indicated at the branch nodes. The scale bar represents a 5% sequence divergence. OTUs were numbered by the order of sequences abundance, i.e., OTU 1 was the most abundant OTU.)

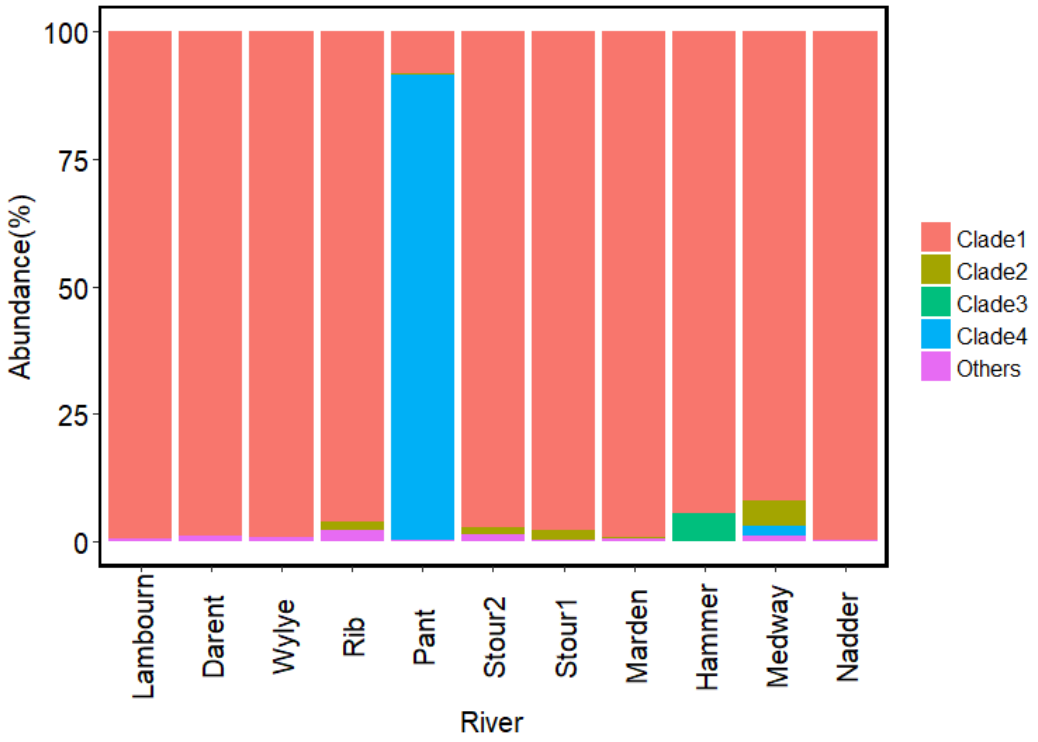

Figure 4.11. Relative abundances of anammox *hzo* within each clade (based on phylogenetic tree) in each riverbed.

Sequencing of anammox *hzsB* showed similar results to the anammox 16S rRNA gene and *hzo* gene. The total number of sequences was 656,880, which were assigned to a total of 84 OTUs at a similarity threshold of 0.97. For the acidic river Broadstone, where no anammox activity could be measured, only 6,046 of sequences were picked up (Table 4.4). In the river Hammer, where anammox activity was low, only 8,907 of sequences were picked up. This was also showed on the rarefaction curves (Figure 4.12), so these two rivers were omitted in the following analysis. The Good's coverage estimator indicated that more than 80.0% of OTUs were picked up in the other riverbeds. Similar as the findings in the anammox 16S rRNA sequencing, the rarefaction curve of the river Darent did not approach saturation (Figure 4.12), indicating that there might be some microbes remained undetermined. All other rarefaction curves tended to approach the

saturation plateaus, indicating a reasonable data volume of sequenced reads. Chao1 richness ranged from 23 to 57 and Shannon diversity indices ranged from 1.15 to 2.32.

Table 4.4. Diversity of *hzsB* gene sequences in each riverbed.

river	No. of sequences	No. of OTUs	Shannon	Chao 1	Coverage (%)
Lambourn	60926	47	1.81	54.00	82.98
Darent	16807	30	1.99	37.50	80.00
Wylye	61113	31	1.70	32.20	87.10
Rib	61287	54	2.32	57.00	94.44
Pant	59916	45	1.84	48.00	93.33
Stour (2)	91142	51	2.23	54.00	94.12
Stour (1)	92530	43	1.88	44.50	93.02
Marden	50251	25	1.50	25.50	92.00
Hammer	8907	17	1.75	32.00	64.71
Medway	61198	37	1.80	40.00	89.19
Broadstone	6046	14	1.95	19.00	64.29
Nadder	86757	23	1.15	23.00	100.00

The plotting of NMDS (without the rivers Broadstone and Hammer) showed that the anammox *hzs*B communities in the gravel-dominated riverbeds tend to cluster together (Figure 4.13). The envfit analysis showed that the nitrite was the most important factor that influence the anammox *hzs*B communities (r^2 = 0.50, p < 0.01). PERMANOVA analysis showed that anammox *hzs*B community compositions between the gravel and sand-dominated riverbeds are not significantly different (p = 0.13).

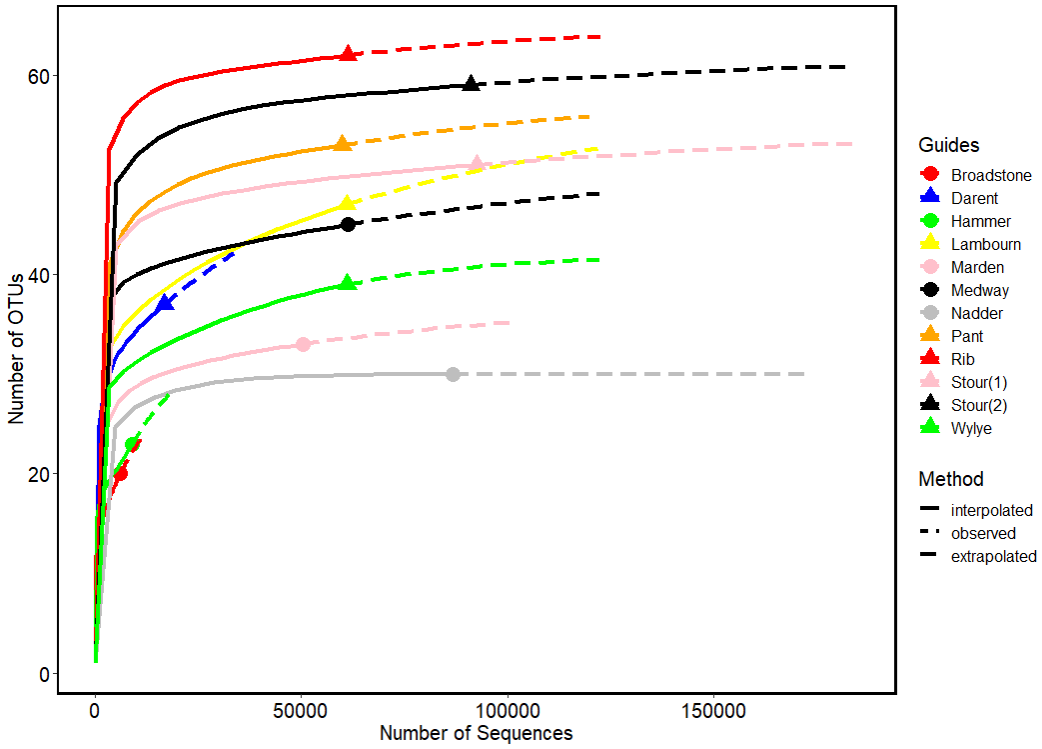

Figure 4.12. Rarefaction/Extrapolation curves of *hzs*B gene sequences from different riverbeds.

(The solid lines represent the rarefaction (interpolation) curves and the dashed lines represent the extrapolation curves, the points/triangles between solid and dashed lines represent the observed sample sizes)

The phylogeny of the *hzs*B was largely congruent with that of the 16S rRNA genes, with OTUs grouped into four clusters (Figure 4.14) and most of the OTUs in Clade 1, Clade 2 and Clade 3 were closely affiliated to *Candidatus.* Brocadia (Figure 4.10). The dominant OTU1, represented 43.2% of the total sequences with 98% sequence identity to an uncultured clone found in sediments of Three Geroge Reservior. Others were similar to the uncultured clones from paddy soils. OTUs in Clade 4 clustered with *Candidatus* Jentenia. Figure 4.15 shows the relative abundances of the different clusters of *hzs*B in the different riverbeds. Clade 1 was the most dominant clade in all of these riverbeds,

with the lowest proportion in the river Stour (1) (79.29%) and the highest proportion in the river Nadder (97.09%). Although with a low sequences number, the most abundant OTUs (OTU1 and OTU2) were also found to dominate in the river Broadstone, indicating the widespread of *Candidatus.* Brocadia in freshwater sediments.

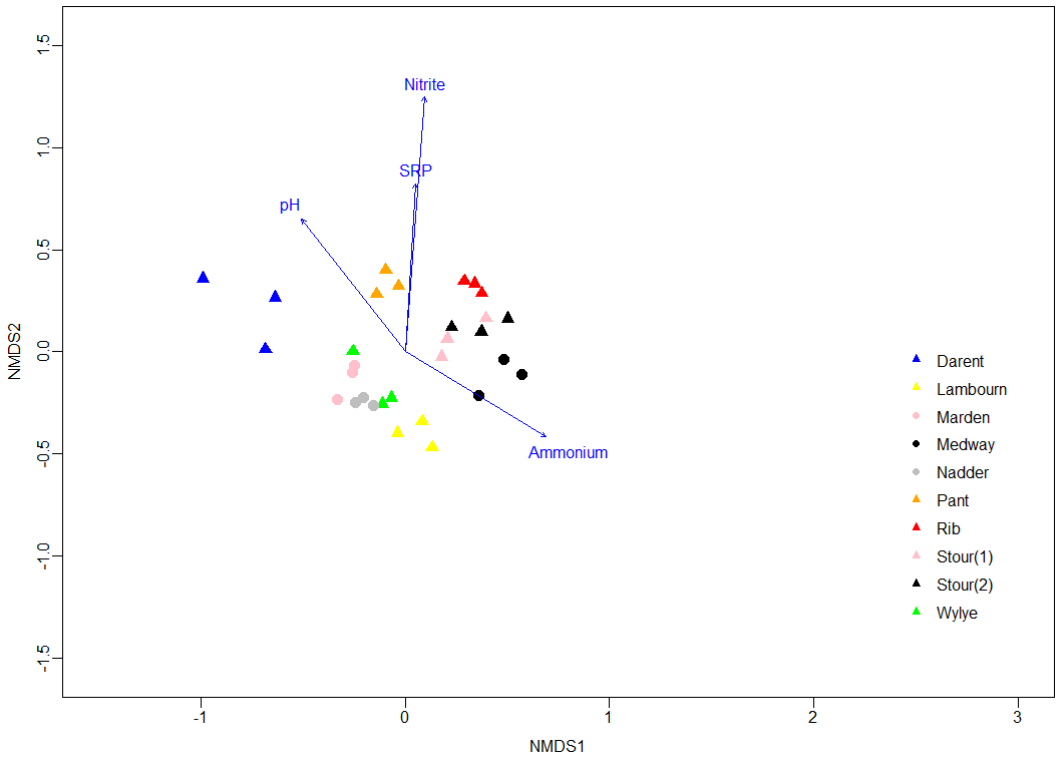

Figure 4.13. Non-metric multidimensional scaling analysis of the community structures of anammox *hzs*B sequences based on Bray-Curtis dissimilarities.

(Dissimilarity in community composition is represented as distance in the diagram. Gravel and sand-dominated riverbed samples were mapped as triangles and circles, respectively. Rivers were mapped was different colours. Environmental factors were fitted to the ordination with arrow length proportional to the correlation between variables and ordination axes. Only vectors with $p < 0.05$ are shown. The rivers Broadstone and Hammer were omitted as their sequence numbers were too low.).

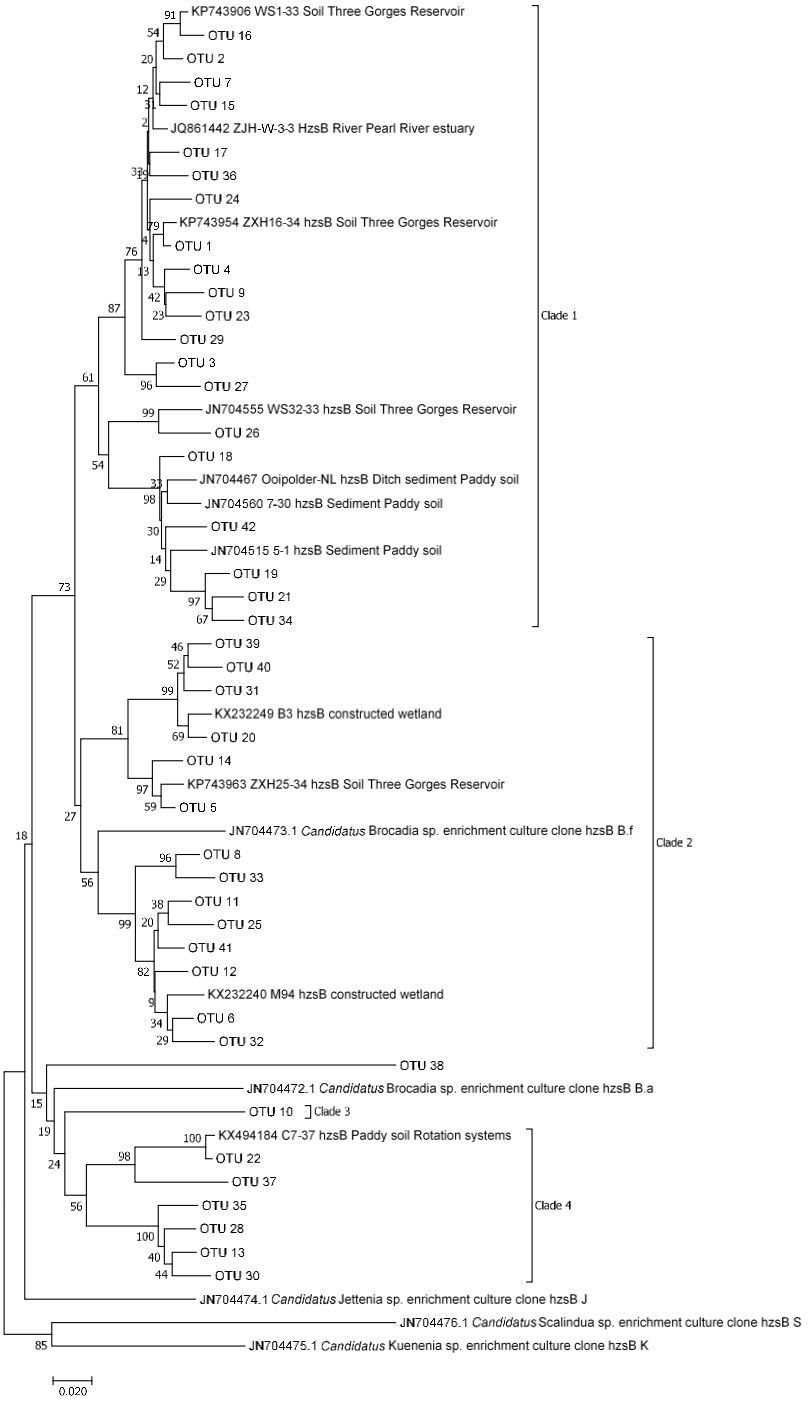

Figure 4.14. Phylogenetic analysis of the anammox *hzs*B amino acid sequences using the neighbour-joining method.

(Tree was constructed from the 42 most abundant OTUs (OTUs that sequences numbers represent higher than 0.1% of the total sequences number). Bootstrap values are indicated at the branch nodes. The scale bar represents a 2% sequence divergence. OTUs were numbered by the order of sequences abundance, i.e., OTU 1 was the most abundant OTU.)

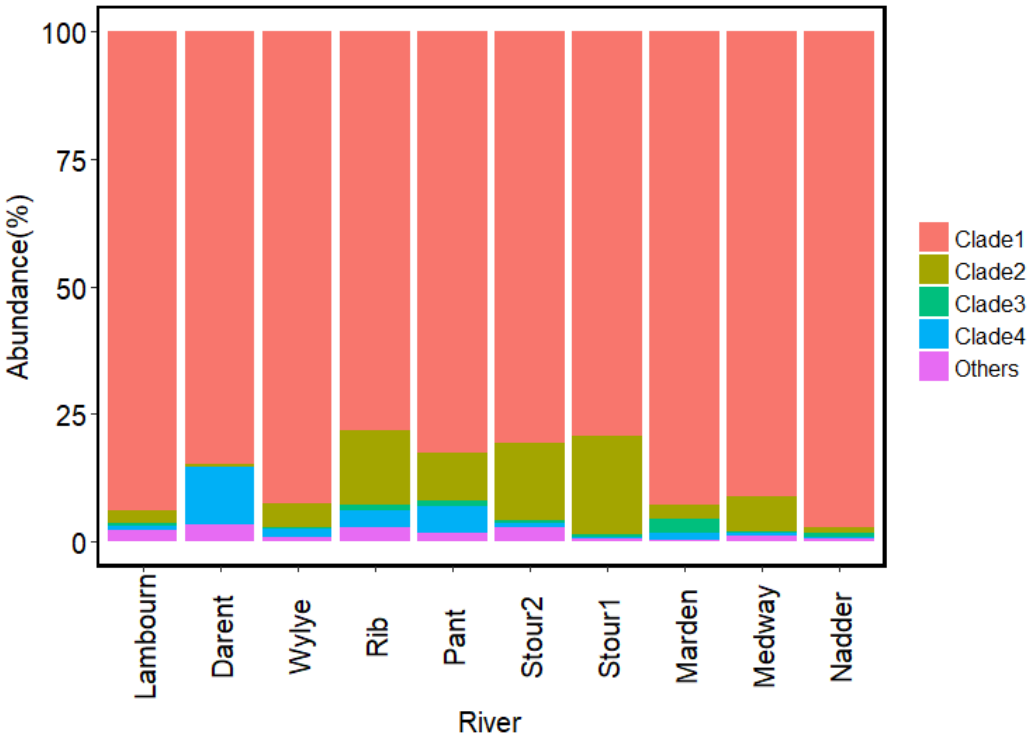

Figure 4.15. Relative abundances of anammox *hzs*B within each clade (based on phylogenetic tree) in each riverbed.

4.3.3. Community structures of AOA and AOB across riverbeds

Sequencing of the *amo*A gene for AOA and AOB was performed to characterise the biodiversity of AOA and AOB in relation to the different chemistries across the riverbeds. The total number of sequences of AOA *amo*A was 656,940, which were assigned to 91 OTUs at a similarity threshold of 0.97. In the river Hammer, where the lowest number of sequences was picked up, the rarefaction curve did not approach saturation (Figure 4.16), indicating that there might be some microbes remained undetermined. The Good's coverage estimator indicated that more than 80.0% of OTUs were picked up in the other riverbeds (Table 4.5). All these rarefaction curves tended to approach the saturation plateaus, indicating these riverbeds were sampled sufficiently. Chao1 richness estimator predicted the presence of 33-74 OTUs in each river, with

Shannon diversity indices ranging from 1.37 to 2.33. The highest AOA *amo*A richness occurred in the river Hammer, while the highest AOA *amo*A diversity occurred in the river Stour (1).

Table 4.5. Diversity of AOA *amo*A gene sequences in each riverbed.

river	No. of sequences	No. of OTUs	Shannon	Chao 1	Coverage (%)
Lambourn	56112	34	1.48	35.00	94.12
Darent	38747	30	1.37	30.75	90.00
Wylye	64662	27	1.48	37.00	81.48
Rib	63610	41	1.66	55.00	80.49
Pant	64069	33	1.85	33.33	93.94
Stour (2)	57829	43	2.20	46.00	93.02
Stour (1)	64033	25	2.33	35.00	80.00
Marden	63825	28	1.69	33.00	82.14
Hammer	28935	38	1.58	74.00	76.32
Medway	56272	32	2.25	32.33	93.75
Broadstone	67194	39	1.64	42.00	89.74
Nadder	52800	34	2.16	35.50	91.18

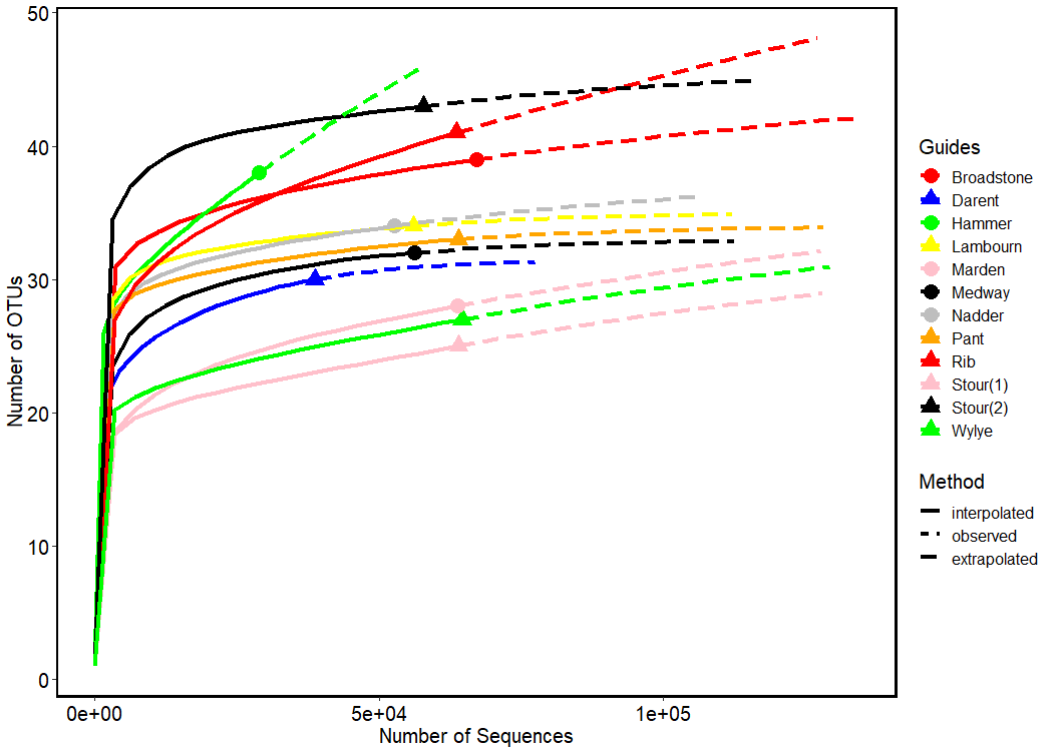

Figure 4.16. Rarefaction/Extrapolation curves of AOA *amo*A gene sequences from different riverbeds.

(The solid lines represent the rarefaction (interpolation) curves and the dashed lines represent the extrapolation curves, the points/triangles between solid and dashed lines represent the observed sample sizes)

The plotting of NMDS showed that the community compositions of AOA in the gravel-dominated riverbeds clustered together and differed from the samples in the sand-dominated riverbeds (Figure 4.17). The envfit analysis showed that the pH and nitrate are the most important factors that influence the AOA community compositions ($r^2 = 0.71$, $p < 0.01$ and $r^2 = 0.62$, $p < 0.01$, respectively). The PERMANOVA analysis showed that community compositions of AOA between the gravel and sand-dominated riverbeds are significantly different ($p < 0.01$).

Phylogenetic analysis showed that these OTUs could be grouped into four clusters (Figure 4.18). The most abundant AOA *amo*A reads (OTU1), represent 26% of the total sequences number, is identical (100% identity) to an uncultured Thaumarchaeote clone (LH-11) from estuary sediment in China. OTU2 represented 10.8% of the total sequences number, has 99% identity to an uncultured Archaeon clone (CFAOA-21) from river water in Mexico. OTU1 and OTU2 belongs to Clade 1 and Clade 2, respectively. Most of the OTUs in Clade 1 were related to *Nitrosopumilus maritimus* and Clade 2 clustered with some uncultured *amo*A sequences from soils or WWTP. Clade 3 and Clade 4 cluster together with Clade 3 closely related to *Nitrosophaera viennensis* while Clade 4 related to some uncultured *amo*A sequences from soils.

Figure 4.19 shows the relative abundances of different clusters of AOA *amo*A in different riverbeds and the distribution of the clades across rivers varied a lot. Except for the river Broadstone, where Clade 2 represented 93.32% of the sequences, others were dominated by either Clade 1 or Clade 4. The proportion of Clade 1 varied from 1.06% (the river Broadstone) to 89.9% (the river Lambourn) and was positively correlated with the porewater nitrate concentration ($r_s = 0.78$, $p < 0.01$), while the relative abundance of Clade 4 ranged from 1.40% (river Broadstone) to 93.60% (river Darent) and was positively correlated with porewater ammonium concentration ($r_s = 0.74$, $p < 0.01$).

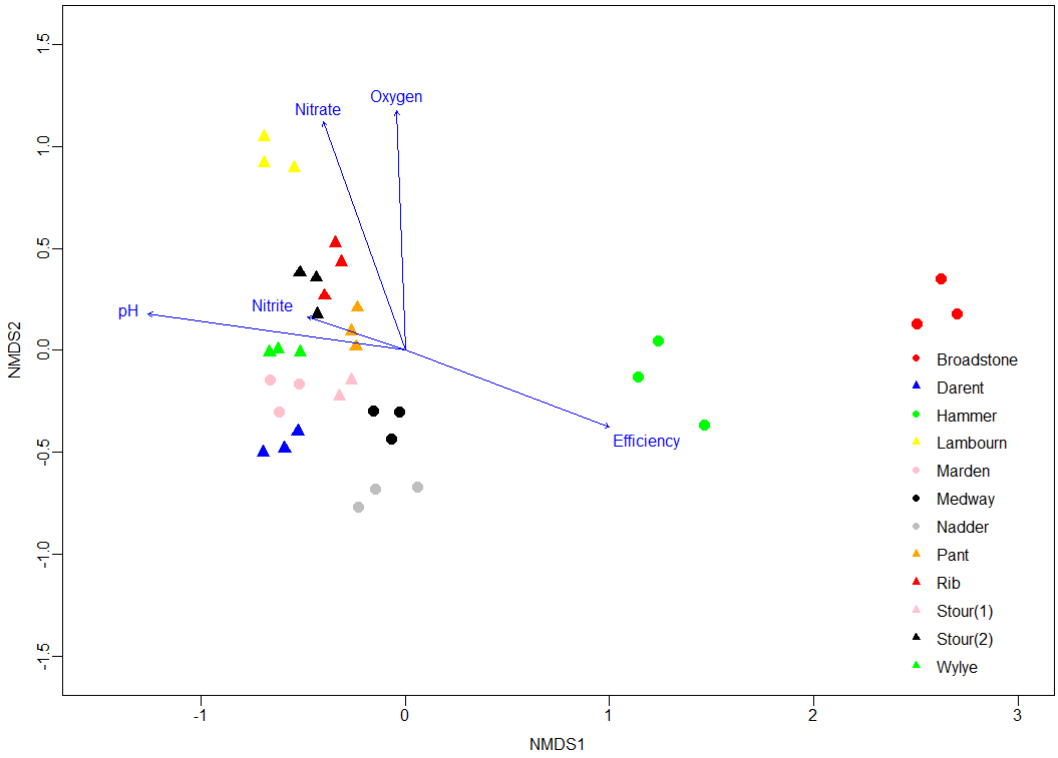

Figure 4.17. Non-metric Multidimensional scaling analysis of the community structures of AOA *amo*A sequences based on Bray-Curtis dissimilarities.

(Dissimilarity in community composition is represented as distance in the diagram. Gravel and sand-dominated riverbed samples were mapped as triangles and circles, respectively. Rivers were mapped was different colours. Environmental factors were fitted to the ordination with arrow length proportional to the correlation between variables and ordination axes. Only vectors with $p < 0.05$ are shown).

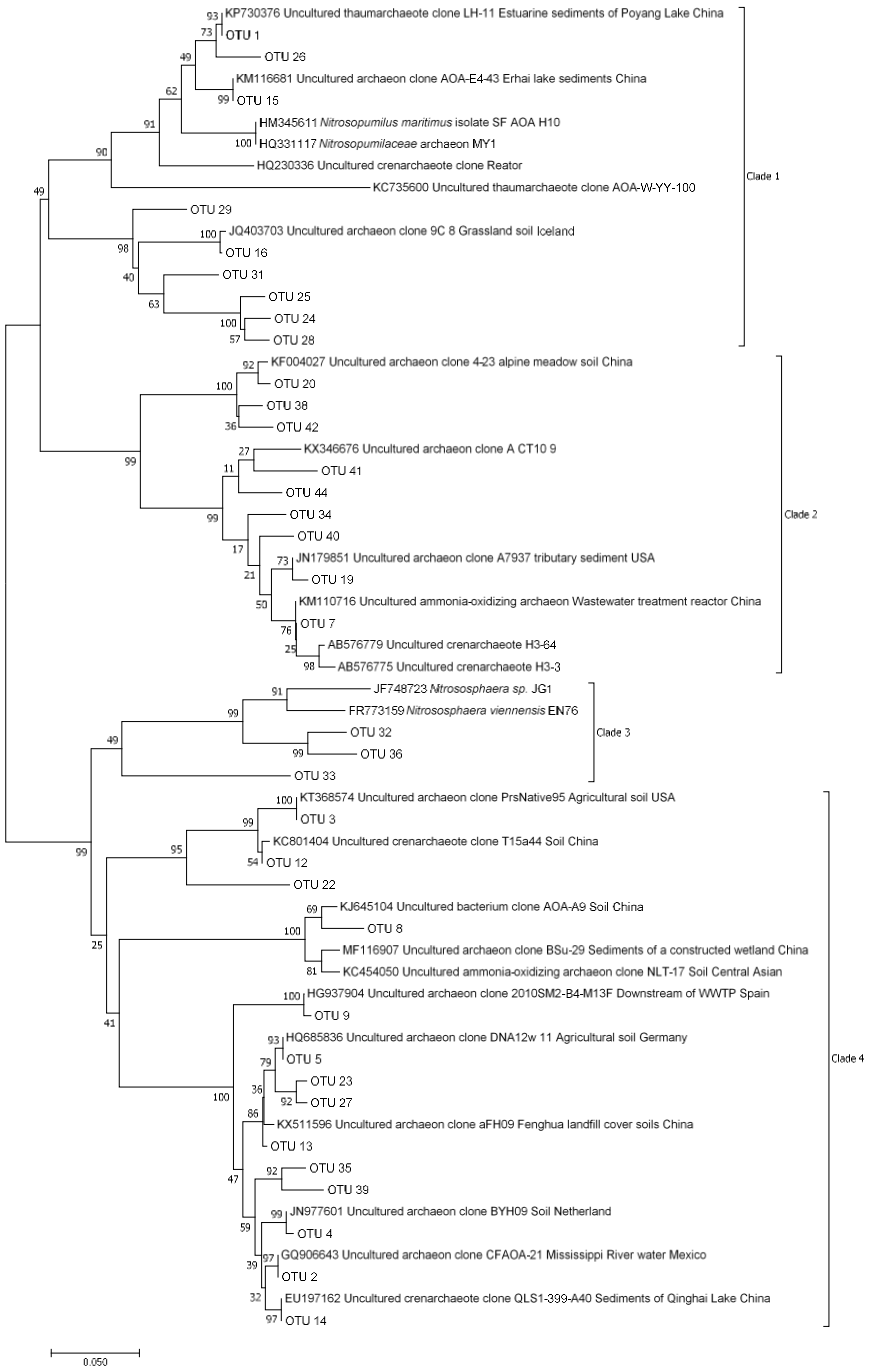

Figure 4.18. Phylogenetic analysis of the AOA *amo*A amino acid sequences using the neighbour-joining method.

(Tree was constructed from the 35 most abundant OTUs (OTUs that sequences numbers represent higher than 0.1% of the total sequences number). Bootstrap values are indicated at the branch nodes. The scale bar represents a 5% sequence divergence. OTUs were numbered by the order of sequences abundance, i.e., OTU 1 was the most abundant OTU).

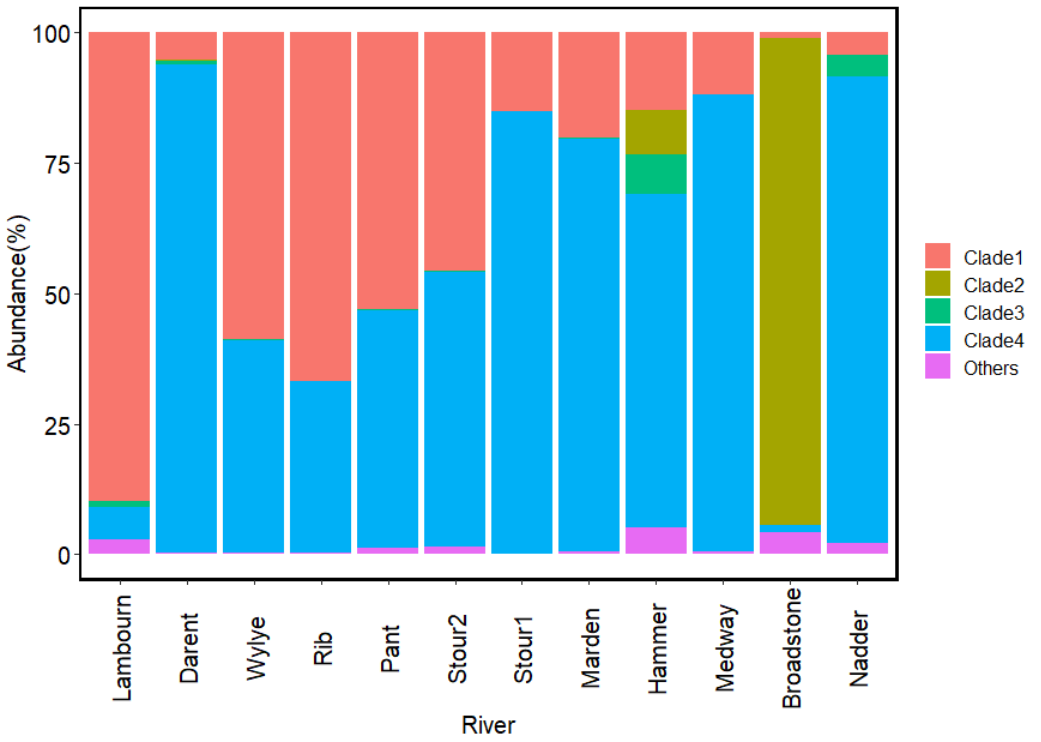

Figure 4.19. Relative abundances of AOA *amo*A OTUs within each clade (based on phylogenetic tree) in each riverbed.

The total number of sequences of AOB *amo*A was 804,008, which were assigned to 54 OTUs at a similarity threshold of 0.97. The Good's coverage estimator indicated that more than 57.1% of OTUs were picked up from riverbeds (Table 4.6). In the river Lambourn, where the lowest number of sequences were picked up, the rarefaction curve did not approach saturation (Figure 4.20), indicating that the sample from the river Lambourn may be not sequenced sufficiently. The other rarefaction curves tended to approach the saturation plateaus, indicating the AOB in these riverbeds could be well-represented by this library. The Chao1 richness estimator predicted the presence of 14-26 OTUs in each location, with Shannon diversity indices ranging from 0.85 to 1.96. The highest AOB richness occurred in the river Rib, while the highest AOB diversity occurred in the river Hammer. Chao 1 richness positively correlated with porewater soluble

reactive phosphorus (SRP) concentration ($r_{(s)}$ = 0.86, p < 0.01), indicating that the rivers with higher SRP concentration may support more diverse AOB.

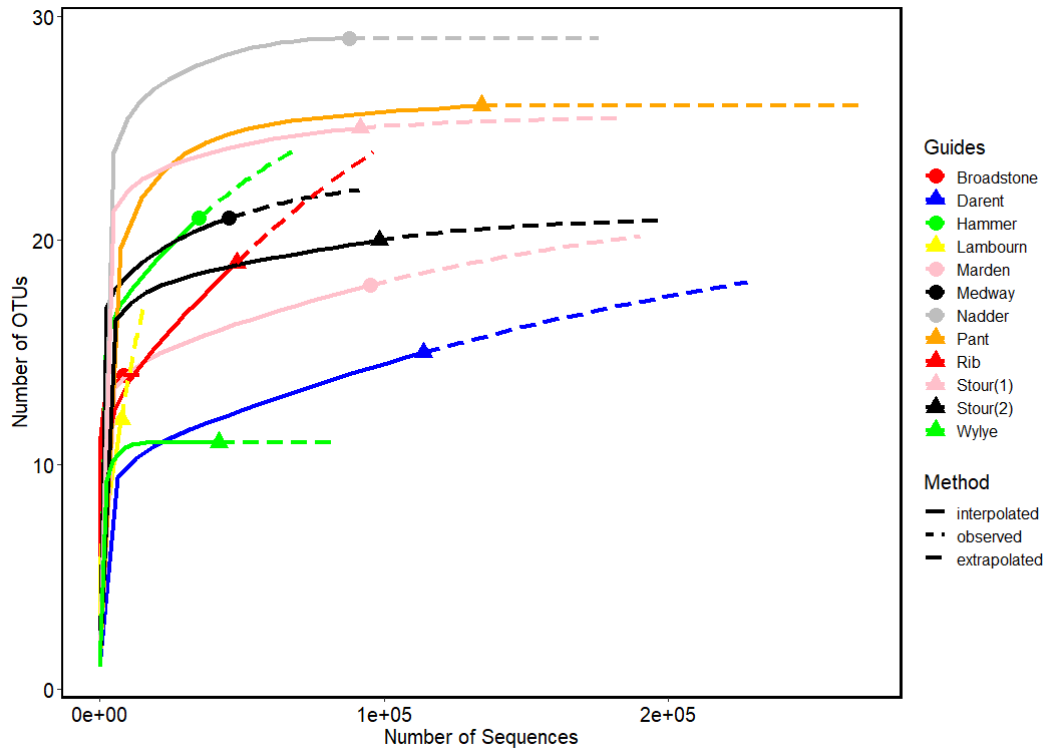

Figure 4.20. Rarefaction/Extrapolation curves of AOB *amo*A gene sequences from different riverbeds.

(The solid lines represent the rarefaction (interpolation) curves and the dashed lines represent the extrapolation curves, the points/triangles between solid and dashed lines represent the observed sample sizes)

Table 4.6. Diversity of AOB *amo*A gene sequences in each riverbed

river	No. of sequences	No. of OTUs	Shannon	Chao 1	Coverage (%)
Lambourn	7612	12	1.19	27	50
Darent	113884	15	0.88	18	73.33
Wylye	41970	11	1.09	11	100
Rib	48132	19	1.27	34	68.42
Pant	134360	26	0.85	26	96.15
Stour (2)	98405	20	1.37	21	90
Stour (1)	91625	25	1.52	25	96
Marden	95044	18	1.22	19.5	83.33
Hammer	35053	21	1.96	24	80.95
Medway	45639	21	1.91	21.5	90.48
Broadstone	8401	14	1.87	14	92.86
Nadder	87744	29	1.57	29	100

The plotting of NMDS showed that the community compositions of AOB in the gravel-dominated riverbeds clustered together and differed from the samples in the sand-dominated riverbeds (Figure 4.21). The envfit analysis showed that the nitrite was the most important factor that influence the AOB *amo*A communities ($r^2 = 0.51$, $p < 0.01$). The PERMANOVA analysis showed that community compositions of AOA between the gravel and sand-dominated riverbeds are significantly different ($p < 0.01$).

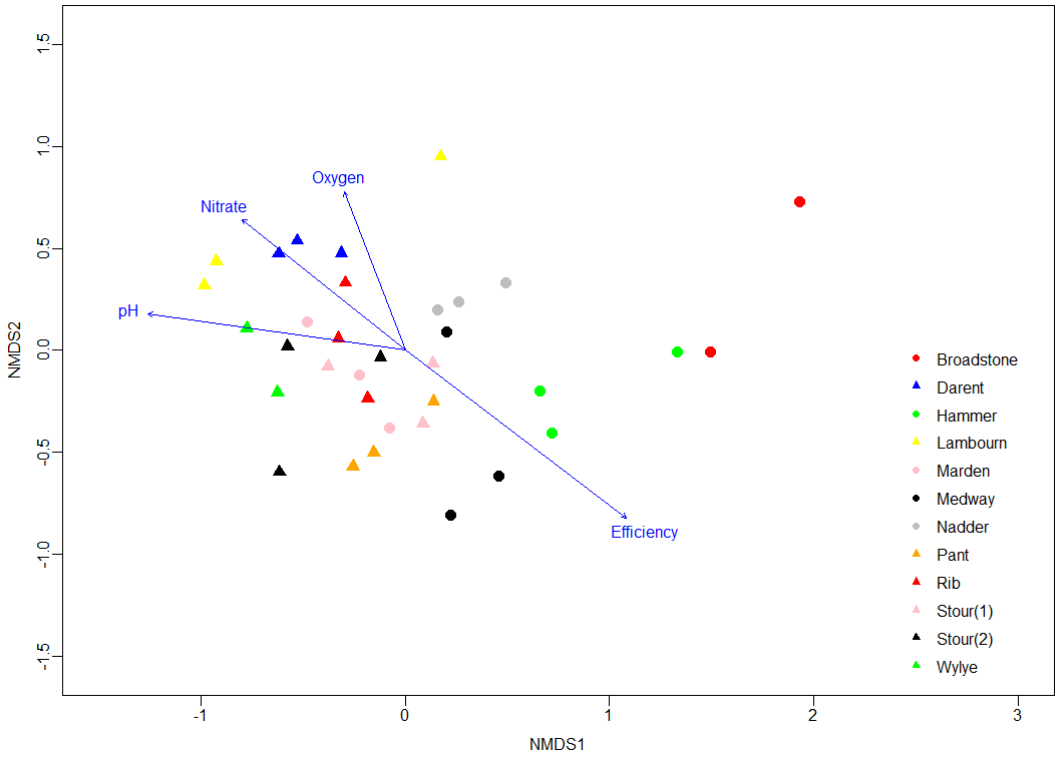

Figure 4.21. Non-metric Multidimensional scaling analysis of the community structures of AOB *amo*A sequences based on Bray-Curtis dissimilarities.

(Dissimilarity in community composition is represented as distance in the diagram. Gravel and sand-dominated riverbed samples were mapped as triangles and circles, respectively. Rivers were mapped was different colours. Environmental factors were fitted to the ordination with arrow length proportional to the correlation between variables and ordination axes. Only vectors with $p < 0.05$ are shown).

AOB sequences clustered predominately with uncultured ammonia-oxidizing clones from soils and river water, closely related to the genus *Nitrosospira* (Figure 4.22). These OTUs could be grouped into four clades. OTUs in Clade 1 and Clade 2 clustered with *Nitrosospira sp.*Wyke2 and *Nitrosospira sp.*EnI299, separately. Clade 3 closely related to *Nitrosospira sp.*Wyke8. Clade 4 separated with other clusters and related to an uncultured bacterium clone from Mississippi river water.

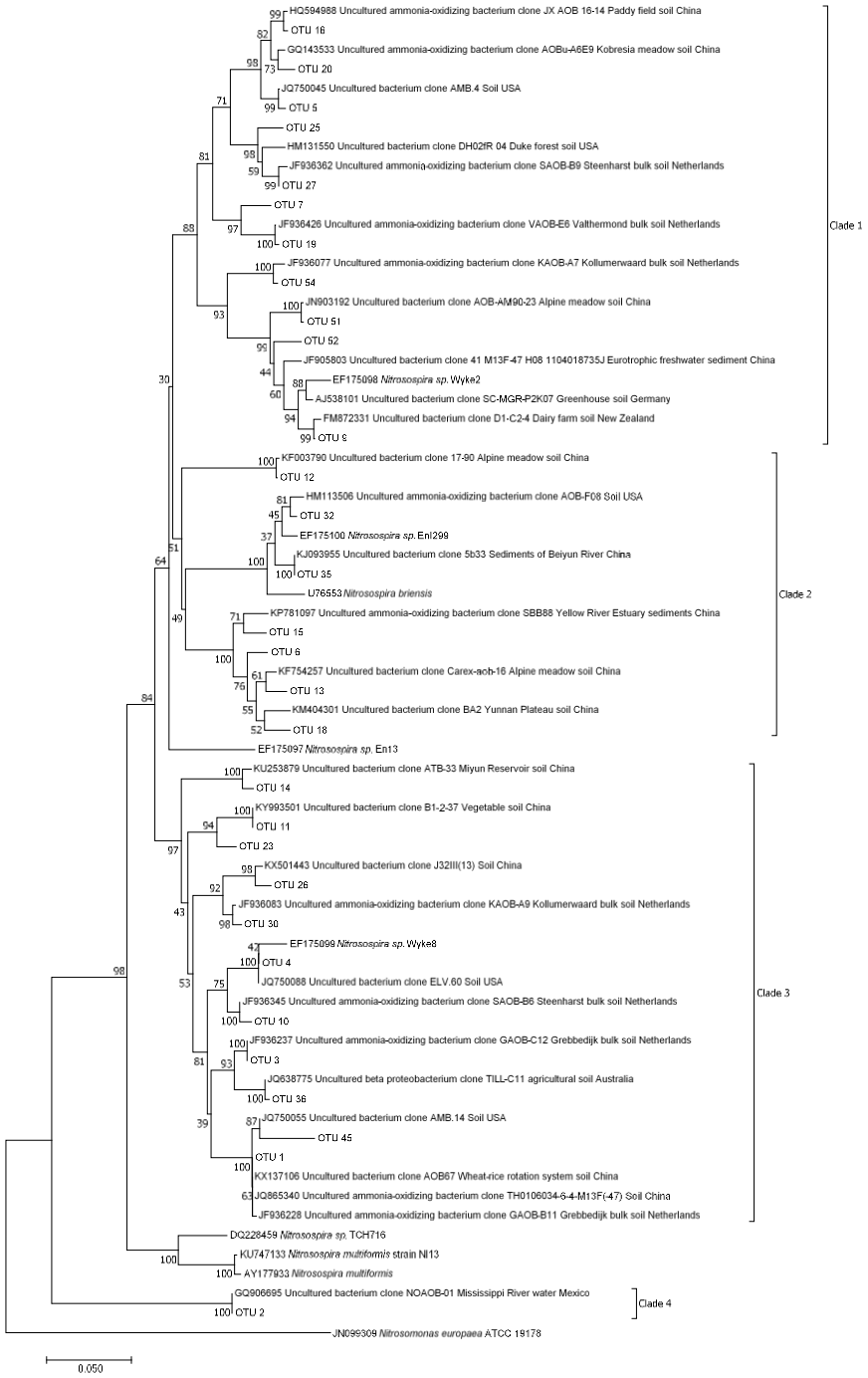

Figure 4.22. Phylogenetic analysis of the AOB *amo*A amino acid sequences using the neighbour-joining method.

(Tree was constructed from the 31 most abundant OTUs (OTUs that sequences numbers represent higher than 0.1% of the total sequences number). Bootstrap values are indicated at the branch nodes. The scale bar represents a 5% sequence divergence. OTUs were numbered by the order of sequences abundance, i.e., OTU 1 was the most abundant OTU.)

Figure 4.23 shows the relative abundances of different clusters of AOB *amo*A in different riverbeds. Clade 1 dominated the proportion of AOB in the rivers Hammer and Broadstone. Other riverbeds were dominated by either Clade 3 or Clade 4. The relative abundance of Clade 3 was positively correlated with pH ($r_{(s)}$ = 0.66, p = 0.02) and NO_3^- ($r_{(s)}$ = 0.65, p = 0.02) while the relative abundance of Clade 4 was positively correlated with porewater SRP concentration ($r_{(s)}$ = 0.61, p = 0.03). These results suggest that the AOB with sequences that group within Clade 3 may prefer the rivers with high pH while those grouped within Clade 4 may favour the rivers with high SRP concentration.

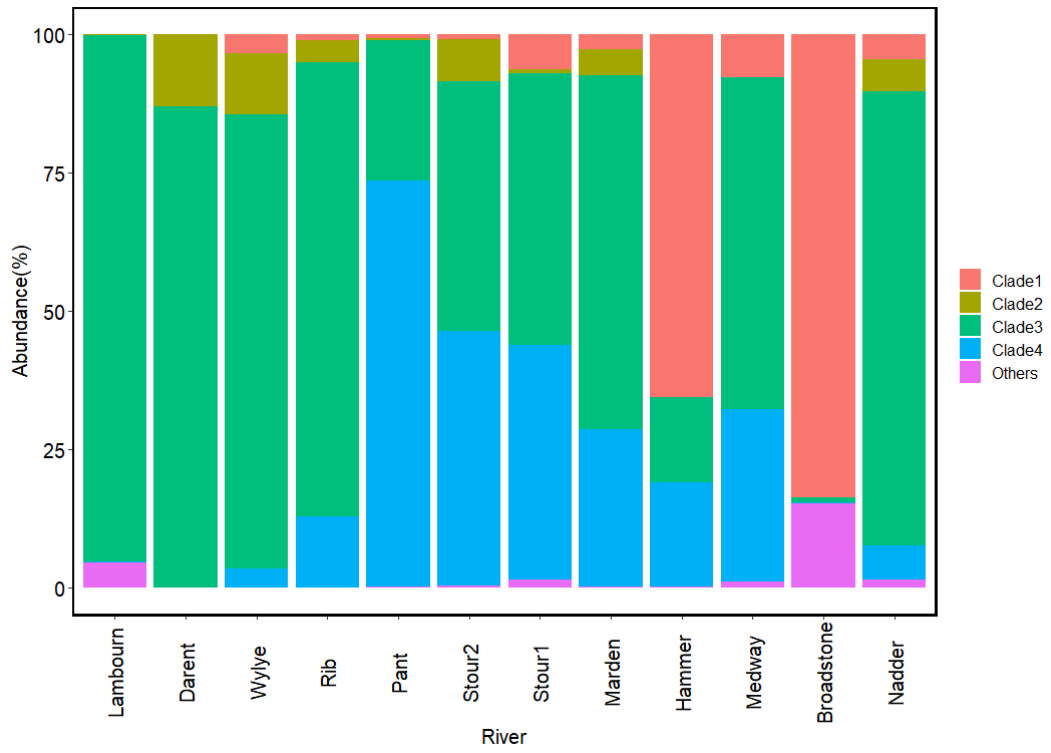

Figure 4.23. Relative abundances of AOB *amo*A within each clade (based on phylogenetic tree) in each riverbed.

4.3.4. Community structures of NOB across riverbeds

Finally, a total of 698,303 *Nitrospira nxr*B gene sequences were obtained, which were assigned to 534 OTUs. Although the sequences numbers varied a lot among riverbeds (Table 4.7), the rarefaction curves tended to approach the saturation plateaus (Figure 4.24), indicating these riverbeds were sampled sufficiently. The Good's coverage estimator indicated that more than 81.4% of OTUs were picked up from the riverbeds. Chao1 richness estimator and Shannon diversity indices ranged from 188 to 321 and from 2.74 to 3.69, respectively. The highest *Nitrospira* richness occurred at the river Stour (2), while the highest *Nitrospira* diversity occurred in the river Pant (Table 4.7).

Table 4.7. Diversity of *Nitrospira nxr*B gene sequences in each riverbed.

river	No. of sequences	No. of OTUs	Shannon	Chao 1	Coverage (%)
Lambourn	280461	204	3.59	219.00	92.65
Darent	24102	156	3.01	206.75	81.41
Wylye	24718	179	3.24	214.10	84.92
Rib	26509	242	2.74	285.59	83.88
Pant	32624	249	3.69	263.29	89.96
Stour (2)	34614	290	3.57	321.17	88.28
Stour (1)	28634	233	3.10	264.00	86.27
Marden	24059	192	3.10	201.56	90.63
Hammer	39642	189	3.35	202.91	90.48
Medway	126405	256	3.25	263.50	94.14
Broadstone	29885	167	3.10	188.23	85.63
Nadder	26650	237	3.05	280.05	82.28

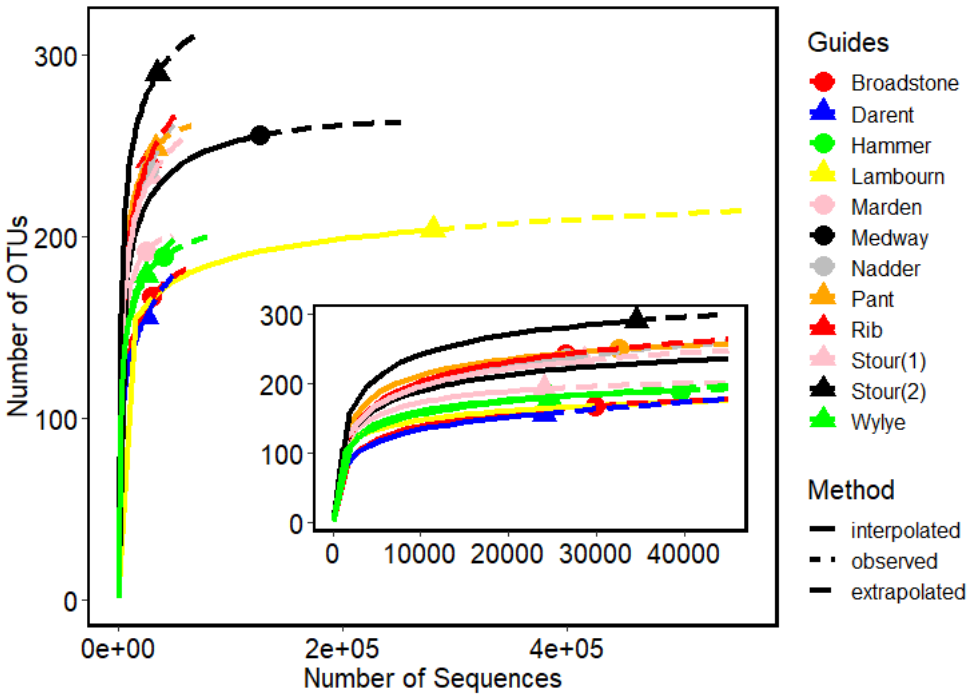

Figure 4.24. Rarefaction/Extrapolation curves of *Nitrospira nxr*B gene sequences from different riverbeds.

(The solid lines represent the rarefaction (interpolation) curves and the dashed lines represent the extrapolation curves, the points/triangles between solid and dashed lines represent the observed sample sizes)

The plotting of NMDS showed that the community compositions of *Nitrospira* in the gravel-dominated riverbeds clustered together and differed from the samples in the sand-dominated riverbeds (Figure 4.25). The envfit analysis showed that the pH, nitrate and nitrite concentrations were the most important environmental factors that influence the *Nitrospira* communities ($r^2 = 0.68$, $p < 0.01$, $r^2 = 0.40$, $p < 0.01$ and $r^2 = 0.51$, $p < 0.01$). A significant correlation between *Nitrospira* community structure and the degree of nitrification efficiency was also observed ($r^2 = 0.74$, $p < 0.01$). The PERMANOVA analysis showed that community compositions of *Nitrospira* between the gravel and sand-dominated riverbeds are significantly different ($p < 0.01$).

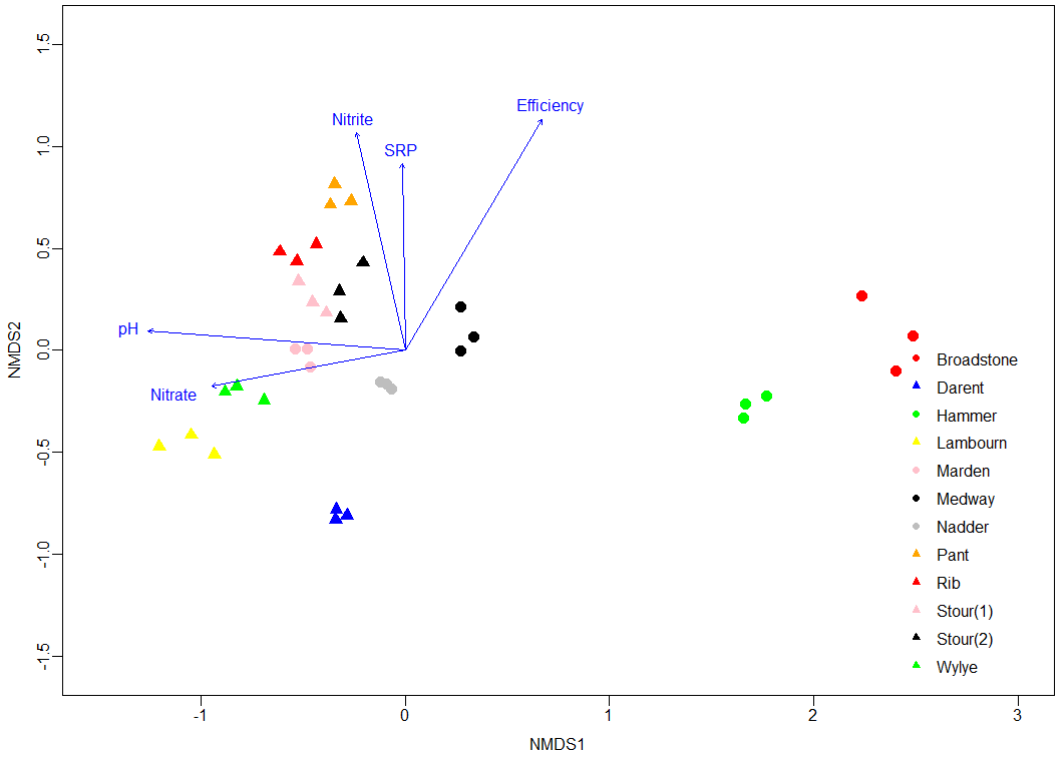

Figure 4.25. Non-metric Multidimensional scaling analysis of the community structures of Nitrospira *nxr*B sequences based on Bray-Curtis dissimilarities.

(Dissimilarity in community composition is represented as distance in the diagram. Gravel and sand-dominated riverbed samples were mapped as triangles and circles, respectively. Rivers were mapped was different colours. Environmental factors were fitted to the ordination with arrow length proportional to the correlation between variables and ordination axes. Only vectors with $p < 0.05$ are shown).

Phylogenetic analysis of sequences revealed that the most abundant *Nitrospira* reads (OTU1), accounted for 17.1% of the total sequences reads and belongs to Clade 1, has an 89% identity to *Nitrospira moscoviensis* strain M-1. The second abundant OTU (OTU2) belongs to Clade 2 and has a 99% identity to an uncultured *Nitrospira sp.* clone (VetMed-B9) found in WWTP in Germany. These OTUs could be grouped into four clades. The OTUs in Clade 1 and Clade 2 clustered with *Nitrospira moscoviensis* and

uncultured *Nitrospira* in Germany WWTP, respectively. Clade 3 clustered with Clade 4, with OTUs in Clade 4 were affiliated to *Nitrospira marina* (Figure 4.26). Figure 4.27 shows the relative abundances of different clades of *Nitrospira* in different riverbeds and the distribution of the clades across the rivers varied a lot. Clade 1 dominated the proportion in all riverbeds, ranging from 40.47% in the river Stour (1) to 77.42% in the river Broadstone.

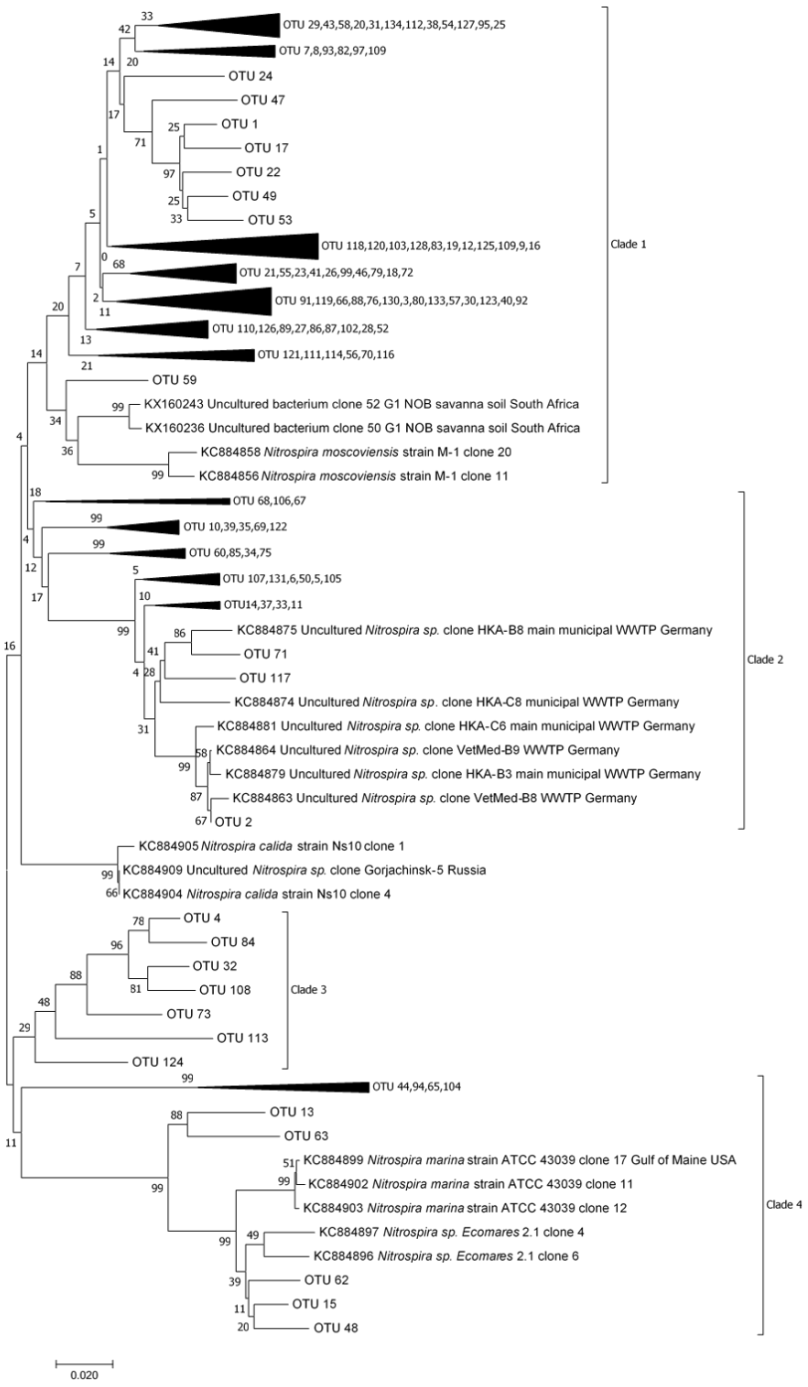

Figure 4.26. Phylogenetic analysis of the *Nitrospira nxr*B amino acid sequences using neighbour-joining method.

(Tree was constructed from the 117 most abundant OTUs (OTUs that sequences numbers represent higher than 0.1% of the total sequences number). Bootstrap values are indicated at the branch nodes. The scale bar represents a 2% sequence divergence. OTUs were numbered by the order of sequences abundance, i.e., OTU 1 was the most abundant OTU.)

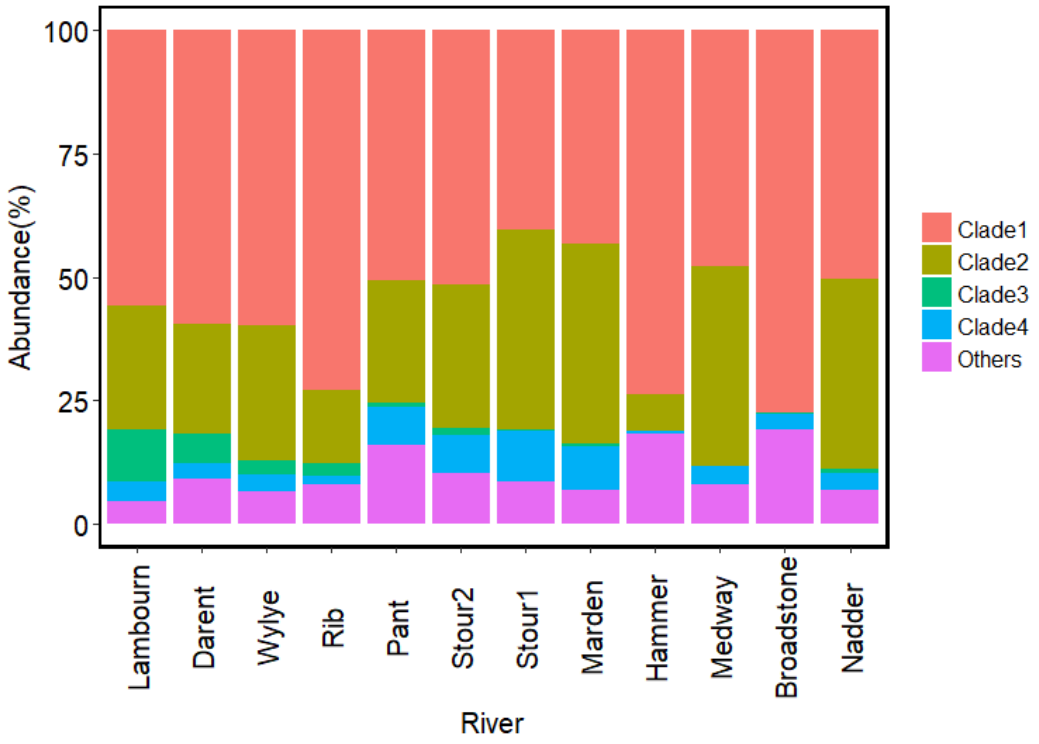

Figure 4.27. Relative abundances of *Nitrospira nxr*B within each clade (based on phylogenetic tree) in each riverbed.

4.3.5. Community structures of comammox *Nitrospira* across riverbeds

Sequencing of the comammox *Nitrospira amo*A gene got a total of 1,908,570 sequences, which were assigned to 390 OTUs. The rarefaction curves tended to approach the saturation plateaus (Figure 4.28), indicating these riverbeds were sampled sufficiently. The Good's coverage estimator indicated that more than 83.33% of OTUs were picked up in the riverbeds (Table 4.8). The Chao1 richness estimator was 200-358 and the Shannon diversity ranged from 2.85 to 3.79. The Chao1 richness estimator was positively correlated with the SRP concentration ($r_{(s)}$ = 0.74, p < 0.01), suggesting that the rivers with higher SRP concentration tend to have more diverse comammox *Nitrospira*.

Table 4.8. Diversity of comammox *Nitrospira amo*A gene sequences in each riverbed

river	No. of sequences	No. of OTUs	Shannon	Chao 1	Coverage (%)
Lambourn	135203	251	2.85	276.5	86.45
Darent	151898	223	2.92	240.55	87.89
Wylye	91098	231	3.06	242.05	90.91
Rib	162063	290	3.13	313.1	92.41
Pant	134164	246	3.04	309.08	83.33
Stour (2)	127728	287	3.07	298	92.33
Stour (1)	118288	279	3.09	321.27	88.89
Marden	82425	260	3.42	295.77	88.08
Hammer	250475	263	3.43	298	86.69
Medway	85255	279	3.55	294.81	91.76
Broadstone	153683	184	2.91	200.67	86.41
Nadder	201893	326	3.79	357.91	91.72

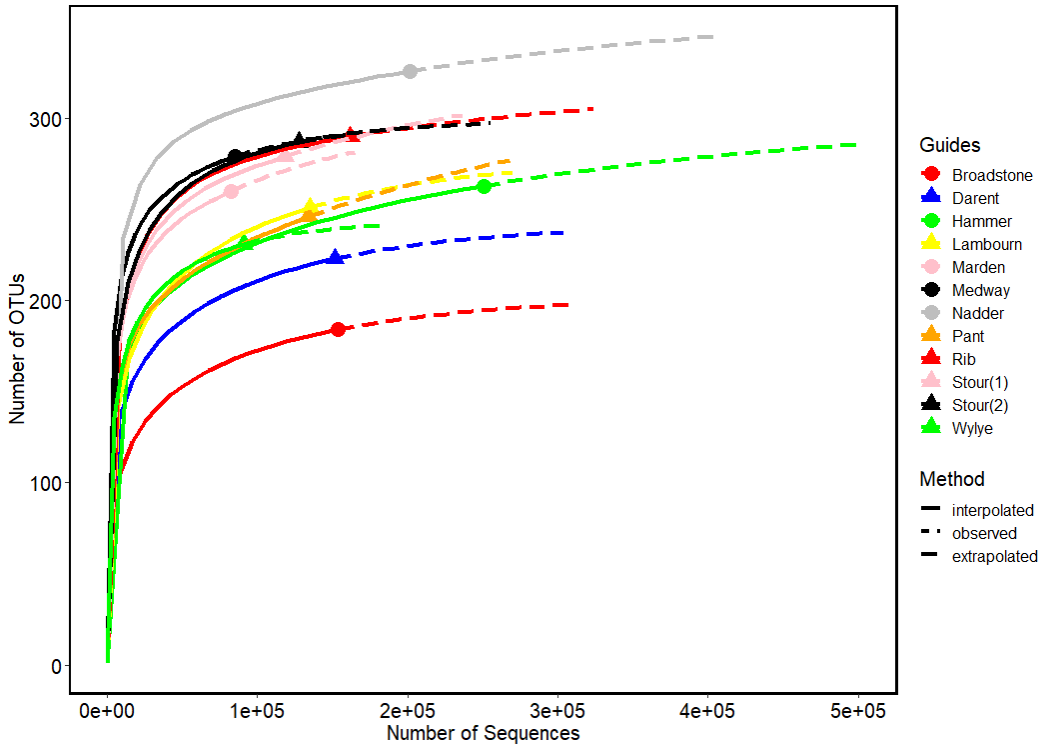

Figure 4.28. Rarefaction/Extrapolation curves of comammox *Nitrospira amo*A gene sequences from different riverbeds.

(The solid lines represent the rarefaction (interpolation) curves and the dashed lines represent the extrapolation curves, the points/triangles between solid and dashed lines represent the observed sample sizes)

The plotting of NMDS showed that the community compositions of comammox *Nitrospira* in the gravel-dominated riverbeds clustered together and differed from the samples in the sand-dominated riverbeds (Figure 4.29). The envfit analysis showed that the pH, nitrate and nitrite concentrations were the most important environmental factors that influence the *Nitrospira* communities ($r^2 = 0.72$, $p < 0.01$, $r^2 = 0.35$, $p < 0.01$ and $r^2 = 0.42$, $p < 0.01$). A significant correlation between *Nitrospira* community structure and the degree of nitrification efficiency was also observed ($r^2 = 0.72$, $p < 0.01$). The

PERMANOVA analysis showed that community compositions of comammox *Nitrospira* between the gravel and sand-dominated riverbeds are significantly different ($p < 0.01$).

Phylogenetic analysis showed that these OTUs could be grouped into five clades (Figure 4.30), and these five clades belong to either clade A comammox *Nitrospira* (Clade 5) or clade B comammox *Nitrospira* (Clades 1,2,3,4), according to the classifications from the former studies (Pjevac et al. 2017, Fowler et al. 2018, Palomo et al. 2018). The most abundant comammox *Nitrospira amo*A reads (OTU1), accounts for 13.2% of the total sequences reads and belongs to Clade 2, has 88% identity to the uncultured bacterium clone 25 from groundwater-fed rapid sand filters in Denmark. The second abundant OTU (OTU2) belongs to Clade 1 and has a 99% identity to the uncultured bacterium clone 14 found in groundwater-fed rapid sand filters in Denmark. Clade 3 and Clade 4 might be novel groups in clade B comammox *Nitrospira* as no reference of comammox can be found. OTUs in Clade 5 clustered with *Candidatus* Nitrospira nitrificans and *Candidatus* Nitrospira inopinata, belonging to clade A comammox *Nitospira* (Figure 4.30). Figure 4.31 shows the relative abundances of different clusters of comammox *Nitrospira* in the different riverbeds, the distribution of the clades in rivers varied a lot. Clade B comammox *Nitrospira* make up 79.5%-94.7% of the comammox abundance in these rivers and are more abundant than clade A comammox *Nitrospira*. The relative abundance of Clade B was negatively correlated with the porewater nitrite concentration (($r_{(s)}$ = -0.69, p = 0.01), while the relative abundance of Clade A comammox *Nitrospira* was positively correlated with both porewater nitrite and nitrate concentrations (($r_{(s)}$ = 0.61, p = 0.03 and $r_{(s)}$ = 0.65, p = 0.02), indicating that nitrite concentration may be the an important factor that influence the distribution of Clade B and Clade A comammox *Nitrospira*.

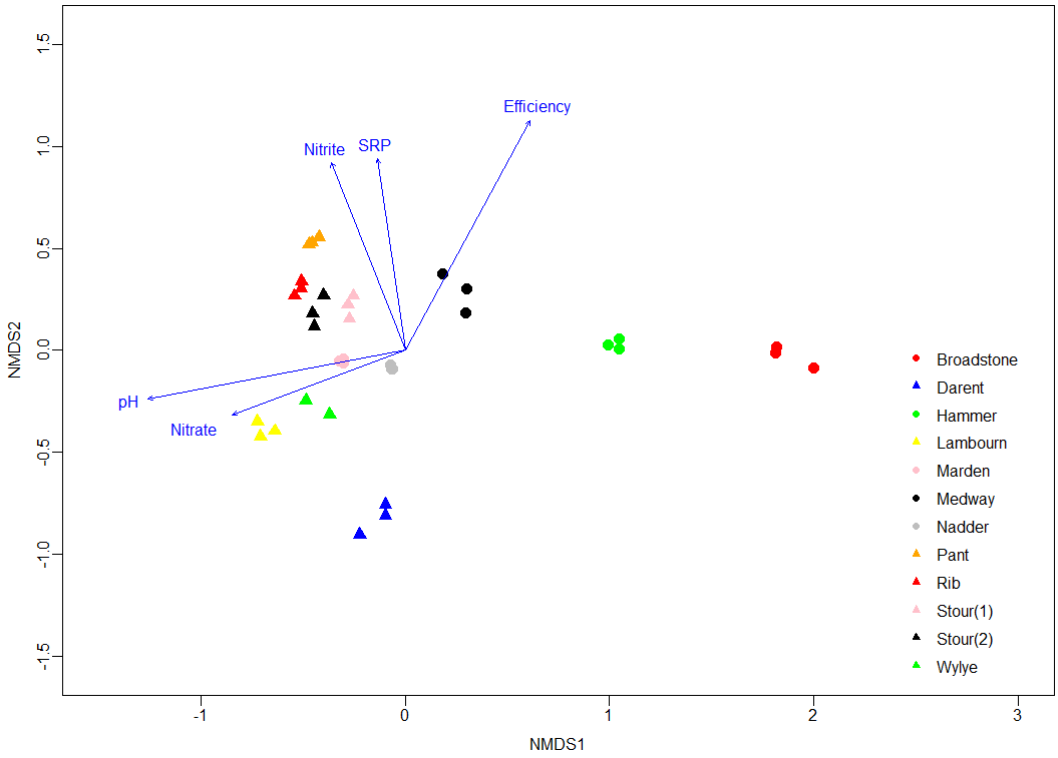

Figure 4.29. Non-metric Multidimensional scaling analysis of the community structures of comammox *Nitrospira amo*A sequences based on Bray-Curtis dissimilarities. (Dissimilarity in community composition is represented as distance in the diagram. Gravel and sand-dominated riverbed samples were mapped as triangles and circles, respectively. Rivers were mapped was different colours. Environmental factors were fitted to the ordination with arrow length proportional to the correlation between variables and ordination axes. Only vectors with $p < 0.05$ are shown).

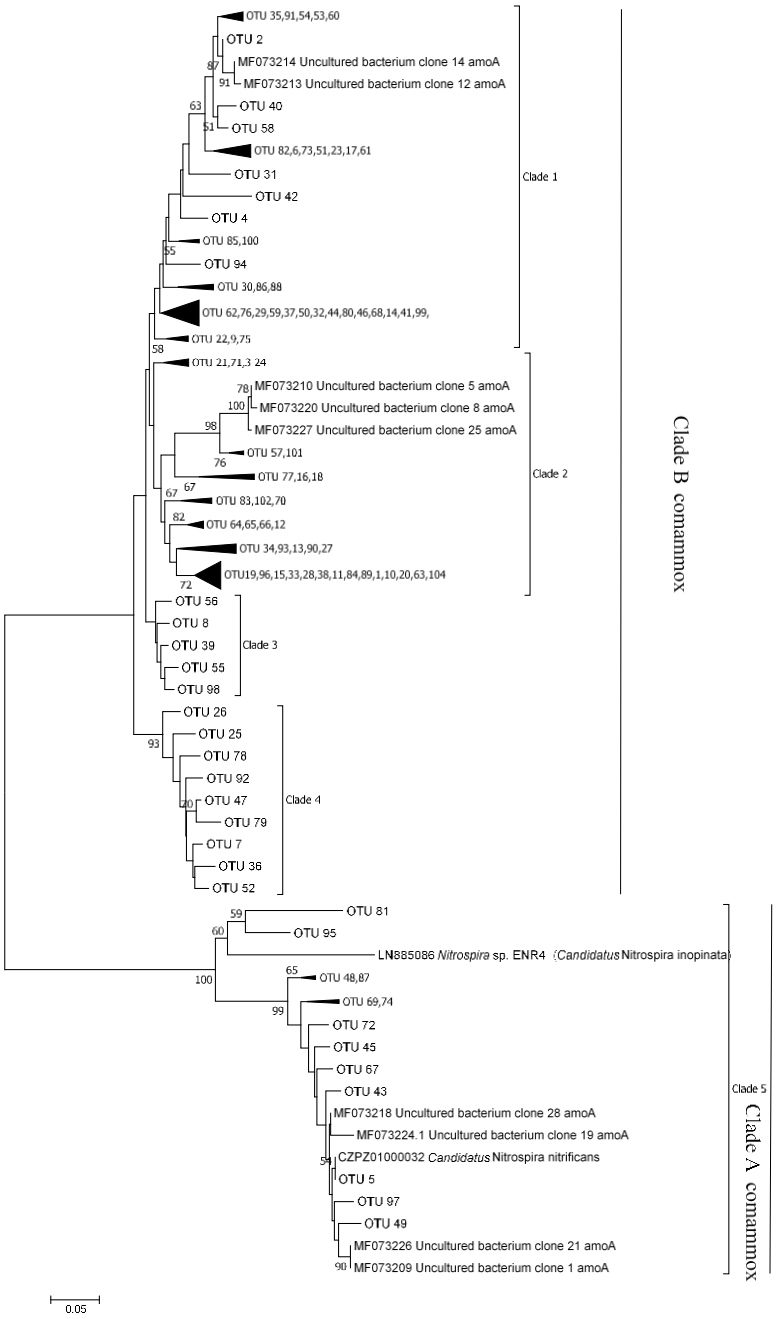

Figure 4.30. Phylogenetic analysis of the comammox *Nitrospira amo*A amino acid sequences using neighbour-joining method.

(Tree was constructed from the 104 most abundant OTUs (OTUs that sequences numbers represent higher than 0.1% of the total sequences number). Bootstrap values greater than 50 are indicated at the branch nodes. The scale bar represents a 5% sequence divergence. OTUs were numbered by the order of sequences abundance, i.e., OTU 1 was the most abundant OTU).

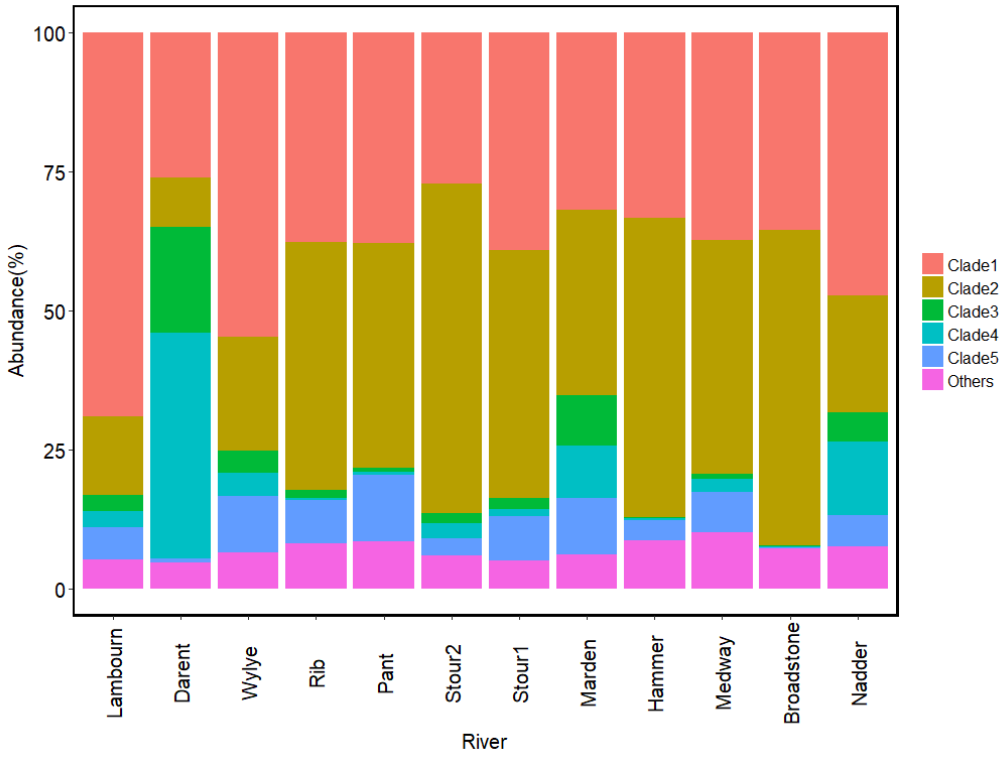

Figure 4.31. Relative abundances of comammox *Nitrospira amo*A within each clade (based on phylogenetic tree) in each riverbed.

4.4. Discussion

The degree of nitrification efficiency was positively correlated with the proportion of NOB in the total 16S rRNA amplicon library (Figure 4.3), suggesting that differences in nitrification efficiency across the riverbeds related to the relative abundance of NOB in the total bacterial community. This is consistent with the finding in Chapter 3 that the abundance of the total *nxr*B gene, as well as the ratio of *Nitrospira* to *Nitrobacter nxr*B gene abundance correlates well with the degree of nitrification efficiency across these rivers, further confirming the primary role of *Nitrospira* in driving the degree of nitrification efficiency.

Phylogenetic analyses revealed that most of the *Nitrospira* sequences clustered with *Nitrospira moscoviensis* and *Nitrospira marina* (Figure 4.26). This is consistent with

other studies on freshwater aquaria (Hovanec et al. 1998), WWTPs (Whang et al. 2009) and a shrimp recirculating aquaculture system (Brown et al. 2013). Clade 1, which groups with *Nitrospira moscoviensis*, dominated in all riverbeds and in the river Broadstone, where the highest nitrification efficiency was observed, the relative abundance of Clade 1 was the highest (77.42%) (Figure 4.28), indicating that *Nitrospira moscoviensis* may be the main species that related to the degree of nitrification efficiency. Nitrite concentration has been reported to influence the community structure of *Nitrospira,* the study of (Maixner et al. 2006) suggested that higher nitrite concentration (5 mg NO_2^- L^{-1} vs. 0.1 mg NO_2^- L^{-1}) selected for *Nitrospira delfluvii* but supressed *Nitrospira moscoviensis*, the low porewater nitrite concentrations (1.06-6.83 µM) across these gravel and sand-dominated riverbeds may provide advantages for the growth of *Nitrospira moscoviensis* over other *Nitrospira* populations. The tolerance for free ammonia has also been reported as an important factor that determines competition among *Nitrospira* populations (Ushiki et al. 2017). The NMDS plot revealed that pH is also an important factor that influence the community structure of *Nitrospira*. It has been reported that the optimal pH value for the growth of *Nitrospira moscoviensis* was 7.6-8.0 (Ehrich et al. 1995), while in a *Nitrospira* bioreactor, the optimal pH for *Nitrospira* was 8.0-8.3 (Blackburne et al. 2007).

Both clade B and clade A comammox *Nitrospira* were harboured in these riverbeds, with clade B are more abundant than clade A comammox *Nitrospira*. This is consistent with the finding in groundwater-fed rapid sand filter communities, where clade B dominated the comammox *Nitrospira* community (Fowler et al. 2018). However, the study of (Yu et al. 2018) showed that all comammox found in tidal sediments belongs to clade A comammox *Nitrospira*. It is reported that comammox *Nitrospira* have high affinity for ammonium (Kits et al. 2017, Yu et al. 2018) and the difference in ammonium affinity might be an important niche-separation factor between the comammox genomes

(Palomo et al. 2018). However, this study shows the nitrite and nitrate concentrations might also influence the distribution of clade A and clade B comammox *Nitrospira*, although comammox *Nitrospira* do not use external nitrite as energy and nitrogen source (Palomo et al. 2018).

Sequences from AOA *amo*A gene clustered with *Nitrosopumilus maritimus*, *Nitrosophaera viennensis* and some uncultured *amo*A sequences from soils. Clade 2 represented 93.32% of the sequences in the river Broadstone, suggesting that this clade may have advantages over others in acidic riverbeds. Other riverbeds were dominated by either Clade 1 or Clade 4, related to *Nitrosopumilus maritimus* and uncultured archaeon clones, respectively. The dominance of *Nitrosopumilus* has been found in estuaries (Jin et al. 2011, Li et al. 2018), a shrimp recirculating aquaculture system (Brown et al. 2013) and marine environments, while *Nitrososphaera* has been demonstrated to more abundant in soils (Tourna et al. 2011, Pester et al. 2012). However, this study suggests that *Nitrosopumilus* also plays an important role in oxic riverbeds. It has been proposed that availability of ammonium is a key factor that driving the populations of AOA, *Nitrosopumilus maritimus* can survive at low ammonium concentration (10 nM) (Martens-Habbena et al. 2009) while *Nitrososphaera viennensis* can tolerate ammonium concentrations at up to 15 mM (Tourna et al. 2011). The positive correlation between the relative abundance of Clade 4 and porewater ammonium concentration further hints at ammonium concentration being an important factor that drives the community structure of AOA, AOA sequences grouped with Clade 4 may favour the riverbeds with higher ammonium concentrations. However, the relative abundance of Clade 1 (clustered with *Nitrosopumilus maritimus*) was positively correlated with the porewater nitrate concentration ($r_s = 0.78$, $p < 0.01$), indicating that AOA sequences grouped with Clade 1 may favour the riverbeds with higher nitrate concentrations. The high nitrate

concentration across the riverbeds, especially in gravel-dominated riverbeds (70.74µM to 484.25µM), may provide a suitable environment for Clade 1.

All of the sequences from AOB *amo*A clustered with *Nitrosospira*, this was consistent with the finding of freshwater marsh wetland (Lee et al. 2014), aquaculture ponds (Zhou et al. 2017) and freshwater sediments (Herrmann et al. 2009). pH and SRP concentration might be the main factors that driving the community structure of AOB, as revealed by the correlations between AOB richness and SRP, as well as the relative abundance of Clade 3 and pH ($r_{(s)} = 0.67$, $p = 0.02$) and the relative abundance of Clade 4 and SRP concentration ($r_{(s)} = 0.62$, $p = 0.03$).

Phylogenetic analyses showed that most of the anammox sequences (from 16S rRNA, *hzo* and *hzs*B) were closely affiliated to *Candidatus* Brocadia. Similarly, *Candidatus* Brocadia has also been found to dominate in the shallow wetland soils (Shen et al. 2015), the sediments of the Xinyi River (Zhang et al. 2007), Lake Kitaura (Yoshinaga et al. 2011) and groundwater environments (Penton et al. 2006). This is different from other findings in freshwater wetland soils, where high diversities of anammox bacteria have been shown (Hu et al. 2011, Zhu et al. 2011). *Candidatus* Brocadia was regarded as freshwater anammox genus (Shen et al. 2016), the dominance of *Candidatus* Brocadia in this study may suggest that it plays a more important role in N_2 removal than other anammox genera in oxic riverbeds. Interestingly, *Candidatus* Scalindua was found in river Pant, *Candidatus* Scalindua is normally found in marine environments (Jetten et al. 2003) or WWTP (Schmid et al. 2003), it is proposed that *Candidatus* Scalindua have a higher tolerance of salinity than *Candidatus* Brocadia and *Candidatus* Kuenenia (Jetten et al. 2003), the specific riverbed characteristic in river Pant (low C:N) may provide an ideal environment for *Candidatus* Scalindua. When comparing the sequencing results from anammox 16S rRNA, *hzo* and *hzs*B, the sequencing of *hzo*

showed a more distinct difference of community structures, the study of (Li et al. 2011) also found that the phylogeny of *hzo* gene showed a more complex anammox community structure than the phylogeny of anammox 16S rRNA gene.

Correlation analysis showed that the porewater SRP concentration positively correlated with the Chao1 richness estimators of the total bacterial 16S rRNA community, AOB community and comammox *Nitrospira amo*A, indicating that the porewater SRP concentration might be an important environmental factor regulating the richness and diversity of the total bacterial community. It has been reported that long-term phosphorus fertilisation increases the bacterial community diversity in pasture soils (Tan et al. 2013). Phosphorus has also been found to be an important factor affecting soil ammonia-oxidizing activity and AOB community structure in a purple soil (Zhou et al. 2014), the aquaculture ponds (Zhou et al. 2017) and nitrifying groundwater filters (De Vet et al. 2012).

Taken together, the above results suggest that these oxic riverbeds are likely to have selected for distinct nitrification and anammox communities, and the tight interactions between AOM, anammox and NOB are related to the physiochemical properties of those riverbeds. pH and SRP concentration were the main factors that influence the community structure of AOB, while the community structure of AOA was mainly driven by ammonium concentration. Nitrite concentration was the main factor that influence the community structure of *Nitrospira* and comammox *Nitrospira*. The community structure of anammox was influenced by ammonium and nitrite concentrations. The community distribution of *Nitrospira* and comammox *Nitrospira* also related to the degree of the nitrification efficiency.

Chapter 5 : Conclusions

As a hydrological connection between terrestrial system and costal system, rivers play an important role in the N cycle. In short term, organic nitrogen is mineralized to ammonia, and then aerobically oxidized and conserved as nitrate through nitrification or returned to the atmosphere as N_2 through denitrification and anammox. The degree of the net nitrification efficiency, i.e., the proportion of ammonia that totally oxidized to nitrate, regulates the primary production and the degree of eutrophication in rivers (Seitzinger 1988, Vitousek et al. 1997, Boyer et al. 2006). In UK, 48% of the rivers are dominated by gravels and pebbles and 26% of sites are dominated by sands and fine sediments (Naura et al. 2016). In these permeable, oxic riverbeds, the advective flows of the porewater can enhance the supply of the oxidants and organic matter, as well as the removal of remineralization by-products, thus resulting in high metabolic activities (Rao et al. 2008).

Coupled nitrification/denitrification is a well-recognized pathway of N loss in permeable marine sands. However, research so far on anammox has mainly focused on both the presence and contribution of anammox to N_2 production, yet how the interaction between nitrification and anammox in permeable, oxic riverbeds is largely unknown. Furthermore, the degree of the net nitrification efficiency is of interest when these processes occurred simultaneously. Here, using ^{15}N tracers and molecular analyses, the potential interactions between nitrification and anammox and/or denitrification and their contributions to the degrees of net nitrification efficiency across twelve oxic riverbeds in southern England were investigated.

In Chapter 2, firstly, $^{15}NH_4^+$ with or without ATU (an inhibitor for aerobic ammonia oxidation) was added into oxic sediment slurries to examine the interactions between nitrification and anammox and/or denitrification. The production of ^{15}N-N_2 in

$^{15}NH_4^+$ amended oxic slurries confirmed the simultaneous aerobic ammonia oxidation, anammox and/or denitrification in oxic riverbeds. Then, to further understand how anammox works in these oxic riverbeds, different combinations of ^{15}N labelling of NH_4^+ and NO_2^- were added into oxic slurries. Results showed that anammox reaction cannot happen in oxic slurries without the presence of aerobic ammonia oxidation. This further confirmed the affiliation between anammox and aerobic ammonia oxidation. It was assumed that aerobic ammonia-oxidizing microorganisms (AOM) and anammox bacteria aggregate together in oxic riverbeds, AOM consume oxygen and create a redox micro-environment for anammox. A micro-respiration system was then used to quantify the consumption of oxygen during aerobic ammonia oxidation. In these oxic riverbeds, AOM consumed oxygen at a rate of 22.28 nmol g^{-1} h^{-1} on average, competing for 8% of the total oxygen consumption through heterotrophic respiration, furthermore, there was more ammonia released through organic respiration than can be oxidised through aerobic ammonia oxidation, making oxygen limited in the aggregates and thus enabling anammox. The aerobic ammonia oxidation can provide nitrite to sustain the anammox bacteria. Furthermore, a standard, anoxic ^{15}N isotope pairing technique was also used in anoxic sediment slurries to confirm the anammox potential in these riverbeds. Anammox activities were also investigated at different depths of two selected riverbeds. Anammox made a higher contribution to N_2 production in gravel-dominated riverbeds compared with the sand-dominated riverbeds. Anammox activity in the surface layer (0-2 cm) of riverbed was higher than at depths and a significant correlation between anammox activity and porewater oxygen was observed in the examined riverbeds (r(s) = 0.90, p < 0.01), further suggesting that porewater oxygen concentration maybe a significant factor controlling anammox activity in the examined riverbeds - through aerobic ammonia

oxidation. In the anoxic conditions, denitrification can provide an alternative source of substrates for anammox.

In the $^{15}NH_4^+$ oxic slurries experiments (Chapter 2), $^{15}N\text{-}NO_3^-$ was also produced through nitrite oxidation process. To further investigate the relationships between aerobic ammonia oxidation, anammox and nitrite oxidation, the degree of nitrification efficiency in each river was calculated in Chapter 3 (based on the production of $^{15}N\text{-}N_2$ and $^{15}N\text{-}NO_3^-$). The degree of nitrification efficiency varied from 22.2% to 99.7% across the riverbeds. The degree of nitrification efficiency was highest where the contribution from anammox to N_2 production (*ra*) was lowest, and maximal where anammox was absent, suggesting a competition between nitrite oxidation and anammox for nitrite. To find out the molecular evidences of aerobic ammonia oxidation, anammox and nitrite oxidation in these riverbeds, as well as their relationships with the degree of nitrification efficiency, the abundances of genes responsible for these processes were quantified by qPCR amplifications. The degree of nitrification efficiency was highest where the abundance of *nxr*B gene (*Nitrospira* + *Nitrobacter*) was greatest, along with the highest abundance of comammox *Nitrospira amo*A gene. These results reveal a gradient in riverbed nitrification efficiency that was related primarily to *Nitrospira* dominating the nitrite oxidising bacteria (NOB) and being spatially separated from anammox. Furthermore, anammox was more important where abundance of *hzs*B and *amo*A genes were greater, indicating an interaction between aerobic ammonia oxidation and anammox - supported by oxygen. The relationships between the degree of nitrification efficiency and riverbed characteristics was also investigated. A positive correlation between the degree of nitrification efficiency and riverbed porewater soluble reactive phosphorus (SRP) concentration was found, suggesting that the availability of the phosphorus may related to the degree of the nitrification efficiency. The effects of SRP on the degree of

nitrification efficiency was then investigated by adding SRP into the oxic slurries. Adding SRP directly into the riverbed slurries may selectively increase the degree of nitrification efficiency in some riverbeds by stimulating nitrite oxidation.

To further identify the microorganisms that involved in these processes, Illumina MiSeq sequencings for total bacteria, AOA, AOB, anammox, *Nitrospira* and comammox *Nitrospira* were conducted in Chapter 4, then the community structures of these microorganisms in different riverbeds were analysed. *Nitrospira* sequences mainly clustered with *Nitrospira moscoviensis* and *Nitrospira marina* species, with the clades clustered with *Nitrospira moscoviensis* dominated in all riverbeds. The AOB *amo*A gene sequences obtained from these oxic riverbeds were all assigned to *Nitrosospira*, while the AOA *amo*A gene sequences were closely related to *Nitrosopumilus maritimus*, *Nitrosophaera viennensis* and some *amo*A sequences from uncultured archaea soils or WWTP. Phylogenetic analysis showed that most of the anammox sequences were closely affiliated to *Candidatus* Brocadia. The comammox *Nitrospira* sequences clustered with *Candidatus* Nitrospira nitrificans, *Candidatus* Nitrospira inopinata and uncultured bacteria clones from groundwater-fed rapid sand filters in Denmark, clade B comammox *Nitrospira* make up 79.5%-94.7% of the comammox abundance in these rivers and are more abundant than clade A comammox *Nitrospira*. These results indicated that these permeable, oxic riverbeds are likely to have selected for distinct AOM, NOB and anammox communities. The main environmental factors that affect the community structures across these riverbeds were also analysed. pH and SRP concentration were the main factors that influence the community structure of AOB, while the community structure of AOA was mainly driven by ammonium concentration. Nitrite concentration was the main factor that influence the community structures of *Nitrospira* and comammox

Nitrospira. The community structure of anammox was influenced by ammonium and nitrite concentrations.

This work has shown the simultaneous occurrence of aerobic ammonia oxidation, anammox and nitrite oxidation in gravel and sand-dominated oxic riverbeds. This phenomenon may also exist in other geologies but is often neglected. So, it is of significance to broaden out the co-occurrence of aerobic and anaerobic process in various environments. Further, the idea of 'the degree of nitrification efficiency' can be applied to any type of aquatic sediments when nitrification activity was examined. The finding in this study can also provide some insights to the researchers work on the N cycle and people who work on the simultaneous nitritation and anammox reactors in wastewater treatment plants (WWTP). The results in this thesis have shown a tight affiliation between aerobic ammonia oxidation and anammox, however, the direct evidence has not been identified. So, the next logical step would be using Fluorescence in situ hybridization (FISH) to detect and locate the distributions of AOM, anammox and NOB in sediment samples. A correlation between the degree of nitrification efficiency and SRP concentration has been found in this study, hinting a tight relationship between N cycle and P cycle in these riverbeds. However, the effect of SRP on the degree of nitrification efficiency has not been clearly illustrated as SRP was not at steady-state in the batch incubations. The effect of the SRP on the degree of nitrification efficiency can be potentially further investigated using continuous reactors (where a constant level of availability of SRP can be achieved).

References

Amano T, Yoshinaga I, Yamagishi T, Thuoc CV, Thu PT, Ueda S, et al. (2011). Contribution of anammox bacteria to benthic nitrogen cycling in a mangrove forest and shrimp ponds, Haiphong, Vietnam. *Microbes Environ* **26**: 1-6.

Anderson IC ,Levine JS. (1986). Relative rates of nitric oxide and nitrous oxide production by nitrifiers, denitrifiers, and nitrate respirers. *Appl Environ Microbiol* **51**: 938-945.

Aspila K, Agemian H ,Chau A. (1976). A semi-automated method for the determination of inorganic, organic and total phosphate in sediments. *Analyst* **101**: 187-197.

Babbin AR ,Ward BB. (2013). Controls on nitrogen loss processes in Chesapeake Bay sediments. *Environ Sci Technol* **47**: 4189-4196.

Bankevich A, Nurk S, Antipov D, Gurevich AA, Dvorkin M, Kulikov AS, et al. (2012). SPAdes: a new genome assembly algorithm and its applications to single-cell sequencing. *J Comput Biol* **19**: 455-477.

Bartelme RP, McLellan SL ,Newton RJ. (2017) Freshwater recirculating aquaculture system operations drive biofilter bacterial community shifts around a stable nitrifying consortium of ammonia-oxidizing archaea and comammox Nitrospira. *Front Microbiol* **8**, 101 doi: 10.3389/fmicb.2017.00101.

Bates D, Mächler M, Bolker B ,Walker S. (2015) Fitting linear mixed-effects models using lme4. *J Stat Softw* **67**, doi: 10.18637/jss.v067.i01.

Belser LW. (1979). Population ecology of nitrifying bacteria. *Ann Rev Microbiol* **33**: 309-333.

Blackburne R, Vadivelu VM, Yuan Z ,Keller J. (2007). Kinetic characterisation of an enriched Nitrospira culture with comparison to Nitrobacter. *Water Res* **41**: 3033-3042.

Blackburne R, Yuan Z ,Keller J. (2008). Partial nitrification to nitrite using low dissolved oxygen concentration as the main selection factor. *Biodegradation* **19**: 303-312.

Boyer EW, Howarth RW, Galloway JN, Dentener FJ, Green PA ,Vörösmarty CJ. (2006) Riverine nitrogen export from the continents to the coasts. *Global Biogeochem Cycles* **20**, GB1S91 doi: 10.1029/2005GB002537.

Bristow LA, Dalsgaard T, Tiano L, Mills DB, Bertagnolli AD, Wright JJ, et al. (2016). Ammonium and nitrite oxidation at nanomolar oxygen concentrations in oxygen minimum zone waters. *Proc Natl Acad Sci U S A* **113**: 10601-10606.

Brown MN, Briones A, Diana J ,Raskin L. (2013). Ammonia-oxidizing archaea and nitrite-oxidizing nitrospiras in the biofilter of a shrimp recirculating aquaculture system. *FEMS Microbiol Ecol* **83**: 17-25.

Burgin AJ ,Hamilton SK. (2007). Have we overemphasized the role of denitrification in aquatic ecosystems? A review of nitrate removal pathways. *Front Ecol Environ* **5**: 89-96.

Camejo PY, Santo Domingo J, McMahon KD ,Noguera DR. (2017) Genome-Enabled Insights into the Ecophysiology of the Comammox Bacterium "Candidatus Nitrospira nitrosa". *mSystems* **2**, e00059-00017 doi: 10.1128/mSystems.00059-17.

Canfield DE, Glazer AN ,Falkowski PG. (2010). The evolution and future of Earth's nitrogen cycle. *Science* **330**: 192-196.

Capone DG. (2001). Marine nitrogen fixation: what's the fuss? *Curr Opin Microbiol* **4**: 341-348.

Caranto JD ,Lancaster KM. (2017). Nitric oxide is an obligate bacterial nitrification intermediate produced by hydroxylamine oxidoreductase. *Proc Natl Acad Sci U S A* **114**: 8217-8222.

Cavan EL, Trimmer M, Shelley F ,Sanders R. (2017). Remineralization of particulate organic carbon in an ocean oxygen minimum zone. *Nat Commun* **8**: 14847.

Cebron A ,Garnier J. (2005). Nitrobacter and Nitrospira genera as representatives of nitrite-oxidizing bacteria: detection, quantification and growth along the lower Seine River (France). *Water Res* **39**: 4979-4992.

Chao Y, Mao Y, Yu K ,Zhang T. (2016). Novel nitrifiers and comammox in a full-scale hybrid biofilm and activated sludge reactor revealed by metagenomic approach. *Appl Microbiol Biotechnol* **100**: 8225-8237.

Chen D, Chalk PM ,Freney JR. (1990). Release of dinitrogen from nitrite and sulphamic acid for isotope ratio analysis of soil extracts containing nitrogen-15 labelled nitrite and nitrate. *Analyst* **115**: 365-370.

Cooper AB. (1983). Population ecology of nitrifiers in a stream receiving geothermal inputs of ammonium. *Appl Environ Microbiol* **45**: 1170-1177.

Daims H, Lebedeva EV, Pjevac P, Han P, Herbold C, Albertsen M, et al. (2015). Complete nitrification by Nitrospira bacteria. *Nature* **528**: 504-509.

Daims H, Nielsen JL, Nielsen PH, Schleifer K-H ,Wagner M. (2001). In Situ Characterization of Nitrospira-Like Nitrite-Oxidizing Bacteria Active in Wastewater Treatment Plants. *Appl Environ Microbiol* **67**: 5273-5284.

Daims H ,Wagner M. (2018). Nitrospira. *Trends Microbiol* **26**: 462-463.

Dalsgaard T, Thamdrup B ,Canfield DE. (2005). Anaerobic ammonium oxidation (anammox) in the marine environment. *Res Microbiol* **156**: 457-464.

Dang H, Zhang X, Sun J, Li T, Zhang Z ,Yang G. (2008). Diversity and spatial distribution of sediment ammonia-oxidizing crenarchaeota in response to estuarine and

environmental gradients in the Changjiang Estuary and East China Sea. *Microbiology* **154**: 2084-2095.

Dapena-Mora A, Fernandez I, Campos J, Mosquera-Corral A, Mendez R ,Jetten M. (2007). Evaluation of activity and inhibition effects on Anammox process by batch tests based on the nitrogen gas production. *Enzyme Microb Technol* **40**: 859-865.

De Brabandere L, Canfield DE, Dalsgaard T, Friederich GE, Revsbech NP, Ulloa O, et al. (2014). Vertical partitioning of nitrogen - loss processes across the oxic - anoxic interface of an oceanic oxygen minimum zone. *Environ Microbiol* **16**: 3041-3054.

De Vet W, Van Loosdrecht M ,Rietveld L. (2012). Phosphorus limitation in nitrifying groundwater filters. *Water Res* **46**: 1061-1069.

Dietl A, Ferousi C, Maalcke WJ, Menzel A, de Vries S, Keltjens JT, et al. (2015). The inner workings of the hydrazine synthase multiprotein complex. *Nature* **527**: 394-397.

Dumbrell AJ, Ferguson RM ,Clark DR (2016). Microbial community analysis by single-amplicon high-throughput next generation sequencing: data analysis–from raw output to ecology. Hydrocarbon and Lipid Microbiology Protocols, *Springer***:** 155-206.

Edgar RC. (2004). MUSCLE: multiple sequence alignment with high accuracy and high throughput. *Nucleic Acids Res* **32**: 1792-1797.

Edgar RC, Haas BJ, Clemente JC, Quince C ,Knight R. (2011). UCHIME improves sensitivity and speed of chimera detection. *Bioinformatics* **27**: 2194-2200.

Ehrich S, Behrens D, Lebedeva E, Ludwig W ,Bock E. (1995). A new obligately chemolithoautotrophic, nitrite-oxidizing bacterium, Nitrospira moscoviensis sp. nov. and its phylogenetic relationship. *Arch Microbiol* **164**: 16-23.

Erguder TH, Boon N, Wittebolle L, Marzorati M ,Verstraete W. (2009). Environmental factors shaping the ecological niches of ammonia-oxidizing archaea. *FEMS Microbiol Rev* **33**: 855-869.

Evrard V, Glud RN ,Cook PL. (2013). The kinetics of denitrification in permeable sediments. *Biogeochemistry* **113**: 563-572.

Fan X, Gao J, Pan K, Li D ,Dai H. (2017). Temporal dynamics of bacterial communities and predicted nitrogen metabolism genes in a full-scale wastewater treatment plant. *RSV Adv* **7**: 56317-56327.

Fernandes SO, Javanaud C, Michotey VD, Guasco S, Anschutz P ,Bonin P. (2016). Coupling of bacterial nitrification with denitrification and anammox supports N removal in intertidal sediments (Arcachon Bay, France). *Estuar Coast Shelf Sci* **179**: 39-50.

Foesel BU, Gieseke A, Schwermer C, Stief P, Koch L, Cytryn E, et al. (2007). Nitrosomonas Nm143-like ammonia oxidizers and Nitrospira marina-like nitrite oxidizers dominate the nitrifier community in a marine aquaculture biofilm. *FEMS Microbiol Ecol* **63**: 192-204.

Folk RL. (1954). The distinction between grain size and mineral composition in sedimentary-rock nomenclature. *J Geol* **62**: 344-359.

Fowler SJ, Palomo A, Dechesne A, Mines PD ,Smets BF. (2018). Comammox Nitrospira are abundant ammonia oxidizers in diverse groundwater - fed rapid sand filter communities. *Environ Microbiol* **20**: 1002-1015.

Francis CA, Beman JM ,Kuypers MM. (2007). New processes and players in the nitrogen cycle: the microbial ecology of anaerobic and archaeal ammonia oxidation. *ISME J* **1**: 19-27.

Francis CA, Roberts KJ, Beman JM, Santoro AE ,Oakley BB. (2005). Ubiquity and diversity of ammonia-oxidizing archaea in water columns and sediments of the ocean. *Proc Natl Acad Sci U S A* **102**: 14683-14688.

Fukushima T, Whang LM, Chiang TY, Lin YH, Chevalier LR, Chen MC, et al. (2013). Nitrifying bacterial community structures and their nitrification performance under sufficient and limited inorganic carbon conditions. *Appl Microbiol Biotechnol* **97**: 6513-6523.

Galán A, Thamdrup B, Saldías GS ,Farías L. (2017). Vertical segregation among pathways mediating nitrogen loss (N2 and N2O production) across the oxygen gradient in a coastal upwelling ecosystem. *Biogeosciences* **14**: 4795-4813.

Galloway JN, Dentener FJ, Capone DG, Boyer EW, Howarth RW, Seitzinger SP, et al. (2004). Nitrogen cycles: past, present, and future. *Biogeochemistry* **70**: 153-226.

Galloway JN, Schlesinger WH, Levy H, Michaels A ,Schnoor JL. (1995). Nitrogen fixation: Anthropogenic enhancement - environmental response. *Global Biogeochem Cycles* **9**: 235-252.

Galloway JN, Townsend AR, Erisman JW, Bekunda M, Cai Z, Freney JR, et al. (2008). Transformation of the nitrogen cycle: recent trends, questions, and potential solutions. *Science* **320**: 889-892.

Gao H, Schreiber F, Collins G, Jensen MM, Kostka JE, Lavik G, et al. (2009). Aerobic denitrification in permeable Wadden Sea sediments. *ISME J* **4**: 417-426.

Geets J, De Cooman M, Wittebolle L, Heylen K, Vanparys B, De Vos P, et al. (2007). Real-time PCR assay for the simultaneous quantification of nitrifying and denitrifying bacteria in activated sludge. *Appl Microbiol Biotechnol* **75**: 211-221.

Gieseke A, Purkhold U, Wagner M, Amann R ,Schramm A. (2001). Community structure and activity dynamics of nitrifying bacteria in a phosphate-removing biofilm. *Appl Environ Microbiol* **67**: 1351-1362.

Gihring TM, Canion A, Riggs A, Huettel M ,Kostka JE. (2010). Denitrification in shallow, sublittoral Gulf of Mexico permeable sediments. *Limnol Oceanogr* **55**: 43-54.

Ginestet P, Audic JM, Urbain V ,Block JC. (1998). Estimation of nitrifying bacterial activities by measuring oxygen uptake in the presence of the metabolic inhibitors allylthiourea and azide. *Appl Environ Microbiol* **64**: 2266-2268.

Gonzalez-Martinez A, Rodriguez-Sanchez A, van Loosdrecht MM, Gonzalez-Lopez J ,Vahala R. (2016). Detection of comammox bacteria in full-scale wastewater treatment bioreactors using tag-454-pyrosequencing. *Environ Sci Pollut R* **23**: 25501-25511.

Graham DW, Trippett C, Dodds WK, O'Brien JM, Banner EB, Head IM, et al. (2010). Correlations between in situ denitrification activity and nir-gene abundances in pristine and impacted prairie streams. *Environ Pollut* **158**: 3225-3229.

Gruber N ,Galloway JN. (2008). An Earth-system perspective of the global nitrogen cycle. *Nature* **451**: 293-296.

Hampel JJ, McCarthy MJ, Gardner WS, Zhang L, Xu H, Zhu G, et al. (2018). Nitrification and ammonium dynamics in Taihu Lake, China: seasonal competition for ammonium between nitrifiers and cyanobacteria. *Biogeosciences* **15**: 733-748.

Hanrahan G, Gledhill M, House WA ,Worsfold PJ. (2003). Evaluation of phosphorus concentrations in relation to annual and seasonal physico-chemical water quality parameters in a UK chalk stream. *Water Res* **37**: 3579-3589.

Hao X, Heijnen JJ ,van Loosdrecht M. (2002). Sensitivity analysis of a biofilm model describing a one - stage completely autotrophic nitrogen removal (CANON) process. *Biotechnol Bioeng* **77**: 266-277.

Harhangi HR, Le Roy M, van Alen T, Hu B, Groen J, Kartal B, et al. (2012). Hydrazine synthase, a unique phylomarker with which to study the presence and biodiversity of anammox bacteria. *Appl Environ Microbiol* **78**: 752-758.

He J, Hu H ,Zhang L. (2012). Current insights into the autotrophic thaumarchaeal ammonia oxidation in acidic soils. *Soil Biol Biochem* **55**: 146-154.

Hellinga C, Schellen A, Mulder JW, van Loosdrecht Mv ,Heijnen J. (1998). The SHARON process: an innovative method for nitrogen removal from ammonium-rich waste water. *Water Sci Technol* **37**: 135-142.

Herbert R. (1999). Nitrogen cycling in coastal marine ecosystems. *FEMS Microbiol Rev* **23**: 563-590.

Herlemann DP, Labrenz M, Jürgens K, Bertilsson S, Waniek JJ ,Andersson AF. (2011). Transitions in bacterial communities along the 2000 km salinity gradient of the Baltic Sea. *ISME J* **5**: 1571-1579.

Herrmann M, Saunders AM ,Schramm A. (2009). Effect of lake trophic status and rooted macrophytes on community composition and abundance of ammonia-oxidizing prokaryotes in freshwater sediments. *Appl Environ Microbiol* **75**: 3127-3136.

Hink L, Gubry-Rangin C, Nicol GW ,Prosser JI. (2018). The consequences of niche and physiological differentiation of archaeal and bacterial ammonia oxidisers for nitrous oxide emissions. *ISME J* **12**: 1084-1093.

Hou L, Zheng Y, Liu M, Gong J, Zhang X, Yin G, et al. (2013). Anaerobic ammonium oxidation (anammox) bacterial diversity, abundance, and activity in marsh sediments of the Yangtze Estuary. *J Geophys Res Biogeosci* **118**: 1237-1246.

Hovanec TA, Taylor LT, Blakis A ,Delong EF. (1998). Nitrospira-like bacteria associated with nitrite oxidation in freshwater aquaria. *Appl Environ Microbiol* **64**: 258-264.

Hsieh T, Ma K ,Chao A. (2016). iNEXT: an R package for rarefaction and extrapolation of species diversity (H ill numbers). *Methods in Ecology and Evolution* **7**: 1451-1456.

Hu B, Shen L, Xu X ,Zheng P. (2011). Anaerobic ammonium oxidation (anammox) in different natural ecosystems. *Biochem Soc Trans* **39**: 1811-1816.

Hu B, Shen L, Zheng P, Hu A, Chen T, Cai C, et al. (2012). Distribution and diversity of anaerobic ammonium‐oxidizing bacteria in the sediments of the Qiantang River. *Env Microbiol Rep* **4**: 540-547.

Hu HW ,He JZ. (2017). Comammox—a newly discovered nitrification process in the terrestrial nitrogen cycle. *J Soils Sed* **17**: 2709-2717.

Hue N ,Adams F. (1984). Effect of phosphorus level on nitrification rates in three low-phosphorus ultisoils. *Soil Sci* **137**: 324-331.

Humbert S, Zopfi J ,Tarnawski SE. (2012). Abundance of anammox bacteria in different wetland soils. *Env Microbiol Rep* **4**: 484-490.

Inwood SE, Tank JL ,Bernot MJ. (2005). Patterns of denitrification associated with land use in 9 midwestern headwater streams. *J N Am Benthol Soc* **24**: 227-245.

Jensen MM, Petersen J, Dalsgaard T ,Thamdrup B. (2009). Pathways, rates, and regulation of N2 production in the chemocline of an anoxic basin, Mariager Fjord, Denmark. *Mar Chem* **113**: 102-113.

Jetten MS. (2008). The microbial nitrogen cycle. *Environ Microbiol* **10**: 2903-2909.

Jetten MS, Sliekers O, Kuypers M, Dalsgaard T, van Niftrik L, Cirpus I, et al. (2003). Anaerobic ammonium oxidation by marine and freshwater planctomycete-like bacteria. *Appl Microbiol Biotechnol* **63**: 107-114.

Jetten MS, Strous M, Van de Pas-Schoonen KT, Schalk J, van Dongen UG, van de Graaf AA, et al. (1998). The anaerobic oxidation of ammonium. *FEMS Microbiol Rev* **22**: 421-437.

Jin T, Zhang T, Ye L, Lee OO, Wong YH ,Qian PY. (2011). Diversity and quantity of ammonia-oxidizing Archaea and Bacteria in sediment of the Pearl River Estuary, China. *Appl Microbiol Biotechnol* **90**: 1137-1145.

Joshi N ,Fass J. (2011). Sickle: A sliding-window, adaptive, quality-based trimming tool for FastQ files (Version 1.33) [Software]. *Available at https://githubcom/najoshi/sickle*.

Kalvelage T, Jensen MM, Contreras S, Revsbech NP, Lam P, Günter M, et al. (2011) Oxygen sensitivity of anammox and coupled N-cycle processes in oxygen minimum zones. *PLoS One* **6**, e29299 doi: 10.1371/journal.pone.0029299.

Kartal B, Maalcke WJ, de Almeida NM, Cirpus I, Gloerich J, Geerts W, et al. (2011). Molecular mechanism of anaerobic ammonium oxidation. *Nature* **479**: 127-130.

Kim H, Bae H-S, Reddy KR ,Ogram A. (2016). Distributions, abundances and activities of microbes associated with the nitrogen cycle in riparian and stream sediments of a river tributary. *Water Res* **106**: 51-61.

Kim SY, Veraart AJ, Meima-Franke M ,Bodelier PL. (2015). Combined effects of carbon, nitrogen and phosphorus on CH4 production and denitrification in wetland sediments. *Geoderma* **259**: 354-361.

Kits KD, Sedlacek CJ, Lebedeva EV, Han P, Bulaev A, Pjevac P, et al. (2017). Kinetic analysis of a complete nitrifier reveals an oligotrophic lifestyle. *Nature* **549**: 269-272.

Koike I ,Hattori A. (1978). Simultaneous determinations of nitrification and nitrate reduction in coastal sediments by a 15N dilution technique. *Appl Environ Microbiol* **35**: 853-857.

Könneke M, Bernhard AE, José R, Walker CB, Waterbury JB ,Stahl DA. (2005). Isolation of an autotrophic ammonia-oxidizing marine archaeon. *Nature* **437**: 543.

Kowalchuk GA, Stephen JR, De Boer W, Prosser JI, Embley TM ,Woldendorp JW. (1997). Analysis of ammonia-oxidizing bacteria of the beta subdivision of the class Proteobacteria in coastal sand dunes by denaturing gradient gel electrophoresis and sequencing of PCR-amplified 16S ribosomal DNA fragments. *Appl Environ Microbiol* **63**: 1489-1497.

Kozlowski JA, Stieglmeier M, Schleper C, Klotz MG ,Stein LY. (2016). Pathways and key intermediates required for obligate aerobic ammonia-dependent chemolithotrophy in bacteria and Thaumarchaeota. *ISME J* **10**: 1836.

Kuenen JG. (2008). Anammox bacteria: from discovery to application. *Nat Rev Microbiol* **6**: 320-326.

Kumar S, Stecher G ,Tamura K. (2016). MEGA7: Molecular Evolutionary Genetics Analysis version 7.0 for bigger datasets. *Mol Biol Evol* **33**: 1870-1874.

Kuypers MM, Lavik G, Woebken D, Schmid M, Fuchs BM, Amann R, et al. (2005). Massive nitrogen loss from the Benguela upwelling system through anaerobic ammonium oxidation. *Proc Natl Acad Sci U S A* **102**: 6478-6483.

Kuypers MM, Marchant HK ,Kartal B. (2018). The microbial nitrogen-cycling network. *Nat Rev Microbiol* **16**: 263-276.

Lam P, Jensen MM, Lavik G, McGinnis DF, Müller B, Schubert CJ, et al. (2007). Linking crenarchaeal and bacterial nitrification to anammox in the Black Sea. *Proc Natl Acad Sci U S A* **104**: 7104-7109.

Lam P, Lavik G, Jensen MM, van de Vossenberg J, Schmid M, Woebken D, et al. (2009). Revising the nitrogen cycle in the Peruvian oxygen minimum zone. *Proc Natl Acad Sci U S A* **106**: 4752-4757.

Lansdown K, Heppell CM, Dossena M, Ullah S, Heathwaite AL, Binley A, et al. (2014). Fine-scale in situ measurement of riverbed nitrate production and consumption in an armored permeable riverbed. *Environ Sci Technol* **48**: 4425-4434.

Lansdown K, McKew B, Whitby C, Heppell C, Dumbrell A, Binley A, et al. (2016). Importance and controls of anaerobic ammonium oxidation influenced by riverbed geology. *Nat Geosci* **9**: 357-360.

Lansdown K, Trimmer M, Heppell C, Sgouridis F, Ullah S, Heathwaite A, et al. (2012). Characterization of the key pathways of dissimilatory nitrate reduction and their response to complex organic substrates in hyporheic sediments. *Limnol Oceanogr* **57**: 387-400.

Lee K-H, Wang Y-F, Zhang G-X ,Gu J-D. (2014). Distribution patterns of ammonia-oxidizing bacteria and anammox bacteria in the freshwater marsh of Honghe wetland in Northeast China. *Ecotoxicology* **23**: 1930-1942.

Li M, Cao H, Hong Y-G ,Gu J-D. (2011). Seasonal dynamics of anammox bacteria in estuarial sediment of the Mai Po Nature Reserve revealed by analyzing the 16S rRNA and hydrazine oxidoreductase (hzo) genes. *Microbes Environ* **26**: 15-22.

Li M, Hong Y-G, Cao H-L ,Gu J-D. (2011). Mangrove trees affect the community structure and distribution of anammox bacteria at an anthropogenic-polluted mangrove in the Pearl River Delta reflected by 16S rRNA and hydrazine oxidoreductase (HZO) encoding gene analyses. *Ecotoxicology* **20**: 1780.

Li M, Hong Y, Klotz MG ,Gu J-D. (2010). A comparison of primer sets for detecting 16S rRNA and hydrazine oxidoreductase genes of anaerobic ammonium-oxidizing bacteria in marine sediments. *Appl Microbiol Biotechnol* **86**: 781-790.

Li M, Wei G, Shi W, Sun Z, Li H, Wang X, et al. (2018) Distinct distribution patterns of ammonia-oxidizing archaea and bacteria in sediment and water column of the Yellow River estuary. *Sci Rep* **8**, 1584 doi: 10.1038/s41598-018-20044-6.

Liu S, Hu JJ, Shen JX, Chen S, Tian GM, Zheng P, et al. (2017). Potencial correlate environmental factors leading to the niche segregation of ammonia-oxidizing archaea and ammonia-oxidizing bacteria: a review. *Appl Environ Biotechnol* **2**: 11-19.

Lu S, Liu X, Ma Z, Liu Q, Wu Z, Zeng X, et al. (2016) Vertical segregation and phylogenetic characterization of ammonia-oxidizing bacteria and archaea in the sediment

of a freshwater aquaculture pond. *Front Microbiol* **6**, 1539 doi: 10.3389/fmicb.2015.01539.

Luther GW, Sundby B, Lewis BL, Brendel PJ ,Silverberg N. (1997). Interactions of manganese with the nitrogen cycle: alternative pathways to dinitrogen. *Geochim Cosmochim Acta* **61**: 4043-4052.

Ma B, Bao P, Wei Y, Zhu G, Yuan Z ,Peng Y. (2015) Suppressing nitrite-oxidizing bacteria growth to achieve nitrogen removal from domestic wastewater via anammox using intermittent aeration with low dissolved oxygen. *Sci Rep* **5**, 13048 doi: 10.1038/srep13048.

Ma Y, Peng Y, Wang S, Yuan Z ,Wang X. (2009). Achieving nitrogen removal via nitrite in a pilot-scale continuous pre-denitrification plant. *Water Res* **43**: 563-572.

Maixner F, Noguera DR, Anneser B, Stoecker K, Wegl G, Wagner M, et al. (2006). Nitrite concentration influences the population structure of Nitrospira - like bacteria. *Environ Microbiol* **8**: 1487-1495.

Marchant HK, Holtappels M, Lavik G, Ahmerkamp S, Winter C ,Kuypers MM. (2016). Coupled nitrification–denitrification leads to extensive N loss in subtidal permeable sediments. *Limnol Oceanogr* **61**: 1033-1048.

Marchant HK, Lavik G, Holtappels M ,Kuypers MM. (2014) The fate of nitrate in intertidal permeable sediments. *PLoS One* **9**, e104517 doi: 10.1371/journal.pone.0104517.

Martens-Habbena W, Berube PM, Urakawa H, José R ,Stahl DA. (2009). Ammonia oxidation kinetics determine niche separation of nitrifying Archaea and Bacteria. *Nature* **461**: 976-979.

Martens - Habbena W, Qin W, Horak RE, Urakawa H, Schauer AJ, Moffett JW, et al. (2015). The production of nitric oxide by marine ammonia - oxidizing archaea and inhibition of archaeal ammonia oxidation by a nitric oxide scavenger. *Environ Microbiol* **17**: 2261-2274.

Masella AP, Bartram AK, Truszkowski JM, Brown DG ,Neufeld JD. (2012). PANDAseq: paired-end assembler for illumina sequences. *BMC Bioinformatics* **13**: 31.

McIlvin MR ,Altabet MA. (2005). Chemical conversion of nitrate and nitrite to nitrous oxide for nitrogen and oxygen isotopic analysis in freshwater and seawater. *Anal Chem* **77**: 5589-5595.

McKew BA ,Smith CJ (2015). Real-Time PCR Approaches for analysis of hydrocarbon-degrading bacterial communities. Hydrocarbon and Lipid Microbiology Protocols, *Springer***:** 45-64.

Meyer RL, Risgaard-Petersen N ,Allen DE. (2005). Correlation between anammox activity and microscale distribution of nitrite in a subtropical mangrove sediment. *Appl Environ Microbiol* **71**: 6142-6149.

Minami K ,Fukushi S. (1983). Effecfs of phosphate and calcium carbonate application on emission of N20 from soils under aerobic conditions. *Soil Sci Plant Nutr* **29**: 517-524.

Mulder A, Graaf A, Robertson L ,Kuenen J. (1995). Anaerobic ammonium oxidation discovered in a denitrifying fluidized bed reactor. *FEMS Microbiol Ecol* **16**: 177-184.

Mulholland PJ, Helton AM, Poole GC, Hall RO, Hamilton SK, Peterson BJ, et al. (2008). Stream denitrification across biomes and its response to anthropogenic nitrate loading. *Nature* **452**: 202-205.

Murphy J ,Riley JP. (1962). A modified single solution method for the determination of phosphate in natural waters. *Anal Chim Acta* **27**: 31-36.

Nakamura Y, Satoh H, Kindaichi T ,Okabe S. (2006). Community structure, abundance, and in situ activity of nitrifying bacteria in river sediments as determined by the combined use of molecular techniques and microelectrodes. *Environ Sci Technol* **40**: 1532-1539.

Naura M, Clark MJ, Sear DA, Atkinson PM, Hornby DD, Kemp P, et al. (2016). Mapping habitat indices across river networks using spatial statistical modelling of River Habitat Survey data. *Ecol Indicators* **66**: 20-29.

Nelson NS. (1987). An acid - persulfate digestion procedure for determination of phosphorus in sediments. *Commun Soil Sci Plant Anal* **18**: 359-369.

Neubacher EC, Parker RE ,Trimmer M. (2011). Short-term hypoxia alters the balance of the nitrogen cycle in coastal sediments. *Limnol Oceanogr* **56**: 651-665.

Nicholls JC ,Trimmer M. (2009). Widespread occurrence of the anammox reaction in estuarine sediments. *Aquat Microb Ecol* **55**: 105-113.

Nicol GW, Leininger S ,Schleper C (2011). Distribution and activity of ammonia-oxidizing archaea in natural environments. Nitrification, *American Society of Microbiology***:** 157-178.

Nielsen M, Bollmann A, Sliekers O, Jetten M, Schmid M, Strous M, et al. (2005). Kinetics, diffusional limitation and microscale distribution of chemistry and organisms in a CANON reactor. *Fems Microbiology Ecology* **51**: 247-256.

Nikolenko SI, Korobeynikov AI ,Alekseyev MA (2013). BayesHammer: Bayesian clustering for error correction in single-cell sequencing. BMC Genomics, BioMed Central.**14**: S7.

Nowak O, Svardal K ,Kroiss H. (1996). The impact of phosphorus deficiency on nitrification-Case study of a biological pretreatment plant for rendering plant effluent. *Water Sci Technol* **34**: 229-236.

Oksanen J, Blanchet FG, Friendly M, Kindt R, Legendre P, McGlinn D, et al. (2017). vegan: Community Ecology Package. R package version 2.4-3. *Available at https://CRANR-projectorg/package=vegan*.

Palomo A, Pedersen AG, Fowler SJ, Dechesne A, Sicheritz-Pontén T ,Smets BF. (2018). Comparative genomics sheds light on niche differentiation and the evolutionary history of comammox Nitrospira. *ISME J* **12**: 1779-1793.

Penton CR, Devol AH ,Tiedje JM. (2006). Molecular evidence for the broad distribution of anaerobic ammonium-oxidizing bacteria in freshwater and marine sediments. *Appl Environ Microbiol* **72**: 6829-6832.

Pester M, Maixner F, Berry D, Rattei T, Koch H, Lücker S, et al. (2014). NxrB encoding the beta subunit of nitrite oxidoreductase as functional and phylogenetic marker for nitrite-oxidizing Nitrospira. *Environ Microbiol* **16**: 3055-3071.

Pester M, Rattei T, Flechl S, Gröngröft A, Richter A, Overmann J, et al. (2012). amoA-based consensus phylogeny of ammonia-oxidizing archaea and deep sequencing of amoA genes from soils of four different geographic regions. *Environ Microbiol* **14**: 525-539.

Pina-Ochoa E ,Alvarez-Cobelas M. (2006). Denitrification in aquatic environments: a cross-system analysis. *Biogeochemistry* **81**: 111-130.

Pinto A, Marcus D, Ijaz U, Bautista-de Lose Santos Q, Dick G ,Raskin L. (2016) Metagenomic evidence for the presence of comammox. *mSystems* **1**, e00054-00015 doi: 10.1128/mSphere.00054-15.

Pjevac P, Schauberger C, Poghosyan L, Herbold CW, van Kessel MA, Daebeler A, et al. (2017) AmoA-targeted polymerase chain reaction primers for the specific detection and quantification of comammox Nitrospira in the environment. *Front Microbiol* **8**, 1508 doi: 10.3389/fmicb.2017.01508.

Pretty J, Hildrew A ,Trimmer M. (2006). Nutrient dynamics in relation to surface–subsurface hydrological exchange in a groundwater fed chalk stream. *J Hydrol* **330**: 84-100.

Purchase B. (1974). The influence of phosphate deficiency on nitrification. *Plant Soil* **41**: 541-547.

Purkhold U, Wagner M, Timmermann G, Pommerening-Röser A ,Koops H-P. (2003). 16S rRNA and amoA-based phylogeny of 12 novel betaproteobacterial ammonia-oxidizing isolates: extension of the dataset and proposal of a new lineage within the nitrosomonads. *Int J Syst Evol Microbiol* **53**: 1485-1494.

Pynaert K, Smets BF, Wyffels S, Beheydt D, Siciliano SD ,Verstraete W. (2003). Characterization of an autotrophic nitrogen-removing biofilm from a highly loaded lab-scale rotating biological contactor. *Appl Environ Microbiol* **69**: 3626-3635.

Rao AM, McCarthy MJ, Gardner WS ,Jahnke RA. (2008). Respiration and denitrification in permeable continental shelf deposits on the South Atlantic Bight: N2: Ar and isotope pairing measurements in sediment column experiments. *Cont Shelf Res* **28**: 602-613.

Raymond J, Siefert JL, Staples CR ,Blankenship RE. (2004). The natural history of nitrogen fixation. *Mol Biol Evol* **21**: 541-554.

Regan JM, Harrington GW ,Noguera DR. (2002). Ammonia-and nitrite-oxidizing bacterial communities in a pilot-scale chloraminated drinking water distribution system. *Appl Environ Microbiol* **68**: 73-81.

Rich JJ, Dale OR, Song B ,Ward BB. (2008). Anaerobic ammonium oxidation (anammox) in Chesapeake Bay sediments. *Microb Ecol* **55**: 311-320.

Risgaard-Petersen N, Meyer RL, Schmid M, Jetten MS, Enrich-Prast A, Rysgaard S, et al. (2004). Anaerobic ammonium oxidation in an estuarine sediment. *Aquat Microb Ecol* **36**: 239-340.

Rognes T, Flouri T, Nichols B, Quince C ,Mahé F. (2016) VSEARCH: a versatile open source tool for metagenomics. *PeerJ* **4**, e2584 doi: 10.7717/peerj.2584.

Rosswall T (1981). The biogeochemical nitrogen cycle. Some perspectives of the major biogeochemical cycles, *SCOPE***:** 25-49.

Saitou N ,Nei M. (1987). The neighbor-joining method: a new method for reconstructing phylogenetic trees. *Mol Biol Evol* **4**: 406-425.

Schmid M, Walsh K, Webb R, Rijpstra WI, van de Pas-Schoonen K, Verbruggen MJ, et al. (2003). Candidatus "Scalindua brodae", sp. nov., Candidatus "Scalindua wagneri", sp. nov., two new species of anaerobic ammonium oxidizing bacteria. *Syst Appl Microbiol* **26**: 529-538.

Schmid MC, Hooper AB, Klotz MG, Woebken D, Lam P, Kuypers MM, et al. (2008). Environmental detection of octahaem cytochrome c hydroxylamine/hydrazine oxidoreductase genes of aerobic and anaerobic ammonium-oxidizing bacteria. *Environ Microbiol* **10**: 3140-3149.

Schmidt I, Sliekers O, Schmid M, Cirpus I, Strous M, Bock E, et al. (2002). Aerobic and anaerobic ammonia oxidizing bacteria–competitors or natural partners? *FEMS Microbiol Ecol* **39**: 175-181.

Schmidt I, van Spanning RJ ,Jetten MS. (2004). Denitrification and ammonia oxidation by Nitrosomonas europaea wild-type, and NirK-and NorB-deficient mutants. *Microbiology* **150**: 4107-4114.

Schramm A, de Beer D, van den Heuvel JC, Ottengraf S ,Amann R. (1999). Microscale Distribution of Populations and Activities ofNitrosospira and Nitrospira spp. along a Macroscale Gradient in a Nitrifying Bioreactor: Quantification by In Situ Hybridization and the Use of Microsensors. *Appl Environ Microbiol* **65**: 3690-3696.

Schubert CJ, Durisch-Kaiser E, Wehrli B, Thamdrup B, Lam P ,Kuypers MM. (2006). Anaerobic ammonium oxidation in a tropical freshwater system (Lake Tanganyika). *Environ Microbiol* **8**: 1857-1863.

Seitzinger S, Harrison JA, Böhlke J, Bouwman A, Lowrance R, Peterson B, et al. (2006). Denitrification across landscapes and waterscapes: a synthesis. *Ecol Appl* **16**: 2064-2090.

Seitzinger SP. (1988). Denitrification in freshwater and coastal marine ecosystems: ecological and geochemical significance. *Limnol Oceanogr* **33**: 702-724.

Shan J, Zhao X, Sheng R, Xia Y, Ti C, Quan X, et al. (2016). Dissimilatory Nitrate Reduction Processes in Typical Chinese Paddy Soils: Rates, Relative Contributions, and Influencing Factors. *Environ Sci Technol* **50**: 9972-9980.

Shaw LJ, Nicol GW, Smith Z, Fear J, Prosser JI ,Baggs EM. (2006). Nitrosospira spp. can produce nitrous oxide via a nitrifier denitrification pathway. *Environ Microbiol* **8**: 214-222.

Shen L, Cheng H, Liu X, Li J ,Liu Y. (2017). Potential role of anammox in nitrogen removal in a freshwater reservoir, Jiulonghu Reservoir (China). *Environ Sci Pollut R* **24**: 3890-3899.

Shen L, Liu S, He Z, Lian X, Huang Q, He Y, et al. (2015). Depth-specific distribution and importance of nitrite-dependent anaerobic ammonium and methane-oxidising bacteria in an urban wetland. *Soil Biol Biochem* **83**: 43-51.

Shen L, Wu H, Gao Z, Cheng H, Li J, Liu X, et al. (2016). Distribution and activity of anaerobic ammonium-oxidising bacteria in natural freshwater wetland soils. *Appl Microbiol Biotechnol* **100**: 3291-3300.

Sliekers AO, Derwort N, Gomez JC, Strous M, Kuenen J ,Jetten M. (2002). Completely autotrophic nitrogen removal over nitrite in one single reactor. *Water Res* **36**: 2475-2482.

Smith LK, Voytek MA, Böhlke JK ,Harvey JW. (2006). Denitrification in nitrate‐rich streams: Application of N2: Ar and 15N‐tracer methods in intact cores. *Ecol Appl* **16**: 2191-2207.

Sonthiphand P, Hall MW ,Neufeld JD. (2014) Biogeography of anaerobic ammonia-oxidizing (anammox) bacteria. *Front Microbiol* **5**, 399 doi: 10.3389/fmicb.2014.00399.

Stein LY ,Klotz MG. (2016). The nitrogen cycle. *Curr Biol* **26**: R94-R98.

Stevens H ,Ulloa O. (2008). Bacterial diversity in the oxygen minimum zone of the eastern tropical South Pacific. *Environ Microbiol* **10**: 1244-1259.

Strous M, Kuenen JG ,Jetten MS. (1999). Key physiology of anaerobic ammonium oxidation. *Appl Environ Microbiol* **65**: 3248-3250.

Strous M, Pelletier E, Mangenot S, Rattei T, Lehner A, Taylor MW, et al. (2006). Deciphering the evolution and metabolism of an anammox bacterium from a community genome. *Nature* **440**: 790-794.

Subbarao G, Ito O, Sahrawat K, Berry W, Nakahara K, Ishikawa T, et al. (2006). Scope and strategies for regulation of nitrification in agricultural systems—challenges and opportunities. *Crit Rev Plant Sci* **25**: 303-335.

Tan H, Barret M, Mooij MJ, Rice O, Morrissey JP, Dobson A, et al. (2013). Long-term phosphorus fertilisation increased the diversity of the total bacterial community and the phoD phosphorus mineraliser group in pasture soils. *Biol Fertility Soils* **49**: 661-672.

Terada A, Zhou S ,Hosomi M. (2011). Presence and detection of anaerobic ammonium-oxidizing (anammox) bacteria and appraisal of anammox process for high-strength nitrogenous wastewater treatment: a review. *Clean Techn Environ Policy* **13**: 759-781.

Thamdrup B ,Dalsgaard T. (2002). Production of N2 through anaerobic ammonium oxidation coupled to nitrate reduction in marine sediments. *Appl Environ Microbiol* **68**: 1312-1318.

Third K, Sliekers AO, Kuenen J ,Jetten M. (2001). The CANON system (completely autotrophic nitrogen-removal over nitrite) under ammonium limitation: interaction and competition between three groups of bacteria. *Syst Appl Microbiol* **24**: 588-596.

Third KA, Sliekers AO, Kuenen JG ,Jetten MSM. (2001). The CANON system (completely autotrophic nitrogen-removal over nitrite) under ammonium limitation: Interaction and competition between three groups of bacteria. *Syst Appl Microbiol* **24**: 588-596.

Tourna M, Freitag TE, Nicol GW ,Prosser JI. (2008). Growth, activity and temperature responses of ammonia - oxidizing archaea and bacteria in soil microcosms. *Environ Microbiol* **10**: 1357-1364.

Tourna M, Stieglmeier M, Spang A, Könneke M, Schintlmeister A, Urich T, et al. (2011). Nitrososphaera viennensis, an ammonia oxidizing archaeon from soil. *Proc Natl Acad Sci U S A* **108**: 8420-8425.

Treusch AH, Leininger S, Kletzin A, Schuster SC, Klenk HP ,Schleper C. (2005). Novel genes for nitrite reductase and Amo - related proteins indicate a role of uncultivated mesophilic crenarchaeota in nitrogen cycling. *Environ Microbiol* **7**: 1985-1995.

Trimmer M, Engström P ,Thamdrup B. (2013). Stark contrast in denitrification and anammox across the deep Norwegian trench in the Skagerrak. *Appl Environ Microbiol* **79**: 7381-7389.

Trimmer M ,Nicholls JC. (2009). Production of nitrogen gas via anammox and denitrification in intact sediment cores along a continental shelf to slope transect in the North Atlantic. *Limnol Oceanogr* **54**: 577-589.

Trimmer M, Nicholls JC ,Deflandre B. (2003). Anaerobic ammonium oxidation measured in sediments along the Thames estuary, United Kingdom. *Appl Environ Microbiol* **69**: 6447-6454.

Trimmer M, Nicholls JC, Morley N, Davies CA ,Aldridge J. (2005). Biphasic behavior of anammox regulated by nitrite and nitrate in an estuarine sediment. *Appl Environ Microbiol* **71**: 1923-1930.

Ushiki N, Jinno M, Fujitani H, Suenaga T, Terada A ,Tsuneda S. (2017). Nitrite oxidation kinetics of two Nitrospira strains: The quest for competition and ecological niche differentiation. *J Biosci Bioeng* **123**: 581-589.

Vadivelu VM, Keller J ,Yuan Z. (2007). Effect of free ammonia on the respiration and growth processes of an enriched Nitrobacter culture. *Water Res* **41**: 826-834.

Vadivelu VM, Yuan Z, Fux C ,Keller J. (2006). The inhibitory effects of free nitrous acid on the energy generation and growth processes of an enriched Nitrobacter culture. *Environ Sci Technol* **40**: 4442-4448.

Van de Graaf AA, de Bruijn P, Robertson LA, Jetten MS ,Kuenen JG. (1996). Autotrophic growth of anaerobic ammonium-oxidizing micro-organisms in a fluidized bed reactor. *Microbiology* **142**: 2187-2196.

Van De Graaf AA, De Bruijn P, Robertson LA, Jetten MS ,Kuenen JG. (1997). Metabolic pathway of anaerobic ammonium oxidation on the basis of 15N studies in a fluidized bed reactor. *Microbiology* **143**: 2415-2421.

Van de Graaf AA, Mulder A, de Bruijn P, Jetten M, Robertson LA ,Kuenen JG. (1995). Anaerobic oxidation of ammonium is a biologically mediated process. *Appl Environ Microbiol* **61**: 1246-1251.

Van Den Berg EM, Van Dongen U, Abbas B ,Van Loosdrecht MC. (2015). Enrichment of DNRA bacteria in a continuous culture. *ISME J* **9**: 2153-2161.

van Kessel MA, Speth DR, Albertsen M, Nielsen PH, den Camp HJO, Kartal B, et al. (2015). Complete nitrification by a single microorganism. *Nature* **528**: 555-559.

Vanparys B, Spieck E, Heylen K, Wittebolle L, Geets J, Boon N, et al. (2007). The phylogeny of the genus Nitrobacter based on comparative rep-PCR, 16S rRNA and nitrite oxidoreductase gene sequence analysis. *Syst Appl Microbiol* **30**: 297-308.

Venter JC, Remington K, Heidelberg JF, Halpern AL, Rusch D, Eisen JA, et al. (2004). Environmental genome shotgun sequencing of the Sargasso Sea. *Science* **304**: 66-74.

Veraart AJ (2012). Denitrification in ditches, streams and shallow lakes, Wageningen University, the Netherlands. **Degree of doctor:** 208.

Verhamme DT, Nicol GW ,Prosser JI. (2011). Ammonia concentration determines differential growth of ammonia-oxidising archaea and bacteria in soil microcosms. *ISME J* **5**: 1067-1071.

Vitousek PM, Aber JD, Howarth RW, Likens GE, Matson PA, Schindler DW, et al. (1997). Human alteration of the global nitrogen cycle: sources and consequences. *Ecol Appl* **7**: 737-750.

Wang B, Zhao J, Guo Z, Ma J, Xu H ,Jia Z. (2015). Differential contributions of ammonia oxidizers and nitrite oxidizers to nitrification in four paddy soils. *ISME J* **9**: 1062-1075.

Wang J, Dong H, Wang W ,Gu JD. (2014). Reverse-transcriptional gene expression of anammox and ammonia-oxidizing archaea and bacteria in soybean and rice paddy soils of Northeast China. *Appl Microbiol Biotechnol* **98**: 2675-2686.

Wang Q, Garrity GM, Tiedje JM ,Cole JR. (2007). Naive Bayesian classifier for rapid assignment of rRNA sequences into the new bacterial taxonomy. *Appl Environ Microbiol* **73**: 5261-5267.

Wang Q, Ye L, Jiang G, Hu S ,Yuan Z. (2014). Side-stream sludge treatment using free nitrous acid selectively eliminates nitrite oxidizing bacteria and achieves the nitrite pathway. *Water Res* **55**: 245-255.

Wang S, Radny D, Huang S, Zhuang L, Zhao S, Berg M, et al. (2017) Nitrogen loss by anaerobic ammonium oxidation in unconfined aquifer soils. *Sci Rep* **7**, 40173 doi: 10.1038/srep40173.

Wang S, Zhu G, Peng Y, Jetten MS ,Yin C. (2012). Anammox bacterial abundance, activity, and contribution in riparian sediments of the Pearl River estuary. *Environ Sci Technol* **46**: 8834-8842.

Wang Y, Ma L, Mao Y, Jiang X, Xia Y, Yu K, et al. (2017). Comammox in drinking water systems. *Water Res* **116**: 332-341.

Wang Y, Zhu G, Harhangi HR, Zhu B, Jetten MS, Yin C, et al. (2012). Co-occurrence and distribution of nitrite-dependent anaerobic ammonium and methane-oxidizing bacteria in a paddy soil. *FEMS Microbiol Lett* **336**: 79-88.

Wang Y, Zhu G, Ye L, Feng X, den Camp HJO ,Yin C. (2012). Spatial distribution of archaeal and bacterial ammonia oxidizers in the littoral buffer zone of a nitrogen-rich lake. *J Environ Sci* **24**: 790-799.

Wang YF, Feng YY, Ma X ,Gu JD. (2013). Seasonal dynamics of ammonia/ammonium-oxidizing prokaryotes in oxic and anoxic wetland sediments of subtropical coastal mangrove. *Appl Microbiol Biotechnol* **97**: 7919-7934.

Wang YF ,Gu JD. (2013). Higher diversity of ammonia/ammonium-oxidizing prokaryotes in constructed freshwater wetland than natural coastal marine wetland. *Appl Microbiol Biotechnol* **97**: 7015-7033.

Wang YF ,Gu JD. (2014). Effects of allylthiourea, salinity, and pH on ammonia/ammonium-oxidizing prokaryotes in mangrove sediment incubated in laboratory microcosms. *Appl Microbiol Biotechnol* **98**: 3257-3274.

Ward B, Glover H ,Lipschultz F. (1989). Chemoautotrophic activity and nitrification in the oxygen minimum zone off Peru. *Deep Sea Res Part 1 Oceanogr Res Pap* **36**: 1031-1051.

Ward BB (2008). Nitrification in marine systems. Nitrogen in the marine environment, *Elsevier*. **5:** 199-261.

Watson SW, Bock E, Valois FW, Waterbury JB ,Schlosser U. (1986). Nitrospira marina gen. nov. sp. nov.: a chemolithotrophic nitrite-oxidizing bacterium. *Arch Microbiol* **144**: 1-7.

Wentworth CK. (1922). A scale of grade and class terms for clastic sediments. *J Geol* **30**: 377-392.

Whang L-M, Chien I-C, Yuan S-L ,Wu Y-J. (2009). Nitrifying community structures and nitrification performance of full-scale municipal and swine wastewater treatment plants. *Chemosphere* **75**: 234-242.

White JR ,Reddy K. (2003). Nitrification and denitrification rates of Everglades wetland soils along a phosphorus-impacted gradient. *J Environ Qual* **32**: 2436-2443.

Wickham H (2016). ggplot2: elegant graphics for data analysis, Springer.

Williams JD, Syers JK, Shukla SS, Harris RF ,Armstrong DE. (1971). Levels of inorganic and total phosphorus in lake sediments as related to other sediment parameters. *Environ Sci Technol* **5**: 1113-1120.

Winterbourn MJ, Hildrew AG ,Orton S. (1992). Nutrients, algae and grazers in some British streams of contrasting pH. *Freshwat Biol* **28**: 173-182.

Wolff J-C, Örnemark U, Taylor PDP ,De Bièvre P. (1998). Stability studies and purification procedure for nitrite solutions in view of the preparation of isotopic reference materials. *Talanta* **46**: 1031-1040.

Wrage N, Velthof G, Van Beusichem M ,Oenema O. (2001). Role of nitrifier denitrification in the production of nitrous oxide. *Soil Biol Biochem* **33**: 1723-1732.

Wu Y, Xiang Y, Wang J, Zhong J, He J ,Wu QL. (2010). Heterogeneity of archaeal and bacterial ammonia-oxidizing communities in Lake Taihu, China. *Env Microbiol Rep* **2**: 569-576.

Xia X, Liu T, Yang Z, Michalski G, Liu S, Jia Z, et al. (2017). Enhanced nitrogen loss from rivers through coupled nitrification-denitrification caused by suspended sediment. *Sci Total Environ* **579**: 47-59.

Ye L, Tang B, Zhao K, Pijuan M ,Peng Y. (2009). Nitrogen removal via nitrite in domestic wastewater treatment using combined salt inhibition and on-line process control. *Water Sci Technol* **60**: 1633-1639.

Yoshinaga I, Amano T, Yamagishi T, Okada K, Ueda S, Sako Y, et al. (2011). Distribution and diversity of anaerobic ammonium oxidation (anammox) bacteria in the sediment of a eutrophic freshwater lake, Lake Kitaura, Japan. *Microbes Environ* **26**: 189-197.

Yu C, Hou L, Zheng Y, Liu M, Yin G, Gao J, et al. (2018). Evidence for complete nitrification in enrichment culture of tidal sediments and diversity analysis of clade a comammox Nitrospira in natural environments. *Appl Microbiol Biotechnol*: 1-15.

Zehr JP, Jenkins BD, Short SM ,Steward GF. (2003). Nitrogenase gene diversity and microbial community structure: a cross-system comparison. *Environ Microbiol* **5**: 539-554.

Zhang J, Kobert K, Flouri T ,Stamatakis A. (2013). PEAR: a fast and accurate Illumina Paired-End reAd mergeR. *Bioinformatics* **30**: 614-620.

Zhang S, Xia X, Liu T, Xia L, Zhang L, Jia Z, et al. (2017). Potential roles of anaerobic ammonium oxidation (anammox) in overlying water of rivers with suspended sediments. *Biogeochemistry* **132**: 237-249.

Zhang X, Liu W, Schloter M, Zhang G, Chen Q, Huang J, et al. (2013) Response of the abundance of key soil microbial nitrogen-cycling genes to multi-factorial global changes. *PLoS One* **8**, e76500 doi: 10.1371/journal.pone.0076500.

Zhang Y, Ruan XH, Op den Camp HJ, Smits TJ, Jetten MS ,Schmid MC. (2007). Diversity and abundance of aerobic and anaerobic ammonium-oxidizing bacteria in freshwater sediments of the Xinyi River (China). *Environ Microbiol* **9**: 2375-2382.

Zhao D, Zeng J, Wan W, Liang H, Huang R ,Wu QL. (2013). Vertical distribution of ammonia-oxidizing archaea and bacteria in sediments of a eutrophic lake. *Curr Microbiol* **67**: 327-332.

Zhao Y, Xia Y, Kana TM, Wu Y, Li X ,Yan X. (2013). Seasonal variation and controlling factors of anaerobic ammonium oxidation in freshwater river sediments in the Taihu Lake region of China. *Chemosphere* **93**: 2124-2131.

Zheng Y, Hou L, Newell S, Liu M, Zhou J, Zhao H, et al. (2014). Community dynamics and activity of ammonia-oxidizing prokaryotes in intertidal sediments of the Yangtze Estuary. *Appl Environ Microbiol* **80**: 408-419.

Zhou S, Borjigin S, Riya S, Terada A ,Hosomi M. (2014). The relationship between anammox and denitrification in the sediment of an inland river. *Sci Total Environ* **490**: 1029-1036.

Zhou Z, Li H, Song C, Cao X ,Zhou Y. (2017). Prevalence of ammonia-oxidizing bacteria over ammonia-oxidizing archaea in sediments as related to nutrient loading in Chinese aquaculture ponds. *J Soils Sed* **17**: 1928-1938.

Zhou Z, Shi X, Zheng Y, Qin Z, Xie D, Li Z, et al. (2014). Abundance and community structure of ammonia-oxidizing bacteria and archaea in purple soil under long-term fertilization. *Eur J Soil Biol* **60**: 24-33.

Zhou Z, Wei Q, Yang Y, Li M ,Gu J-D. (2018). Practical applications of PCR primers in detection of anammox bacteria effectively from different types of samples. *Appl Microbiol Biotechnol*: 1-13.

Zhu G, Jetten MS, Kuschk P, Ettwig KF ,Yin C. (2010). Potential roles of anaerobic ammonium and methane oxidation in the nitrogen cycle of wetland ecosystems. *Appl Microbiol Biotechnol* **86**: 1043-1055.

Zhu G, Wang S, Wang W, Wang Y, Zhou L, Jiang B, et al. (2013). Hotspots of anaerobic ammonium oxidation at land-freshwater interfaces. *Nat Geosci* **6**: 103-107.

Zhu G, Wang S, Wang Y, Wang C, Risgaard-Petersen N, Jetten MS, et al. (2011). Anaerobic ammonia oxidation in a fertilized paddy soil. *ISME J* **5**: 1905-1912.